

# Therapeutic Strategies for the Treatment of Atrial Fibrillation: New Insights from Biophysical Modeling and Signal Processing

THÈSE N° 5107 (2011)

PRÉSENTÉE LE 19 AOÛT 2011

À LA FACULTÉ SCIENCES ET TECHNIQUES DE L'INGÉNIEUR

GROUPE SCI STI JMV

PROGRAMME DOCTORAL EN GÉNIE ÉLECTRIQUE

ÉCOLE POLYTECHNIQUE FÉDÉRALE DE LAUSANNE

POUR L'OBTENTION DU GRADE DE DOCTEUR ÈS SCIENCES

PAR

Laurent ULDRY

acceptée sur proposition du jury:

Prof. J. R. Mosig, président du jury  
Dr J.-M. Vesin, Prof. L. Kappenberger, directeurs de thèse  
Prof. G. Carrault, rapporteur  
Prof. M.-O. Hongler, rapporteur  
Dr E. Pruvot, rapporteur



ÉCOLE POLYTECHNIQUE  
FÉDÉRALE DE LAUSANNE

Suisse  
2011



*“Toutes les sciences ont leur chimère, après laquelle elles courent, sans la pouvoir attraper ; mais elles attrapent en chemin d’autres connaissances fort utiles.”*

Bernard le Bovier de Fontenelle



# Abstract

---

Atrial fibrillation is the most common cardiac rhythm disorder encountered in clinical practice, often leading to severe complications such as heart failure and stroke. This arrhythmia, increasing in prevalence with age, already affects several millions of people in the United States, with a rising occurrence of the disease during the past two decades. In spite of these warning signals, atrial fibrillation is still difficult to treat, because basic mechanisms of the arrhythmia remain poorly understood and current treatments are therefore based on empirical considerations.

The future of therapeutic solutions for the treatment of complex diseases such as atrial fibrillation relies on a strong collaboration between medicine, biology and engineering. Only through such synergies will efficient monitoring, diagnostic and therapeutic devices be created. The goal of the present thesis was to adopt this multidisciplinary approach, and develop new strategies for atrial fibrillation therapy using both computer modeling and advanced signal processing methods.

Biophysical modeling is a practical and ethically interesting approach to develop innovative therapies, since physiological phenomena of interest are reproduced numerically and the resulting framework is then used with full repeatability to explore mechanisms and test treatments. A model of the human atria, that was developed in our group, was used to simulate atrial fibrillation and perform mechanistic and therapeutic investigations. In a first study, computer simulations were used to observe spontaneous terminations of two models of atrial fibrillation corresponding to different developmental stages of the arrhythmia. Dynamical parameters were observed during several seconds prior to termination in order to describe the underlying mechanisms of this natural phenomenon, showing that different levels of fibrillation complexity led to different termination patterns. The mechanisms highlighted by the study were successfully compared to those described in the existing literature and could suggest interesting guidelines to better investigate spontaneous terminations of atrial fibrillation in experimental and clinical settings. Moreover, a more precise understanding of the natural extinction of atrial fibrillation will certainly be crucial for future therapy developments.

The potential of rapid low-energy pacing for artificially terminating atrial fibrillation was also thoroughly investigated. First, the possibility to entrain and thereby control fibrillating atrial activity by rapid pacing was studied in a systematic manner. Results showed that optimized pacing parameters provided sustained entrainment of electrical activity, although total extinction of atrial fibrillation was never observed. The ability

to control atrial activity by pacing was also shown to depend on specific properties of the atrial tissue, showing that patients with atrial fibrillation may not all respond in the same way to pacing treatments. Finally, this study suggested different guidelines for the development of pace-termination algorithms for atrial fibrillation. Based on these results, a new pacing sequence for the automatic termination of atrial fibrillation was designed, implemented and tested in the biophysical model. The pacing protocol comprised two distinct phases involving a succession of rapid and slow pacing stimulations. The results of the tests suggest that this pacing scheme could represent an alternative to current treatments of atrial fibrillation, and could easily be implemented in patients who already have an indication for pacing.

Advanced signal processing techniques were also used in this thesis to analyze real cardiac signals and develop new diagnosis tools. Multivariate spectral analysis and complexity measures were combined to develop an automatic method able to describe subtle changes in atrial fibrillation organization as measured by non-invasive ECG recordings. Accurate discrimination between persistent and permanent AF was shown possible, and potential applications in clinical settings to optimize patient management were demonstrated.

Collectively, the results of this thesis show that major public health issues such as atrial fibrillation can strongly benefit from the contribution of biomedical engineering. The modeling and signal processing approaches used in the present dissertation proved effective and promising, and synergies between clinicians and scientists will definitely be at the basis of future therapies.

**Keywords :** Atrial fibrillation, Biophysical modeling, Computer Simulations, Low-energy pacing, Surface electrocardiogram, Spectral analysis, Complexity measures.

# Résumé

---

La fibrillation auriculaire est le trouble du rythme cardiaque le plus commun rencontré en clinique, menant bien souvent à de sévères complications telles que défaillances cardiaques et accidents vasculaires cérébraux. Cette arythmie, dont la prévalence augmente avec l'âge, affecte par exemple plusieurs millions de personnes aux États-Unis, et a vu sa présence se renforcer de manière notoire durant les deux dernières décennies. Bien que ces faits appellent à des développements cliniques importants, la fibrillation auriculaire reste difficile à traiter, car les mécanismes fondamentaux de cette arythmie sont encore mal compris et les traitements actuels sont dès lors basés sur des considérations empiriques.

Les futures solutions thérapeutiques dédiées aux maladies complexes telles que la fibrillation auriculaire reposent sur une forte collaboration entre les univers de la médecine, de la biologie, et de l'ingénierie. Ce n'est que par de telles synergies que des systèmes efficaces de surveillance, de diagnostic assisté et de thérapie pourront voir le jour. Le but de cette thèse est d'adopter cette approche multidisciplinaire et de développer de nouvelles stratégies thérapeutiques pour le traitement de la fibrillation auriculaire au moyen de méthodes ayant recours à la modélisation informatique ainsi qu'à des techniques avancées de traitement de signal.

La modélisation biophysique est une approche pratique et intéressante du point de vue éthique pour le développement de nouvelles thérapies, puisque les phénomènes physiologiques observés sont reproduits numériquement et que le cadre résultant se prête à l'exploration des mécanismes et aux tests de thérapies avec une répétabilité illimitée. Un modèle d'oreillettes humaines développé dans notre équipe de recherche a été utilisé pour simuler la fibrillation auriculaire et entreprendre une analyse des mécanismes et une recherche de thérapies potentielles. Durant une première étude, des simulations informatiques furent utilisées afin d'observer des terminaisons spontanées dans deux modèles de fibrillation auriculaire correspondant à différents stades développementaux de la maladie. Les paramètres dynamiques d'intérêt furent observés pendant plusieurs secondes avant terminaison afin de décrire les mécanismes sous-jacents de ce phénomène naturel, démontrant que des fibrillations de différents niveaux de complexité présentent des scénarios de terminaison différents. Les mécanismes mis en valeur par l'étude furent comparés avec succès à ceux décrits par la littérature existante et purent ainsi suggérer des lignes de recherche intéressantes visant à examiner de manière plus détaillée les terminaisons spontanées de fibrillation auriculaire en laboratoire et en clinique. De plus,

une compréhension plus précise du phénomène d'extinction naturelle de la fibrillation auriculaire sera certainement cruciale pour le développement de futures thérapies.

Le potentiel des méthodes de stimulation rapide à basse intensité dédiées à la terminaison artificielle de la fibrillation auriculaire a également été investigué en détail. Tout d'abord, la possibilité d'entraîner, et par-là même de contrôler l'activité auriculaire au moyen d'une stimulation rapide, a été étudiée de manière systématique. Les résultats obtenus montrent que des paramètres de stimulation optimisés peuvent fournir un entraînement soutenu de l'activité électrique, bien qu'aucune extinction totale de fibrillation auriculaire n'ait pu être observée. Il a aussi été démontré que l'aptitude à contrôler l'activité auriculaire par stimulation dépend de propriétés spécifiques du tissu des oreillettes, ce qui tend à prouver que des patients en fibrillation auriculaire pourraient ne pas tous réagir à ce traitement de la même manière. Finalement, l'étude a permis de formuler des suggestions pour le développement des futures solutions de stimulation thérapeutique. Grâce à ces résultats, une nouvelle procédure de stimulation menant à la terminaison automatique de la fibrillation auriculaire a été conceptualisée, implémentée et testée dans le modèle biophysique. Le protocole de stimulation proposé comprend deux phases distinctes mettant en oeuvre des stimulations électriques rapides puis lentes. Les résultats des tests suggèrent que cette procédure de stimulation pourrait représenter une alternative aux traitements courants de la fibrillation auriculaire, et pourrait être facilement implémenté chez des patients ayant déjà une indication pour un pacemaker.

Des méthodes avancées de traitement de signal ont aussi été utilisées durant cette thèse pour analyser des signaux cardiaques réels et développer de nouveaux outils de diagnostic. Une combinaison d'analyse spectrale multivariée et de mesures de complexité permirent le développement d'une méthode automatique permettant de quantifier finement des changements d'organisation de l'activité fibrillatoire des oreillettes dans des signaux d'ECG de surface. Une distinction précise entre signaux de fibrillations auriculaires persistentes et permanentes a été proposée, et de potentielles applications cliniques visant à optimiser la prise en charge du patient ont été démontrées.

Pris collectivement, les résultats de cette thèse montrent que des problèmes de santé publique majeurs comme la fibrillation auriculaire peuvent clairement bénéficier de la contribution du domaine de l'ingénierie biomédicale. Les approches par la modélisation et le traitement de signal utilisées dans ce travail de thèse se sont montrées efficaces et prometteuses, et des synergies entre médecins et scientifiques seront assurément à l'origine du développement des thérapies du futur.

Mots-clés : Fibrillation auriculaire, Modélisation biophysique, Simulations informatiques, Stimulation électrique à basse intensité, Électrocardiogramme de surface, Analyse spectrale, Mesures de complexité.



# Remerciements

---

Ce travail n'aurait pas été possible sans la contribution, directe ou indirecte, d'une multitude de personnes que j'aimerais ici sincèrement remercier :

- J'aimerais commencer par remercier mon co-directeur de thèse, le Prof. Lukas Kappenberger, pour son soutien continu, sa disponibilité et son immense expertise dans le domaine de recherche que j'ai exploré. Votre vision, votre enthousiasme et votre passion intacte pour la recherche ont véritablement guidé notre projet, et continuent à lui donner son souffle !
- Merci au président du jury, Prof. Juan Mosig, et aux rapporteurs, Prof. Guy Carraut, Prof. Max-Olivier Hongler et Dr. Etienne Pruvot pour les intéressantes discussions qui ont ponctué cette thèse.
- Merci également aux nombreux collaborateurs qui participèrent à ce projet, et le rendirent ainsi possible. Je pense bien sûr à nos partenaires industriels représentés par Dr. Frederic Lindemans et Dr. Nathalie Virag, mais aussi au Prof. Adriaan Van Oosterom pour m'avoir initié à la modélisation de l'activité cardiaque avec une justesse et un enthousiasme impressionnants, ainsi qu'aux Drs. Andrei Forclaz et Lam Dang pour leurs précieux conseils. Tout particulièrement, j'adresse un énorme merci au Prof. Vincent Jacquemet pour m'avoir montré avec patience et brio les finesses du modèle biophysique dont il est le principal créateur, et qui permit les recherches présentées plus loin. Vince, ta disponibilité sans faille, ta rigueur et ton génie ont été plus qu'essentiels dans la réussite de ce travail.
- Je tiens bien sûr à rendre un immense hommage aux mythiques "Jean-Marc Boys" de l'ASPG, très justement rebaptisés "Jean-Marc People" pour des raisons évidentes de genre, qui ont mis du bonheur et des rires dans chaque journée de cette période dorée : Florian Jousset, Mathieu Lemay, Andréa Buttu, Aline Cabasson, coach Cédric Duchêne, "Lapin" Yann Prudat, Jérôme Van Zaen (alias mon Jérôme), Alain Viso, Zenichi Ihara, Vincent Jacquemet, ainsi que nos complices Elda, Bobo, Benoît, Alex, Meri, ma chère Nawal, et tous les autres !
- Plus généralement, c'est chaque membre de nos laboratoires de traitement de signaux (ASPG, LTS et MMSPG) que j'aimerais remercier pour l'ambiance conviviale et amicale qui règne dans chaque couloir ! En particulier, un grand merci à nos secrétaires, Rosie De Pietro et Christine Gabriel, pour leur disponibilité, leur efficacité, et leurs sourires quotidiens !
- J'aimerais également dire toute ma gratitude à ma famille et mes proches pour leur soutien inconditionnel dans chaque moment, bon comme plus difficile : merci à

mes parents pour leur attention continuelle, à Julien, à Júlia, et au reste de ma famille : vous m'avez donné l'énergie dont j'avais besoin !

- Le dernier remerciement, et peut-être le plus important : pour Jean-Marc Vesin, mon directeur de thèse. Sa passion pour son métier et son érudition sans limite ont été un vrai moteur pour moi durant toute ma thèse. Jean-Marc, tu ne nous apprends pas seulement le traitement de signal et les compétences requises pour réussir notre doctorat, mais aussi l'amitié, la culture générale, l'humour, et tout cela dans un cadre professionnel. Quelle chance d'avoir pu travailler avec toi ! Merci pour les moments géniaux passés tous ensemble, merci pour m'avoir tenu à bout de bras quand il le fallait, merci pour rendre magique la période du doctorat pour chacun de tes boys, **MERCI POUR TOUT !**

# Contents

---

<b>1</b>	<b>Introduction</b>	<b>1</b>
1.1	Motivation and Problem Statement . . . . .	1
1.2	Organization of the Dissertation . . . . .	5
1.3	Original Contributions . . . . .	6
<b>I</b>	<b>Biophysical Modeling of Atrial Fibrillation Dynamics</b>	<b>7</b>
<b>2</b>	<b>Biophysical Modeling of the Human Atria</b>	<b>9</b>
2.1	Introduction . . . . .	9
2.2	Modeling the cardiac cell . . . . .	10
2.2.1	Properties of the cardiac cell . . . . .	10
2.2.2	Modeling the cardiac cell membrane . . . . .	12
2.3	Modeling cardiac tissue . . . . .	15
2.3.1	The Bidomain Model . . . . .	15
2.3.2	The Monodomain Model . . . . .	17
2.3.3	Simulated Electrograms . . . . .	17
2.4	Atrial Geometry . . . . .	18
2.4.1	Monolayer 3D Surface . . . . .	18
2.5	Conclusion . . . . .	19
<b>3</b>	<b>Simulating Atrial Fibrillation</b>	<b>21</b>
3.1	Introduction . . . . .	21
3.2	Simulating Sinus Rhythm . . . . .	22
3.3	Simulating Atrial Fibrillation . . . . .	22
3.3.1	The Polymorphic Beast . . . . .	22

3.3.2	Initiation and Perpetuation of Atrial Fibrillation . . . . .	23
3.3.3	A Model of Recent Chronic Atrial Fibrillation . . . . .	25
3.3.4	A Model of Paroxysmal Atrial Fibrillation . . . . .	31
3.4	Conclusion . . . . .	36
<b>4</b>	<b>Dynamics of Atrial Fibrillation during Spontaneous Termination</b>	<b>37</b>
4.1	Introduction . . . . .	37
4.2	Methods . . . . .	39
4.2.1	Biophysical Modeling of Atrial Fibrillation . . . . .	39
4.2.2	Simulating Atrial Fibrillation Spontaneous Termination . . . . .	41
4.2.3	Analysis of Spontaneous Terminations . . . . .	42
4.3	Results . . . . .	44
4.3.1	Examples of Simulated Spontaneous Terminations . . . . .	45
4.3.2	Temporal Analysis . . . . .	48
4.3.3	Spatial Analysis . . . . .	50
4.3.4	Subgroup Analysis in the Model of Paroxysmal Atrial Fibrillation	52
4.4	Discussion . . . . .	54
4.4.1	Mechanisms of Spontaneous Termination of Atrial Fibrillation .	56
4.4.2	Termination Patterns during Simulated Paroxysmal Atrial Fibrillation . . . . .	57
4.4.3	Study Limitations . . . . .	60
4.4.4	Future Works and Clinical Implications . . . . .	60
4.5	Conclusion . . . . .	62
<b>II</b>	<b>Towards New Therapeutic Strategies for Atrial Fibrillation</b>	<b>63</b>
<b>5</b>	<b>Rapid Pacing of Atrial Fibrillation</b>	<b>65</b>
5.1	State of the Art of Therapeutic Pacing for AF . . . . .	65
5.1.1	Pacing Algorithms for AF Prevention . . . . .	66
5.1.2	Pacing Algorithms for AF Termination . . . . .	68
5.2	Motivation of the Proposed Study . . . . .	71
5.3	Methods . . . . .	71
5.3.1	Reference Model for Sustained AF . . . . .	71
5.3.2	Variants of the Reference Model . . . . .	72

5.3.3	Characterization of AF Dynamics . . . . .	73
5.3.4	Rapid Pacing Protocol . . . . .	73
5.3.5	Assessment of AF Capture . . . . .	74
5.3.6	Statistical Analysis . . . . .	75
5.4	Results . . . . .	75
5.4.1	Local Capture of AF . . . . .	75
5.4.2	Temporal Aspects of AF Capture . . . . .	76
5.4.3	Spatial Aspects of AF Capture . . . . .	77
5.4.4	Effect of AF Dynamics on Capture . . . . .	78
5.5	Discussion . . . . .	80
5.5.1	Local Capture and Capture Window . . . . .	80
5.5.2	Comparison of Pacing Sites . . . . .	81
5.5.3	Effect of Modified AF Dynamics on Capture . . . . .	82
5.5.4	Limitations of the Study . . . . .	82
5.5.5	Clinical Implications . . . . .	83
5.6	Conclusion . . . . .	84
<b>6</b>	<b>Atrial Septal Pacing For the Termination of Atrial Fibrillation</b>	<b>85</b>
6.1	Introduction . . . . .	85
6.2	Methods . . . . .	86
6.2.1	Biophysical Model of AF . . . . .	86
6.2.2	Study Protocol . . . . .	87
6.3	Results . . . . .	91
6.3.1	Capture Window for Septal Rapid Pacing . . . . .	91
6.3.2	Example of Successful AF Termination . . . . .	92
6.3.3	Example of Unsuccessful Septal Pacing . . . . .	92
6.3.4	Performance of the Septal Pacing Algorithm . . . . .	93
6.3.5	Effect of the Capture Pattern on AF Termination . . . . .	95
6.4	Discussion . . . . .	97
6.4.1	Possibility of AF Termination by Septal Pacing . . . . .	97
6.4.2	Rapid Pacing Phase . . . . .	99
6.4.3	Slow Pacing Phase . . . . .	100
6.4.4	Practical Aspects of Septal Pacing . . . . .	101
6.4.5	Importance of Capture Patterns . . . . .	101

6.4.6	Study Limitations . . . . .	102
6.4.7	Clinical Implications . . . . .	103
6.5	Conclusion . . . . .	103
<b>7</b>	<b>Measures of Atrial Fibrillation Organization</b>	<b>105</b>
7.1	Introduction . . . . .	105
7.1.1	Quantifying Atrial Fibrillation Complexity: a State of the Art . . . . .	105
7.1.2	Motivation of the Proposed Study . . . . .	107
7.2	Clinical Electrocardiogram Database and Data Preprocessing . . . . .	109
7.3	Multivariate Analysis of Atrial Fibrillation Organization . . . . .	110
7.3.1	Multivariate Spectral Analysis: the Spectral Envelope . . . . .	110
7.3.2	Two measures of Atrial Fibrillation Organization . . . . .	115
7.3.3	Feature Selection and Classification . . . . .	119
7.4	Results . . . . .	120
7.4.1	Two-Feature Classification Results . . . . .	120
7.4.2	Three-Feature Classification Results . . . . .	123
7.5	Discussion . . . . .	123
7.5.1	A Discriminative Measure of Atrial Fibrillation Chronification . . . . .	124
7.5.2	Advantages of the Multivariate Approach . . . . .	125
7.5.3	Clinical Implications . . . . .	128
7.6	Conclusion . . . . .	129
<b>8</b>	<b>Conclusion</b>	<b>131</b>
8.1	Summary of Achievements . . . . .	132
8.2	Perspectives . . . . .	134

# List of Acronyms

---

AF	Atrial fibrillation
AFCL	Atrial fibrillation cycle length
AFL	Atrial flutter
APD	Action potential duration
AT	Atrial tachyarrhythmia
ATP	Antitachycardia pacing
CL	Cycle length
CRN	Courtemanche-Ramirez-Nattel
CS	Coronary sinus
CV	Conduction velocity
ECG	Electrocardiogram
ERP	Effective refractory period
IC	Initial condition
IVC	Inferior vena cava
LA	Left atrium
LR	Luo-Rudy
MOI	Multivariate organization index
MSE	Multivariate spectral entropy
MV	Mitral valve
OI	Organization index
PCL	Pacing cycle length
PV	Pulmonary veins
RA	Right atrium
SAF	Simulated atrial fibrillation

SE Spectral entropy  
SR Sinus rhythm  
SVC Superior vena cava  
TV Tricuspid valve



# List of Figures

---

2.1	Electrical response of a simulated cardiac cell . . . . .	11
2.2	Definition of action potential parameters and restitution properties for the Luo-Rudy model . . . . .	12
2.3	Schematic representation of the Luo-Rudy membrane kinetics model . .	14
2.4	Schematic representation of the Courtemanche et al. human atrial model	15
2.5	Geometry of a model of human atria based on MR images . . . . .	20
3.1	Activation map and isochrones during normal sinus rhythm . . . . .	22
3.2	Action potential shape and restitution curve of the modified Luo-Rudy model . . . . .	26
3.3	SAF initiation by 20 Hz burst pacing in the modified Luo-Rudy model .	27
3.4	Dynamics of sustained SAF using the remodeled modified Luo-Rudy model . . . . .	28
3.5	Local and global dynamical properties of sustained SAF using the remodeled modified Luo-Rudy model . . . . .	29
3.6	Action potential shape and restitution curve of the Courtemanche model	32
3.7	SAF initiation by ramp pacing in the modified Courtemanche model . .	33
3.8	Dynamics of sustained SAF using the modified Courtemanche model .	34
3.9	Local and global dynamical properties of sustained SAF using the modified Courtemanche model . . . . .	35
4.1	Geometry of the biophysical model of human atria . . . . .	40
4.2	Simulation protocol and temporal analysis of SAF spontaneous termination	42
4.3	Example of SAF wavelet with multiple wavefronts. . . . .	43
4.4	Histograms of the durations of the 50 episodes of SAF for each AF model	45
4.5	Example of spontaneous AF termination for the model of paroxysmal AF	47
4.6	Example of spontaneous AF termination for the model of recent chronic AF . . . . .	49

4.7	Temporal analysis of AF spontaneous termination in the model of paroxysmal AF . . . . .	50
4.8	Temporal analysis of AF spontaneous termination in the model of recent chronic AF . . . . .	51
4.9	Spatial distribution of extinction sites for the model of paroxysmal AF and the model of recent chronic AF . . . . .	52
4.10	Mean temporal evolution of <i>AFCL</i> for the subgroups of simulations defined for the model of paroxysmal AF . . . . .	54
4.11	Mean temporal evolution of <i>#WF</i> for the subgroups of simulations defined for the model of paroxysmal AF . . . . .	55
5.1	The biophysical model of AF and its components . . . . .	72
5.2	Simulation of rapid pacing in the biophysical model of AF . . . . .	73
5.3	Description of AF capture assessment . . . . .	75
5.4	Example of local capture by rapid pacing in the RA free wall . . . . .	76
5.5	Summary of the temporal aspects of AF capture . . . . .	77
5.6	Summary of the spatial aspects of AF capture . . . . .	79
5.7	Effect of AF dynamics on capture . . . . .	80
6.1	The biophysical model of AF . . . . .	88
6.2	Study protocol for the testing of the septal pacing algorithm . . . . .	89
6.3	Capture window for septal pacing . . . . .	90
6.4	Example of application of the septal pacing algorithm with successful AF termination . . . . .	93
6.5	Example of application of the septal pacing algorithm without AF termination . . . . .	94
6.6	Histogram of the AF termination rates obtained when applying septal rapid pacing only vs. the whole atrial septal pacing algorithm . . . . .	95
6.7	Impact of the number of anchored waves around anatomical obstacles on AF termination rates . . . . .	97
6.8	Assessment of a critical number of anchored waves . . . . .	98
7.1	Pharmacological management of patients with persistent AF or permanent AF . . . . .	109
7.2	Block diagram of the multivariate analysis framework . . . . .	110
7.3	Detection of common oscillations in a noisy environment through spectral envelope computation . . . . .	115

7.4	Spectral envelope of an ECG recording of AF . . . . .	116
7.5	Examples of MOI and MSE measures on ECG signals . . . . .	118
7.6	Two-feature classification of persistent and permanent AF signals . . . . .	122
7.7	Multivariate three-feature classification of persistent and permanent AF signals . . . . .	125
7.8	Univariate three-feature classification of persistent and permanent AF signals . . . . .	126



# List of Tables

---

2.1	Ionic currents of the Luo-Rudy model . . . . .	14
2.2	Ionic currents of the Courtemanche et al. model . . . . .	16
2.3	Dimensions of the atrial geometry . . . . .	19
4.1	Dynamical characteristics of each AF model . . . . .	45
4.2	Temporal analysis of spontaneous terminations . . . . .	48
4.3	Summary of the spatial analysis of spontaneous terminations . . . . .	51
5.1	Capture windows computed from published data . . . . .	78
6.1	AF termination rates for the septal pacing algorithm compared to rapid pacing only . . . . .	95
6.2	Locations of anchored waves with significant impact on termination rates as computed with an ANOVA . . . . .	98
7.1	Summary of two-feature classification results . . . . .	121
7.2	Multivariate features statistics . . . . .	121
7.3	Summary of three-feature classification results . . . . .	124



# 1

## Introduction

---

### 1.1 Motivation and Problem Statement

#### Atrial Fibrillation

Atrial Fibrillation (AF) is the most common cardiac rhythm disorder (*arrhythmia*), increasing in prevalence with age. During an episode of AF, the upper chambers of the heart (the *atria*) do not beat in a normal way, the so-called *sinus rhythm*, but present rapid and uncoordinated activations. A general consensus classifies this arrhythmia according to its degree of recurrences [1, 2, 3]: when AF lasts less than seven days and returns spontaneously to sinus rhythm, it is called *paroxysmal AF*. When the AF episode lasts more than seven days, and may require a clinical intervention (called *cardioversion*) to restore normal rhythm, it is called *persistent AF*. *Long-standing persistent AF* has lasted for more than one year when it is decided to adopt a rhythm control strategy. Finally, when cardioversion fails to suppress AF on a long-term run, the arrhythmia is described as *permanent AF*.

This abnormal tachyarrhythmia results in an impaired atrial mechanical activity, irregular ventricular response, rapid heart rate, and decreased cardiac output [1, 3], which in turn can cause symptoms such as severe palpitations, dizziness, angina, dyspnea, decreased exercise tolerance, and more generally decreased quality of life [4, 5]. Although not directly life-threatening, AF was shown to potentially lead to severe complications, such as a tendency to precipitate or worsen heart failure; besides, the loss of atrial contractility promotes the formation of blood clots, resulting in increased risks for stroke and thromboembolic events. Therefore, AF was associated with substantial morbidity and mortality [6].

Recently, it has been estimated that more than 2.2 millions of people in the United States are affected by AF [1], and a rising occurrence of the disease was observed during the past two decades, so that projective studies estimated that 15.9 millions of people will be affected by 2050 if present trends continue [7]. As a consequence, the financial costs

of AF, which constitute already a substantial part of health expenditures, will become a crucial issue in the following years [8]. Therefore, the need for efficient therapies for the treatment of AF is now obvious.

### **Therapy of Atrial Fibrillation: a Challenging Future**

Several guidelines for the management of AF have been proposed, and provide a practical basis for the treatment of the arrhythmia in clinical settings [1, 3, 9]. Nowadays, possible treatments of AF include:

- pharmacological solutions using anti-arrhythmic drugs (AAD) to slow down the pathologic rapid heart rate or switch it back to normal sinus rhythm by modulating pharmacologically the ionic properties of the cardiac tissue,
- electrical cardioversion, where an electric shock resets the atrial activity towards normal rhythm,
- ablation procedures, where portions of the atrial tissue are ablated either surgically (surgical ablation) or with high-frequency electrical impulses (catheter-based ablation) for artificially restraining the pathway of AF electrical propagation and therefore suppressing the fibrillatory activity,
- low-energy pacing solutions by means of implanted atrial pacemakers, where the atrial rhythm is regulated by electrical stimulations of low intensity in order to prevent or terminate AF.

Thus far, none of the above solutions has proven to be fully satisfactory, and presently available treatment options are suboptimal. The current guidelines for the treatment of AF recommend the use of AAD such as flecainide, dofetilide, propafenone, ibutilide, amiodarone and dronedarone for pharmacological conversion [1, 2]. However, the long-term efficacy of pharmacological cardioversion as well as the problem of its related cardiac and extracardiac side effects (frequent intolerance, organ toxicity, pulmonary fibrosis, photosensitivity and neurological disorders) are still a matter of debate [10, 11, 12]. Moreover, pharmacological treatments may increase mortality by causing proarrhythmia [10, 11, 13, 14, 15]. Although electrical cardioversion by means of electric shocks applied either internally or externally shows high success rates for restoring sinus rhythm, it was also shown to have a rather high rate of AF recurrence and a weak maintenance of sinus rhythm [1, 11]. It was also suggested that the procedure has a substantial risk of proarrhythmic effects, in that the shock could subsequently trigger ventricular arrhythmia. Another risk related to electrical cardioversion is the creation of thromboembolic events, when a newly formed blood clot is ejected by the shock out of the atria. Finally, an acute pain is perceived by patients during electrical cardioversion [16], and the systematic need for conscious sedation or anesthesia makes the procedure unsuitable for regular use. Ablation procedures are promising approaches to treat AF but are still facing major issues before becoming first-line treatments. On one hand, surgical ablation requires open-heart surgery, and linear lesions are placed during cardiac arrest, which contributes to a risk of complications [17]. Therefore, surgical ablations are restricted to patients undergoing concomitant heart surgery for other purposes or to patients with contraindications to other treatments of AF. On the other hand, catheter-based ablation



is often considered as a serious alternative to AAD treatments [12]. Nevertheless, this technique still raises several questions [18]. First, it was shown that AF catheter ablation often results in the occurrence of an atrial tachyarrhythmia (AT), which can be seen from the patient point of view like an adverse event more than a success [19]. Moreover, the late-phase AF recurrence in patients initially defined as successfully ablated is reported to occur at a rate of approximately 5% per year [20], probably because the technique is less efficient with persistent AF than with paroxysmal AF [21]. Another drawback is that, as for any invasive procedure, catheter ablation does not allow trial-and-error therapy, and its success rate and the occurrence of complications are dependent on the skills of the operator. Moreover, the technique has not been standardized and differs across institutions and operators, which leaves open the search for a specific sequence of ablations leading to optimal AF termination rates. Finally, the field of low-energy pacing still lacks a reliable solution for the specific treatment of AF. Although many atrial anti-tachycardia pacing (ATP) algorithms have been developed either to prevent or terminate AF [22, 23], recent long-term clinical surveys tend to confirm that current ATP strategies fail to provide long-term benefits in AF patients with implanted pacemakers [24, 25].

Taken together, these results suggest that the quest for an optimal treatment of AF still remains an opened question, and future directions for the developments of new therapeutic strategies remain to be proposed. Regarding the diversity of suboptimal treatments available, it would be of strong interest to develop automatic diagnostic tools that could determine, based on the analysis of the AF dynamics of a specific patient, which treatment would have the most chance to succeed. Treatments themselves can also be optimized. Of course, the development of new AADs is ongoing [11, 26, 27], but the biggest surprise could also come from the field on non-pharmacological therapies. Indeed, the field of catheter-based ablation benefits from the development of new energy sources and technical equipments ensuring single and highly effective procedures [17, 28], so that ablation could slowly become a potential candidate for routine treatment of AF [29]. In this perspective, it would be of crucial interest to develop optimized sequences of ablation lines, as well as automated algorithms able to describe and track changes in the organization of AF dynamics during the ablation procedure. Eventually, the final goal would be to have a dedicated monitoring system providing patient-specific solutions for optimal ablation procedures. In the same direction, implanted pacemakers could provide a minimally invasive solution to treat AF without adverse effects. The major challenge for future research will be to design new ATP algorithms for specifically terminating AF, and thus reducing AF burden for patients with paroxysmal as well as chronic AF. On one hand, systematic studies of the response of AF dynamics to various pacing protocols still remain to be done, in order to better understand the strengths and weaknesses of current ATP algorithms and design new AF-specific protocols with better therapeutic properties. On the other hand, targeted research on the dynamical properties of spontaneous AF termination could bring fruitful information about the way AF naturally disappears; such insights may give rise to a new generation of efficient pacing algorithms. Ultimately, it would be of crucial importance to create an automatic algorithm embedded in current implantable devices, able to continuously monitor atrial activity, quickly detect and terminate AF if necessary, and therefore maintain sinus rhythm

without the need of drugs.

Collectively, the non-pharmacological approaches of ablation or low-energy pacing, as well as possible combinations of these methods with drugs (so-called *hybrid solutions*) show great promise in the field of AF therapy, and will surely require extensive engineering developments in the next decade before a reliable and efficient therapeutic solution to AF will be proposed.

## **Biophysical Modeling of Atrial Electrophysiology**

Computer modeling of biophysical phenomena has gained increasing importance in the field of physiology and biology research, particularly because improvements in computational speed now allow the simulation and analysis of very detailed and realistic biological models. Indeed, computer models for the analysis of biological systems lead to the precise description of the underlying phenomena under controlled conditions, because all the variables of interest can be observed at any temporal or spatial scales. Compared to experimental research, biophysical modeling also benefits from a perfect reproducibility of any experiment at any time.

The field of cardiac electrophysiology strongly benefits from the coupling and comparison of findings coming from clinical and experimental research on one hand, and from biophysical modeling on the other hand [30]. Specifically, computer models of AF in realistic atrial geometries can be implemented to better understand the functional and dynamical features of the arrhythmia under fully controlled conditions [31, 32, 33, 34, 35, 36]. Such models can thus be an ideal framework for the development of therapeutic strategies for AF treatment, and have already proven to be fruitful, for instance in the field of catheter-based ablation of AF [37].

## **Objectives**

The present dissertation has to be considered in the continuation of a series of research projects made by former PhD students of the Lausanne Heart Group<sup>1</sup>. During these previous contributions, a biophysical model of AF was created [38] and developed [39, 40]. Especially, a realistic geometry of the human atria derived from magnetic resonance images was developed together with models of atrial cells with relevant excitability, propagation and restitution properties [35]. Optimized numerical schemes made the use of this model possible for *in silico* simulations of cardiac arrhythmias with reasonable computational load. Subsequently, the dynamics of simulated AF could be analyzed [40, 41], and strategies of AF ablation could be explored [41].

Within this framework, the major goal of the present dissertation is to further develop therapeutic strategies for AF using both the aforementioned biophysical model and real clinical signals. The main objectives are:

- to investigate the dynamical processes underlying the phenomenon of AF spontaneous termination in the biophysical model,

---

1. <http://lausanneheart.epfl.ch/>

- to provide a detailed analysis of the effect of rapid pacing on simulated AF dynamics, and determine its ability to control atrial activity,
- to propose innovative pacing schemes dedicated to the automatic termination of AF, and assess their performance in the biophysical model,
- to develop new signal processing methods measuring the level of organization of AF electrical activity, in order to provide potential diagnostic tools that could better discriminate between different types of AF and subsequently propose appropriate treatments.

This work has been realized in the framework of a collaboration between Medtronic Europe and the Applied Signal Processing Group<sup>2</sup> of the Swiss Federal Institute of Technology. This collaboration between industry and academic research, supported by the Commission for Innovative Technology and the Theo-Rossi-Di-Montelera Foundation, is an ideal opportunity for fruitful interactions between complementary entities. The ultimate goal of this thesis is to provide concrete diagnostic schemes and therapeutic tools, promoting industrial implementation for future clinical use. Hopefully, such contribution could help bridge gaps between academic research, biomedical industry and clinics.

## 1.2 Organization of the Dissertation

The dissertation is divided into two parts:

- I. **Modeling of Atrial Fibrillation Dynamics:** the first part is devoted to the presentation of a biophysical model of human atria, and its applications to the simulation of cardiac arrhythmias. In chapter 2, the electrophysiological and numerical properties of the biophysical model used throughout this work are reviewed. In chapter 3, the ability of the model to simulate atrial fibrillation is described. Using this framework, a model-based study of the phenomenon of spontaneous termination of AF is presented in chapter 4.
- II. **Therapeutic Strategies for Atrial Fibrillation:** in the second part, low-energy pacing approaches to treat AF are analyzed and improved, and diagnostic tools are proposed. In chapter 5, a detailed study of the properties of rapid pacing during AF is presented. In particular, the effect of both pacing parameters and atrial tissue properties on the ability to control electrical activity through rapid pacing is studied. Based on these results, a novel pacing protocol for the termination of AF is presented and tested in the biophysical model (chapter 6). In chapter 7, measures of AF organization based on multivariate spectral analysis are presented and used as a diagnostic tool to automatically characterize the type of a newly discovered AF, and thereby improve patient management and therapeutic decisions.

Finally, a summary of the whole project as well as possible future directions of research are given as conclusion in chapter 8.

---

2. <http://aspg.epfl.ch/>

### 1.3 Original Contributions

The main contributions<sup>1</sup> of this work are:

- Advances in fundamental research and therapeutic testing for atrial fibrillation using a biophysical model of human atria.
  - A dynamical study of the phenomenon of AF spontaneous termination comparing different models of AF dynamics, and relating mechanisms to existing literature.
  - A systematic study of the effect of pacing parameters and atrial tissue properties on AF capture during rapid pacing.
  - The development and testing of a multi-stage pacing scheme dedicated to the automatic termination of AF.
- Advances in signal processing techniques for the non-invasive analysis of atrial fibrillation.
  - Development of organization measures based on multivariate spectral analysis to assess the spatiotemporal organization of AF based on the spectral information of multiple surface ECG electrodes.
  - Automatic classification of persistent and permanent AF signals to improve current patient management.

---

1. See also the list of patents and publications at the end of the text.

## Part I

---

# **Biophysical Modeling of Atrial Fibrillation Dynamics**

The first part of the dissertation is devoted to the presentation of the modeling approach used to study the dynamical properties of atrial fibrillation. In chapter 2, a brief review of the biophysical model of human atria used in this project is proposed, including basic concepts and mathematical formulations. The third chapter shows the ability of the model to simulate realistic atrial fibrillation dynamics. As an application, a study of the dynamics of spontaneous termination in atrial fibrillation is presented in chapter 4.



# Biophysical Modeling of the Human Atria

---

# 2

## 2.1 Introduction

The mechanisms underlying cardiac arrhythmias are highly complex, and far from being understood. Since a more precise description of these mechanisms is needed to target efficient therapeutic solutions, physicians and researchers have made extensive efforts to tackle this problem with different approaches. On one hand, animal models have been largely used in a successful way to uncover various electrophysiological mechanisms of cardiac arrhythmias. However, the results obtained using these models can not be directly translated to human patients, since it is not sure that the nature of the arrhythmias under study are similar in animals and in humans. Moreover, repeatability issues as well as ethical concerns make the use of animal experiments sometimes relatively difficult. In parallel, complementary approaches based on the biophysical modeling of cardiac activity was developed as early as in the 1960's to offer new insights into cardiac processes [42]. The dramatic increase of computer power over the last decade as well as fruitful collaborations between physicians and engineers accelerated the development of such approaches in an exponential way, leading to precise computerized models of cardiac activity, in turn opening the way to *in silico* experiments for investigating pathophysiological processes under controlled conditions.

A model of cardiac electrophysiology is usually performed following a bottom-up approach. First, channel gating kinetics must be modeled at the molecular level. Then, ionic currents, pumps, and ion exchangers can be integrated in a model of cell membrane. The sum of the contributions of each ionic current and its effect on ionic concentration provide a model of the cardiac cell. Furthermore, cells can be coupled to form a tissue, and eventually a model of the whole organ through the reproduction of the desired anatomy. Finally, measurement of stimulation devices such as electrodes are also simulated, in order to give clinicians the opportunity to observe and analyze the processes produced by the model in a realistic way. Today's computer models incorporate all these features, and allow the simulation of realistic cardiac arrhythmias as well as the

evaluation of potential therapies. Among them, several models have been developed to specifically describe the atrial myocardial cell. The first models of atria were based on measurements in rabbit [43, 44], but models extended to describe the human atrial cell were proposed later [31, 32, 33, 34, 45]. Specific configurations of the Courtemanche model described in [45] were then proposed in order to account for structural or electrical remodeling [46, 47], offering the framework needed to investigate the underlying mechanisms of atrial arrhythmias and their corresponding potential therapies [48].

In this chapter, the biophysical model of human atria that was created and developed in the Lausanne Heart Group [35, 38, 39, 40, 41] is briefly reviewed, following the bottom-up approach that was used to create it. First, the cellular properties of the model are presented in the light of some general physiological concepts. Then, the integration of this cellular description into a tissue model is exposed. Finally, the construction of a realistic geometry of human atria is presented. Further details on the spatial and temporal discretization schemes that were used to implement the model numerically can be found in previous works [39, 40].

## 2.2 Modeling the cardiac cell

### 2.2.1 Properties of the cardiac cell

The cardiac tissue can be thought of as a dense array of cells arranged into bundles. Each cardiac cell is typically 30-100  $\mu\text{m}$  long and 8-20  $\mu\text{m}$  wide [49], with a *plasma membrane* defining its boundary, and maintaining the characteristic differences between the intracellular and extracellular environments. The cell membrane is a thin film of lipid and protein molecules held together by non-covalent interactions [50]. The lipid molecules are arranged as a continuous double layer about 5 nm thick. Protein molecules embedded in this *lipid bilayer* form channels allowing specific ions to cross the membrane either through passive or active transport<sup>1</sup>. The *transmembrane potential*  $V_m$  is defined by the difference in voltage between the interior and exterior of a cell ( $V_{\text{interior}} - V_{\text{exterior}}$ ). In cardiac cells, the major ions contributing to the net value of  $V_m$  are the  $\text{Na}^+$ ,  $\text{K}^+$  and  $\text{Ca}^{2+}$  ions. At steady-state equilibrium, the transmembrane potential  $V_m$  is approximately maintained at  $-80$  mV.

Cardiac cells have the property to be *excitable*. As long as the transmembrane potential stays under a critical value called the *threshold potential*, no specific response of the cell membrane is elicited (*subthreshold response*). But when the transmembrane potential reaches the threshold potential, for instance due to a sufficiently strong external stimulation, an *action potential* is automatically triggered by voltage-gated cation channels. During such *superthreshold stimulation*, the typical time-course of the induced action potential is shown in Figure 2.1, and consists of 5 phases [51, 52]. In a first step (phase 0), a rapid depolarization (action potential upstroke) due to a large inward  $\text{Na}^+$

1. During *passive transport*, specific ions diffuse rapidly down their electrochemical gradients across the lipid bilayer, whereas during *active transport*, carrier proteins actively pump ions across the membrane against their electrochemical gradient.



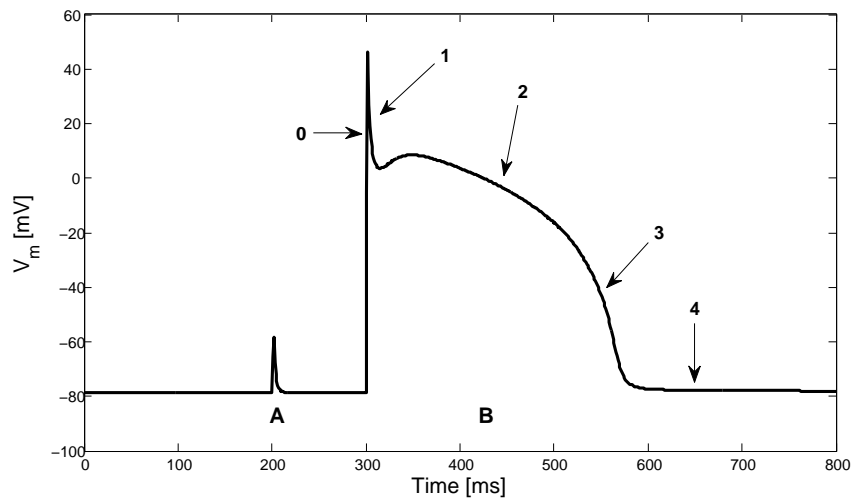


**Figure 2.1:** Electrical response of a cardiac cell simulated with a Luo-Rudy membrane kinetics model. (A) Subthreshold stimulation. (B) Suprathreshold stimulation. The different phases of the action potential are numbered from 0 to 4 and are explained in the text.

current ( $I_{Na}$ ) shifts the cell potential from its resting value to about +40-50 mV within a fraction of a millisecond. Then, an early repolarization takes place (phase 1), where transient outward  $K^+$  currents ( $I_{to}$ ) cause the cell to briefly repolarize. During phase 2, the cell repolarizes slowly, giving rise to a relatively flat portion of the action potential, called the plateau, and maintained by an inward  $Ca^{2+}$  current ( $I_{si}$ ). Finally, during the late repolarization phase (phase 3), a series of  $K^+$  currents ( $I_K$ ) called *delayed rectifiers* ( $I_{Kur}$ ,  $I_{Kr}$ ,  $I_{Ks}$ ,  $I_{K1}$ ) lead to cellular repolarization, and thus bring the potential back to the resting value (phase 4).

A characteristic feature of excitable cells is that once they get depolarized, they cannot generate supplementary action potentials during an interval of time called the *effective refractory period* (ERP). This intrinsic parameter of cardiac tissue is crucial for the occurrence of arrhythmia [52]. Estimation of ERP requires sequences of repeated stimulations of the cell tissue with various timings until the excitability threshold can be found. This protocol is not well adapted to computer simulation settings, so a measure of the *action potential duration* (APD) is used instead [53, 54]. As shown in Figure 2.2(A), the APD is usually measured between the onset of the action potential upstroke and the point at which the cell repolarizes to a certain fraction of the maximum reached [49]. For instance, a commonly used measurement is the  $APD_{90}$  representing the APD at 90% repolarization. By definition, the APD depends on the preceding *diastolic interval* (DI), defined as the time interval between the end of the last action potential and the onset of the next one. The dependent behavior of APD values for various DI is described by the corresponding *restitution curve* (Figure 2.2(B)). This curve has been shown to be a crucial indicator of the susceptibility of the cardiac tissue to initiate and perpetuate arrhythmias [55, 56]. Similarly, the *conduction velocity* (CV) of wavefronts and the ERP are modulated by the preceding DI, and possess their respective restitution curves.

Finally, the *cycle length* (CL) is the sum of APD and DI, which is the total time elapsed between two successive action potential upstrokes.

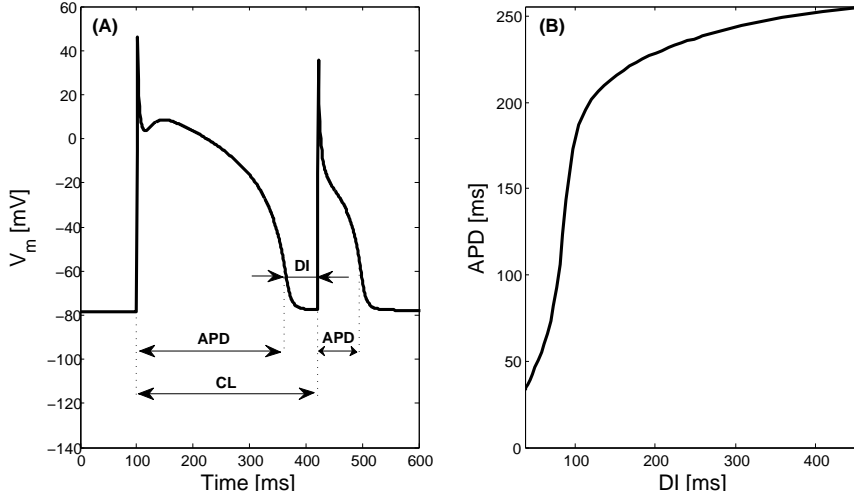


**Figure 2.2:** Definition of action potential parameters and restitution properties for the Luo-Rudy membrane kinetics model. (A) Action potential duration (APD), diastolic interval (DI) and cycle length (CL). (B) Restitution curve computed on a 1D cable.

## 2.2.2 Modeling the cardiac cell membrane

Most of the available models of cardiac cell membrane were derived based on the mathematical formulation first introduced by Hodgkin and Huxley [57] for neuronal cells and then applied to cardiac ventricular cells [58, 59, 60, 61]. In this mathematical description, the cell membrane, consisting of a dielectric lipid bilayer, acts as a transmembrane capacitor denoted by  $C_m$ , and the membrane potential  $V_m$  varies according to the following evolution equation:

$$I_m = C_m \frac{dV_m}{dt} + I_{\text{ion}} - I_{\text{stim}} \quad (2.1)$$

$$V_m = \Phi_i - \Phi_e \quad (2.2)$$

where  $I_m$  is the total transmembrane current,  $I_{\text{ion}}$  is the sum of the ion currents,  $I_{\text{stim}}$  is an external stimulation current possibly used to trigger an action potential, and  $\Phi_i$  and  $\Phi_e$  are the intracellular and extracellular potentials, respectively. Each of the individual currents  $I_k$  contributing to the total ionic current  $I_{\text{ion}}$  can be put in the following form:

$$I_k = \bar{g}_k y (V_m - E_k). \quad (2.3)$$

$I_k$  represents the current associated with the ion of type  $k$ ,  $\bar{g}_k$  is the maximum conductance of the related ion channels, and  $y$  is a *gating variable* ( $0 \leq y \leq 1$ ) indicating the

state (open when  $y = 0$  and closed when  $y = 1$ ) of the ionic channels.  $E_k$  stands for the potential of the Nernst equation [50] of an ion of type  $k$  given by:

$$E_k = \frac{RT}{zF} \cdot \ln \left( \frac{[k]_e}{[k]_i} \right) \quad (2.4)$$

where  $R$  is the universal gas constant,  $T$  is the absolute temperature,  $z$  is the valence of ion  $k$ ,  $F$  is the Faraday constant, and  $[k]_i$  and  $[k]_e$  are the intracellular and extracellular ion concentrations, respectively. Thus, each individual ionic current  $I_k$  in (2.3) has its own *gating kinetics*, which describes the transition of the gate  $y$  between the open ( $O$ ) and the closed ( $C$ ) state. Let  $\alpha_y$  (resp.  $\beta_y$ ) be the forward (resp. backward) rate of the reaction  $C \rightleftharpoons O$ . The fraction  $y(t)$  of open gates at time  $t$  is then governed by the equation

$$\frac{dy}{dt} = \alpha_y(1 - y) - \beta_y y. \quad (2.5)$$

In the next subsections, two membrane kinetics models that were widely used throughout the presented research projects are described more specifically.

### The Luo-Rudy Membrane Kinetics Model

The Luo-Rudy membrane kinetics model was originally dedicated to the modeling of cardiac ventricular cells [60, 61]. In its first version [60], called the Luo-Rudy I (LRI) model, the total ionic current  $I_{\text{ion}}$  is the sum of six individual currents involving six gating variables and the intracellular calcium concentration (see also Figure 2.3):

$$I_{\text{ion}} = I_{\text{Na}} + I_{\text{si}} + I_{\text{K}} + I_{\text{K1}} + I_{\text{Kp}} + I_{\text{b}}. \quad (2.6)$$

Each individual ionic current is characterized by its own gating kinetics equation of the form (2.5). In Table 2.1, the main characteristics of each current are documented. The LRI model is a *passive* model, because the ion concentration inside the cell remains unchanged; a dynamic version called LRII model was later proposed, which included a dynamic regulation of the intracellular ionic balance for sodium and potassium [61].

In this work, the LR1 model was largely used to simulate atrial arrhythmias for several reasons. First, this model has a reduced set of variables, making the computational load more tractable, especially when a large number of simulations is needed for systematic test studies. In addition, the original LR1 model could be modified in order to mimic atrial membranes by adjusting some ionic conductance properties [55, 62]. This "atrialized" LR1 model was further developed to mimic electrical remodeling as observed in permanent AF, such as shortening of action potential duration (APD) [56].

### The Courtemanche-Ramirez-Nattel Membrane Kinetics Model

The Courtemanche et al. membrane kinetics model (CRN) can be considered as a refinement of the LRII model, and was derived using specific formulations of ionic currents based on direct measurements in human atrial myocytes [45]. It is therefore

Symbol	Current	Direction
<i>Sodium channel</i>		
$I_{Na}$	fast inward $Na^+$ current	E $\rightarrow$ I
<i>Calcium channel</i>		
$I_{si}$	slow inward current	E $\rightarrow$ I
<i>Potassium channels</i>		
$I_K$	time-dependent outward $K^+$ current	I $\rightarrow$ E
$I_{Kp}$	time-independent outward plateau $K^+$ current	I $\rightarrow$ E
$I_b$	time-independent outward background $K^+$ current	I $\rightarrow$ E
$I_{K1}$	time-independent outward $K^+$ current	I $\rightarrow$ E

**Table 2.1:** Ionic currents of the Luo-Rudy membrane kinetics model. In the column "Direction", E stands for extracellular space and I for intracellular space.

one of the first model of the human atrial cell. The model includes the dynamics of intracellular currents of the *sarcoplasmic reticulum*<sup>1</sup> (SR). According to the CRN model, the total current  $I_{ion}$  of the modeled cell membrane is the sum of 12 individual ionic currents as follows (see also Figure 2.4):

$$I_{ion} = I_{Na} + I_{Na,b} + I_{Ca,L} + I_{Ca,b} + I_{p,Ca} + I_{to} + I_{Kur} + I_{Kr} + I_{Ks} + I_{K1} + I_{Na/K} + I_{Na/Ca}. \quad (2.7)$$

Table 2.2 summarizes the main properties of the membrane currents of the model, including those involved in the dynamics of intracellular currents. More details about the functions of each individual current can be found in [45]. The underlying gate kinetics of each ionic current is governed by differential equations of the form (2.5). The Courtemanche et al. model became very popular for the simulation of cardiac arrhythmias, because several studies proposed specific modifications of parameters to reproduce

1. The sarcoplasmic reticulum is a network of tubules and sacs in skeletal muscle fibers. It plays an important role in muscle contraction and relaxation by releasing and storing calcium ions.

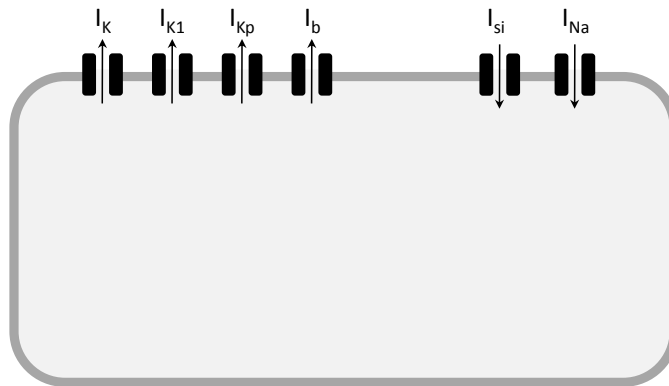


**Figure 2.3:** Schematic representation of the Luo-Rudy membrane kinetics model. The Luo-Rudy model includes six membrane currents listed in Table 2.1.

structural or electrical remodeling, which are crucial substrate alterations in order to be able to simulate arrhythmias [46, 47].

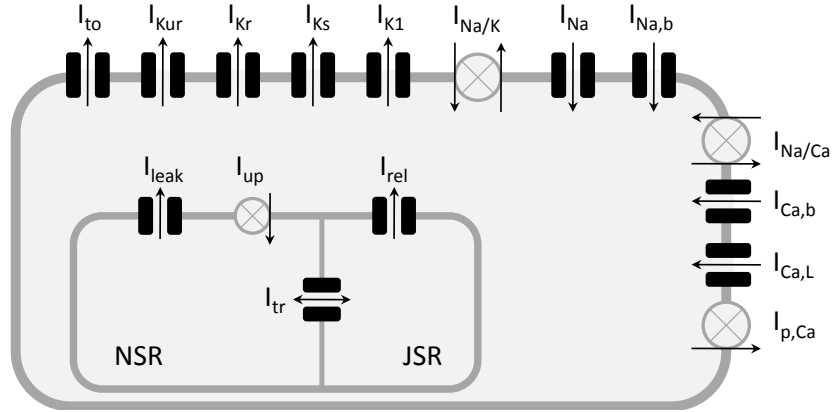


**Figure 2.4:** Schematic representation of the Courtemanche et al. human atrial model. The different membrane currents of the model are listed in Table 2.2. In addition, the model includes a model of sarcoplasmic reticulum (SR) subdivided into the network SR (NSR) and the junctional SR (JSR). Circles represent active pumps and exchangers.

## 2.3 Modeling cardiac tissue

At the tissue level, equations of electrical propagations have to be derived in order to model the propagation of electrical impulses on a piece of cardiac tissue. In this section, both bidomain and monodomain approaches are presented.

### 2.3.1 The Bidomain Model

In the bidomain theory [49, 63], the propagation equations are expressed in a continuous model of excitable tissue composed of an intracellular and an extracellular medium. The evolution equations are derived from the law of conservation of charge. Moreover, one has to take into account boundary conditions. The complete system of a bidomain model is represented by the following reaction-diffusion equations:

$$S_v^{-1} \nabla \cdot \sigma_i \nabla \phi_i = C_m \frac{\partial V_m}{\partial t} + I_{ion} \quad (2.8)$$

$$\nabla \cdot (\sigma_i \nabla \phi_i + \sigma_e \nabla \phi_e) = 0 \quad (2.9)$$

where  $V_m = \Phi_i - \Phi_e$ , with  $\Phi_i$  and  $\Phi_e$  the intracellular and extracellular potentials,  $S_v$  is the cell surface-to-volume ratio, and  $\sigma_i$  and  $\sigma_e$  are the intracellular and extracellular conductivity tensors summarizing gap junction resistivities, and reflecting electrical properties that are spatially averaged over several cardiac cells. It is assumed that there is

Symbol	Current	Direction
<i>Sodium channels</i>		
$I_{Na}$	fast inward $Na^+$ current	E $\rightarrow$ I
$I_{Na,b}$	background $Na^+$ current	E $\rightarrow$ I
<i>Calcium channel</i>		
$I_{Ca,L}$	L-type inward $Ca^{2+}$ current	E $\rightarrow$ I
$I_{Ca,b}$	background $Ca^{2+}$ current	E $\rightarrow$ I
<i>Potassium channels</i>		
$I_{to}$	transient outward $K^+$ current	I $\rightarrow$ E
$I_{Kur}$	ultra-rapid delayed rectifier $K^+$ current	I $\rightarrow$ E
$I_{Kr}$	rapid delayed rectifier $K^+$ current	I $\rightarrow$ E
$I_{Ks}$	slow delayed rectifier $K^+$ current	I $\rightarrow$ E
$I_{K1}$	inward rectifier $K^+$ current	E $\rightarrow$ I
<i>Pumps</i>		
$I_{Na/K}$	$Na^+$ - $K^+$ pump current	I $\rightarrow$ E
$I_{p,Ca}$	sarcolemmal $Ca^{2+}$ pump current	I $\rightarrow$ E
<i>Ion exchanger</i>		
$I_{Na/Ca}$	$Na^+$ - $Ca^{2+}$ exchanger current	E $\rightarrow$ I
<i>Sarcoplasmic reticulum fluxes</i>		
$I_{leak}$	$Ca^{2+}$ leak current	NSR $\rightarrow$ I
$I_{up}$	$Ca^{2+}$ uptake current	I $\rightarrow$ NSR
$I_{rel}$	$Ca^{2+}$ transfer current	NSR $\rightarrow$ JSR
$I_{tr}$	$Ca^{2+}$ release current	JSR $\rightarrow$ I

**Table 2.2:** Ionic currents of the Courtemanche et al. model. In the column "Direction", E stands for extracellular space, I for intracellular space, NSR for network sarcoplasmic reticulum and JSR for junctional sarcoplasmic reticulum.

no current flow between the intracellular and extracellular domain through gap junctions. This can be expressed as the following von Neumann boundary conditions:

$$\mathbf{n}^T \cdot \sigma_i \nabla \phi_i = 0 \quad (2.10)$$

where  $\mathbf{n}$  is a unit vector perpendicular to the tissue interface. On the exterior boundary of the surrounding bath, which could for instance correspond to the body surface, a no-flux boundary condition is also assumed:

$$\mathbf{n}^T \cdot \sigma_e \nabla \phi_e = 0 \quad (2.11)$$

Moreover, the extracellular domain, in the absence of any source current, is governed by the following equation:

$$\nabla \cdot \sigma_e \nabla \phi_e = 0 \quad (2.12)$$

It has to be noted that other boundary conditions may be imposed [49, 64], depending on the targeted application. For instance, during defibrillation modeling, the electrodes used for the defibrillation must be considered.

### 2.3.2 The Monodomain Model

The *monodomain approximation* consists in a simplification of the bidomain problem, in that only one medium is considered for the resolution of the propagation equation [49]. While the numerical resolution of the bidomain equations involve complex computations [65, 66], the monodomain approach provides a significant reduction of computational load. A monodomain model can be built in several ways. A first approach consist in starting from the following assumptions [39]:

- the tissue is thin and lies in an extensive bath,
- the extracellular potential variations are sufficiently small, so that the intracellular potential variations are approximately equal to the transmembrane potential variations,
- the effect of the extracellular potential on the transmembrane current sources is small, so the bidomain equations can be decoupled.

Under these assumptions, a cardiac tissue can be modeled by the monodomain propagation equation below:

$$S_v^{-1} \nabla \cdot \boldsymbol{\sigma} \nabla V_m = C_m \frac{\partial V_m}{\partial t} + I_{\text{ion}} - I_{\text{stim}} \quad (2.13)$$

where the conductivity tensor  $\boldsymbol{\sigma}$  is equal to  $\boldsymbol{\sigma}_i$ . The related boundary condition reads:

$$\mathbf{n}^T \cdot \boldsymbol{\sigma} \nabla V_m = 0. \quad (2.14)$$

Another way to conceive a monodomain model is to consider that the anisotropy ratios of the intracellular and extracellular domain are equal,  $\boldsymbol{\sigma}_e(\mathbf{x}) = \kappa \boldsymbol{\sigma}_i(\mathbf{x})$ , where  $\kappa$  is a constant [67]. Under this assumption, the bidomain equations (2.8) and (2.9) can be decoupled, so that only one medium has to be considered [49], and equations (2.13) and (2.14) still hold, with  $\boldsymbol{\sigma}^{-1} = \boldsymbol{\sigma}_i^{-1} + \boldsymbol{\sigma}_e^{-1}$ . A particular case is to consider an isotropic homogeneous conductivity tensor

$$\boldsymbol{\sigma} = \rho^{-1} \mathbb{I} \quad (2.15)$$

where  $\mathbb{I}$  is the identity matrix and  $\rho$  is the scalar resistivity. In this case, the passive resistivity can be used to determine the CV, according to the approximate power law  $\rho \propto CV^{-2}$  [68]. In a more general framework, anisotropic conduction can be simulated by modifying the conductivity tensor  $\boldsymbol{\sigma}$  [40].

### 2.3.3 Simulated Electrograms

In clinical settings, transmembrane potentials are only rarely accessible for the practitioners, and cardiologists are rather used to deal with less invasive cardiac signal recordings, such as *electrogram signals*<sup>1</sup> (EGM) or *electrocardiogram signals*<sup>2</sup> (ECG). As a

1. A cardiac electrogram is a recording of the heart's activity as measured directly on the surface of the myocardium.

2. An electrocardiogram is a graphic signal representing the global electrical activity of the heart as measured by skin electrodes placed on the thorax.

consequence, it is necessary to include simulated EGMs and ECGs as measured by virtual electrodes in any model aiming at providing valuable information to clinicians.

A virtual *unipolar electrode* can be modeled as a point measurement of the (extracellular) electric potential. Such virtual electrodes are ideal, since they do not alter the tissue or the geometry of the model. As a convention, the reference electrode (zero potential) is located at infinity. The distance of the electrode to the tissue surface determines the spatial extent of the area of cardiac tissue the electrode considers for averaging. Unipolar EGMs are simulated through the computation of the extracellular potential  $\Phi_e$ , which can be obtained using a current source approximation for a large volume conductor [35, 69]:

$$\Phi_e(\mathbf{x}, t) = \frac{1}{4\pi\sigma} \int_{\Omega_{\text{epi}}} d\mathbf{y} \delta \frac{S_v I_m(\mathbf{y}, t)}{\|\mathbf{x} - \mathbf{y}\|}, \quad (2.16)$$

where  $\Omega_{\text{epi}}$  is the epicardial surface,  $d\mathbf{y}$  is an infinitesimal surface element,  $\delta$  is the thickness of the tissue,  $\sigma$  is the surrounding bath conductivity,  $I_m$  is the current source per unit area of membrane surface, and  $S_v$  is the cell surface-to-volume ratio. As a supplementary step, this formula can be extended to take into account the finite size of the torso as well as its inhomogeneity (lung, blood cavity) in order to provide simulated ECGs [70, 71].

## 2.4 Atrial Geometry

The propagation equations presented in the previous section have to be defined on a specified tissue geometry. In this section, we briefly present the monolayer 3D surface atrial geometry that was used in this work. It should be mentioned that multilayer versions of the presented atrial geometry were also developed, as well as geometries with additional anatomical details [40]. Although these geometries are slightly more realistic than the one presented below, they were not appropriate for the studies conducted in this thesis, in which massive amounts of simulations were performed to systematically test potential AF therapies. Thus, for obvious computational reasons, the monolayer 3D surface geometry was used exclusively and is described below.

### 2.4.1 Monolayer 3D Surface

Nowadays, the majority of the biophysical models are based on real medical imaging, such as magnetic resonance imaging (MRI). Below, the different processing steps that were needed to create the biophysical model of human atria used in the Lausanne Heart Group are enumerated:

- **Data acquisition:** An MRI acquisition was first performed on a normal human subject <sup>1</sup>.

---

1. The raw data was kindly provided by Ryan Lahm, Dr. Josée Morissette and Dr. Arthur Stillman (Medtronic Inc.). The segmentation was also done by the same group.



- **Segmentation:** The epicardial surface of the atria was semi-automatically segmented slice-by-slice, so that a 3D reconstruction of the atrial structure could be performed, resulting in a coarse triangular mesh. At this point, the original mesh could not be directly used for partial differential equation solving, because of important geometrical problems [38]. Indeed, appendages as well as several valves were poorly segmented, and the definition of the septal wall was unclear.
- **Surface design:** In order to solve these problems, the surface was smoothed and parametrized using 3D splines by means of the software Ideas<sup>®</sup> (SRDC Inc.). The sizes of the appendages, veins and valves were corrected to better correspond to published values [72]. Finally, a septal wall was created [38].
- **Meshing:** From this parametrized surface, several triangular meshes with different spatial resolutions were generated [40]. Among them, two meshes were extensively used in the present work: the first mesh contains 50'000 nodes for a spatial resolution of  $\Delta x = 0.6$  mm, and the second contains 100'000 nodes for a spatial resolution of  $\Delta x = 0.4$  mm.

The resulting geometry is a monolayer 3D-surface shown in Figure 2.5 that includes most of the important anatomical features of the human atria: mitral valve (MV), tricuspid valve (TV), left/right superior pulmonary vein (LSPV/RSPV), left/right inferior pulmonary vein (LIPV/RIPV), inferior/superior vena cava (IVC/SVC) and coronary sinus (CS). Indeed, the geometry comprises both atrial chambers, and openings corresponding to the location of veins and valves. The septum wall has a non-conducting hole representing the fossa ovalis. The total excitable area of the right atrium (resp. left atrium) is 84 cm<sup>2</sup> (resp. 72 cm<sup>2</sup>). The dimensions of the other anatomical features of the geometry are detailed in Table 2.3.

Right atrium	total RA	SVC	IVC	TV	CS	
	84.20	2.84	3.14	4.29	0.54	
Left atrium	total LA	LSPV	RSPV	LIPV	RIPV	MV
	72.10	1.07	1.02	0.89	1.08	4.57
Septum	total septum					
	4.36					

**Table 2.3:** Dimensions of the atrial geometry. RA/LA stand for right atrium/left atrium. Values are indicated in cm<sup>2</sup>.

## 2.5 Conclusion

In this chapter, the biophysical model of human atria that was developed in the Lausanne Heart Group over almost two decades has been briefly reviewed. The bottom-up approach used to create the model was followed step by step, starting from the molecular level with the presentation of cell membrane kinetics, to the organ level and the creation of a realistic anatomy of human atria. Throughout this dissertation, the 3D monolayer surface version of the model was preferred to a multilayer one. This choice is inherent to

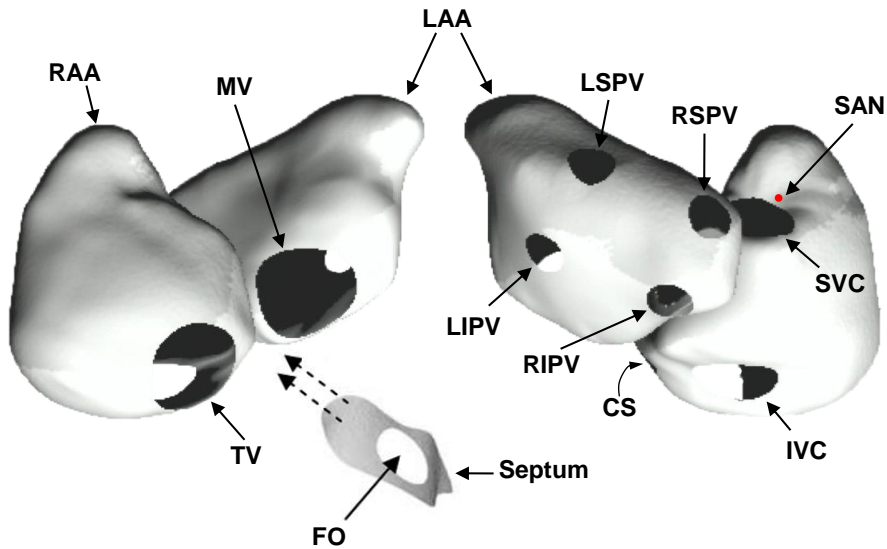


**Figure 2.5:** Geometry of a model of human atria based on MR images: anterior view (on the left) and posterior view (on the right). The left/right atrium appendages are indicated by LAA/RAA. The major anatomical obstacles are also indicated: mitral valve (MV), tricuspid valve (TV), left/right superior pulmonary vein (LSPV/RSPV), left/right inferior pulmonary vein (LIPV/RIPV), inferior/superior vena cava (IVC/SVC) and coronary sinus (CS). A cut of the septum is also shown with its fossa ovalis (FO). The location of the sino-atrial node (SAN) is represented as a red dot.

the trade-off between model accuracy and computational load needed to perform large scale evaluations such as the ones presented in the next chapters.

Two different membrane kinetics models (the Luo-Rudy I and the Courtemanche et al. models) were successively described, because both are used in the studies presented in the next chapters. The interest of using these models is that they present very different simulated AF dynamics: while the Courtemanche et al. model gives rise to a fibrillating activity of relatively low complexity, the Luo-Rudy model can generate highly complex simulated AF patterns. These variations in AF complexity was also observed in clinical and experimental settings [73, 74], and comparisons could be made between different AF dynamics by using both models (see chapter 3 and 4).

# Simulating Atrial Fibrillation

# 3

---

## 3.1 Introduction

The quality of a biophysical model is mostly determined by its ability to reproduce a physiological phenomenon with satisfying reliability and to suggest innovative hypotheses based on its output. Although models can be made very complex to exactly mimic reality, the real challenge is to create a simple model with the lowest possible number of parameters, and still be able to conduct relevant analyzes and make predictions about the underlying phenomena [75]. Thus, the real strength of a biophysical model lies in its simplicity, and not in its complexity. With this philosophy in mind, the biophysical model of the Lausanne Heart Group was designed in such a way that realistic AF could be simulated with a small number of parameters and a relatively simple anatomy. Thanks to this simplicity, the model could be used to run systematic analyzes involving a very large number of simulations in a reasonable time.

The major goal of this dissertation is to use computer modeling and signal analysis for the study of AF and its related therapies. In order to achieve such investigations, simulated AF (SAF) must be first artificially induced in the model, so that the modeled atria keep fibrillating in a stable and realistic way. Once this situation is reached, subsequent analyses and therapeutic testing can be performed. In this chapter, the ability of the biophysical model used in this dissertation to simulate cardiac arrhythmias is demonstrated. First, the model is used to simulate normal sinus rhythm. Then, the simulation of different dynamics of SAF are presented using two different membrane kinetics models. It should be mentioned that the simulation of atrial flutter<sup>1</sup> (AFL) is not presented here, since it was not the object of the studies presented in this dissertation. Nevertheless, atrial flutter was also successfully simulated by the model in a previous study [41].

---

1. Atrial flutter is an abnormality of the heart rhythm, resulting in a rapid and sometimes irregular heartbeat. It often degenerates into atrial fibrillation.

## 3.2 Simulating Sinus Rhythm

The normal sinus rhythm originates from the sinoatrial node (SAN), which is a cluster of pacemaker cells located in the posterior right atrium that fire spontaneously approximately every second [76]. Each depolarization wave triggered by the SAN spreads uniformly from the right to the left atrium down to the atrio-ventricular node (AVN) via the interatrial septum area, and then triggers ventricular contraction. In Figure 3.1, the typical pattern of activation time for normal sinus rhythm as simulated by the atrial model is displayed, together with its corresponding isochrones. The total duration of a normal sinus propagation is about 110 ms. Atrial activation propagates from the right to the left side and terminates in the left lateral wall, where wavefronts coming from both sides of the left atrium converge. It is worth mentioning that this activation pattern is comparable to experimental findings [77] or to other anatomical models [32], although several anatomical structures such as Bachman’s bundle or crista terminalis have not been included in the geometry.

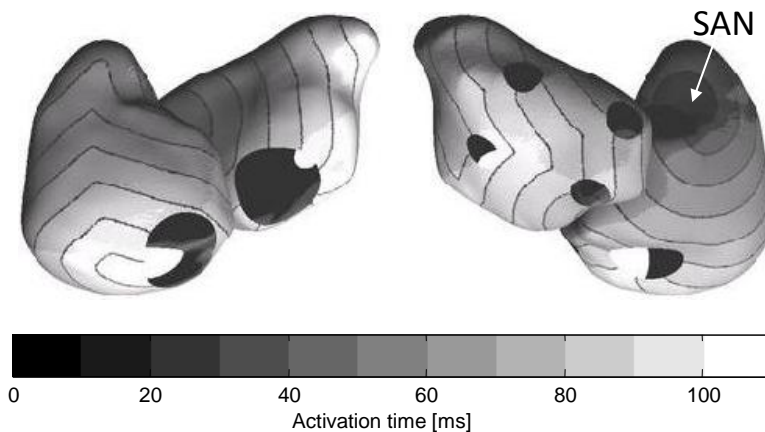


**Figure 3.1:** Activation map and isochrones during normal sinus rhythm initiated from the sinoatrial node (SAN). Isochrones are indicated every 10 ms. (Reprinted with permission from Dr. V. Jacquemet)

## 3.3 Simulating Atrial Fibrillation

### 3.3.1 The Polymorphic Beast

Atrial fibrillation was first described specifically at the end of the 19<sup>th</sup> century [78], although many observations of the phenomenon were made before without clear understanding of the underlying disease [79, 80]. In 1906, the first electrocardiographic recordings of AF were performed [81], and led quickly to a definitive identification of the arrhythmia and its self-sustained nature [82]. Quickly, discussions about the mechanistic nature of atrial fibrillation became a subject of intense debate. Very early, two

opposed hypotheses were proposed to describe the basic mechanism accounting for AF perpetuation [80]. On one hand, AF was thought to be created and maintained by the rapid spiking of a single focus [83]. Another theory called "circus movement" stated that multiple rotating electrical waves could perpetuate atrial fibrillation in a self-sustained manner [84]. The latter theory progressively prevailed as the dominant explanation of the mechanism of AF, and was further supported by pioneering computer studies [42]. In this modeling work, the so-called "multiple wavelet" model was first introduced, with multiple independent wavelets maintaining fibrillation. Moreover, electrophysiological experiments demonstrated the crucial role of the wavelength of rotating waves for this multiple reentry model [85, 86].

This classical view of AF mechanisms was soon challenged in the beginning of the 21<sup>st</sup> century by new theories built on experimental findings [52]. Indeed, mapping studies suggested that AF could either be created and sustained by the automatic discharge of ectopic foci in specific areas of the atria [87], or alternatively by one or a small number of stable and self-sustained high frequency rotors [88]. Which of these three theories is the most probable description of AF mechanisms remains a matter of debate [89]; it is often suggested that different stages of the disease could be better represented by one or another of the above theories. In this context, it is of major importance to be able to generate different types of AF dynamics with a biophysical model in order to take into account all the proposed dynamical frameworks mentioned in this section. For this reason, several models of AF have been developed by the Lausanne Heart Group. In this dissertation, two models presented below are used, namely a model of recent chronic AF that could be linked to the multiple wavelet model, and a model of paroxysmal AF based on meandering wavelets. Nevertheless, it should be noted that other AF types were also implemented in the model for specific studies, such as a model of ectopic foci [90] or models of cholinergic AF as well as AF with refractoriness heterogeneity [91].

### 3.3.2 Initiation and Perpetuation of Atrial Fibrillation

In order to study AF dynamics in the biophysical model, SAF must be first induced in the model by means of a direct intervention aiming at creating a substrate for arrhythmogenesis. In animal models, this procedure can be achieved by the application of a drug or chronic pacing. Several clinical pacing protocols known to lead to AF induction can be mentioned:

- Burst-pacing protocol [92]: during this protocol, a single atrial site is paced at a periodic fixed frequency of 20-50 Hz during a few seconds until atrial fibrillation is induced.
- Ramp protocol [93]: during ramp pacing, a sequence of stimuli is delivered with a progressively decrementing time interval between two subsequent pulses. The ramp is designed such that AF is triggered by the successive pulses at a given point.
- Programmed stimulation protocol ( $S_1 - S_2 - S_3$ ) [94, 95]: these pacing schemes are a little bit more complex, and involve three different pacing sites. Each site is stimulated with a different timing that must be specified, and the interactions

between the created wavefronts trigger the arrhythmia.

In this dissertation, initiation of SAF was performed either by means of a 20 Hz burst-pacing protocol applied during 3 seconds on the sinoatrial node for the recent chronic AF model, or by a ramp pacing protocol for the initiation of the paroxysmal SAF. These simple pacing protocols were preferred because no complex time adjustment is required between stimuli, and SAF could be reliably induced.

Once SAF has been initiated, its ability to be sustained must be considered, especially in the context of therapy testing. Indeed, in order to assess reliably the success rate of a therapy in the model, it must be assured that a termination of SAF observed in the simulations is directly caused by the therapeutic intervention, and is not due to spontaneous termination of an unsustained SAF. According to the multiple wavelet hypothesis, the number of fibrillating waves evolving on the atrial tissue at a given time is a critical parameter for AF maintenance [42, 96]. It was indeed observed that a high number of fibrillating wavelets increase overall AF complexity and ensure AF perpetuation, and that AF can not be maintained reliably when this number of wavelets falls below a critical value [97, 98]. More generally, different alterations of the atrial substrate were shown to promote AF perpetuation [99]:

- *Electrical remodeling*: it has been shown that rapid atrial pacing provokes a shortening in atrial refractoriness through electrical remodeling, which increases susceptibility to AF [92]. This progressive remodeling in atrial ionic properties causes the remodeled cells to present shorter APDs as well as a loss of rate adaptation [46] and a flattening of the restitution dependence. These factors largely contribute to AF maintenance. Conversely, steep restitution curves lead to spontaneous wavebreaks [100, 101].
- *Structural remodeling*: the presence of structural heterogeneities such as fibrosis, heterogeneities in specific ionic concentrations or gradients in APD is also a potential contributor to AF perpetuation. It was shown in human and animal studies as well as in modeling studies that these structural changes were associated with AF inducibility and sustainability [102, 103, 104, 105]. From a mechanistic point of view, these structural alterations can be thought to cause spatial dissociation of wavelets and therefore promote AF maintenance.
- *Inflammation*: Finally, it has been recently suggested that inflammation could play a role in the progressive development of AF. C-reactive proteins (CRP), which are acute-phase proteins of the innate immune system, were shown to be correlated with the level of chronicity of AF [106]. Moreover, the level of specific proinflammatory cytokines was also positively correlated with the duration of AF episodes, indicating a potential role of inflammation in the process of atrial remodeling [107].

Both electrical and structural remodeling were implemented in the presented biophysical model, leading to sustained SAF dynamics useful for subsequent analyses [40, 91]. However, in the different studies presented in this dissertation, only models including electrical remodeling were used.

### 3.3.3 A Model of Recent Chronic Atrial Fibrillation

The first model of AF proposed is based on the multiple wavelet hypothesis, which states that several independent fibrillating waves evolve randomly on the atrial tissue and maintain AF by their self-sustained interactions [42, 96]. Such SAF dynamics was reproduced using the Luo-Rudy I (LRI) membrane kinetics model presented in section 2.2.2 [60]. Although this model was first derived for ventricular cells, some modifications of its ionic properties were performed to shorten the resulting APD and therefore better approximate the specific ionic properties of atrial cells [108]. Thus, the channel conductance  $G_{\text{Si}}$  was set to  $0.085 \text{ mS/cm}^2$ ,  $G_{\text{K}}$  was set to  $0.423 \text{ mS/cm}^2$ , and  $G_{\text{Na}}$  was reduced to  $16 \text{ mS/cm}^2$ , as was proposed in [109]. Each channel conductance mentioned can be easily linked to its corresponding ionic current as depicted in Table 2.1 for further details. As a result, the APD was in the range of reported values for atrial refractory periods in humans [77]. In addition, an isotropic homogeneous tissue with resistivity  $\rho = 200 \text{ }\Omega\text{cm}$  was selected, providing an average conduction velocity during sinoatrial propagation of  $70 \text{ cm/s}$ . This "atrialized" baseline version of the LRI model can be considered as a model of healthy atrial cell, and will be called *baseline modified LRI model* in the remaining of the dissertation. In Figure 3.2, the action potential shape as well as the corresponding restitution curve of this baseline model are illustrated (continuous line). Interestingly, the maximal slope of the restitution curve is greater than one, meaning that SAF can be easily initiated in this model [101]. However, as was shown in previous studies, the baseline version of this AF model could not give rise to sustained SAF, since all episodes terminated after 4-5 seconds, either through mutual annihilations of wavefronts, or through interactions with refractory tissue [40]. This dynamical behavior of the baseline modified LRI model is typical of normal human atria, in which AF episodes usually terminate after a few seconds [110]. In order to mimic electrical remodeling as observed in permanent AF, the channel conductance  $G_{\text{Si}}$  was further reduced to  $0.055 \text{ mS/cm}^2$ . The main effect of this modification was a shortening of the APD and a flattening of the restitution curve, as displayed in Figure 3.2 (dashed line). Under these conditions, SAF could be maintained in a stable manner, with wavebreaks continuously occurring and ensuring AF perpetuation. Consequently, this model of fibrillating atria was called *remodeled modified LRI model*.

In order to initiate SAF in the biophysical model, it was therefore necessary to use a combination of the baseline model and the remodeled model in a sequential way, as illustrated in Figure 3.3. In a first step, the baseline atrial model was stimulated at the sinoatrial node by a  $20 \text{ Hz}$  rapid pacing protocol during 3 seconds. Each stimulating pulse was modeled by the injection of intracellular current ( $I_{\text{stim}} = 80 \text{ }\mu\text{A/cm}^2$ ) during  $2 \text{ ms}$  (square pulse). After the first induced pulse, the atrial surface was entirely depolarized and stayed for several hundreds of milliseconds in a refractory state. However, as mentioned above, the steep restitution characteristics of the baseline version provides an ideal framework for wavebreak occurrence [101], and the first SAF wavelet was created after 500 milliseconds, as illustrated on the color maps of Figure 3.3. From this point, wavebreaks occurred continuously under the influence of the pacing, and fibrillating waves could progressively spread to the left atrium. After 3 seconds, the pacing

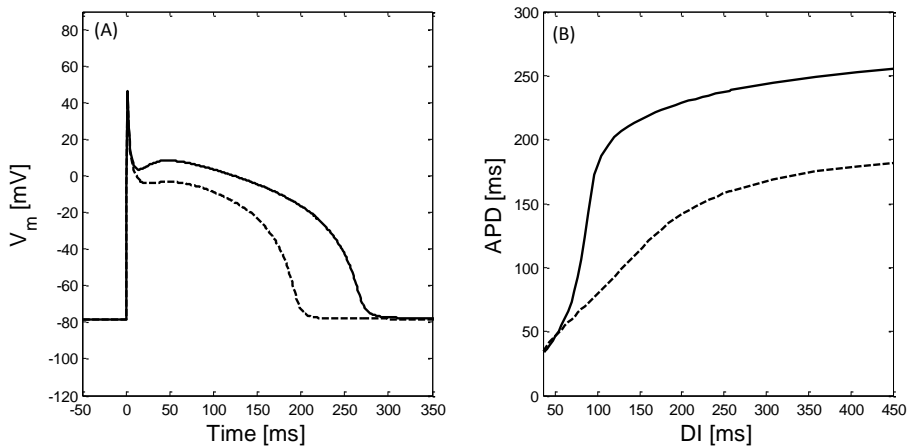


**Figure 3.2:** Action potential shape and restitution curve of the modified Luo-Rudy membrane kinetics model. (A) Transmembrane potential. (B) Restitution curves. Two configurations of the model are presented: the baseline model with  $G_{si} = 0.085 \text{ mS/cm}^2$  (continuous line), and the remodeled version with  $G_{si} = 0.055 \text{ mS/cm}^2$  (dashed lines).

sequence had created a sufficient number of fibrillating wavefronts circulating over both atria; pacing was stopped and a switch towards the remodeled tissue and its flattened restitution could be performed to ensure AF perpetuation (red bar on the EGM traces, panel (A) of Figure 3.3). The resulting fibrillating activity could be maintained during more than 10 minutes, which is to our knowledge one of the longest simulations ever performed in a biophysical model of AF.

In Figure 3.4, an example of SAF as simulated by the modified LRI model is presented together with its related physiological parameters. In panel (A), a sequence of instantaneous transmembrane potential maps equally spaced by 15 ms increments is shown, illustrating the dynamical behavior of this model during a short period of time (135 ms). Clearly, the dynamics observed in these space plots is a multiple wavelet AF, including numerous wavebreaks and spiral formations. In this example, a typical pattern of this type of dynamics can be observed in the right lateral wall, where a spiral wave (pointed by the red arrow in the first space plot) progressively rotates, until it hits its own refractory tail and gives rise to a wavelet that will in turn create several spiral waves. A 10 seconds time segment of this self-sustained SAF can be observed in panel (B), together with examples of simulated unipolar electrograms and membrane potentials, as well as dynamical parameters such as the number of wavelets present on the atria or the percentage of excited atrial tissue. These curves illustrate well the chaotic nature of the simulated fibrillating activity. In Figure 3.5, the histograms of AF cycle length (AFCL) and of the number of fibrillating wavelets detected on the tissue were computed over the whole 10 minutes episode of SAF. In panel (A), local measures of AFCL were performed, with two sites in the left atrium and two in the right atrium. Mean AFCL values were slightly different from one site to another, demonstrating the influence of atrial anatomy on the fibrillating activity. Interestingly, the AFCL computed in the pulmonary



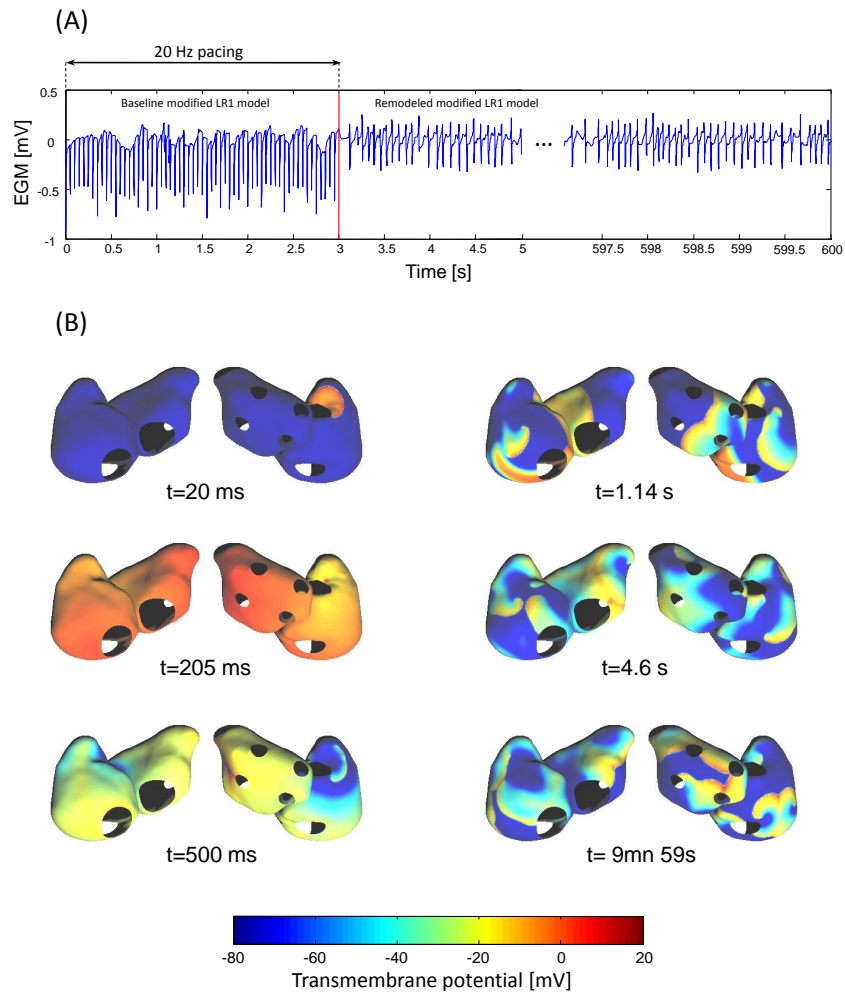


**Figure 3.3:** SAF initiation by 20 Hz burst pacing in the modified Luo-Rudy membrane kinetics model. (A) Simulated unipolar electrogram as measured on the sinoatrial node. The modified LR1 model was switched from the baseline to the remodeled version after the three seconds of 20 Hz burst pacing (red line) and was then let to evolve freely during 10 minutes. (B) Space plots of membrane potentials during SAF initiation and perpetuation.

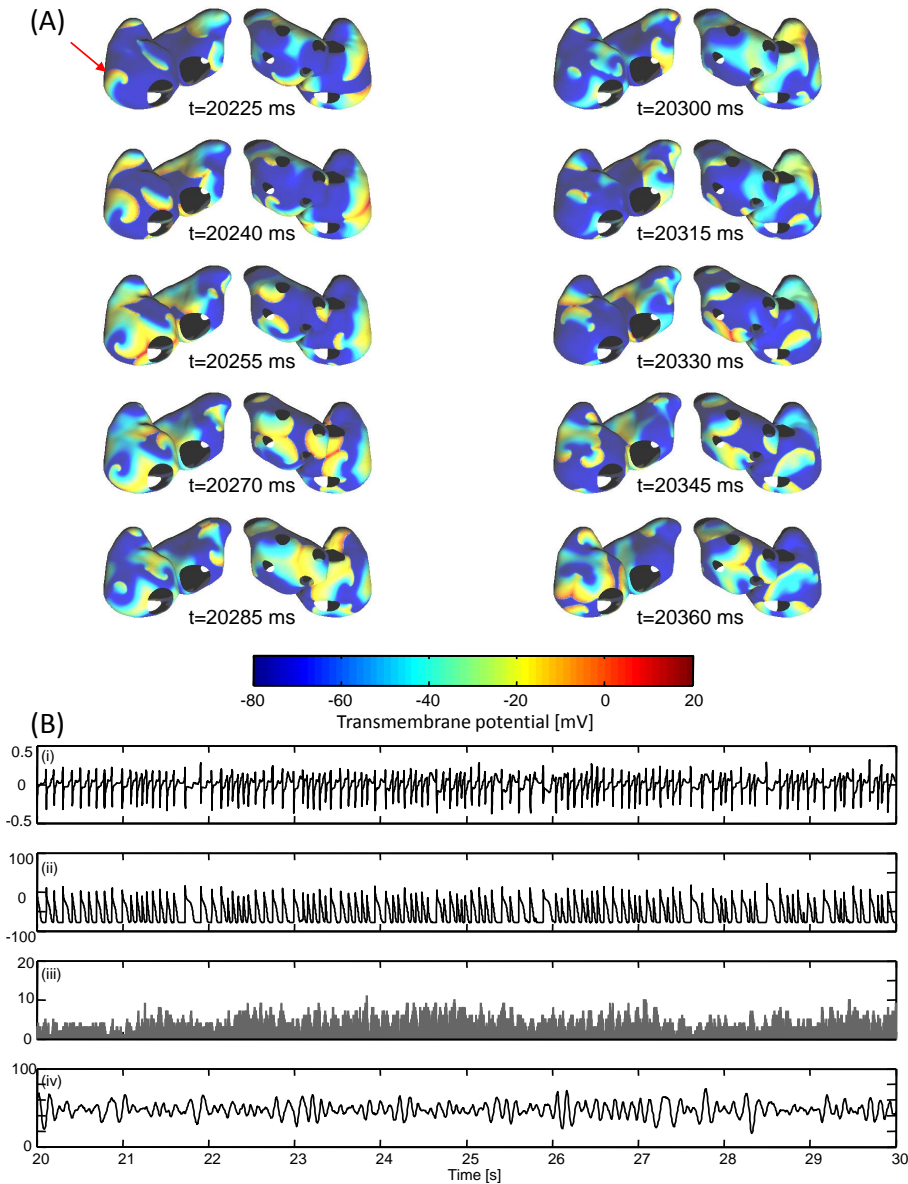


**Figure 3.4:** Dynamics of sustained SAF using the remodeled modified Luo-Rudy membrane kinetics model. (A) Space plots of membrane potentials during SAF showing self-sustained multiple wavelet dynamics with wavefront fusions and wavebreaks. (B) Dynamical analysis of a 10 seconds segment of SAF: (i) Simulated unipolar electrogram as measured in the right anterior wall. (ii) Simulated transmembrane potential as measured in the right anterior wall. (iii) Number of fibrillating wavelets present on the total atrial surface. (iv) Percentage of excited tissue.

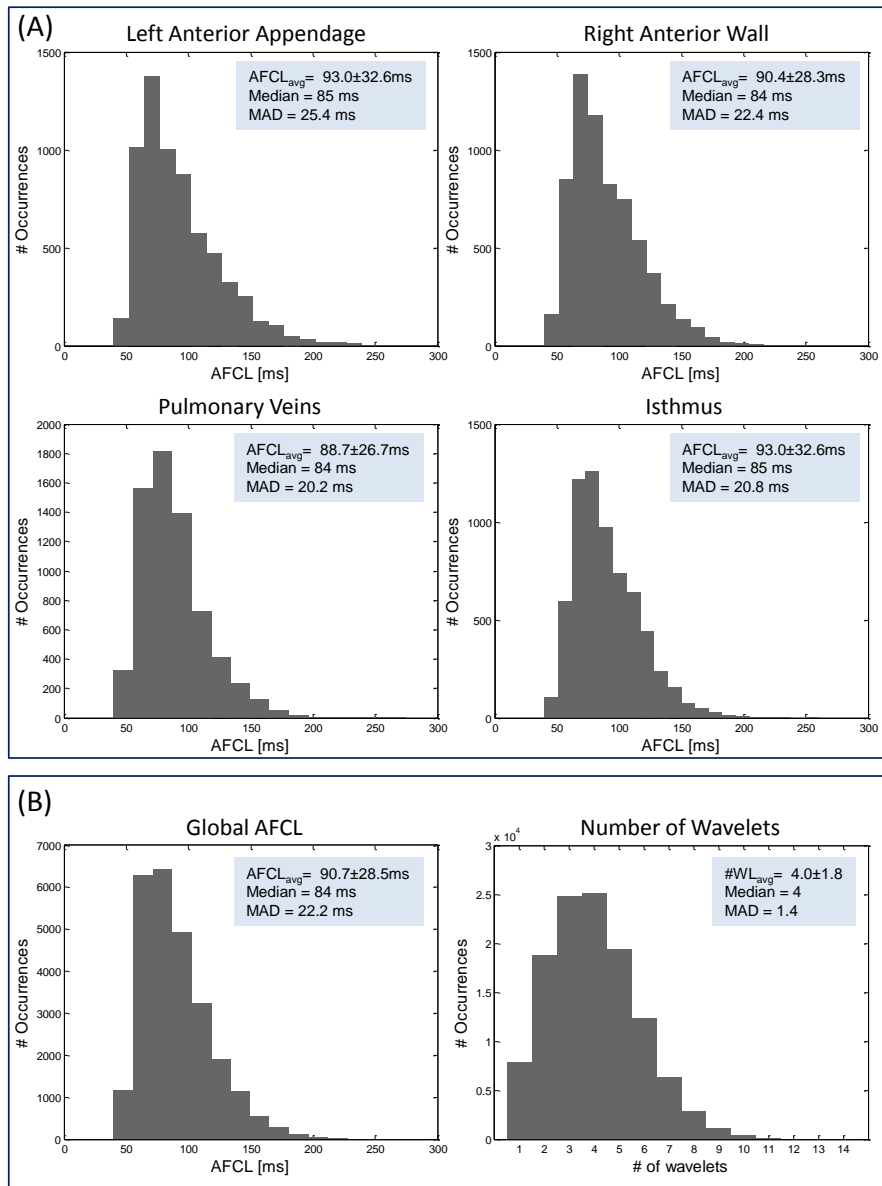


**Figure 3.5:** Local and global dynamical properties of a 10 minutes episode of sustained SAF using the remodeled modified Luo-Rudy membrane kinetics model. All histograms were based on the total SAF of 10 minutes duration. For all plots, mean values, standard deviations, medians and median absolute deviations are indicated in shaded blue. (A) AF cycle length (AFCL) in local atrial sites: AFCL was measured in two sites of the left atrium and two sites of the right atrium. (B) Global measures of AFCL and of the number of wavelets present on the tissue. The global AFCL was computed by grouping the four sites of the upper panel.

veins was the lowest, meaning that this area tends to fibrillate faster than the others. This behavior was also observed during experimental studies on sheep [111]. In panel (B), the AFCL measures of each site were grouped to give a global measure of AFCL, and the number of wavelets was also documented. It should be noted that the average AFCL observed with the modified LRI model is slightly lower than the values usually reported in humans, since AFCL under 100 ms are only rarely measured. Nevertheless, other parameters such as APD or CV are in the range of reported values. The number of wavelets present in the tissue varied between 1 and 14, with an average of 4. In terms of complexity, this SAF dynamics can be defined as a type II-III AF, as described by Konings et al. [74].

The numerical implementation of this AF model was done as follows. Propagation of atrial electrical activity was computed on the atrial geometry discretized using triangular elements. A finite volume approach was used to solve the monodomain propagation equations [35, 39]. This approach considers the atrial tissue as a network of resistors [112]. The actual values of the resistors depends on the geometry of the neighboring triangles (edge length and angles) as described in Zozor and colleagues [39]. The discretized surface of 50,000 nodes resulting in a spatial resolution of 0.6 mm was retained. This coarse discretization was motivated by the need to simulate thousands of runs of AF in the studies presented throughout next chapters. It represents a trade-off between accuracy and computational load that has been used before to reproduce clinical observations [113, 114]. Moreover, the whole procedure was also tested with a finer mesh (100,000 nodes,  $\Delta x = 0.4$  mm) in previous studies, and no major difference was observed between the two configurations [41]. The resulting error in conduction velocity (CV) was about 20% compared to a very fine mesh, but tissue resistivity was adjusted to compensate for this effect [39]. Operator splitting and adaptive time steps were used for time integration [35]. The time steps varied between 12.5  $\mu\text{s}$  for depolarization and 50  $\mu\text{s}$  for repolarization.

Overall, the remodeled modified LRI model simulates the existence of a long-lasting and sustained AF affected by electrical remodeling, but without structural remodeling or ectopic activity. Therefore, this model is proposed as a *model of recent chronic AF*, in which fibrillation has already altered the ionic properties of the atria, but structural damages are not yet visible. Interestingly, this AF model is characterized by a complex dynamics, and its resulting fibrillatory activity is not likely to terminate spontaneously without any external intervention. As a consequence, this model was appropriate for the testing of simulated therapeutic interventions such as ablation procedures or low-energy pacing protocols, since it was sure that any observed termination could be attributed to the therapy under investigation and not to a spontaneous termination. Moreover, this model was preferentially used compared to other highly complex models because of its reduced computational load, and its overall simplicity in reproducing recent chronic AF dynamics. Moreover, past studies demonstrated that results obtained during AF ablation simulations using this model were not significantly different from clinical findings in humans [113]. For all these reasons, the modified LRI membrane kinetics model was largely used in this dissertation, and is at the core of the following studies:

- A study of the phenomenon of spontaneous termination of complex SAF dynamics

(chapter 4). For this particular study, some ionic properties of the model were slightly modified in order to make spontaneous terminations more frequent.

- A detailed investigation of AF rapid pacing as observed in the biophysical model, in order to better understand the effect of rapid pacing on atrial tissue and on AF electrical activity (chapter 5).
- The presentation and testing of a novel therapeutic solution for AF suppression based on low-energy pacing (chapter 6).

### 3.3.4 A Model of Paroxysmal Atrial Fibrillation

The second type of AF that was simulated and studied in this dissertation is characterized by a much simpler dynamics, and can be viewed as a type I-II AF according to Koning's classification [74]. For this purpose, the Courtemanche et al. model was used [45]. In its original configuration of healthy atrial cell, the Courtemanche model could not provide sustained SAF episodes of more than one second due to long spatial wavelengths [115]. To permit self-sustained SAF, electrical remodeling was simulated with the modification of specific parameters of the membrane model, as proposed in [46], in order to better match restitution properties measured experimentally in humans during AF [56]. Therefore, the currents  $I_{to}$ ,  $I_{CaL}$ , and  $I_{Kur}$  were reduced by 80%, 30% and 90% respectively, and  $I_{Kr}$  was increased by 50%, so that APDs were significantly shortened as shown in Figure 3.6 (panel A), and the flattened APD restitution curve shown in panel B of Figure 3.6 was relatively similar to the experimental findings of Kim and colleagues [56]. This model will be referred to the *modified Courtemanche model* from now on. However, the refractory period of the modified Courtemanche model is 230 ms at rest and 120 ms for the shortest diastolic interval, which is still slightly too long to ensure SAF perpetuation. In order to shorten the spatial wavelength and thus maximize the maintenance of SAF after initiation, the resistivity parameter  $\rho$  was set to 500  $\Omega\text{cm}$ , resulting in a CV of 40 cm/s. Structural remodeling was not implemented in this specific model, but other types of SAF based on the same biophysical model and including heterogeneities in vagal action or in APD were also proposed elsewhere [91].

SAF was initiated in the modified Courtemanche model by applying a ramp pacing protocol in the sinoatrial node. Based on previous studies [40], the ramp pacing sequence was set to start with a cycle length of 280 ms. The pacing cycle length was then decremented by 1 ms at each beat. Such pacing protocol was extensively used in clinical studies to induce AF or atrial flutter [93]. The ramp pacing was applied during 11 seconds and then stopped to let AF evolve freely on the atrial surface. In Figure 3.7, the simulated unipolar electrogram as measured on the sinoatrial node as well as space plots of membrane potentials during SAF initiation are presented. A progressive change of atrial activity towards fibrillatory conduction can be observed. After 5 seconds of pacing, patterns of alternans appeared as the stimulation cycle length decreased. After approximately 9.3 seconds (35<sup>th</sup> stimulating pulse), the first fibrillating patterns could be observed (Figure 3.7, panel B). From that point on, fibrillating wavelets started meandering on the tissue in a self-sustained manner. Interestingly, clinical studies in patients also found that large APD oscillations were triggered just before AF initiation [116]. After

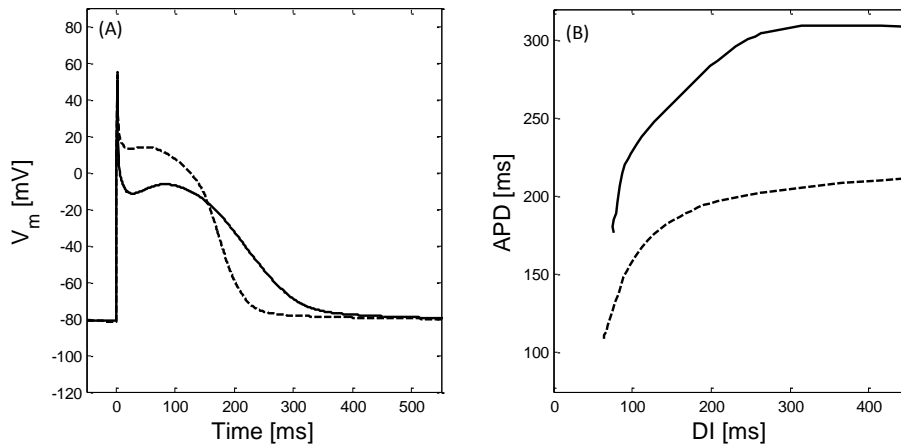


**Figure 3.6:** Action potential shape and restitution curve of the Courtemanche model. (A) Transmembrane potential. (B) Restitution curves. Two configurations of the model are presented: the baseline model (continuous line), and the remodeled version (dashed lines).

11 seconds, pacing was stopped and SAF was maintained for more than 28 seconds.

In Figure 3.8, a typical sequence of SAF using the modified Courtemanche model is presented together with its dynamical properties. In panel (A), a sequence of membrane potential maps equally spaced by 60 ms increments is shown, while panel (B) presents the analysis of a 10 seconds time segment, where simulated unipolar electrograms, transmembrane potentials, the number of wavelets evolving on the tissue and the percentage of excited tissue are documented. Clearly, the dynamics of this SAF is very different from the one provided by the modified Luo-Rudy membrane model. Here, fibrillating electrical activity is characterized by very simple dynamical patterns. Wavebreaks and spiral formation are not frequent, so the resulting electrical activity only involves a few spirals drifting randomly on the atrial surface at the same time. For this reason, this type of SAF is considered as a model of meandering AF. This regularity in dynamics can also be observed in the curves displayed in Figure 3.8 (panel(B)). In particular, the number of wavelets present in the tissue is only rarely higher than two. In Figure 3.9, the histograms of AFCL in different atrial sites and of the number of fibrillating wavelets detected on the tissue were computed over an AF episode of 30 seconds to provide more global statistics. The shapes of the AFCL histograms in the Figure are very similar to the AFCL distribution corresponding to a type I AF in Konings *et al.* [74]. In addition, the small number of wavelets detected in average on the atrial surface also suggest that the SAF presented in this section is of type I.

Although the modified Courtemanche model is specific of human atrial cells and is well accepted as a detailed and realistic description of atrial cellular activity, it remains very difficult to make it fibrillate in a sustained manner. In most cases, the SAF provided by the model tends to terminate spontaneously after a few seconds. Even when using the modified ionic properties proposed in this section, the duration of SAF episodes simulated and analyzed throughout this dissertation ranged between 1.8 seconds and 45.3

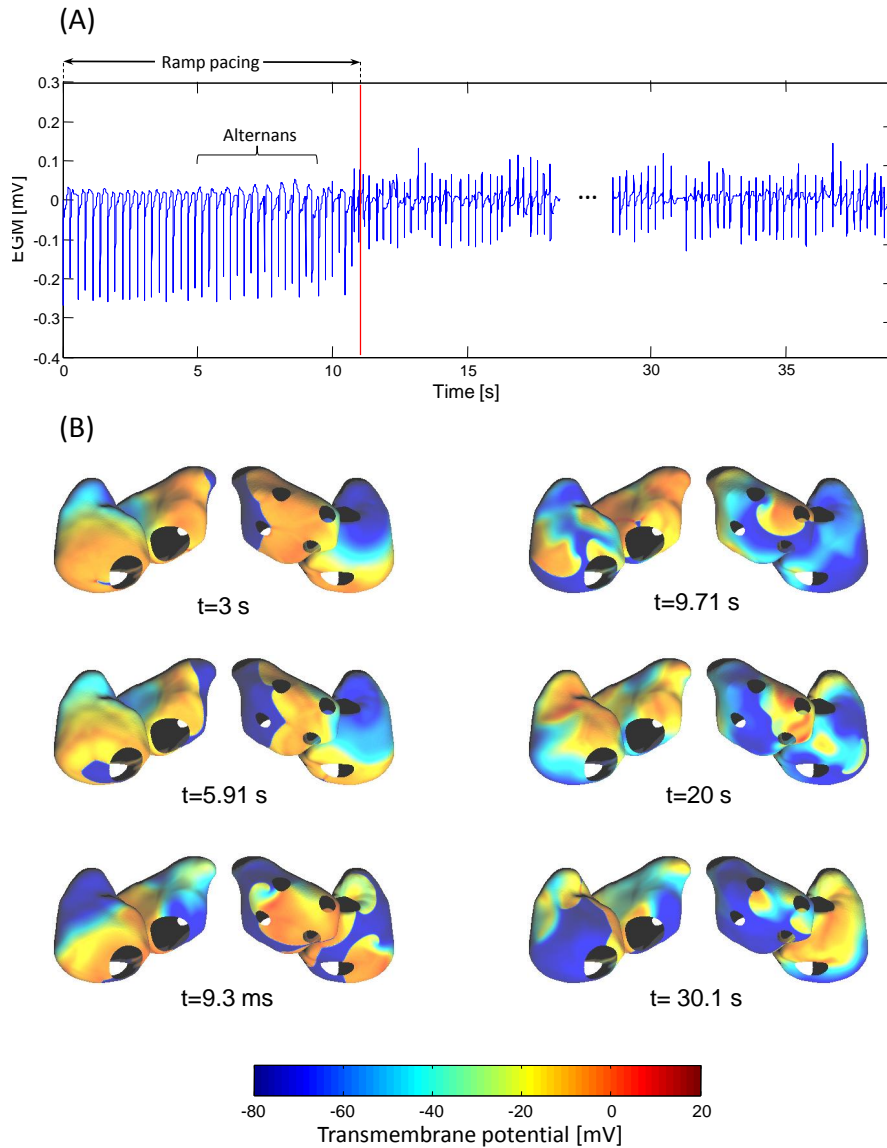


**Figure 3.7:** SAF initiation by ramp pacing in the modified Courtemanche model. (A) Simulated unipolar electrogram as measured on the sinoatrial node. The model was electrically remodeled, and ramp pacing was abruptly stopped after 11 seconds (red line). In this example, the SAF episodes lasted 28.1 seconds. (B) Space plots of membrane potentials during SAF initiation and perpetuation.

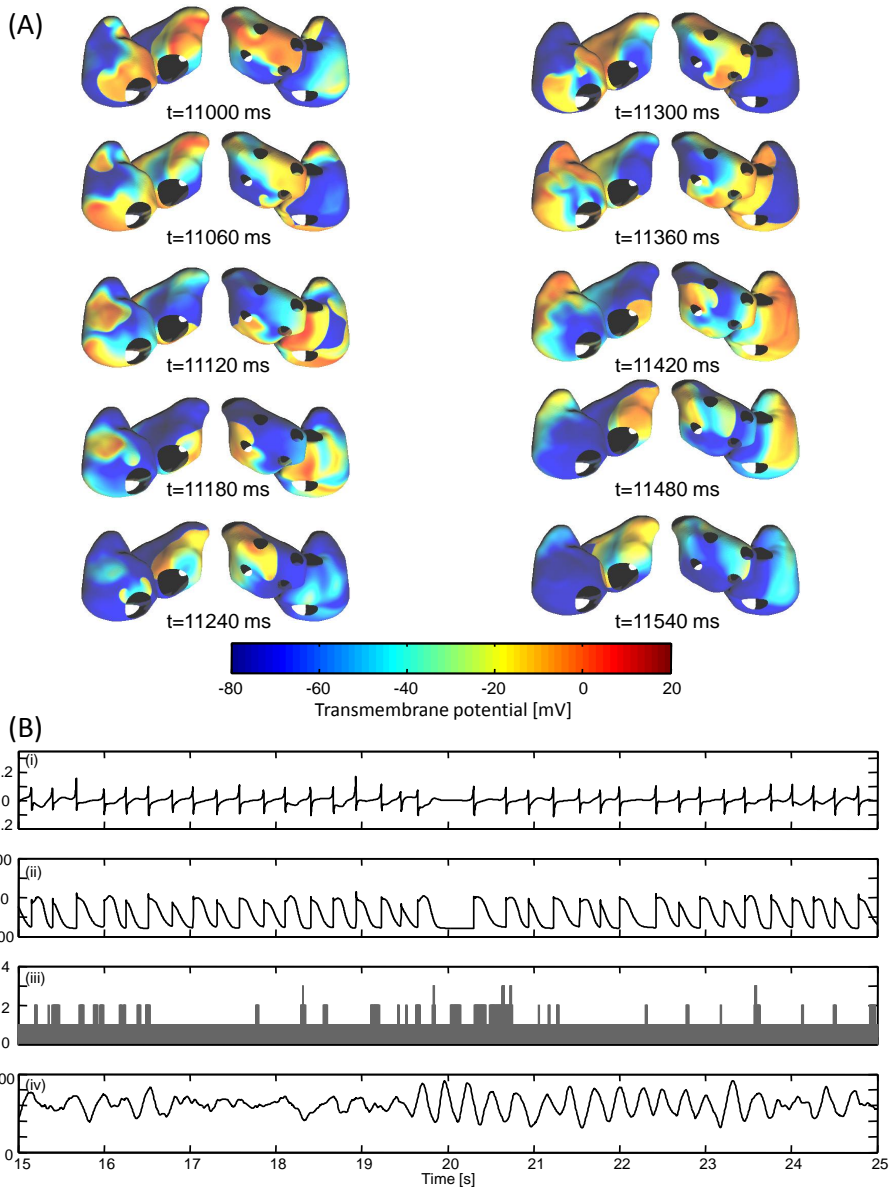


**Figure 3.8:** Dynamics of sustained SAF using the modified Courtemanche model. (A) Space plots of membrane potentials during SAF showing self-sustained SAF with meandering wavelets. (B) Dynamical analysis of a 10 seconds segment of SAF: (i) Simulated unipolar electrogram as measured in the right anterior wall. (ii) Simulated transmembrane potential as measured in the right anterior wall. (iii) Number of fibrillating wavelets present on the total atrial surface. (iv) Percentage of excited tissue.



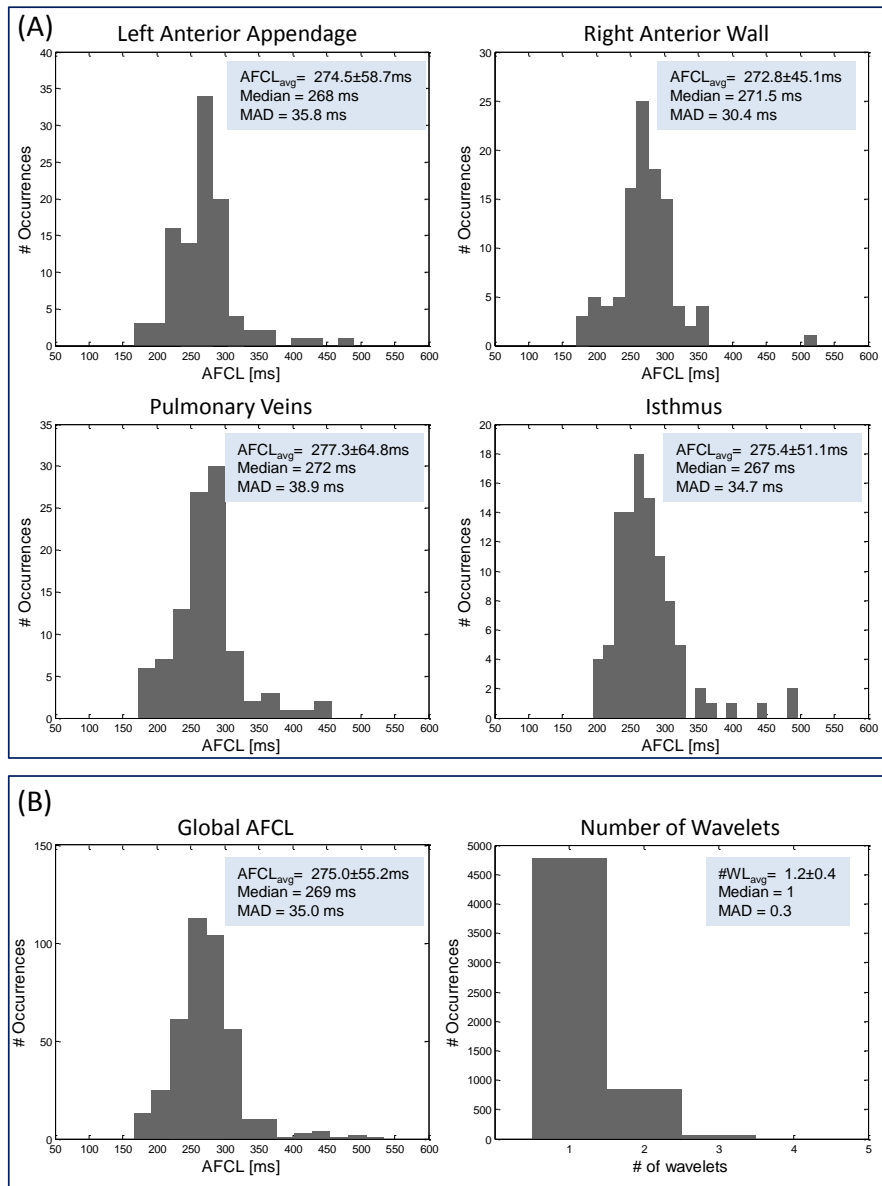


**Figure 3.9:** Local and global dynamical properties of a 30 seconds episode of sustained SAF using the modified Courtemanche model. All histograms were based on the total SAF of 30 seconds duration. For all plots, mean values, standard deviations, medians and median absolute deviations are indicated in shaded blue. (A) AFCL in local atrial sites: AFCL was measured in two sites of the left atrium and two sites of the right atrium. (B) Global measures of AFCL and of the number of wavelets present on the tissue. The global AFCL was computed by grouping the four sites of the upper panel.

seconds, with an average value of  $8.5 \pm 7.1$  seconds (see chapter 4 for more details). This tendency towards spontaneous termination combined with its relatively simple "meandering wavelets" dynamics and the fact that no structural heterogeneities were considered for this model motivated the decision to propose it as a *model of paroxysmal AF*. However, it could be argued that paroxysmal AF often involve ectopic activity stemming from pulmonary veins [87]. Indeed, continuous ectopic activity was not simulated in the proposed model. Nevertheless, our model can be thought of as simulating ongoing episodes of acute AF that could have been triggered by a transient firing of ectopic foci. Due to its inherent properties, this model was not adapted to therapy testing, where sustained SAF is absolutely needed. Indeed, in order to assess therapy efficiency in a reliable way, it must be certain that an observed SAF termination was provoked by the therapy, and not by a spontaneous phenomenon. Thus, this model was used exclusively in chapter 4 to study the mechanisms of spontaneous AF termination.

The advantage of simulating short AF episodes is that the computational load is not a constraint anymore. Therefore, the numerical implementation of this AF model was done in a surface mesh of 100,000 nodes giving a spatial resolution of  $\Delta x = 0.4$  mm. The resulting error in conduction velocity (CV) was smaller than 15% compared to a very fine mesh, but tissue resistivity was again adjusted to compensate for this effect. The numerical integration of the numerous differential equations of the Courtemanche model was performed the same way as for the modified LRI model.

### 3.4 Conclusion

In this chapter, the biophysical model of human atria presented in chapter 2 was used to simulate both normal and altered cardiac activity. SAF could be successfully initiated using two distinct cellular models showing different propensities to be sustained over time. A detailed documentation of the parameters and integration methods used to simulate these two AF models was provided, and will be largely used throughout the rest of this dissertation.

In addition, a complete description of the dynamics of both AF models was presented, emphasizing the difference in their respective levels of complexity. AF is known to cover a wide range of complexities depending on its type and its state of progression. The models used in this dissertation can be considered as representative of either early stages (paroxysmal AF) or later stages (recent chronic AF) of the arrhythmia. Being able to simulate AF of different families can be an advantage, as it can be considered as simulating different sub-populations of patients. For instance, in chapter 4, the phenomenon of spontaneous termination could be studied and compared between early and later stages of AF, which is not easily feasible in clinical settings. Similarly, the methods developed in chapters 5 and 6 for AF therapeutic pacing were based on the AF model of section 3.3.3. Thus, these methods can be considered as targeted to patients with recently diagnosed chronic AF.

# Dynamics of Atrial Fibrillation during Spontaneous Termination: A Biophysical Modeling Study

# 4

---

## 4.1 Introduction

In this chapter, a modeling study of the dynamics of AF spontaneous termination is exposed. After a state of the art of this widely observed, but poorly understood phenomenon, a description of the mechanisms of spontaneous termination of two different types of SAF is presented. This study was at the origin of two publications [117, 118].

### **Spontaneous Termination: a Poorly Understood Phenomenon**

The first case reports of spontaneous termination of long-lasting AF were described as early as in the 1950's [119]. Since then, a growing interest in the understanding of this phenomenon could be observed across the medical and scientific community, as a better understanding of this process of spontaneous AF termination could lead to a more accurate dynamical description of AF in its last instants, and eventually to the development of more effective therapies. However, the mechanisms of spontaneous AF termination are difficult to study in detail due to their transient nature. Nevertheless, several studies investigated this phenomenon during clinical, electrophysiological or computer-based experiments, and illustrated the difficulty to precisely describe the time course as well as the spatial patterns underlying spontaneous AF termination.

Indeed, describing the exact timing of AF spontaneous termination is a major challenge, sometimes leading to contradictory results. While a study on patients with paroxysmal AF reported that changes in the global organization of electrocardiographic sig-

nals could be detected up to one minute prior to paroxysmal AF termination [120], it was shown on a similar population of patients that frequency changes in the surface electrocardiogram are abrupt and occur only during the last 1-2 s of the AF episode [121]. Moreover, during a mapping study of spontaneous AF termination using a basket catheter, the earliest detectable event was shown to occur on average 4 s before termination [122].

Similarly, the spatial patterns of electrical activity underlying AF terminations are difficult to describe accurately. According to the "multiple wavelet" AF model [96], AF might terminate either by a simultaneous block of all fibrillating wavelets, or by a progressive fusion of wavelets into one massive wavefront. Once again, results and conclusions were mixed. In a study based on intra-atrial recordings of both drug-induced and spontaneous termination of AF in humans, observations failed to show any wavelet linking measured by coherence increase or cycle length increase before spontaneous AF termination, therefore supporting, but not proving, the hypothesis that AF wavelets are simultaneously annihilated [123]. The same conclusions were also drawn in a study of surface ECG recordings [124]. On the other hand, opposite results were obtained in other electrophysiologic studies, where AFCL was shown to increase several seconds before spontaneous terminations of AF, suggesting an organization process through wavelet fusion directly preceding AF extinction [120, 122, 125]. This latter hypothesis was further supported by investigations using signal processing methods dedicated to the quantification of organization, such as mutual information or sample entropy [120, 126, 127]. Organization tended to increase progressively several seconds before AF termination, as fibrillating wavelets progressively fused into a few major waves prior to AF termination [126]. In terms of spectral parameters, it was observed that AF termination could be better predicted by a low and stable fibrillatory frequency, which also suggests some organizing process [121, 128]. Nevertheless, these studies were conducted on different types of AF encompassing a continuous spectrum of complexity. AF with different dynamics can possibly have different termination processes, as will be shown in the next sections.

Alternatively, several attempts to mechanistic descriptions of the phenomenon were also published, including both experimental and computer modeling studies [129, 130, 131, 132, 133, 134, 135, 136]. In these studies, the crucial role of wavefront curvature changes during conduction slowing and block was underlined [131, 134, 135], and mechanisms of termination through spiral wave collisions were largely described [132, 133]. Especially, two studies based both on computer modeling and animal experiments when considering AF models based on rotors [137] suggested that AF termination was triggered by a destabilization of spiral rotors evolving on the atrial tissue during AF through  $\text{Na}^+$  inhibition [135, 136]. When  $\text{Na}^+$  decreased, rotors started to increase in size, which in turn increased their core meander and their wavefront curvature. These dynamical instabilities promoted rotor extinction either through mutual annihilation with other rotors, or through collision with anatomic boundaries. Moreover, they were also observed in another computer modeling study as a critical parameter for AF termination through wave collision [138]. Finally, it was demonstrated during mapping studies that spontaneous AF termination was polymorphic with spatially heterogeneous groups of

unstable rhythms [122]. In particular, different dynamical behaviors between the right atrium (RA) and the left atrium (LA) were observed.

## **A Modeling Perspective**

Taken together, these results illustrate the complexity of the phenomenon of AF spontaneous termination. Although several parameters were mentioned as good descriptors of the termination process, more detailed studies are needed to understand the phenomenon in a more systematic way. Such knowledge would be of the utmost importance, since a precise description of AF spontaneous termination mechanisms could be used through "reverse engineering" to elaborate more targeted therapies, such as AF-dedicated pacing algorithms or ablation patterns.

In this perspective, computer studies are of interest to complement clinical and experimental findings in the search for a more complete understanding of the underlying mechanisms of AF spontaneous termination. Indeed, computer simulations can be used to generate a high number of spontaneously terminated AF episodes in a much easier way than in clinical settings. Moreover, a refined analysis of the dynamical mechanisms coming into play can be conducted at different temporal and spatial scales, since all variables of interest are accessible over time and space, including the number of fibrillating wavelets as well as their trajectories and mutual interactions.

In the present model-based study, we analyzed simulated episodes of spontaneous AF termination to assess the temporal and spatial scales of the mechanisms involved. In order to account for the polymorphic nature of AF, models of either paroxysmal or recent chronic AF with distinct dynamical properties were investigated, and differences in SAF dynamics between the RA and the LA were documented.

## **4.2 Methods**

### **4.2.1 Biophysical Modeling of Atrial Fibrillation**

Different computer models of the atria with realistic anatomy and electrophysiology were developed over the last decade [31, 32, 33, 34, 36, 69]. In order to alleviate the computational load, simplified versions of these models were derived to make the large-scale simulation of atrial arrhythmias possible, for instance to investigate therapies, such as AF ablation [36, 113] or low-energy pacing (see chapter 6 or [139]).

In this study, two biophysical models of AF with an identical anatomical structure but with different cellular kinetics were successively used to simulate AF dynamics with distinct levels of complexity: (A) the model of paroxysmal AF presented in section 3.3.4, depicted as a meandering or type I AF according to the classification of Konings et al. [74], where only a few reentries wander on the atria, and (B) the model of recent chronic AF developed in section 3.3.3, i.e. a model of multiple-wavelet AF [96] that could be classified as a type III AF due to the high number of reentries observed on the tissue.

The dynamics of spontaneous termination was then analyzed in each of these AF models in both the temporal and spatial domains.

### Atrial Geometry

The atrial geometry used in this work in combination with the cellular models mentioned above is the 3-D monolayer surface described in chapter 2. The resulting geometry includes all major anatomical obstacles to propagation, as shown in Figure 4.1. Three-dimensional anatomical structures such as Bachmann's bundle, pectinate muscles or crista terminalis are not included, so that the effect of the major anatomical features on the process of spontaneous termination can be specifically investigated.

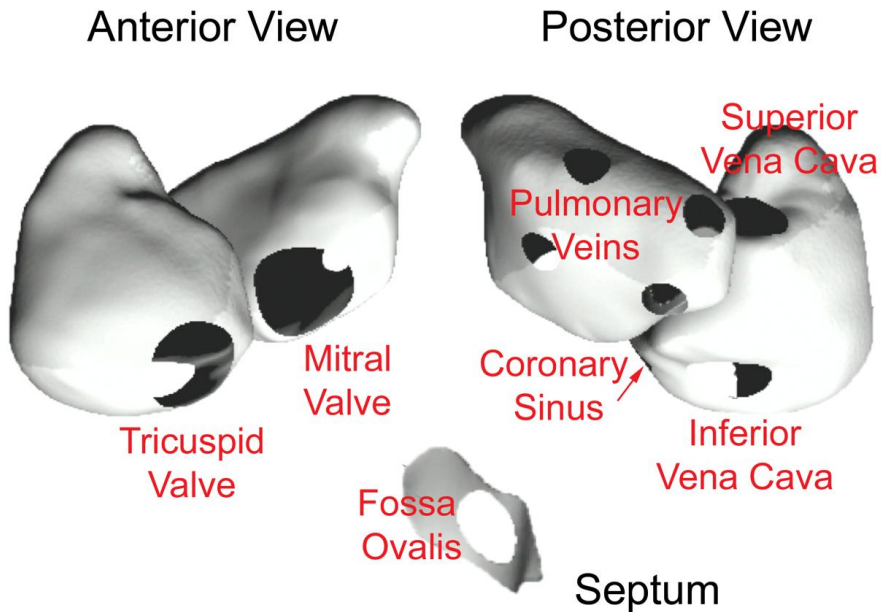


**Figure 4.1:** Geometry of the biophysical model of human atria used in this chapter: anterior view (on the left) and posterior view (on the right), with a cut of the septum in the middle. The major anatomical obstacles including valves and veins are indicated in red.

### Atrial Cell Models

In order to generate SAF dynamics with distinct levels of complexity, two different cellular models were successively used at each node of the atrial geometry to simulate atrial electrical activity. First, the modified Courtemanche model introduced in section 3.3.4 was used to simulate a paroxysmal AF based on meandering AF dynamics. The modifications in the parameters of the membrane accounting for AF tissue properties shortened the action potential duration to 210 ms, while reproducing the restitution prop-

erties measured in human atrial cells during chronic AF [56]. The atrial substrate was kept homogeneous, and conduction anisotropy was not considered. The resistivity  $\rho$  was set to 500  $\Omega\text{cm}$ , resulting in a conduction velocity of 40 cm/s. With this configuration, SAF could occasionally be self-sustained for more than 20 seconds, although most of simulations terminated spontaneously in a shorter period of time.

For the second type of SAF investigated, the remodeled modified LRI model presented in section 3.3.3 was used, namely a model of recent chronic AF. In its original configuration, this model tends to keep AF sustained for several minutes of simulation, which is useful to create the initial database of SAF signals, but is computationally demanding when it comes to observing SAF terminations. For this reason, a slight modification in the tuning of channel conductance parameters was abruptly made at the beginning of each simulation of spontaneous termination using this model. The  $\text{K}^+$  channel conductance was still set to  $G_{\text{K}} = 0.423 \text{ mS/cm}^2$ , and the  $\text{Na}^+$  channel conductance to  $G_{\text{Na}} = 16 \text{ mS/cm}^2$ , but the L-type  $\text{Ca}^{2+}$  channel conductance  $G_{\text{si}}$  was increased to a value of  $0.06 \text{ mS/cm}^2$  instead of  $0.055 \text{ mS/cm}^2$ . This abrupt increase in  $G_{\text{si}}$  lengthened the APD from 195 ms to 210 ms compared to the original model used to generate the SAF, and subsequently forced spontaneous termination in a shorter time window.

#### 4.2.2 Simulating Atrial Fibrillation Spontaneous Termination

First, SAF had to be triggered properly in each of the configurations depicted above, in order to be able to observe spontaneous termination mechanisms in a second step. Each type of SAF, paroxysmal AF model and recent chronic AF model, was initiated successfully following the protocols of section 3.3.3 and 3.3.4 respectively. Then, a database of SAF initial conditions was created by selecting 50 instantaneous transmembrane potential maps during ongoing SAF, and keeping them as initial conditions (IC) for the subsequent simulations of spontaneous terminations. An illustration of this procedure is given for the model of recent chronic AF in the upper panel of Figure 4.2. For this model, the first IC was taken after 30 seconds of freely evolving SAF (IC1), and the remaining ones were selected every 5 seconds, IC50 being therefore picked after 4 minutes and 15 seconds of SAF. For the model of paroxysmal AF, the 50 ICs were taken from 9.6 s to 19.4 s after the beginning of pacing, with 200 ms steps. For this model, there was a slight difference in the initiation protocol compared to the one presented in section 3.3.4. Indeed, the ramp pacing protocol was not stopped after 11 s, but was maintained during 20 s. This small modification ensured that each IC was radically different from the others, and therefore led to distinct termination patterns, since at least one pacing pulse could be observed between the different time instants when ICs were taken. Finally, for each of these ICs, SAF simulations were let to evolve freely until spontaneous termination occurred. Following this protocol, 50 different AF termination episodes for each model of AF could be simulated, resulting in a total of 100 simulations of different durations.

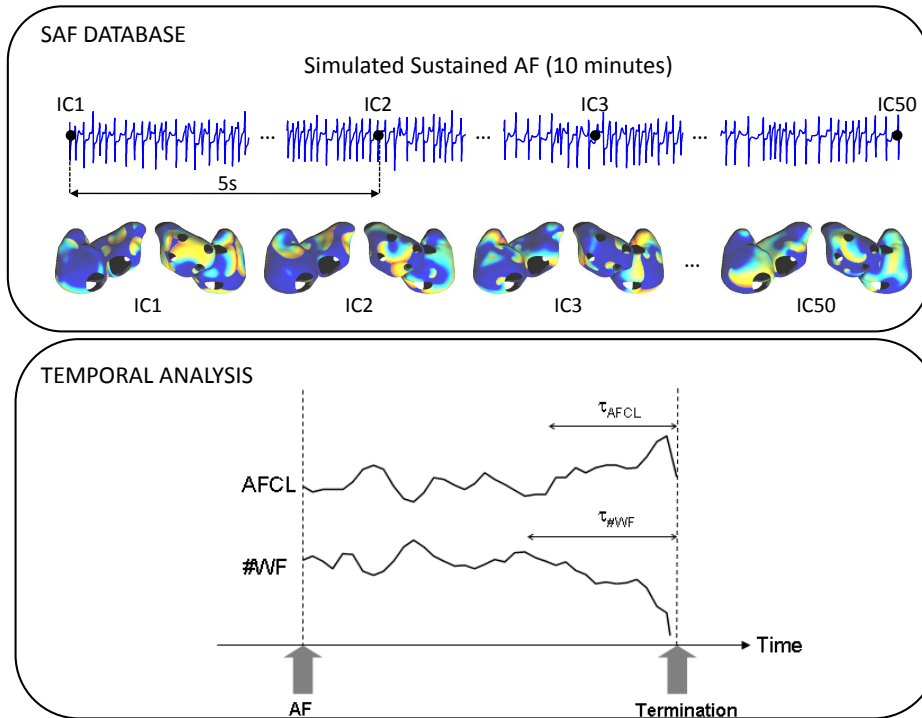


**Figure 4.2:** Simulation protocol and temporal analysis of SAF spontaneous termination. Upper panel: Creation of a database of SAF initial conditions by selecting 50 transmembrane potential maps at regular intervals from simulated sustained AF (Example of the model of recent chronic AF is shown). Lower panel: Scheme of the temporal analysis of both AFCL and #WF averaged across the 50 initial conditions. AFCL represents the spatially averaged AF cycle length and #WF the number of wavefronts present in the atria.  $\tau_{AFCL}$  and  $\tau_{\#WF}$  are respectively the times from the onset of the last AFCL increase or the last #WF decrease prior to AF termination.

### 4.2.3 Analysis of Spontaneous Terminations

#### Temporal Analysis

To assess the time scales involved in the SAF termination process, different parameters were measured during the 8 s preceding termination (Figure 4.2, lower panel). First, the durations of each SAF episode until spontaneous termination were computed. Then, the temporal evolution of AFCL was documented. AFCL was computed as a spatial average of the beat-to-beat intervals measured with 64 electrodes uniformly distributed over the surfaces of both atria (32 on the RA and 32 on the LA). The SAF dynamics was then characterized by two parameters: the number of wavelets present in the atria and the number of wavefronts (#WF). A wavelet was defined as a spatial zone of neighboring atrial cells with a transmembrane potential higher than  $-60$  mV. Wavefronts were defined as the depolarizing fronts of wavelets, computed as the zones located at the edge of a wavelet with a positive derivative of the transmembrane potential. Therefore, there could be more wavefronts than wavelets, as illustrated in Figure 4.3. Finally, the mea-



asures  $\tau_{AFCL}$  and  $\tau_{\#WF}$  were respectively computed as the time from the onset of the last *AFCL* increase and the last *#WF* decrease prior to SAF termination, as illustrated in the lower panel of Figure 4.2. These instants were measured because they were presumed to be triggering mechanisms of termination.

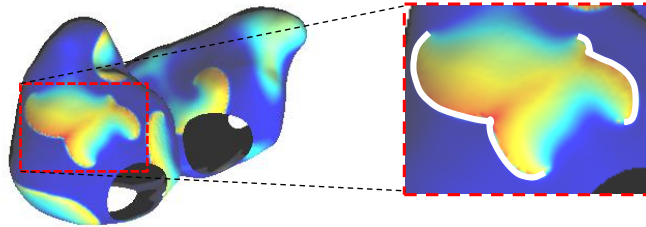


**Figure 4.3:** Example of SAF wavelet with multiple wavefronts observed on an instantaneous transmembrane potential map of freely evolving SAF. The SAF wavelet is shown by a red dashed rectangle. On the enlarged version of the wavelet, two wavefronts can be observed (white continuous lines), which shows that a single wavelet can possibly contain more than one wavefront.

Each measure was systematically computed globally in both atria, and separately in the RA and the LA: statistical comparisons between atria could then be conducted using Wilcoxon ranksum test with differences considered to be significant at  $p < 0.001$ . The sampling period was 1 ms for *AFCL* and 5 ms for *#WF*. In order to observe the temporal evolution of each measure in a smooth manner, a moving average was performed on the *AFCL* and *#WF* with a sliding window of 1000 ms with 100 ms increments.

### Spatial Analysis

The second part of the analysis is aimed at describing systematically the underlying spatial patterns of SAF spontaneous terminations in the AF models under study. For each simulation, the location of the extinction sites of the last active reentrant wavefronts before SAF termination was documented. In most cases, these last wavefronts were annihilated by one or several collisions, generating a bigger and more uniform wavefront that died out in one of the extremities of the geometry a few hundredths of milliseconds later. Therefore, an extinction site was defined as the site where SAF activity terminated, but not necessarily where electrical activity was present last in the atrial tissue. Spatial patterns of spontaneous termination were distinguished according to three different classes of increasing spatial complexity:

- Spontaneous terminations involving a single extinction site.
- Spontaneous terminations involving multiple extinction sites located in the same atrium.
- Spontaneous terminations involving multiple extinction sites located in both atria.

A termination pattern was considered to involve a single extinction site whenever the last reentry observed in the tissue was the only remaining one for a sufficient period of

time  $T_{single}$  before its extinction. Based on preliminary tests, this minimal time interval  $T_{single}$  was defined empirically for each model of AF separately as  $0.3 \cdot AFCL_{mean}$ , where  $AFCL_{mean}$  is the  $AFCL$  averaged across the 50 simulations. This choice was motivated by the fact that the models of AF compared in this study showed very different dynamical properties; adjusting  $T_{single}$  on the mean  $AFCL$  of each model made it independent from these dynamical discrepancies. Finally, whether unilateral termination patterns occurred in the RA or the LA was also documented. Thus, all simulations could be classified within this analysis framework, and binomial tests were run to investigate which spatial patterns had a statistically significant (0.1% significance level) tendency to occur more frequently.

Finally, it was attempted, whenever possible, to group simulations according to the location of their last extinction sites, and to investigate through temporal analysis possibly different termination mechanisms between these groups.

### 4.3 Results

SAF was consistently observed across the 100 simulations as several fibrillating wavelets propagating on both atria, but the dynamics observed presented clear differences depending on the AF model under study. In Table 4.1, average values of  $AFCL$  and  $\#WF$  computed on a SAF episode of 30 s are given for each AF model. Simulated paroxysmal AF was characterized by a smaller number of fibrillating wavefronts ( $6.0 \pm 2.8$ ) present on the atrial tissue compared to the recent chronic AF model, for which an average of  $7.8 \pm 2.7$  wavefronts were detected. Similarly, differences between the models could be observed in the average  $AFCL$  measured on the 30s segment, as the mean  $AFCL$  of the paroxysmal AF model was  $275.0 \pm 53.0$  ms, which is a very slow AF dynamics, whereas the recent chronic AF model had a very fast dynamics with an average  $AFCL$  of  $106.8 \pm 39.8$  ms. Based on these observations, the variable  $T_{single}$  could be set at 80 ms for the model of paroxysmal AF, and at 30 ms for the model of recent chronic AF. Finally, in order to relate each SAF dynamics to the well-accepted classification proposed by Konings et al. [74], an average number of fibrillating wavelets detected on the RA was computed for each SAF model across the 50 simulations. For the model of paroxysmal AF, the average number of wavelets in the RA was  $1.1 \pm 0.4$ . This corresponds to type I and type II AF as described in [74], a dynamics of relatively low complexity. On the other hand, the average number of wavelets in the RA as observed in the model of recent chronic AF was  $2.5 \pm 1.3$ , which represents a more complex AF dynamics of type II to type III.

All 100 simulations performed in this study had different durations, but ended with a spontaneous termination. In Figure 4.4, the histograms of the durations of the 50 episodes of SAF for each AF model are presented. For the model of paroxysmal AF, the mean episode duration was  $8.49 \pm 7.11$  s. However, when looking at the histogram in panel (A) of Figure 4.4, most episodes terminated in an average time of about 6 s and only four episodes lasted much longer (up to 45 s). For this reason, the median and median absolute deviation of the episode duration distribution were also computed,

resulting in a value of  $7.5 \pm 3.93$  s. For the model of recent chronic AF, the mean and median values for episode durations were  $58.47 \pm 56.29$  s and  $47.10 \pm 37.94$  s respectively. The range of possible episode durations was much wider than for the meandering AF model (Figure 4.4(B)), and some particular simulations could show sustained SAF for more than 4 minutes.

#### Paroxysmal AF model

	LA	RA	LA+RA
<i>AFCL</i>	$275.2 \pm 54.3$ ms	$274.9 \pm 51.7$ ms	$275.0 \pm 53.0$ ms
<i>#WF</i>	$3.4 \pm 2.0$	$3.8 \pm 2.0$	$6.0 \pm 2.8$

#### Recent chronic AF model

	LA	RA	LA+RA
<i>AFCL</i>	$106.1 \pm 39.5$ ms	$107.6 \pm 40.1$ ms	$106.8 \pm 39.8$ ms
<i>#WF</i>	$4.6 \pm 2.0$	$4.8 \pm 2.1$	$7.8 \pm 2.7$

**Table 4.1:** Dynamical characteristics of each AF model as computed on a 30s segment of ongoing SAF. Mean values and standard deviations are given for both *AFCL* and *#WF* measures.

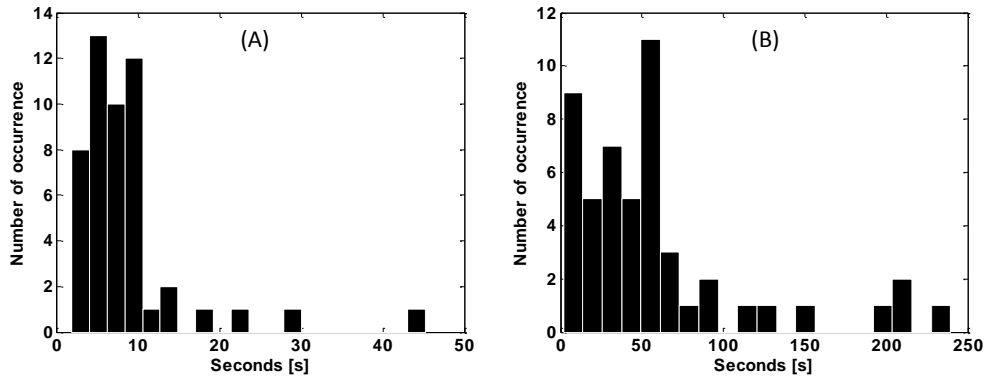


**Figure 4.4:** Histograms of the durations of the 50 episodes of SAF for each AF model. (A) Paroxysmal AF model. (B) Recent chronic AF model.

### 4.3.1 Examples of Simulated Spontaneous Terminations

In this section, two examples of SAF spontaneous terminations are presented, one for each of the AF models under study. Instantaneous membrane potential maps as well as dynamical parameters of the eight seconds preceding termination are systematically shown, in order to illustrate in detail the mechanisms in action during these particular simulations. For the purpose of clarity, a spontaneous termination episode involving a single extinction site is shown for each model.

### Termination in a Model of Paroxysmal Atrial Fibrillation

Figure 4.5 presents an example of SAF spontaneous termination as simulated by the model of paroxysmal AF. In this model characterized by a meandering AF dynamics, SAF showed a low dynamical complexity. Indeed, only 1 to 3 fibrillating wavelets (translating into approximately 6 wavefronts) could be observed on the tissue, and periods with more than 2 wavelets (e.g.  $t = -5470$  ms) were generally short. Most of the time, only 1 or 2 wavelets were observed, and SAF was therefore characterized by massive wavefronts circulating slowly on the atrial surface. Repolarization alternans was also observed during SAF evolution on both unipolar electrogram and transmembrane potentials (panel (B)-(i)-(ii)). Approximately 2.5 seconds before termination, the number of wavelets present in the tissue increased more durably, as can be seen on space plots ( $t = -2450$  ms), and the percentage of excited tissue started to oscillate a few hundredths of milliseconds later. From this point, several collisions between wavefronts progressively decreased the overall complexity of the global activity ( $t = -1310$  ms). At time  $t = -790$  ms, several wavefronts were still present in both atria, but a series of blocks provoked by refractory fronts ( $t = -710$  ms, blocks indicated by thick red lines) occurred; as a result, only one reentry still survived in the RA, while the LA was already free from any fibrillating activity ( $t = -460$  ms). The last reentry spiraled rapidly before being blocked by its own refractory tail ( $t = -380$  ms). At this point, no more reentries were present in the tissue, and only a massive uniform wavefront remained ( $t = -290$  ms), propagating from the RA to the LA appendage and finally leaving the tissue free from any activity ( $t = -130$  ms). Interestingly, repolarization alternans was less present in the 2 last seconds of this example, which supports the hypothesis that the phenomenon of repolarization alternans could be related to vulnerability to AF [140].

### Termination in a Model of Recent Chronic Atrial Fibrillation

Figure 4.6 shows an example of SAF spontaneous termination from the model of recent chronic AF. In this model, the number of fibrillating wavelets observed on the atrial surface could occasionally reach a value of 10, which illustrates the high level of complexity embedded in the dynamics of this particular SAF. Between 8 and 3 seconds before termination, SAF was stable and present on the whole atrial surface. Especially, the number of wavelets was often above five and the percentage of excited tissue remained relatively constant on this time interval, resulting in a globally installed fibrillating activity. Interestingly, a transient oscillation in the percentage of excited tissue could be observed 3 seconds before termination (dashed red circle in panel (B)-(iv)), as if the activity was near termination but somehow found a way to perpetuate itself. This short phenomenon was due to a collision of wavefronts in the LA momentarily depolarizing a major portion of the atrium ( $t = -2820$  ms). Nevertheless, fibrillating wavefronts still present in the RA could rapidly reinitiate SAF in both atria and keep it stable for 2 more seconds. The termination process could be observed only in the 500 last milliseconds, as the percentage of excited tissue started to oscillate strongly and the number of wavelets decreased progressively. This sudden change was provoked by the collisions of multiple wavefronts in the RA ( $t = -490$  ms). As a result, only one wavelet survived (red

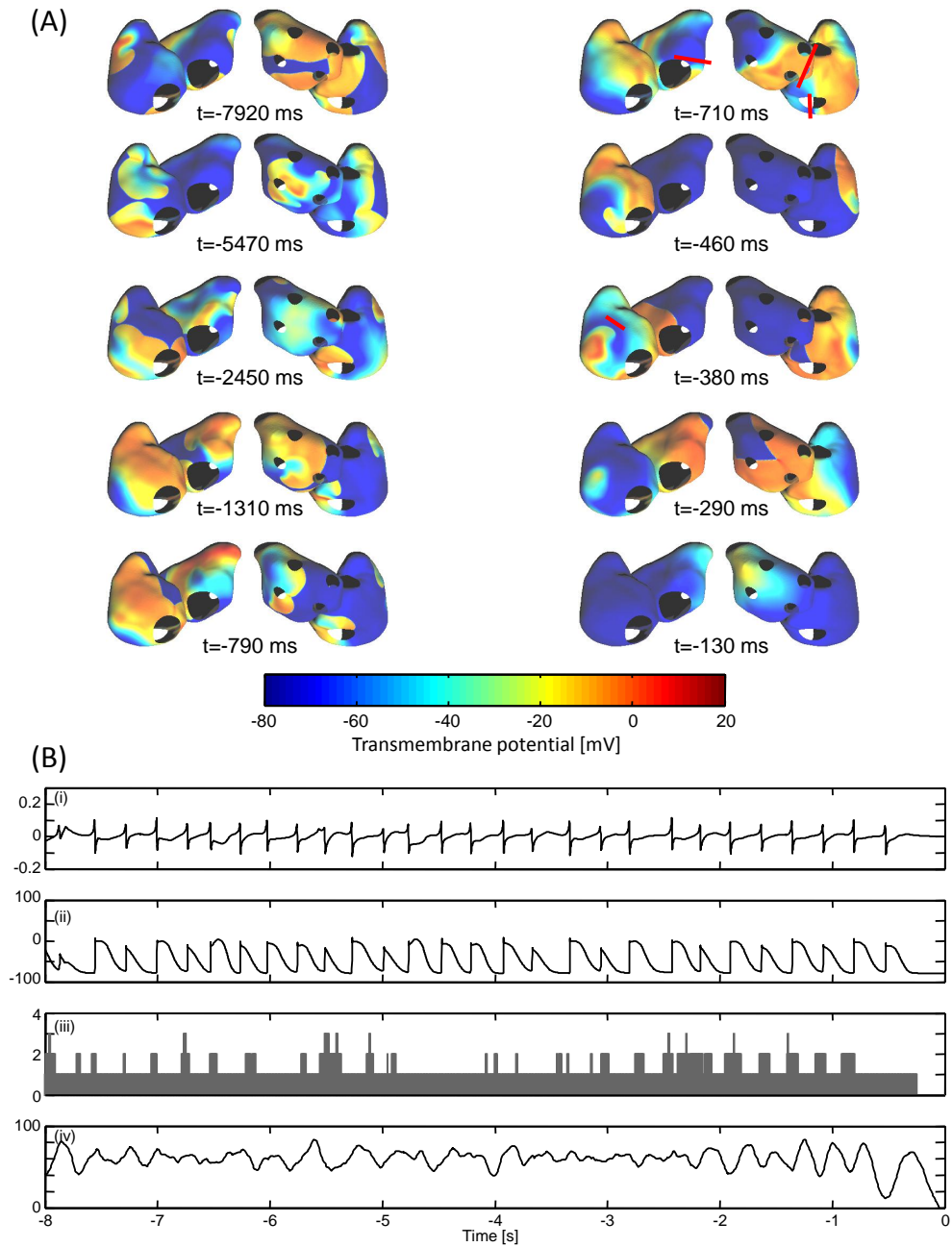


**Figure 4.5:** Example of spontaneous AF termination for the model of paroxysmal AF. This example corresponds to the 8 s preceding spontaneous termination for IC35. In this figure, time 0 stands for the exact instant when no more electrical activation is observed on the atria. (A) Space plots of membrane potentials during SAF directly preceding spontaneous termination. (B) Dynamical analysis of the 8 s preceding spontaneous termination : (i) Simulated unipolar electrogram as measured in the right anterior wall. (ii) Simulated transmembrane potential as measured in the right anterior wall. (iii) Number of fibrillating wavelets present on the total atrial surface. (iv) Percentage of excited tissue.

arrow) and immediately spread into the whole surface of the RA ( $t = -390$  ms) before annihilating itself on its refractory tail ( $t = -370$  ms), leaving the RA free from any reentry. Nevertheless, one or two reentries were still present in the LA ( $t = -280$  ms), but tended to be rapidly extinguished through refractory blocks. The last reentry present in the pulmonary veins ( $t = -230$  ms) was finally blocked ( $t = -210$  ms), creating a last uniform wavefront propagating from LA to RA before total extinction.

### 4.3.2 Temporal Analysis

The temporal evolution of  $AFCL$  and  $\#WF$  averaged on the 50 AF termination episodes for the models of paroxysmal AF and recent chronic AF is presented in this section. On Figures 4.7 and 4.8, dynamical parameters were computed either globally for both atria (continuous line), or separately for the RA and the LA (dashed and dotted line respectively). Thus, differences in the timing of termination between the right and the left atria could be documented.

The mean temporal evolution of the paroxysmal AF model during spontaneous termination is presented in Figure 4.7 and Table 4.2. In this model, termination was characterized by a progressive increase in  $AFCL$  and decrease in the number of fibrillating wavefronts several seconds before SAF extinction.  $AFCL$  started to increase about 3 s before termination on a global scale, but 800 ms earlier in the LA ( $\tau_{AFCL} = 3200$  ms) than in the RA ( $\tau_{AFCL} = 2400$  ms). During these three last seconds,  $AFCL$  became significantly higher in the LA than in the RA, meaning that the LA started to fibrillate more slowly than the RA. In a similar way,  $\#WF$  started to decrease 1800 ms earlier in the LA ( $\tau_{\#WF} = 3000$  ms) than in the RA ( $\tau_{\#WF} = 1200$  ms). Finally, an  $AFCL$  increase in the LA could be observed between 7 and 6 seconds before termination. During this transient of 1 s, the LA was shown to fibrillate more slowly than the RA, as if termination was about to occur. However, during the following second, the number of wavefronts in LA temporarily increased and became similar to the number of waves in the RA, and  $AFCL$  in LA returned to lower values, ensuring SAF maintenance for 5 more seconds.

	Paroxysmal AF model	Recent chronic AF model
$\tau_{AFCL}$ in RA	2400 ms	1600 ms
$\tau_{AFCL}$ in LA	3200 ms	1600 ms
$\tau_{\#WF}$ in RA	1200 ms	1600 ms
$\tau_{\#WF}$ in LA	3000 ms	1600 ms

**Table 4.2:** Temporal analysis of spontaneous terminations. The average timings of the last  $AFCL$  increase and  $\#WF$  decrease ( $\tau_{AFCL}$  and  $\tau_{\#WF}$ ) are given for each model of AF, separately for the RA and the LA.

Figure 4.8 and Table 4.2 depict the mean temporal evolution of spontaneous termination as observed in the recent chronic AF model. Here again, termination was associated with an increase in  $AFCL$  and a sudden decrease in the number of wavefronts circulating on the atria, but the timings involved and the overall dynamics were different from the model of paroxysmal AF, as is shown in Table 4.2. Indeed, dynamical changes in  $AFCL$

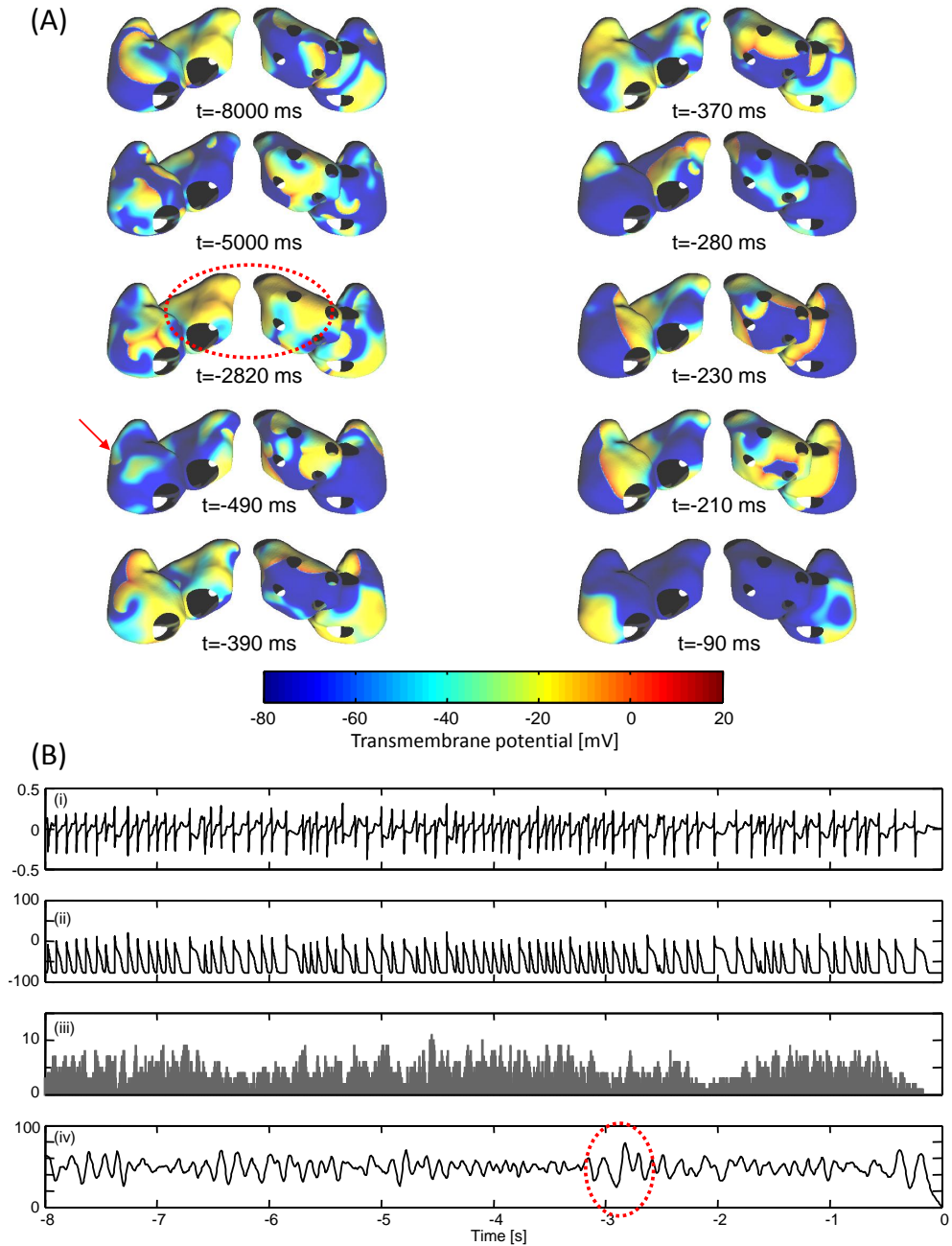


**Figure 4.6:** Example of spontaneous AF termination for the model of recent chronic AF. This example corresponds to the 8 s preceding spontaneous termination for IC37. In this figure, time 0 stands for the exact instant when no more electrical activation is observed on the atria. (A) Space plots of membrane potentials during SAF directly preceding spontaneous termination. (B) Dynamical analysis of the 8 s preceding spontaneous termination : (i) Simulated unipolar electrogram as measured in the right anterior wall. (ii) Simulated transmembrane potential as measured in the right anterior wall. (iii) Number of fibrillating wavelets present on the total atrial surface. (iv) Percentage of excited tissue.

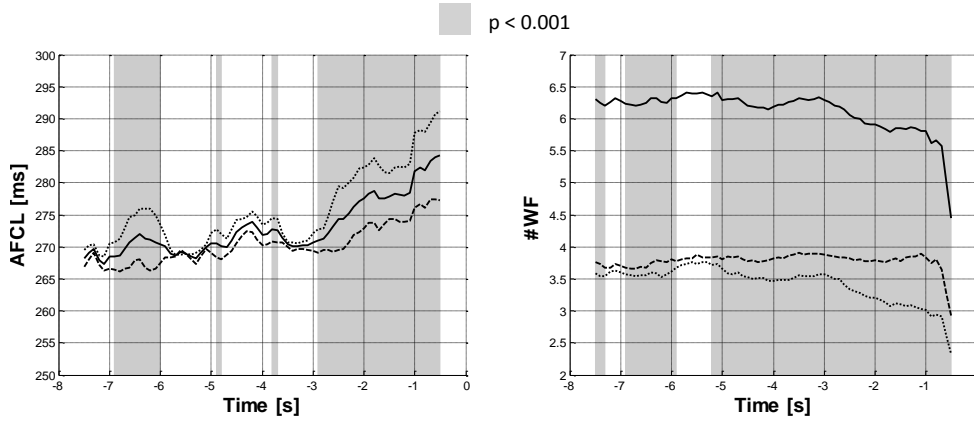


**Figure 4.7:** Temporal analysis of AF spontaneous termination in the model of paroxysmal AF. (A) Mean temporal evolution of AFCL in both atria (solid line), in the RA alone (dashed line) and in the LA alone (dotted line). (B) Same as (A) for the mean temporal evolution of #WF. Instants when a significant difference ( $p < 0.001$ ) could be observed between the RA and the LA are highlighted in grey.

or #WF triggering termination occurred at the same time in the RA and the LA, and at a short time scale compared to the model of paroxysmal AF ( $\tau_{AFCL} = \tau_{\#WF} = 1600$  ms in both atria). During this termination process, AFCL was similar in the RA and the LA, although AFCL had a non-significant tendency to be higher in the RA than in the LA. In addition, there was most of the time a significantly higher number of wavefronts in the RA than in the LA. Finally, like with the paroxysmal AF model, a transient sequence occurring around 6 seconds before termination could be observed; during this short time period, AFCL was higher in the RA than in the LA, and the number of wavefronts in each atrium became temporarily similar.

### 4.3.3 Spatial Analysis

The results of the spatial analysis assessing the localizations of extinction sites for both AF models are summarized in Table 4.3 and Figure 4.9. As before, observations differed depending on the AF model under study. In the model of paroxysmal AF, a clear asymmetry between atria was found in the spatial distribution of extinction sites. First, it was observed that only five simulations presented termination patterns involving multiple extinction sites located simultaneously on both atria, which represents a significant tendency towards unilateral termination patterns compared to bilateral ones ( $p < 0.001$ ). Moreover, among the 45 unilateral terminations, significantly more extinction sites were located in the RA ( $N = 38$ ) compared to the LA ( $N = 7$ ). While the extinction sites of the LA were randomly distributed over the whole atrium, those located in the RA tended to form clusters around anatomical obstacles (Figure 4.9(2)). This was especially so in the posterior part of the atrium, where extinction sites were found to create clusters near the inferior vena cava (IVC) and the superior vena cava (SVC). Finally, no preference for



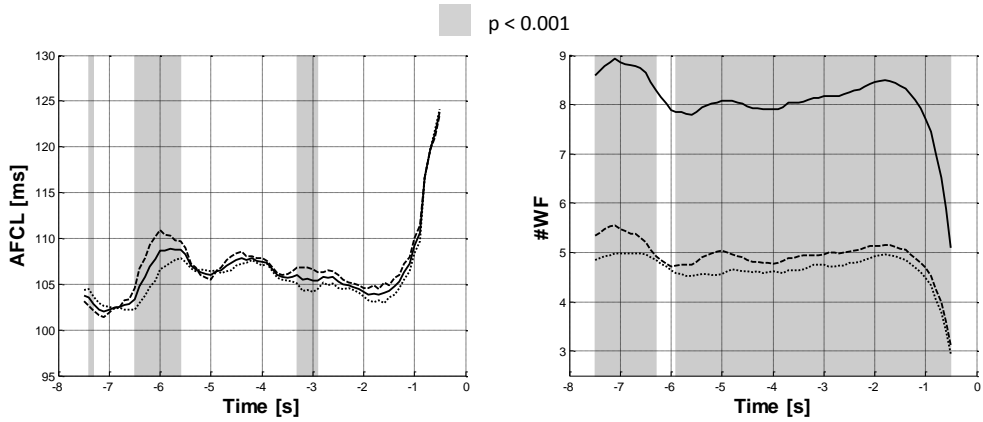


**Figure 4.8:** Temporal analysis of AF spontaneous termination in the model of recent chronic AF. (A) Mean temporal evolution of AFCL in both atria (solid line), in the RA alone (dashed line) and in the LA alone (dotted line). (B) Same as (A) for the mean temporal evolution of #WF. Instants when a significant difference ( $p < 0.001$ ) could be observed between the RA and the LA are highlighted in grey.

termination patterns involving a single extinction site or multiple extinction sites could be observed across simulations.

The spatial asymmetries in termination dynamics observed in the paroxysmal AF model were not present as clearly in the model of recent chronic AF. Indeed, although unilateral terminations were observed significantly more often than bilateral ones, there were no preferred atrial side for termination to occur, as there were no statistical difference in the number of extinction sites observed in each atria. Moreover, it can be seen in Figure 4.9 that extinction sites were regularly distributed over the whole atrial surface, such that no cluster of extinction sites possibly indicating a specific termination pattern could be extracted. Finally, there were no statistical preference for single or multiple simultaneous extinction sites, as for the model of paroxysmal AF.

	Paroxysmal AF model	Recent chronic AF model
Number of terminations in RA	38 (25/13)	25 (14/16)
Number of terminations in LA	7 (5/2)	17 (11/6)
Bilateral terminations	5	8
<b>Statistics</b>		
Termination in LA vs. RA	$p < 0.001$	N.S.
Single vs. Multiple extinction sites	N.S.	N.S.
Unilateral vs. Bilateral terminations	$p < 0.001$	$p < 0.001$

**Table 4.3:** Summary of the spatial analysis of spontaneous terminations. The number of terminations occurring in each atrium and for each AF model is shown. Between brackets, the corresponding number of terminations through single/multiple extinction site(s) is given. Binomial tests are applied to assess the properties of termination patterns.

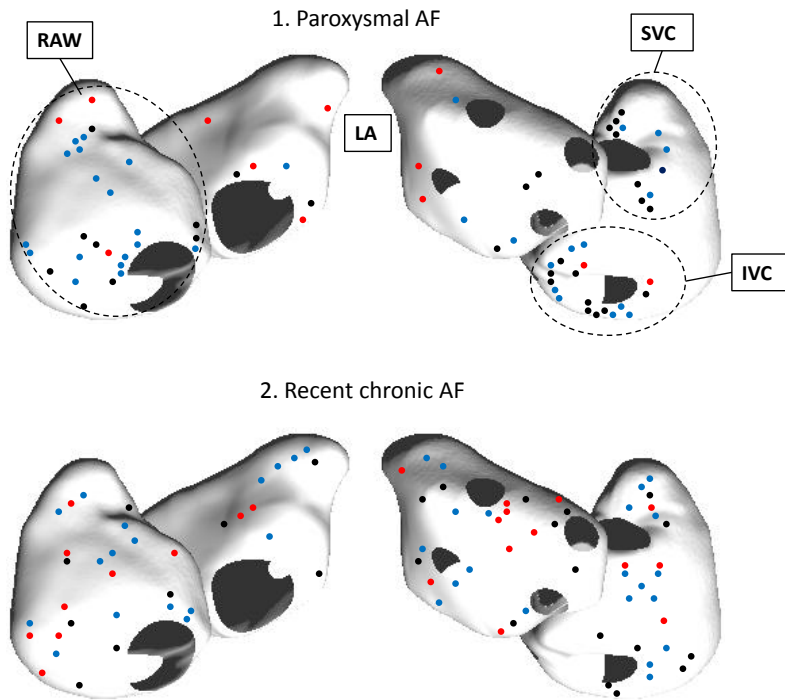


**Figure 4.9:** Spatial distribution of extinction sites for: 1. the model of paroxysmal AF 2. the model of recent chronic AF. Black dots represent spontaneous terminations with a single extinction site, blue dots stand for multiple extinction sites located on the same atrium, and red dots for multiple extinction sites located on both atria. For the model of paroxysmal AF, four subgroups of simulations are distinguished, depending on whether the extinction site(s) are located near the superior vena cava (SVC group), the inferior vena cava (IVC group), the right anterior wall (RAW group) or the left atrium (LA group).

#### 4.3.4 Subgroup Analysis in the Model of Paroxysmal Atrial Fibrillation

Since it was observed in the case of a paroxysmal AF model that clusters of extinction sites located in different areas of the RA could be delineated, it was hypothesized that these clusters could represent subgroups of distinct termination mechanisms. To test this hypothesis, the 50 simulations were divided into four groups of termination episodes, each one corresponding to a specific location of the AF extinction sites (See Panel 1, Figure 4.9). The IVC group (17 simulations) comprised the simulations involving extinction sites in the IVC area (including simulations with multiple extinction sites but at least one in the IVC area). The SVC group (12 simulations) and the right anterior wall (RAW) group (22 simulations) were constructed the same way. Finally, the LA group (12 simulations) was formed by simulations terminating in LA. Figure 4.10 shows the temporal evolution of  $AFCL$  resulting from the separate analysis of the termination episodes in the four groups defined in Figure 4.9. The results confirm that, although there is an increase of global  $AFCL$  a few seconds before termination in all groups, the individual curves differ both in their temporal evolution and in the differences observed

between the RA and the LA, suggesting distinct termination mechanisms.

In the IVC group, it could be observed on the space plots of membrane potentials that the termination process was systematically characterized by the installation of an anchored wave around the IVC approximately three seconds before termination. This macroreentry progressively took control of the LA before auto-annihilating itself on its own refractory tail, leaving the tissue free from reentries. Looking at Panel A of Figure 4.10 and 4.11, this process could be described in more detail. Indeed, three seconds before termination, the *AFCL* in LA increased suddenly from 275 ms to 295 ms in one second, and the number of wavefronts in LA decreased abruptly at the same time. At this point, the macroreentry around the IVC was installed and controlled the LA by sending periodic waves in its direction. Then, the global *AFCL* decreased slowly during the two last seconds, meaning that the macroreentry accelerated progressively, till the point where it hit its own refractory tail and extinguished itself. Interestingly, it can be observed on the *AFCL* evolution that similar patterns could be observed at  $-7$  s and  $-5$  s, where LA was transiently slower than RA. At the same instants, the number of wavefronts in LA decreased to lower values. A possible interpretation is that the installation of the anchored wave around the IVC was done in several steps, during which the macroreentry tried to control the LA but could not do it successfully, because the LA was fibrillating too fast and was not entrained. However, after each aborted attempt, the overall *AFCL* was increased and the number of wavefronts decreased, so that eventually a critical value of global *AFCL* was reached that made it possible for the macroreentry to push away fibrillating activity in LA and take control of it. According to the graphs, the critical values of global *AFCL* and *#WF* for LA control and subsequent termination were  $\sim 275$  ms and  $\sim 3.5$  wavefronts in the LA.

In the SVC group, the average termination pattern showed large variations in *AFCL* during the five last seconds prior to termination. Atrial activity was strongly accelerated and became homogeneous across atria between  $-6$  s and  $-4$  s, as shown by the sudden drop in *AFCL* and the similar value of *#WF* in this time frame. Then, the global activity progressively slowed down. At time  $t = -2.5$  s, the LA started to fibrillate more slowly than the RA (differences in *AFCL*), although the difference was not significant until the last second before total AF extinction. Interestingly, at the same time ( $t = -2.5$ ), the global *AFCL* was near 275 ms and *#WF* decreased below 3.5 in the LA, which are the same critical values found in the IVC group that triggered termination.

In the RAW group, the *AFCL* evolution did not show the instabilities of IVC and SVC group, but remained stable before the first termination mechanisms occurred. Five seconds before termination, the number of wavefronts in the LA started to be significantly lower than in the RA, but remained stable during a couple of seconds. At time  $t = -3$  s, *#WF* in the LA started to decrease under the critical value of 3.5, while global *AFCL* increased to values just below 275 ms. Less than 0.5 s later, *AFCL* became significantly different between LA and RA, as the LA decelerated strongly while the RA kept on fibrillating. Again, this dynamical pattern can be interpreted as a progressive entrainment of the LA by the fibrillating activity of the RA, which was confirmed by visual inspection of the membrane potential space plots. This brutal change in LA dynamics led to termination after two seconds.

Finally, the LA group was characterized by a much more chaotic behavior. Both *AFCL* and *#WF* variables were continuously changing between eight and three seconds prior to termination with no predominance of either atrium, making any interpretation of the phenomenon very difficult. Nonetheless, three seconds before termination, a pattern typical of the other groups could be observed, as the LA started to fibrillate more slowly than the RA when the global *AFCL* crossed the value of 275 ms. However, 1.5 s before termination, a dramatic change in *AFCL* evolution could be observed. The fibrillation in LA suddenly accelerated, simultaneously with an abrupt increase of *AFCL* in RA, leading to termination within one second. Thus, consistently with the other groups of simulations, the atrium where the last reentry was observed had a shorter *AFCL* immediately before termination.

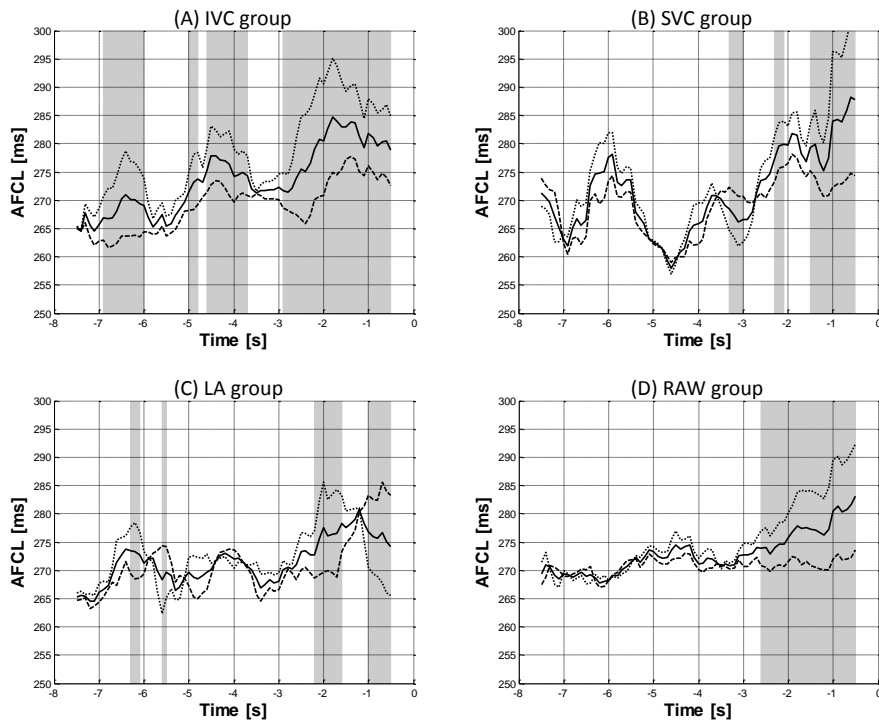


**Figure 4.10:** Mean temporal evolution of *AFCL* in both atria (solid line), in the RA alone (dashed line) and in the LA alone (dotted line) for the different subgroups of simulations defined for the model of paroxysmal AF: (A) IVC group (B) SVC group (C) LA group and (D) RAW group. Instants when a significant difference ( $p < 0.001$ ) was observed between the RA and the LA are highlighted in grey.

## 4.4 Discussion

Spontaneous termination of AF is very difficult to observe, and by extension, to study in detail. First, its occurrence is poorly predictable, and collecting multiple occurrences of the phenomenon requires long observation times. Such acquisitions can be made

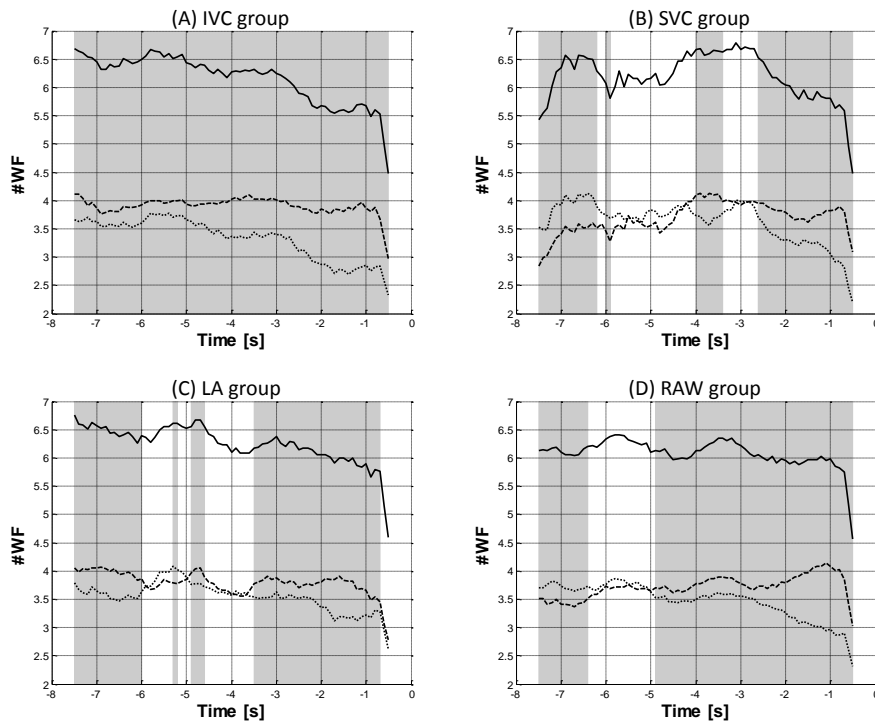


**Figure 4.11:** Mean temporal evolution of #WF in both atria (solid line), in the RA alone (dashed line) and in the LA alone (dotted line) for the different subgroups of simulations defined for the model of paroxysmal AF: (A) IVC group (B) SVC group (C) LA group and (D) RAW group. Instants when a significant difference ( $p < 0.001$ ) was observed between the RA and the LA are highlighted in grey.

using Holter recordings, but the resulting quality of the signals acquired in terms of spatial and temporal resolutions is often relatively low. Finer recordings such as mapping studies can be performed in electrophysiological settings, but with fewer observations. For this reason, only a few studies tried to describe the underlying mechanisms of AF spontaneous termination in the past. In this context, modeling studies represent a complementary approach to provide detailed descriptions of a phenomenon under controlled conditions and with sufficient repeatability, but of course with diminished reliability due to the simplifying hypotheses embedded in the model. This study presented a detailed description of SAF spontaneous termination in both temporal and spatial domains, using two types of AF models with different dynamics. Comparing modeling results and previous experimental findings can shed light on the putative mechanisms of spontaneous termination, and explain why past studies on spontaneous terminations of AF have sometimes led to contradictory conclusions.

The two models of AF used in this study were different in many aspects, including dynamical parameters such as  $AFCL$  or the average number of fibrillating wavelets present on the tissue. More generally, these models made it possible to study termination mechanisms in AFs with different embedded complexities: the model of paroxysmal AF characterized by meandering wavelets could be related to a type I-II AF according

to Konings classification [74], while the model of recent chronic AF was associated to a type II-III. Such observations of increasing disorganization of atrial activity during chronic AF compared to acute AF were reported during epicardial mapping in dogs [141]. Moreover, these dynamical differences could also be observed and interpreted in the results obtained when studying spontaneous termination mechanisms. Indeed, it was observed that the duration of episodes before spontaneous termination was much longer in the model of recent chronic AF than in the paroxysmal AF model. This result is in line with evidence that AF episode durations are longer in persistent and permanent AF than in paroxysmal AF [1, 2, 3]. Taken together, these observations tend to confirm that using the modified Courtemanche model presented in section 3.3.4 based on meandering AF dynamics can be considered as a reasonable model of paroxysmal AF.

#### 4.4.1 Mechanisms of Spontaneous Termination of Atrial Fibrillation

When looking more precisely at the dynamical mechanisms underlying spontaneous terminations, differences could be found between the AF models used in the present study. In the model of recent chronic AF, detectable changes before termination only occurred in the last 1-2 seconds before termination, indicating an abrupt and rapid process. In addition, no difference in timings between LA and RA were observed, nor was it possible to find any recurrent spatial pattern in reentry extinctions. On the other hand, spontaneous termination mechanisms in the model of paroxysmal AF were characterized by a progressive change to increased organization before termination and clear differences in timings between the LA and the RA, with termination mechanisms being triggered earlier in the LA. Moreover, the extinction sites of the last observed fibrillatory activity were also asymmetrically distributed, with a bias towards RA. Therefore, an asymmetry in dynamics between atria was observed in this model in both temporal and spatial domains. A temporal decoupling of atria prior to termination was already reported in clinical observations on human patients with acute or persistent AF, where the earliest detectable event occurred on average 4 s before termination with a significant increase of cycle length in the LA first, followed by an increase in the RA only 1 s later [122]. Similar timings were measured in the present study. The propensity of extinction sites to be distributed asymmetrically and near anatomical obstacles, however, could not be demonstrated yet in clinical studies, although evidence of interactions between AF waves and anatomical boundaries during AF terminations was already demonstrated in modeling and experimental studies [135, 142]. It would be of interest to extend past clinical investigations and search for preferential locations of extinction sites in order to test the additional hypothesis of spatial asymmetry that our modeling approach emphasized. But current acquisition systems such as high-density mapping electrodes still offer limited spatial resolution, and observing the exact spatial patterns of fibrillating activity will represent a major challenge for future studies.

The discrepancies in termination mechanisms between these two models of AF can be better interpreted in the light of the long-lasting debate about putative mechanisms of AF termination that can be found in literature. Indeed, whether AF spontaneous termination is preceded by a progressive fusion of wavelets or involves a simultaneous block

of all wavelets present in the tissue remains an opened question, and past results were mixed. Several studies could demonstrate organization processes preceding spontaneous terminations [120, 122, 125], while other studies could not [123, 124]. Furthermore, no consensus was found about the appropriate time scale of AF spontaneous termination, ranging from several minutes [120] to one second [121]. In the present study, it was shown that for both AF models considered, it was equally likely to observe terminations with single or multiple extinction sites. Therefore, a mechanism of simultaneous blocks of multiple wavelets during termination cannot be discarded. Nevertheless, some organization processes could be observed in both models, although at different degrees. Indeed, in both AF models, spontaneous terminations more often involved extinction sites located in one atrium only. This lateralization of fibrillatory activity prior to termination can be interpreted as an organizing process, as one of the atrium started to control the other before termination occurred. However, additional indicators of organization were observed in the model of paroxysmal AF, such as the progressive decrease of the number of wavefronts or the progressive increase of global *AFCL* several seconds before termination.

Thus, the present study suggests that spontaneous termination mechanisms may differ depending on the dynamics of the AF under study, and especially its underlying complexity. This proposition is in line with previous mapping studies demonstrating the polymorphic nature of spontaneous AF [122]. According to our simulation results for low-complexity AF dynamics such as the ones encountered in simulated acute AF, spontaneous termination processes can be precisely described in both time and space and are characterized temporally by a progressive increase in global atrial organization with distinct timings in LA and RA as in previous studies [122, 125], and spatially by preferential sites of extinction. On the other hand, spontaneous terminations in highly complex AF such as long-lasting persistent AF or recent chronic AF are more difficult to obtain and take place in a less predictable way. This interpretation seems relatively intuitive, since it is well known that the complexity of AF increases over time [141]. However, it remains difficult to confirm these hypotheses experimentally, because observing spontaneous terminations in long-lasting AF such as recent chronic AF is a very difficult task, and no study, to the best of our knowledge, could describe such phenomena on a large recorded database. In this context, modeling studies represent an attractive alternative to investigate the differences in AF termination patterns between distinct stages of the arrhythmia, since it is possible to generate spontaneous terminations of developed AF through the fine-tuning of specific ionic properties as described in section 4.2.1.

#### **4.4.2 Termination Patterns during Simulated Paroxysmal Atrial Fibrillation**

An interesting aspect of modeling studies is the possibility to have access at any instant to the temporal evolution of transmembrane potential maps over the whole atrial surface together with its corresponding dynamical parameters such as *AFCL* or the number of fibrillating wavefronts present on the tissue. Based on this extensive amount of information, we tried to perform in-depth analyses of termination mechanisms in each

AF models with special attention to the spatial distribution of extinction sites. While the model of recent chronic AF did not show any preferential termination sites and was therefore not appropriate for such investigation, it was possible for the simulated paroxysmal AF to identify recurrent termination patterns by grouping simulations according to the location of their extinction sites. Doing so, termination mechanisms that were particular to each group as well as common mechanisms across the four groups were extracted.

Figures 4.10 and 4.11 showed that spontaneous termination mechanisms can vary widely from one termination episode to another. Indeed, temporal traces of both *AFCL* and *#WF* differed markedly in simulations associated to one subgroup of termination or another. For instance, short periods where *AFCL* was transiently longer in LA than in RA could be observed in the IVC group several times before termination, as if termination took place after multiple attempts. In opposition, there was no sign in the *AFCL* evolution of the RAW subgroup that could announce the imminence of termination onset. Another feature is the difference in wavefronts dynamics between the IVC and SVC groups: while there were more wavefronts in RA than in LA in the IVC group during the whole termination process, simulations of the SVC group were characterized by a more homogeneous number of wavefronts between atria during most of the eight seconds preceding termination. Taken together, these differences between spontaneous termination mechanisms illustrate well the multiple facets of the phenomenon and the difficulty to describe it in a complete manner.

Nevertheless, common mechanisms could also be observed between the subgroups of terminations. These mechanisms are of particular interest, as they may constitute a more robust basis for the development of therapeutical approaches. Indeed, the detailed analysis of section 4.3.4 helped to clarify the average termination process of simulated paroxysmal AF that was presented in sections 4.3.2 and 4.3.3. In all four groups of terminations, it could be confirmed that termination involved a decoupling of atria in terms of dynamical parameters several seconds before termination. Indeed, it was consistently observed that one of the atrium systematically started to present higher *AFCL* values and a decreased fibrillating activity, while the other atrium maintained its fibrillatory rate for a longer period of time before termination. Moreover, it was shown that the atrium with the lower *AFCL* was the one where the last reentrant activity could be observed. This decoupling of left and right atria prior to termination was also observed during mapping studies [122], and the modeling approach presented here could therefore further describe the putative mechanisms leading to this decoupling. The proposed mechanistical interpretation of these observations is that several seconds prior to spontaneous AF termination, one of the atria starts fibrillating faster than the other one. As a consequence, the faster atrium sends regular waves towards the other side and entrains the activity of the slower atrium, therefore taking progressively control of it, the same way as a pacemaker would do to capture the atrial electrical activity. The multiple annihilations of reentries taking place in the slower atrium due to the overdriving waves of the faster atrium can explain the progressive decrease of *#WF* and increase of *AFCL* observed before termination. Thus, fibrillating activity becomes lateralized in one atrium, therefore reducing the surface available for reentries to propagate. Following the principle of critical mass



[138, 143], this lateralization in AF dynamics makes it subsequently more probable that wavefronts get annihilated, provoking AF termination.

When looking specifically at *AFCL* and *#WF* prior to termination onset, it was also possible to determine critical values of these parameters provoking terminations. Indeed, it was observed across the four groups of simulations that the decoupling phase between LA and RA was triggered whenever the combination of a global *AFCL* superior to  $\sim 275$  ms and a number of wavefronts in LA inferior to  $\sim 3.5$  were measured. Interestingly, this situation leading to dynamical decoupling of atria occurred with different timings (ranging between 3 and 2 seconds prior to spontaneous termination) depending on the location of the last extinction site. As such, the absolute values of these critical *AFCL* and *#WF* are of little physiological interest, because they are strongly specific to the AF model used in the study. Indeed, due to the low CV of the paroxysmal AF model, its average *AFCL* is known to be higher than accepted values for *AF*. Nevertheless, this observation suggests that specific dynamical states of the atria may act as bifurcation points triggering termination. These dynamical states could be described with information about *AFCL* and wavefront dynamics. In a study of AF ablation, the usefulness of *AFCL* as a quantitative tool for monitoring substrate changes during ablation of ongoing AF was already demonstrated, and prolongation of *AFCL* indicated successful extinction of fibrillating foci [144]. Similarly, it was hypothesized and verified very early that the number of fibrillating wavefronts present on the atria was proportional to the ability of AF to be sustained [96, 97]. Thus, a decrease in *#WF* under a certain level is likely to announce spontaneous termination. Overall, these results suggest that paroxysmal AF spontaneous termination is likely to be preceded by a specific dynamical state of atrial electrical activity. Such consideration is of interest for therapy development, since forcing AF towards this particular dynamical states (*AFCL* increase and *#WF* decrease) could make spontaneous terminations more likely to occur. Interestingly, antiarrhythmic drugs (AADs) somehow provoke similar dynamical changes [11]. For instance, class III AADs prolonge refractoriness without altering CV. Thus, the resulting shortening of the excitable gap is likely to reduce the average number of wavefronts, which can in turn trigger conversion to sinus rhythm. Besides, class I AADs provoke an *AFCL* increase (AF deceleration) through CV reduction.

Despite the various mechanisms of termination proposed above, some observations lack a clear interpretation. First, the reason why AF lateralization prior to termination occurs more often in the RA than in the LA is still unknown. It can be suggested that atrial geometry may have an influence on this phenomenon. Indeed, the total area of the RA is larger than the LA area in the biophysical model used in this study. Therefore, according to the critical mass principle, SAF should more likely terminate in the LA first [138, 143]. However, further investigations will be needed to better understand why extinction sites tended to form clusters near RA valves. For instance, using different geometries (with atria of equal size, differences in diameters of valves and veins, or with a dilated LA) could bring new information about the putative role of atrial anatomy on the process of termination. Finally, termination patterns involving extinction sites located in the LA could not be described in a precise manner. Possibly, the presence of small obstacles such as the PVs make the whole termination process less predictable.

Clearly, more simulations will have to be conducted, because there were not enough occurrences of such termination episodes to obtain a sufficiently clear average pattern.

Although the interpretations proposed in this section remain speculative, the proposed modeling approach brings new insights into the possible mechanisms underlying spontaneous termination and appears useful to complement clinical experiments based on surface electrocardiograms or mapping studies in which detailed and systematic observations of AF terminations cannot be easily performed.

### **4.4.3 Study Limitations**

The biophysical models of AF used in this study have several limitations. First, both cell models used in this work only provide approximate AF dynamics. On one hand, the model of recent chronic AF presents AFCL values between 100 ms and 110 ms, which is slightly shorter than reported clinical values for highly complex AF [74]. On the other hand, the CV of the paroxysmal AF model is too slow, and the resulting AFCL is consequently longer than accepted values. Moreover, the models did not include fibrosis or anisotropy.

Another limitation is that the atrial geometry was based on a three-dimensional monolayer surface and therefore did not take into account atrial tissue thickness. Modeling studies suggested that increasing tissue thickness could add dynamical instability and therefore modulate termination processes [138]. Moreover, several three-dimensional anatomical structures such as Bachmann's bundle, pectinate muscles or crista terminalis were not added to our monolayer geometry. This choice was motivated by the need to assess the effect of more fundamental anatomical structures such as valves or veins on termination. Moreover, in the case of simulated paroxysmal AF, the observed mechanisms of termination seem to be consistent with what has been reported in the literature.

### **4.4.4 Future Works and Clinical Implications**

#### **Guiding Future Fundamental Research**

There is only sparse experimental research investigating the mechanisms of AF spontaneous termination because it is difficult to observe this phenomenon with sufficient precision to accurately describe it. Several guidelines could be derived from the results obtained in this study, in order to design future studies trying to validate experimentally what was obtained in this model-based investigation. First, it was shown that spontaneous termination mechanisms could be very different depending on the stage of the arrhythmia. Most studies so far investigated populations of patients with various histories of AF, sometimes mixing patients with paroxysmal and persistent AF. Special care should be taken in the future to document AF duration and to group patients according to their AF development stage. Such procedure may help uncovering termination mechanisms specific to each AF type. More generally, several observations made in the present work could be the object of targeted experimental validation. For instance, bia-

trial high-density mapping of patients with paroxysmal AF could be used to assess the potential existence of a lateralization process of fibrillating activity prior to AF spontaneous termination. Similarly, such studies could be conducted to explore the spatial distribution of AF extinction sites during termination. However, the latter investigation requires extensive methodological developments, as automatic detection methods to track AF wavelets are better suited for model data and reliable reentry tracking during ongoing AF has not been demonstrated so far [145, 146, 147]. Finally, it was suggested that specific dynamical states of atrial electrical activity could act as bifurcation points and trigger termination, and that changes in *AFCL* or *#WF* could potentially act as indicators of this transition. Recent studies on population dynamics demonstrated that the extinction of a population through transcritical bifurcation could be predicted early by simple variables such as population size [148]. Besides, it was shown that multiple fibrillating spiral waves could be modeled by interacting populations of predators and preys and could be analyzed with this innovative point of view [149]. Merging these studies could provide an interesting analysis framework to better understand dynamical processes preceding AF extinction.

### **Towards New Therapeutic Approaches**

A better understanding of spontaneous AF termination can also inspire new therapeutic approaches that would imitate nature by forcing AF activity towards termination. A major finding of the present work is that different types of AF can potentially present different mechanisms of spontaneous termination. As a consequence, therapeutic strategies aiming at provoking spontaneous terminations should be different depending on whether the patient under treatment is diagnosed with acute or chronic AF. Moreover, in the specific case of a paroxysmal AF, our study suggests that guiding current AF activity towards certain dynamical states, including increased global *AFCL* or decreased number of wavefronts, could promote spontaneous terminations of ongoing AF. Based on these guidelines, innovative non-pharmacological solutions could be designed and tested for the termination of AF; we propose some solutions here, although they remain highly speculative. For instance, low-energy rapid pacing sequences of short duration could be applied to transiently reduce the number of fibrillating waves in the atrial surface, and hopefully trigger termination processes. Ablation schemes involving a minimal number of ablation lines could aim at the same goal, or hybrid solutions could combine both strategies for an optimal outcome. Finally, a better description of the spatial patterns preceding spontaneous terminations could help finding preferential anatomical areas for terminations to occur. Such knowledge could lead to the development of refined ablation procedures that would constrain fibrillating wavefronts into a controlled and robust termination process.

## 4.5 Conclusion

In this chapter, the biophysical modeling framework introduced in chapter 2 and 3 was used to describe important dynamical processes of AF several seconds before its spontaneous termination. Due to the transient nature of AF spontaneous terminations, a modeling approach appears useful as spontaneous termination in various types of AF can be provoked by modifying ionic properties of different AF substrates at will. As a result, it was demonstrated that different levels of AF complexity led to different termination mechanisms, which illustrates the polymorphic nature of AF.

As such, a better understanding of AF spontaneous termination through model-based studies is valuable, since computer simulations can bring new insights into the fundamental mechanisms underlying AF terminations. Based on these modeling results, future experimental studies will hopefully use optimized designs targeted to the precise description of these putative mechanisms. Furthermore, the field of AF therapy may benefit from a better understanding of AF spontaneous terminations, since AF termination processes could be imitated and artificially reproduced to provide more robust and natural therapeutic solutions.

## Part II

---

# **Towards New Therapeutic Strategies for Atrial Fibrillation**

The second part of the dissertation is devoted to the development of new lines of research for atrial fibrillation therapy with the help of biophysical modeling and signal processing methods. The properties of low-energy rapid pacing and its influence on atrial fibrillation is studied in detail in chapter 5. In chapter 6, a novel pacing scheme for the suppression of chronic atrial fibrillation is presented, together with a statistical analysis of its performance in the biophysical model of human atria. In chapter 7, innovative signal processing methods to characterize the level of organization of atrial fibrillation activity are presented, and their use as potential diagnostic tools for AF patient management is demonstrated.



# Rapid Pacing of Atrial Fibrillation: Influence of Pacing Sites, Pacing Cycle Length and Tissue Property

---

# 5

## 5.1 State of the Art of Therapeutic Pacing for AF

The properties of cardiac stimulation were already known in the early 1800s [150], and the first cases of cardiac resuscitations through defibrillation were reported in the 1870s [151, 152]. From 1932, when Hyman first proved the clinical applicability of pacing devices [153], the therapeutic potentials of cardiac pacing became a major focus of attention in the quest for cardiac therapies. In parallel with pioneering studies of cardiac pacemaking allowing ventricular defibrillation [154], valuable efforts were made during the remaining of the 20<sup>th</sup> century to further develop pacemaker devices in terms of battery efficacy, electrode design, transvenous implantation procedures [155] and portability [156]. At the end of the 1980s, some ventricular and atrial arrhythmias could already be treated either by defibrillation [154, 157] or low energy pacing [158, 159].

Therapies for AF were also developed in the light of cardiac pacing. Following the successful model of implantable devices for ventricular fibrillation, internal atrial defibrillation was first proposed in 1993 as a way to reach cardioversion with an energy shock [157, 160]. However, unlike for ventricular fibrillation, an electrical shock aiming at cardioverting an episode of AF cannot be considered as life saving [16]. Thus, the acute pain perceived during such electrical shocks could be considered unacceptable. Moreover, a risk of proarrhythmic effects following atrial defibrillation, possibly leading to ventricular fibrillation, could not be discarded. Such considerations raised doubts about the reliability and justification of atrial defibrillation for the treatment of AF, suggesting the need to find other protocols involving low-energy stimulations<sup>1</sup>.

---

1. From now on, the term "pacing" will implicitly refer to low-energy stimulations.

Overdrive pacing is a sequence of atrial pacing at a cycle length that is shorter than the detected arrhythmia. The goal of the procedure is to access reentrant circuits during any potential excitable gap, take control of AF activity, and possibly terminate it. In 1991, Allesie et al. first demonstrated the existence of an excitable gap during AF induced in dogs, meaning that AF could be paced and entrained with overdrive pacing [161]. This observation was then refined by high resolution mapping [162], and finally demonstrated in humans [163] and during spontaneous chronic AF [164]. In these pioneering studies, the capture obtained was local, restricted to a small area around the pacing site. Nevertheless, it was shown that a local capture in one of the atrium could have a distant effect on the underlying organization of the contralateral atrium [165]. Thus, these results demonstrated the potential of low-energy pacing for the therapy of AF, and an increasing number of both clinical and experimental studies were conducted to investigate therapeutic pacing solutions to AF. Among these solutions, the pacing strategies proposed for the treatment of AF can be divided into two main categories, namely methods for *prevention* of AF on one hand and for *termination* of AF on the other hand. These distinct families of pacing therapies will be reviewed below.

### 5.1.1 Pacing Algorithms for AF Prevention

Preventive methods aim at providing prophylactic pacing schemes to either prevent the appearance of paroxysmal AF or minimize the early recurrences of AF episodes. Since a suppression of compensatory pauses or "short-long-short" cycles is supposed to reduce arrhythmia onsets, most of the preventive pacing schemes are designed to reach this goal [22]. Three families of pacing algorithms were developed for AF prevention [166]:

- *Preferential atrial pacing*: this pacing protocol consists in pacing the atrium at a rate slightly superior to sinus rate in order to entrain the cardiac rhythm and thereby prevent abrupt pauses.
- *PAC response*: it was shown during analysis of stored pacemaker memory data that a significant portion of episodes of paroxysmal AF are triggered by premature atrial complexes (PACs) [167]. Therefore, PAC response algorithms are designed to initiate atrial pacing whenever a PAC is detected, in order to take control of atrial activity.
- *Post-atrial fibrillation termination response*: this algorithm applies atrial pacing for a sustained duration immediately upon AF termination, and then returns gradually to sinus rate in order to suppress PACs. This method is motivated by the fact that AF is more likely to be reinitiated just after an AF episode, as a consequence of electrophysiologic remodeling [92].

Several large clinical studies tried to assess the effectiveness of these preventive pacing algorithms for AF, but reported results have been mixed. During the Atrial Dynamic Overdrive Pacing Trial (ADOPT), preferential atrial pacing efficacy was investigated in 319 patients [168]. Only a small, but significant reduction in symptomatic AF burden over the subsequent six months was observed. The Atrial Septal Pacing Efficacy Clinical Trial (ASPECT) was designed to test a combination of the three preventive pac-



ing schemes described above, randomized to septal or non-septal atrial lead placement [169]. No significant difference in AF burden could be demonstrated, but the frequency of symptomatic AT/AF episodes was significantly lower in therapy group compared with control group only in the septal pacing recipients. During the same year, the Atrial Therapy Efficacy and Safety Trial (ATTEST) evaluated a combination of prevention and termination therapies for AF [170]. The study showed that such pacing strategies did not reduce AT/AF burden or frequency in the patient population under study. One year later, the Prevention of Atrial Fibrillation (PIPAF) study reported a lower AF burden only in a subgroup of patients with a low percentage of ventricular pacing, but no significant difference over the total patient population [171]. In 2006, the so-called PMOP study assessed the efficacy of the post-mode switch overdrive pacing algorithm (utilized by the AT500 pacemaker, Medtronic Inc.), which was designed to prevent new episodes of AF occurring shortly after the termination of a previous AF episode [172]. The study demonstrated that overdrive pacing could be effective in preventing early recurrence of AT/AF, although no significant differences in burden and total number of AF episodes were found in the overall patient population. Nevertheless, a significant reduction in AT/AF burden could be demonstrated in a subgroup of patients with high percentage of early recurrence of AF [173]. In 2007, the AFTherapy study evaluated four different preventive pacing algorithms on patients with paroxysmal AF [174]. Although a 37% lower mean AF burden was observed in the therapy group, no statistically significant difference could be found compared with patients treated with conventional pacing. The same year, the Pacemaker Atrial Fibrillation Suppression (PAFs) study evaluated the effect of atrial overdrive and ventricular rate stabilization pacing algorithms in patients with paroxysmal AF. Although the percentage of AF induced by PACs was significantly reduced, total AF burden, patients' symptoms and quality of life did not show any differences between therapy and control groups. A more recent study of Atrial Pacing Preference (APP) presented in 2008 showed that preferential atrial pacing could possibly reduce the number of AF episodes and thus represent a promising alternative, although the observed reduction of the total duration of AT episodes did not reach statistical significance [175]. Finally, a large-scale Study of Atrial Fibrillation Reduction (SAFARI) tested different preventive algorithms in a worldwide prospective randomized clinical trial [176]. This study reported a modest but significant reduction of AF burden in the group with prevention therapies, while no change in AF burden was observed in the control group. Moreover, a subgroup of patients with high AF burden at baseline showed an even greater decrease of AF burden when treated with preventive pacing schemes.

Taken together, these results are not conclusive on the real potential of preventive AF pacing, and several limitations of these studies and of the proposed pacing schemes have to be kept in mind. Importantly, these algorithms have not been studied over long periods of time. Potential problems of patient discomfort or tachycardia-induced cardiomyopathy may arise during long-term application of the proposed pacing sequences. Especially, continuous overdrive pacing is unlikely to be well-tolerated in the long term. In addition, several studies found significant results only in subgroups of the total patient population under study. Since each preventive pacing algorithm presented above aims at specific but different AF-inducing mechanisms to prevent AF occurrence, this

observation suggests that the exact AF-onset mechanism of a given patient plays a determining role in the efficacy of the algorithms used to prevent AF [177]. It would be therefore necessary to treat each case on an individual basis, which would considerably complicate the preventive approach for AF pacing therapy.

### 5.1.2 Pacing Algorithms for AF Termination

On the other hand, pacing solutions for the direct termination of detected AF episodes were also investigated, both during clinical studies and in electrophysiological experiments. The demonstration of the existence of an excitable gap in dogs and humans during AF [161, 163] motivated the testing of overdrive pacing. Moreover, standard overdrive pacing protocols such as 50 Hz pacing bursts and ramps were already programmed in implanted devices, and could directly be tested for AF treatment. In 1997, three pioneering studies tested the ability of overdrive pacing to terminate AF. The first study applied 50 Hz burst pacing at the high right atrium in patients with atypical atrial flutter or AF [178]. While burst pacing of AFL patients resulted in a termination success rate of 60%, no termination could be observed in patients with AF. Similarly, Paladino and colleagues tried to terminate AF in 28 patients with a 50 Hz burst pacing either by single-site pacing in the high right atrium or by multi-site pacing in the high right atrium, mid septum and coronary sinus [179]. As a result, no pace-induced termination of AF was observed. Finally, in electrophysiological settings, Pandozi et al. were able to capture atrial tissue with rapid pacing but failed to terminate AF [164].

These pioneering studies were followed some years later by large-scale clinical studies made possible by the refinement of implanted devices and by the development of automatic detection of AT/AF episodes integrated in the devices [180, 181]. The performance of the 50 Hz burst pacing applied to detected AT/AF episodes was assessed by Gold and colleagues, resulting in a termination success rate of 22.7% for AF episodes [182]. A similar study found an AF termination success rate of 24%, with a significant decrease of arrhythmia burden [183]. Two other studies with the same protocol showed slightly lower, but still impressive AF termination success rates of 13.5% and 16.8% [184, 185].

These termination success rates can be considered surprisingly high, and even misleading when compared with the first electrophysiological experiments, where AF could not be terminated at all [164, 178, 179]. However, it was rapidly demonstrated that the embedded automatic detection algorithms could not always reliably distinguish between AF and more organized AT episodes, resulting in misclassifications of arrhythmia [181, 186]. Therefore, since AT episodes are more easily terminated by burst pacing, overestimated success rates for pace-induced AF termination could be expected. Moreover, it was shown by Schmitt and colleagues that spontaneous terminations of AF were sometimes detected and classified as successful therapeutic interventions by implanted devices [181, 187]. Thus, the above results must be considered carefully. In a large-scale evaluation of the 50 Hz burst pacing on paroxysmal AF episodes, a termination success rate of 29.8% was first observed for detected AF episodes [180]. However, after careful inspection of the detected AF episodes, an average AF cycle length of more than 200 ms

was observed, which is too high for AF and is certainly due to imperfect classifications of the automatic detection algorithms. Selecting only the episodes with an AF cycle length under 160 ms, the termination success rate dropped to 11%. The issue of wrongly classified spontaneous termination episodes was not considered in this study. In another work by Mitchell and colleagues, in which spontaneous termination episodes were controlled, both ramp pacing protocols and 50 Hz burst pacing failed to terminate a single case of persistent AF [25]. Other studies sorted the detected AF episodes in terms of their underlying organization. Israel and colleagues distinguished atrial flutter, highly organized AF episodes, and complex AF episodes [188], and applied both adaptive ramps and 50 Hz burst pacing on each group. While termination success rates of 62% and 34% were obtained for atrial flutter and highly organized AF respectively, no success at all was observed for the complex AF group. Similarly, an organization index based on spectral analysis was used to detect periods of highly organized AF in dogs and to trigger a 20 Hz burst pacing [189]. The study showed that synchronizing the burst pacing sequence with the beginning of an organized AF segment could significantly improve subsequent termination success rates during both single-site and bi-atrial pacing.

Several larger clinical studies were then conducted to assess the efficacy of ATP protocols for AT/AF termination on a larger scale. Published in 2003, the Atrial Therapy Efficacy and Safety Trial (ATTEST) was a prospective and randomized study to evaluate preventive pacing and two ATP protocols (ramp and burst pacing) in patients with AF and AT [170]. Using the automatic criteria for successful termination embedded in the device, ATP protocols applied to AT and AF episodes indifferently resulted in a termination success rate of 54%. Once again, AF episodes could not be clearly separated from AT episodes, and spontaneous terminations were possibly counted by the device as successful therapeutic interventions, which explains this high score. Moreover, the study failed to demonstrate statistically significant differences in AT/AF burden and AT/AF frequency between the groups with ATP algorithms engaged and controls. During the same year, Hügl and colleagues tested the possible benefits of more aggressive ATP protocols (incremental programming) compared to the usual sequences programmed in implanted devices [190]. Although aggressive programming showed a modest but significant improvement in efficacy compared to nominal programming, no differences were found in AT/AF burden or frequency. During a similar study to test the efficacy of ATP sequences and their effect on AT/AF burden, the patient population was divided in a group with high ATP efficacy and low ATP efficacy [191]. In the high efficacy group, following ATP initiation, total AT/AF burden decreased significantly; however, total AT/AF burden increased slightly but significantly in the low efficacy group, illustrating the issue of patient-specific performance of ATP therapies. In 2006, during the Pitagora (Prevention Investigation and Treatment: A Group for Observation and Research on Atrial arrhythmias) study, another comparison was made between ramp pacing and 50 Hz burst pacing [192]. Ramp pacing was shown to be more effective in terminating AT episodes, with its efficacy being directly correlated with the cycle length of the AT under treatment. However, neither ramp pacing nor burst pacing showed any clear ability to terminate AF episodes. Similar findings were obtained in the Prevention and Termination (POT) study, where ATP sequences were tested on top of preventive

pacing algorithms [193]. While a significant reduction of AF burden could be obtained when performing preventive pacing, no incremental benefit was observed when ATP was activated in the therapeutic sequence. A recent study of Gillis and colleagues with the same design resulted in even worse conclusions [24]. When applying preventive pacing combined with ATP sequences, the AT/AF burden did not change over a 3-years follow-up period. However, when applying ATP pacing sequences alone, the AT/AF burden increased significantly over time.

These results demonstrate that current pacing strategies to terminate AF are not efficient, if not inappropriate; considerable research and developments will be needed to finally come up with a reliable pacing solution for AF termination. Recently, innovative developments were proposed as an alternative to low-energy pacing for terminating AF episodes [194, 195, 196, 197]. The method called *far-field antifibrillation pacing* consists in the delivery of a short train of low-intensity electric pulses at the frequency of current ATP sequences, but from field electrodes surrounding the atria. The electric field created by the field electrodes during the applied burst sequence takes advantage of the heterogeneities of the atrial tissue by abruptly changing their potential, and therefore creating secondary sources that act as virtual pacing electrodes [194]. The number of these virtual electrodes increases as the electric field becomes stronger, which in turn maximizes the efficacy in terminating AF. When testing the method in isolated perfused canine atrial preparations, it was shown that a series of pulses from field electrodes is sufficient to terminate atrial arrhythmias including AF and atrial flutters with a success rate of 93% [195]. A recent study conducted in a rabbit model using the same method was shown to be even more successful, with AF termination rates of 100% [197]. Although this method could be a promising approach, important drawbacks must be mentioned. First, it is not clear whether the stimulations applied would be below the pain threshold. Although a single pulse uses only 13% of the energy required for defibrillation, it is likely that a series of pulses during a burst pacing sequence could affect pain perception, as it is well known that a series of shocks seems more painful than a single shock, and subsequent shocks subjectively feel stronger even when they are weaker than previous shocks [198]. Finally, such pacing system with field electrodes is more complicated to design and implant than catheter-based pacing devices, and could certainly not be implanted in a minimally invasive way with current technologies. Therefore, it is still of the utmost importance to search for low-energy pacing algorithms that could be directly programmed in current implanted devices and terminate AF in a reliable way. Very recently, the septal area was proposed as a potentially serious pacing site candidate. The Septal Pacing for Atrial Fibrillation Suppression Evaluation (SAFE) study, launched in 2009 and currently ongoing, is a single-blinded, parallel randomized multicenter study to assess the therapeutic potential of septal pacing in patients with paroxysmal AF [199]. In this dissertation, several studies were conducted with our biophysical model to better understand the mechanisms and influences of pacing applied to AF. A systematic study of rapid pacing in several pacing sites including the septum is proposed in this chapter, and in chapter 6, a septal pacing algorithm for AF suppression is presented together with its termination success rates when tested in the biophysical model.

## 5.2 Motivation of the Proposed Study

So far, rapid pacing of AF was shown to induce a local capture of the atrial tissue but no pacing solution was successfully proposed to terminate AF consistently, although these algorithms are of interest since they appear to be safe and usually add little incremental cost [176, 200]. Moreover, clinical studies often focus on AF frequency and burden but few of them are aimed at evaluating the effect of AF pacing on the atrial tissue [201]. A better understanding of the ability to induce local capture in atrial tissue may have implications for the design of pacing algorithms for AF termination.

The purpose of the study presented in this chapter is to systematically determine the conditions leading to capture of AF by rapid pacing and to understand more fully the influence of atrial tissue properties in our biophysical model of human atria. Mapping experiments are routinely carried out on a limited fraction of the atrial tissue and thus provide an incomplete view of its electrical activity. Moreover, a large variability in the range of frequencies leading to AF capture has been observed in different experimental models. We propose here a model-based approach, which enables access to any variable of interest at any time and provides the possibility of repeating experiments under controlled conditions. Different AF dynamics in terms of conduction velocity and action potential duration as well as multiple pacing sites were studied, in order to have a general view of AF capture properties in the computer model used. This work was the object of two publications [139, 202].

## 5.3 Methods

### 5.3.1 Reference Model for Sustained AF

In this study, the MRI-based biophysical model of human atria described in chapters 2 and 3 was used. The simplified design of its three-dimensional monolayer geometry permitted the simulation of long runs of AF (minutes of real time), while the geometry still included all major anatomical obstacles to propagation, as shown in the left panel of Figure 5.1. Three-dimensional anatomical structures such as Bachmann's bundle, pectinate muscles or crista terminalis were not included. The model was specifically designed to investigate the effect of the dynamics of AF (wavelength, excitable gap) on the success of rapid pacing of AF regardless of structural factors (although thought to probably play an important role).

The propagation of atrial electrical activity was computed on the atrial geometry exactly as presented in detail in section 3.3.3. The coarse discretization (0.6 mm) selected for this model was motivated by the need to simulate thousands of 30-seconds runs of AF, which represented a significant amount of computational load.

At each node, electrical cellular activity was modeled by the remodeled modified LRI model presented in section 3.3.3 [35, 60, 91]. All nodes were assigned the same ionic properties, and conduction anisotropy was not considered. The model was adjusted

to mimic electrical remodeling as observed in permanent AF, such as shortening of APD, as shown in the right panel of Figure 5.1 [56]. For the reference model for sustained AF, channel conductances were parametrized exactly as in section 3.3.3: the  $K^+$  channel conductance was set to  $G_K = 0.423 \text{ mS/cm}^2$ , the  $Na^+$  channel conductance  $G_{Na} = 16 \text{ mS/cm}^2$ , and the L-type  $Ca^{2+}$  channel conductance to  $G_{si} = 0.055 \text{ mS/cm}^2$ , resulting in an APD value of 242 ms. With the resistivity value  $\rho$  set at  $250 \text{ }\Omega\text{cm}$  the mean CV during sinus rhythm was  $60 \text{ cm/s}$ .

SAF was initiated as described in section 3.3.3, by 20 Hz pacing for 3 seconds in the sinoatrial node region (Figure 5.2). When pacing was stopped, SAF was sustained and was allowed to evolve freely during 10 minutes. The resulting SAF dynamics showed multiple reentrant wavelets that continuously changed in size and direction, accompanied by important variations in AFCL over time. This model provides a tool to explore the mechanisms of rapid pacing applied to AF sustained by multiple wavelet reentries, in the absence of ectopic foci or influence of the autonomic nervous system.

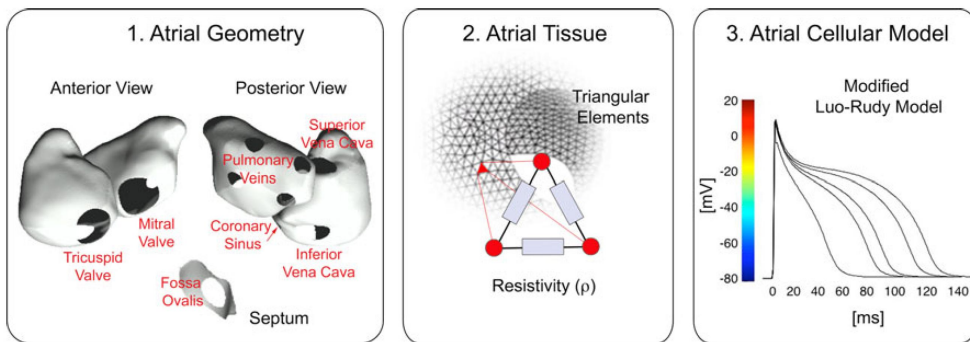


**Figure 5.1:** *The biophysical model of AF and its components. 1. Atrial geometry. 2. Atrial tissue: resistivity  $\rho$  sets CV values. 3. Atrial cellular model:  $K^+$  channel conductance  $G_K$  sets APD values. The shape of the action potential is represented for the reference model of sustained AF for the following pacing cycle length values: 80, 100, 120, 150 and 200 ms.*

### 5.3.2 Variants of the Reference Model

Using the same geometry, four variants of the reference model were specified by setting either the CV values at  $50 \text{ cm/s}$  ( $\rho = 300 \text{ }\Omega\text{cm}$ ) or  $70 \text{ cm/s}$  ( $\rho = 200 \text{ }\Omega\text{cm}$ ), or by changing the intrinsic APD values of the cells through modifications of  $G_K$  (Figure 5.1), all other parameters remaining the same. Longer APD values of 248 ms were obtained with  $G_K = 0.402 \text{ mS/cm}^2$ , while  $G_K = 0.5 \text{ mS/cm}^2$  provided shorter APDs of 228 ms. These four variants represent models with different AF dynamics.

### 5.3.3 Characterization of AF Dynamics

In computer modeling, a direct and complete access to transmembrane potential maps is possible at any time. These maps were color-coded, red representing a depolarized cell and blue, the resting potential (Figure 5.1). The link between simulation results and clinical or electrical mapping data was provided by the simulation of endocardial electrograms at any location of interest. The extracellular potential (unipolar electrogram) was modeled using a current source approximation for large homogeneous volume conductor as described in section 2.3.3 and in Jacquemet and colleagues [69]. AFCLs were computed from electrogram interbeat intervals.

During sinus rhythm the average CV value across all nodes was obtained from a map of activation gradients computed over the whole surface. APD values were defined as the intervals between  $-60$  mV level crossings during propagation, paced at 100 bpm. An estimate of the wavelength [91], defined as the distance traveled by the depolarization wave during the effective refractory period, was obtained by the product of CV and APD, the latter being taken as a surrogate for the effective refractory period [53].

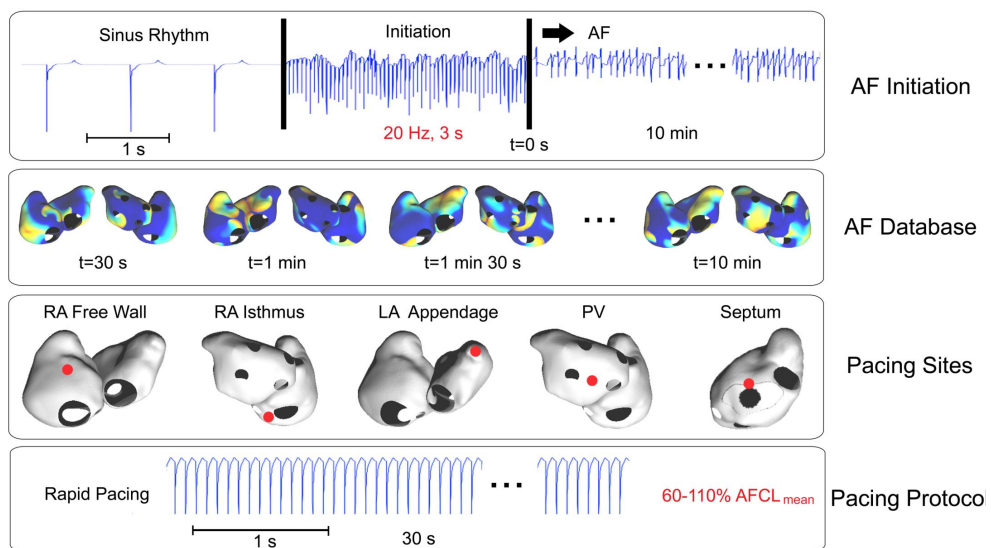


**Figure 5.2:** Simulation of rapid pacing in the biophysical model of AF. 1. AF initiation. 2. AF database created from 20 transmembrane potential maps at 30 seconds intervals during sustained AF. 3. The five pacing sites studied. 4. Application of rapid pacing at cycle lengths based on  $AFCL_{mean}$ .

### 5.3.4 Rapid Pacing Protocol

#### AF Database

From the 10 minutes of sustained SAF, 20 instantaneous transmembrane potential maps were selected at 30-second intervals to form an SAF database. These maps dif-

ferred in terms of activation patterns (Figure 5.2, second row) and were taken as initial conditions for the application of the rapid pacing protocol, for purposes of subsequent statistical analysis.

### **Pacing Sites and AF Dynamics**

Single-site rapid pacing during SAF was evaluated at five sites (Figure 5.2, third row): two sites on the RA, two on the LA, and one on the septum. These pacing sites are regions that are accessible with clinically used stimulation electrodes. For each atrium, one site was located away from anatomical obstacles and the other site was close to major vessels. A comparison of the results at the five pacing sites was performed using the reference model for sustained SAF. Pacing results for the four variants of the reference model (changes in CV or APD) were simulated for the pacing site located in the RA free wall only.

### **Pacing Protocol**

Rapid pacing at constant cycle length was studied systematically. For each pacing site, pacing cycle lengths were based on a mean AFCL ( $AFCL_{\text{mean}}$ ) computed at the pacing site over 1 minute of sustained SAF. Twenty-six pacing intervals were tested in the range 60-110%  $AFCL_{\text{mean}}$  with 2% increments. The duration of each pacing episode was 30 seconds, a value based on preliminary studies indicating that AF capture could be typically achieved within this time window.

#### **5.3.5 Assessment of AF Capture**

The assessment of local capture was based on results published on humans [164]. For each pacing site, electrograms were computed at four nodes on a circle of  $\sim 2$  cm radius centered on the pacing site. During pacing, a node on the circle was considered to be entrained if during at least five consecutive beats the measured cycle length was within  $\pm 3$  ms around the pacing cycle length. Capture was achieved if at least three out of four nodes were entrained (Figure 5.3, panel A). By definition, this type of capture is local only, and can not be generalized to a global capture of both atria. Temporal properties of capture were quantified by the following variables (Figure 5.3, panel B). The percentage of capture was the percentage of time spent in capture during the total pacing sequence of 30 seconds. The capture window was defined as the range of pacing cycle lengths for which the percentage of capture was above 70%. Within the capture window, time to capture was defined as the duration from the beginning of pacing to the onset of the first capture episode. Capture robustness was the percentage of time spent in capture between the first capture episode and the end of pacing. The spatial extent of capture, specified by the area of capture, was assessed for each pacing site.



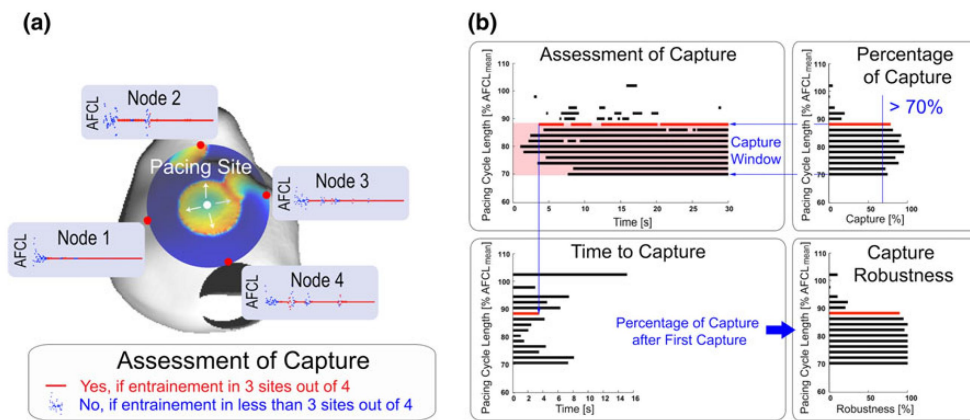


**Figure 5.3:** AF capture assessment. (a) Local capture defined if 3 out of 4 nodes on a circle of 2 cm radius around the pacing site were entrained. (b) The quality of capture, quantified by percentage of capture, capture window, time to capture, and capture robustness. The bars highlighted in red correspond to the example in panel (a), representing one simulation at 88%  $AFCL_{mean}$  pacing cycle length.

### 5.3.6 Statistical Analysis

Results were averaged across the 20 SAF initial conditions in order to minimize the bias resulting from a single, random testing of the pacing protocol. Variables were reported as mean  $\pm$  SD. Comparisons were performed using Wilcoxon's rank sum test. Results were considered to be statistically significant at  $p < 0.01$ .

## 5.4 Results

### 5.4.1 Local Capture of AF

For each of the five pacing sites tested in the reference model, all 26 pacing cycle lengths were tested and results were documented for 20 SAF initial conditions, resulting in a total of 2600 simulations. Similarly, 2080 simulations were carried out for the four AF models with modified dynamics at the single RA pacing site. In all the 4680 simulations performed no AF termination could be observed. Different degrees of local capture could be achieved depending on the pacing site, the pacing cycle length and the SAF dynamics.

Figure 5.4 shows an example of progressive local capture in the RA free wall. After one second of pacing at 80%  $AFCL_{mean}$ , a capture episode was observed with the pacing-induced wavefront being fast enough to spread in the RA free wall, gradually blocking AF reentries. However, AF reentrant wavefronts could still enter the paced area during the installation of capture, resulting in a transient loss of capture after two seconds of pacing. After about four seconds, robust local capture was achieved in the anterior RA,

with a regular electrogram phase-locked to the pacing cycle length.

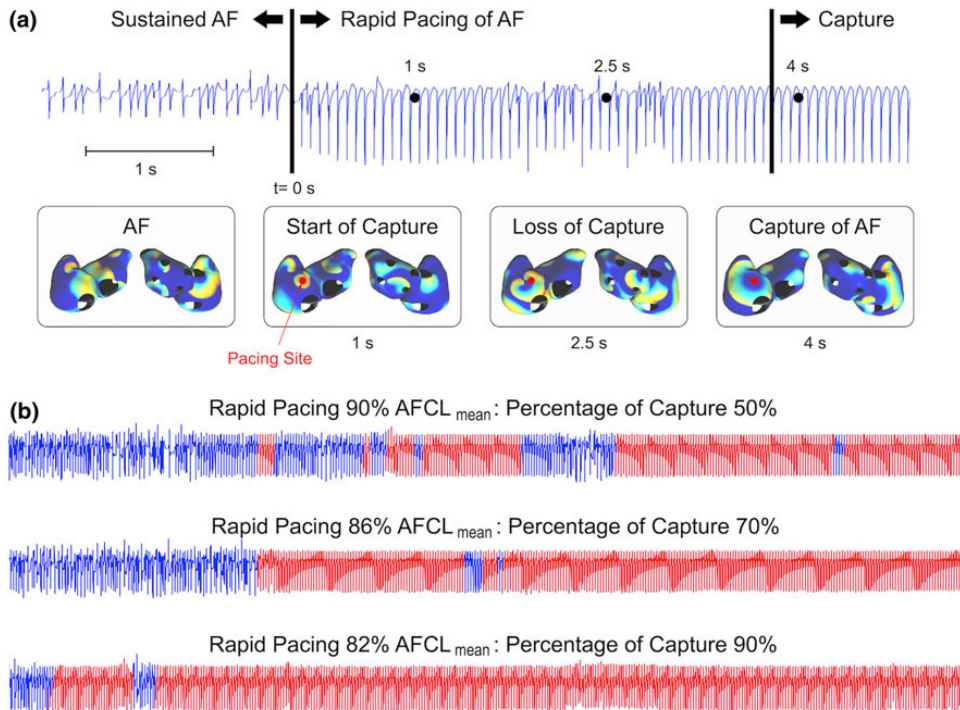


**Figure 5.4:** Example of local capture by rapid pacing in the RA free wall. (a) Upper row: electrogram at the pacing site. Bottom row: transmembrane potential maps at the time of the black dots on the electrogram. The transmembrane potential map on the left represents the element of AF database on which rapid pacing at 80% AFCL<sub>mean</sub> was started. After 1 second of pacing, the first phases of capture can be observed, followed by a loss of capture after 2.5 seconds. Finally, at about 4 seconds, the RA is captured. (b) Examples of electrograms and percentages of capture for rapid pacing in the RA free wall at 90, 86 and 82% AFCL<sub>mean</sub>. Rapid pacing was applied during 30 seconds, and the segments where local capture was observed are represented in red.

## 5.4.2 Temporal Aspects of AF Capture

### Successful AF Capture

Three pacing sites led to capture during more than 70% of the total pacing simulation time (Figure 5.5): RA free wall, LA appendage, and PV, with capture windows of 72-88%, 68-80%, 70-84% AFCL<sub>mean</sub> respectively. The capture window bounds, expressed as a percentage of AFCL<sub>mean</sub>, were not statistically different for PV and RA free wall ( $p > 0.03$ ), but significantly lower for the LA appendage ( $p < 0.01$ ). No significant difference was found between the widths of the capture window at these three sites ( $p > 0.23$ ), which was on average  $14.6 \pm 3.0\%$  AFCL<sub>mean</sub>. Capture windows computed from the literature are shown in Table 5.1. Widths of the capture window were in the range 14-16% AFCL<sub>median</sub> in dogs and 8-25% AFCL<sub>mean</sub> in humans.

For each of these three pacing sites, an optimal pacing cycle length was identified in the middle of the capture window, which also corresponded to the shortest time to capture and the highest capture robustness (Figure 5.5). For these optimal pacing cycle lengths, no significant difference in time to capture ( $p > 0.16$ ) and capture robustness ( $p > 0.19$ ) was observed across pacing sites.

### Unsuccessful AF Capture

When pacing in the RA isthmus or in the septum, the average percentage of capture did not reach 70%, although sporadic capture episodes could be observed in the same range of pacing cycle lengths as reported for the other sites (Figure 5.5). Interestingly, the different curves obtained for the septum were bimodal, although one of the modes (78% AFCL<sub>median</sub>) tended to show better capture with greater robustness. Compared to the pacing sites with capture above threshold, capture robustness was significantly reduced ( $p < 10^{-4}$ ) at optimal pacing cycle length for both RA isthmus and septum, while time to capture remained similar ( $p > 0.06$ ). Pacing the septum tended to yield a higher percentage of capture ( $p < 0.03$ ) and higher capture robustness ( $p < 0.02$ ) than for RA isthmus pacing.

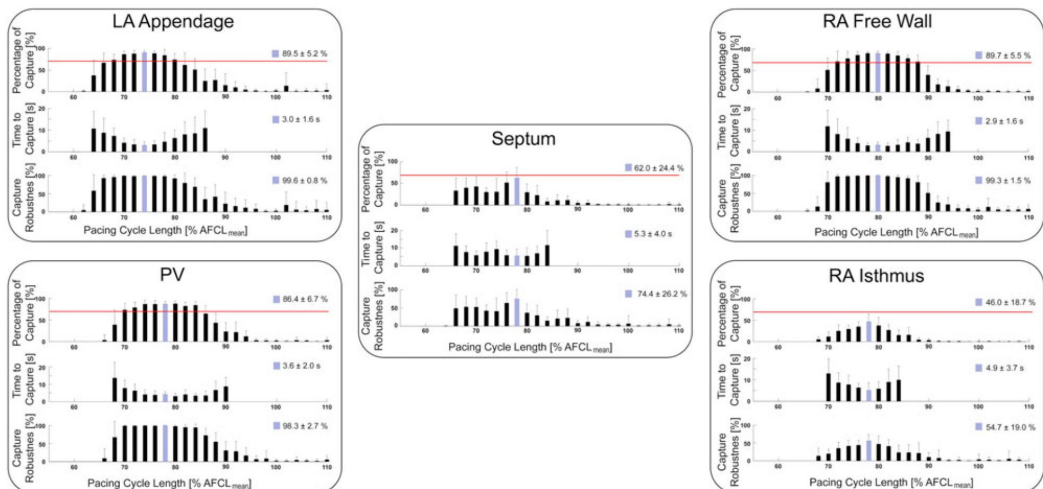


**Figure 5.5:** Summary of the temporal aspects of AF capture. For each pacing site, the measures of AF capture are presented, averaged over the 20 pacing simulations. The horizontal red line represents the 70% capture threshold. The blue bar indicates the optimal pacing cycle length within the capture window.

### 5.4.3 Spatial Aspects of AF Capture

Areas of capture were comparable for the group of three pacing sites with capture above threshold (RA free wall, LA appendage and PV): the area encompassed most of

Publication	Subjects	Pacing Sites	AFCL mean or median	Capture Window (Width) [ms]	Capture Window (Width) [%AFCL <sub>med/mean</sub> ]
Allessie et al. [161]	Dogs (5)	LA/RA appendage LA/RA lateral wall	85 ± 8 ms	60-80 ms (12 ms)	80-94% (14%)
Kirchhof et al. [162]	Dogs (6)	LA appendage	98 ± 16 ms	89-105 ms (16 ms)	91-107% (16%)
Kalman et al. [163]	Humans (3)	Anterolateral RA	170 ± 27 ms	150-178 ms (28 ms)	88-104% (16%)
			180 ± 17 ms	157-175 ms (18 ms)	87-97% (10%)
			165 ± 30 ms	157-170 ms (13 ms)	95-103% (8%)
Daoud et al. [165]	Humans (24)	High RA/Distal CS	163 ± 22 ms	113-153 ms (40 ms)	69-94% (25%)
Capucci et al. [125]	Humans (7)	RA/Septum/CS	151 ± 16 ms	129-158 ms (29 ms)	85-104% (19%)

**Table 5.1:** Capture windows computed from published data. Capture windows expressed in percents were computed by dividing the range of capturing pacing cycle lengths by the mean or median AFCL. CS = Coronary sinus.

the atrium under pacing without implying capture in the non-paced fibrillating atrium (Figure 5.6). For a given pacing site and cycle length, experiments with different AF initial conditions could lead to variations in the time needed to reach the state of local capture, but the final area of capture was the same. The pacing-induced wavefronts highlighted in red in Figure 5.6 show that propagation around the pacing site was uniform. The presence of PV did not alter the ability to capture the LA. On the contrary, the presence of bigger anatomical obstacles near the pacing site, such as valves, greatly decreased the ability to capture. In the RA isthmus, the capture pattern resembled a macro-reentry around the inferior vena cava; pacing did not capture the whole atrium. The only pacing site likely to consistently capture both atria was the septum, although fibrillating wavefronts survived in the RA lateral wall and the LA appendage.

#### 5.4.4 Effect of AF Dynamics on Capture

Capture results obtained when pacing in the RA free wall with the modified AF dynamics of Figure 5.1 are summarized in Figure 5.7. Moving left/right of the center panel of Figure 5.7 corresponds to a selective increase/decrease in CV, while moving up/down corresponds to a selective increase/decrease in APD.

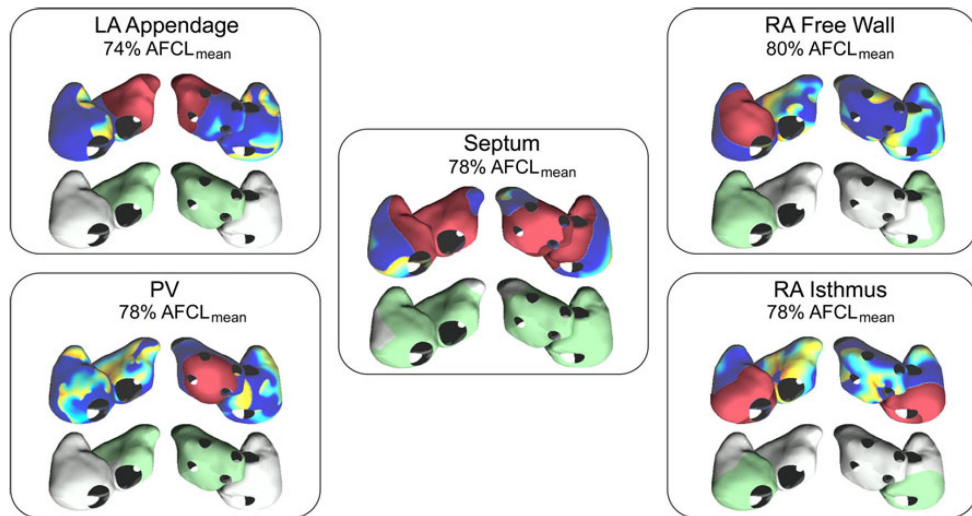


**Figure 5.6:** Summary of the spatial aspects of AF capture. For each pacing site, the upper transmembrane potential map represents an instant during rapid pacing where the most favorable capture is achieved and the pace-induced wavefronts are highlighted in red. The lower transmembrane potential shows the maximum area of capture.

### Effect of CV

Increasing CV led to a significant decrease of the capture window width (horizontal shrinking from  $14.6 \pm 3.0\%$  to  $11.4 \pm 1.7\%$  AFCL<sub>mean</sub>,  $p < 0.002$ ), meaning that the threshold of capture could still be reached, however, for fewer values of the pacing cycle length (Figure 5.7). Inversely, a decrease in CV was related to a significant stretching of the capture window ( $18.7 \pm 2.0\%$  AFCL<sub>mean</sub>,  $p < 10^{-5}$ ). No significant effect of CV was found on the percentage of capture, time to capture or capture robustness observed at optimal pacing cycle length.

### Effect of APD

Decreasing APD led to a significant stretching of the capture window ( $21.0 \pm 1.8\%$  AFCL<sub>mean</sub>,  $p < 10^{-7}$ ) (Figure 5.7). In addition, at the optimal pacing cycle length, percentage of capture was significantly increased ( $p < 10^{-5}$ ) and time to capture significantly reduced ( $p < 0.002$ ). On the other hand, an increase in APD implied an important decrease in percentage of capture and capture robustness, meaning that capture was lost.

### Prediction of AF Pacing Outcome

Simulation results suggest that AFCL is not a good predictor of the response of SAF to rapid pacing. Indeed, a decrease in AFCL induced by an increase in CV led to a shorter capture window, while a decrease in AFCL induced by a shorter APD led to the

opposite effect, i.e., a longer capture window (Figure 5.7). On the other hand, the estimate of wavelength could be linked to capture effectiveness, with a shorter wavelength corresponding to a better capture and *vice versa*.

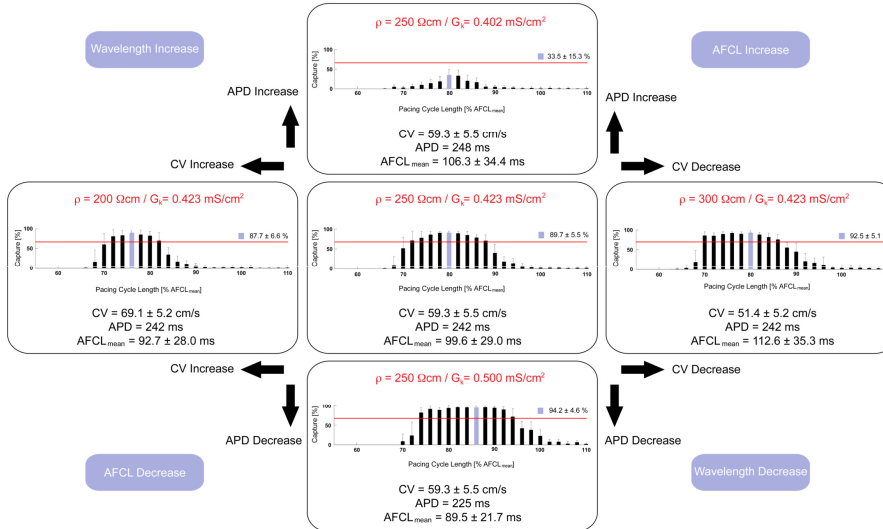


**Figure 5.7:** Effect of AF dynamics on capture. Measures of AF capture are presented in the case of rapid pacing in the RA free wall for the different AF dynamics. Central panel: reference model. Upper/lower panel: effect of a increase/decrease in APD. Left/right panel: effect of an increase/decrease in CV.

## 5.5 Discussion

### 5.5.1 Local Capture and Capture Window

In a theoretical AF model based on multiple reentries, wavelets reenter after they have recovered excitability from previous activation, so that no excitable gap should exist. However, an excitable gap can appear if a newly excitable area is not immediately invaded by a reentrant wavelet. Allesie et al. first demonstrated the presence of such an excitable gap in dogs and the fact that pacing could influence a fibrillating atrium [161]. By pacing at a cycle length shorter than the median fibrillation interval, it was possible for the pacing-induced wavefronts to penetrate into the excitable gap and to induce local capture. The feasibility of local capture of AF in humans has also been shown [163, 164, 165]. Daoud et al. demonstrated the presence of an excitable gap and the possibility to entrain either RA or LA by rapid pacing during AF in humans [165].

This chapter presents a systematic exploration of the mechanisms of local capture induced when applying rapid pacing during SAF. Five different pacing sites were compared and a large range of pacing cycle lengths was scanned. Our computer simulations are in agreement with the observation made in animals [161] and humans [163, 164, 165]

that it is possible to obtain local SAF capture using rapid pacing. An optimal pacing cycle length could be determined for each specific pacing location, although no termination could be achieved. Results were consistent across repeated simulations. For the three pacing sites with capture above the 70% threshold (RA free wall, LA appendage and PV), the optimal pacing cycle length corresponded simultaneously to the maximum percentage of capture, the minimum time to capture and the highest capture robustness. Capture window widths obtained in the computer model ( $14.6 \pm 3.0\%$  AFCL<sub>mean</sub>) were in the range of values reported for animal and human experiments, if pacing cycle lengths were expressed as a percentage of the median or mean AFCL. This formulation led to comparable results in terms of capture window even for different values of baseline AFCL. This formulation was also used by Capucci et al. when performing a study on the time window of capture during AF [203]. In the study by Daoud et al. on 24 patients, pacing cycle lengths of 69%, 75%, 81%, 87% and 94% AFCL<sub>mean</sub> led to capture in 29%, 42%, 75%, 96%, and 87% of patients respectively [165]. This distribution is similar to that of the percentage of capture obtained in the present study with comparable pacing cycle lengths.

Protocol for *in vivo* studies varied widely across published studies. First, the type of AF and patient population varied. Second, the pacing protocols were different and did not necessarily scan the whole range of cycle lengths. Finally, capture assessment differed across studies. Many only addressed the feasibility of AF entrainment, stopping pacing once capture was achieved. In the present work, the accent was put on capture reproducibility through the computation of an average over 20 SAF initial conditions, and on long-term capture properties, since capture robustness and time to capture were measured during sequences of 30 seconds of continuous pacing. This explains why the resulting capture windows tended to be slightly shorter than published values.

### 5.5.2 Comparison of Pacing Sites

Robust and consistent capture was achieved both temporally and spatially for the RA free wall, the LA appendage and the PV. Percentage of capture in the septum and in the RA isthmus did not reach the 70% threshold. This is in agreement with data in humans published by Pandozi et al., in which capture was achieved more frequently in the RA lateral wall (96.8%) than in the septum (66.7%) [164]. The published values for the radius of the capture region in the RA were 2-3 cm in dogs [161, 162] and 2.8 cm in humans [163]. It should be noted that in clinical mapping experiments, due to the limited number of recording sites, it is difficult to assess the exact area of capture or to determine if capture is uniform in all directions. In computer simulations, a precise identification of the area of capture was possible, and higher values were obtained compared to clinical data, such as for example a capture radius of 4.5 cm in the RA. This can be explained by the choice of a computer model with homogeneous and isotropic substrate, which provided a theoretical limit to the maximum area of capture. However, pacing at any of the three sites with robust capture did not lead to a systematic capture in the non-paced atrium. This can be explained by the asymmetric location of these pacing sites and the inhomogeneous distribution of refractory periods during multiple reentrant AF, creating

conduction disturbances of the pacing-induced wavefronts between the pacing sites and potentially distant reentry circuits in the opposite atrium [162].

In a simplified geometry such as a sphere, single-site pacing would lead to a full capture of SAF after some time. Therefore the differences in ability to capture AF from one pacing site to another can be explained by the strong influence of atrial anatomy on the propagation of pacing-induced wavefronts around the pacing site. Results obtained in this study suggest that pacing sites located close to major anatomical obstacles such as valves should be avoided. Indeed, the presence of large obstacles interacting with pacing-induced waves promotes anchoring and the formation of macroreentries, as it is the case with RA isthmus pacing. On the contrary, the presence of smaller obstacles such as PV did not alter the ability to capture. Robust capture was obtained when pacing from the RA free wall and the LA appendage due to the relatively uninterrupted propagation of the pacing-induced wavefronts. Interestingly, septum pacing was the only location allowing for sporadic capture episodes of both atria from a single site due to its specific location. However, this capture was difficult to maintain and occurred at best during 62% of the time, compared to 89% for the RA free wall.

### 5.5.3 Effect of Modified AF Dynamics on Capture

The effect of changes in cellular properties (APD changes) and in tissue properties (CV changes) on SAF capture was investigated separately. An increase/decrease in CV led to a significant shrinking/stretching of the capture window, yet keeping percentage of capture above the 70% threshold. This can be explained by the fact that when CV increased, the excitable gap between two successive wavefronts became shorter, making capture more difficult to achieve. Inversely, a decrease in CV led to an increase of the excitable gap, and therefore a stretching of the capture window. Interestingly, the effect on capture window width was proportionally less important than during CV increase, probably due to the fact that the CV decrease facilitated reentrant processes, thus reducing the net increase in the excitable gap. Similarly, decreasing APD led to a significant stretching of the capture window via increasing the excitable gap. However, when increasing APD, the capture window was not only shortened, but also lost its efficacy and robustness, reducing capture ability to the point that it did not reach the 70% threshold that we arbitrarily defined. Therefore, APD changes were shown to have a more dramatic impact on rapid pacing outcomes than CV changes. In animal and clinical experiments, variations in capture window widths were frequently observed across different subjects [162, 163]. However, these experiments cannot dissociate the impact of CV and APD changes, whereas computer simulations can.

### 5.5.4 Limitations of the Study

The biophysical model used in this study was based on a three-dimensional monolayer surface and did not take into account anatomical details such as Bachmann's bundle, pectinate muscles or crista terminalis. The tissue had homogeneous properties and did not include fibrosis or anisotropy. These simplifications are part of the trade-off



between model accuracy and computational load needed to perform large-scale evaluations such as the ones presented here. A similar approach using the same model has been successfully applied in a previous study for the simulation of different ablation procedures, showing that ablation outcomes were not significantly different from clinical experience in humans [113]. In the case of pacing, it is suspected that substrate heterogeneities could influence capture properties, in particular the area of capture. The results presented here can be considered as a theoretical limit of the highest achievable capture. This simple model has the advantage that simulations are done under controlled conditions and therefore that underlying mechanisms of AF capture could be derived.

Although values of CV and APD are within values reported for the human atria, AFCL values in the model are slightly lower than human responses, with AFCL values of 100 ms only rarely measured [74]. However, our study focused more on the effect of changes in AF dynamics (varying CV and/or APD) during rapid pacing than on the absolute values of these parameters.

Burst pacing sequences (30 seconds) were much longer than those currently used in implantable devices. This choice was a feature of our systematic study, in which not only the capture intervals were assessed but also the ability to maintain capture during long periods of time.

Finally, clinical AF is a polymorphic disease varying from one individual to another and different types of AF may respond in different ways to atrial pacing. The model-based study conducted here was based exclusively on a model of permanent AF, and results cannot be generalized to other types of AF.

### 5.5.5 Clinical Implications

#### Prediction of the Ability to Capture AF

This study suggests that AFCL is not predictive of the ability to capture AF by rapid pacing, since simulations with similar measured AFCL could end with opposed capture window values. This was also observed in clinical data in which subjects with the same AFCL had different capture responses [203]. The ability to capture SAF in our simulations depended on the atrial substrate as characterized by its wavelength, computed as a combination of CV and APD. Better capture was consistently achieved when wavelength was decreased, as highlighted in Figure 5.7. This implies that patients may not be equal with respect to rapid pacing of AF since different AF substrates (CV and APD) can lead to different capture outcomes for a given pacing site and cycle length. Therefore, a measure proportional to wavelength could give an estimate of the capture abilities in a specific patient. This value could be assessed using an S1-S2 protocol from which simultaneous measures of CV and APD could be derived.

## Towards Pacing Strategies for AF Termination

This model-based study also confirms the clinical observations that single-site rapid pacing of AF does not lead to AF termination in a model of permanent AF. For pacing sites such as the RA free wall, the LA appendage and the PV, rapid pacing can lead to a robust local capture of the paced atrium, but multi-site pacing schemes would be needed to control both atria. The only pacing site leading to a capture of both atria is the septum, at the expense, however, of having residual wavelets still present in LA appendage and the RA free wall that reinitiate AF when the pacing cycle length is increased. The systematic results on local capture presented in this chapter may help in the design of future AF pacing protocols, which may include more complex pacing protocols to avoid AF reinitiation due to residual wavelets and/or multi-site stimulation for the control of AF.

## 5.6 Conclusion

In this chapter, a model-based approach to the study of AF rapid pacing offered new insights into its underlying mechanisms. To conduct such analyses, a considerable amount of simulations was performed in order to understand in a systematic way the effect of very different parameters on the outcome of AF pacing, such as pacing sites, pacing frequencies, or properties of the tissue under stimulation.

An automatic algorithm to assess the presence of local capture of AF by rapid pacing was implemented in the biophysical model of atria, as well as different measures describing the quality of this capture. Thanks to these quality measures, not only were episodes of local capture detected, but their efficacy and robustness could also be quantified. Pacing sites and pacing frequencies could be compared to find optimal pacing configurations.

Pacing sites in the RA or LA lateral wall provided consistent local capture of the atrium under pacing, whereas pacing on the inter-atrial septum led to sporadic capture episodes of both atria. The ability to capture AF depended on the atrial substrate as characterized by its wavelength, a better capture being consistently achieved for shorter wavelengths. An optimal pacing cycle length was determined for specific pacing locations, although no termination could be achieved. Nevertheless, this study underlined the necessity to capture both atria before considering any attempt to terminate AF. Taking these considerations into account, a new pacing algorithm based on septum stimulation is proposed in chapter 6 as a new therapy for AF termination.

# A Novel Atrial Septal Pacing Algorithm for the Termination of Atrial Fibrillation

---

# 6

## 6.1 Introduction

Pacemaker-based therapies for AF offer an alternative to drugs and ablation for patients with a conventional indication for pacing [166]. Today, many pacemakers and implantable defibrillators include pacing algorithms developed for the prevention or the termination of AF. Most existing pacing algorithms have a preventive nature, designed to suppress AF triggers and to reduce the dispersion of atrial refractoriness [23]. In this context, different single- or multi-site atrial pacing strategies have been compared. Pacing at a single site offers the advantage of simplicity. On the other hand dual-site or multi-site pacing strategies are considered as promising approaches for achieving a more complete atrial synchronization, but experimental studies have not yielded conclusive results [204, 205].

One factor that predisposes to reentry is the dispersion in atrial refractoriness. Therefore, it might be desirable to find a pacing location from which the stimulation of both atria is rapid and uniform. Septal pacing has been proposed as a simple and attractive alternative to multi-site pacing since it may produce simultaneous biatrial stimulation using a single pacing location, without the need of complex methods for synchronizing pacing sites. The feasibility of pacing both atria simultaneously from a single lead placed in the interatrial septum has been demonstrated [206]. These results motivated the testing of atrial septal pacing both as a way to prevent AF occurrence, or to terminate ongoing AF. Clinical studies evaluating the preventive effect of atrial septal pacing have led to mixed results [207]. Becker et al. showed in a canine model that septal pacing produced comparable results as quadruple site pacing in terms of prevention of paroxysmal AF and activation times [208]. Kale et al. showed that atrial septal pacing in combination with antiarrhythmic drugs resulted in a subjective improvement of symptoms in patients with drug-refractory paroxysmal AF [209]. On the other hand, Hermida et al.

showed that atrial septal pacing did not prevent the occurrence of AF [210]. Hakacova et al. found no significant difference between septal and high atrial preventive pacing, using AF duration and the number of AF episodes as endpoints [211]. A multicenter prospective randomized study by Padeletti et al. showed that preventive pacing of atrial tachycardias from the septum was associated with a decreased frequency of symptomatic episodes and premature atrial contractions [169]. In all these studies safety of interatrial septal pacing was demonstrated [169, 211]. Interest in septal pacing still persists, as seen in a multicenter parallel randomized study on 380 patients with paroxysmal AF, currently being conducted to evaluate whether septal pacing with or without atrial overdrive pacing could have an effect on AF suppression [199].

In this chapter, we propose a novel algorithm of septal pacing for AF termination. It is aimed at terminating an atrial arrhythmia by applying rapid (overdrive) pacing at a cycle length shorter than that of the detected arrhythmia [23]. In chapter 5, during a systematic testing of single site rapid pacing of SAF in a biophysical model of human atria, septal rapid pacing was shown to lead to SAF capture in both atria [139]. However, the capture obtained was not robust enough to provoke SAF termination when rapid pacing was stopped, because of residual fibrillating activity near the atrial appendages. In the pacing scheme presented in this chapter, the initial rapid septal pacing leads to capture in both atria. This is followed by a transition to a slow septal pacing phase at a cycle length longer than that of the detected arrhythmia. In both experimental and computer studies, perpetuation of AF was shown to be promoted by short cardiac wavelength [86, 91]. The sharp transition to slow pacing presented here, translating into a brutal lengthening of the wavelength of paced waves, contributes to eliminate any residual SAF activity and thus leads to termination. The effectiveness of this new septal pacing algorithm was tested and optimized in a model-based study, and compared to the one using rapid pacing only.

## 6.2 Methods

### 6.2.1 Biophysical Model of AF

#### Model of Electrical Propagation on an Atrial Geometry

The MRI-based biophysical model of human atria described in chapters 2 and 3 was used. The simplified design of its three-dimensional monolayer geometry permitted the simulation of long runs of AF (several minutes in real time), while the geometry still included all major anatomical obstacles to propagation including the septal area, as shown in panel A of Figure 6.1.

The model of recent chronic AF was used with ionic properties and numerical integration parameters set exactly as described in section 3.3.3. The same ionic properties were assigned to all nodes and conduction anisotropy was not taken into account. The resistivity value between two neighboring atrial cells was set to 200  $\Omega\text{cm}$ , resulting in a mean CV during sinus rhythm of 70 cm/s. ERP and CV restitution properties of the proposed model as computed in a 1-D cable are presented in panels B and C of Figure 6.1.

## Creation of a Database of AF Initial Conditions

As already presented in section 3.3.3, SAF was initiated by 20 Hz pacing for 3 s in the sinoatrial node region of the model. When pacing was stopped, SAF was sustained and allowed to evolve freely for 10 minutes. The resulting SAF dynamics showed multiple reentrant wavelets that continuously changed in size and direction, accompanied by important variations in AFCL over time. As in the systematic model-based study of AF rapid pacing presented in chapter 5 and in [139], from the 10 minutes of sustained SAF, 40 instantaneous transmembrane potential maps (IC1 to IC40) were selected at 15 s intervals to form an SAF database (Figure 6.2). These maps differed in terms of activation patterns, making them equivalent to a randomly chosen set of SAF initial conditions. They were used to test the effectiveness of the proposed septal pacing algorithm.

### 6.2.2 Study Protocol

#### Proposed Septal Pacing Algorithm

Pacing was applied from the septal area (Figure 6.1, panel A). Septal pacing consisted in the simultaneous stimulation of the 1248 nodes located in the septal area (corresponding to a surface of  $4.36 \text{ cm}^2$ ) by injecting an intracellular current of  $80 \text{ A/cm}^2$  (total injected current: 0.3 mA). This relatively large area was considered as a theoretical limit of an ideal stimulation site, ignoring the potential issues of imperfect electrodes placement. Using this stimulation, the specific efficiency of the pacing protocol could be studied. Pacing cycle length (PCL) values were based on a mean AFCL ( $\text{AFCL}_{\text{mean}}$ ) computed as the 10 minutes average on 4 endocardial electrograms from the septal area during sustained SAF. The extracellular potential (unipolar electrogram) was modeled using a current source approximation for large homogeneous volume conductor [69]. The septal pacing algorithm comprised two phases (Figure 6.2): 1) a rapid pacing phase for 10 to 30 s at a PCL shorter than  $\text{AFCL}_{\text{mean}}$  in order to capture the electrical activity of a substantial portion of both atria, 2) a slow pacing phase lasting 1.5 s at a PCL longer than  $\text{AFCL}_{\text{mean}}$ , aimed at lengthening the wavelength of the paced wavefronts, and thus eliminating any residual fibrillating wavelets that might have survived in areas distant from the septum during the rapid pacing phase. An abrupt transition was applied between these two phases.

#### Rapid Pacing Phase

During the first phase of the proposed AF pacing algorithm, capture of both atria (bilateral capture) has to be established by rapid septal pacing. In order to select the PCL needed to achieve this bilateral capture, the capture window was first determined following the same procedure as in chapter 5. PCLs were systematically tested in the range of 50-100%  $\text{AFCL}_{\text{mean}}$  with 2% increments. The duration of each pacing episode was 30 s and capture results were averaged across the 40 initial conditions of the SAF database (IC1 to IC40). The percentage of capture was computed as the percentage

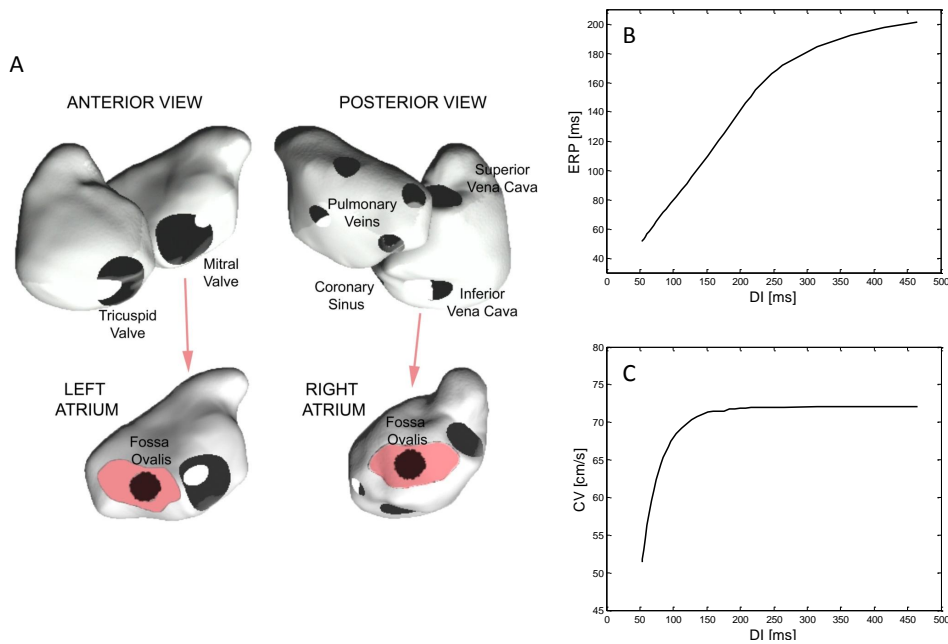


**Figure 6.1:** The biophysical model of AF. (A) Anterior and posterior view of the atrial geometry. The septal area where the pacing protocol is applied (1248 nodes of the atrial geometry,  $4.36 \text{ cm}^2$ ) is highlighted in red for the LA and RA separately. (B) ERP restitution curve of the modified Luo-Rudy model with  $G_{si} = 0.055 \text{ mS/cm}^2$ . Restitution properties are measured in a cable with the same parameters as the ones used for the three-dimensional atrial geometry, and following a standard  $S_1$ - $S_2$  protocol. (C) CV restitution curve for the same set of parameters.

of time spent in bilateral capture during the total pacing sequence of 30 s. The capture window was defined as the range of the PCL for which the percentage of bilateral capture was above 70%. Within this capture window, PCL values corresponding to stable capture results (standard deviation of the mean percentage of capture less than 5%) were retained to test the proposed septal pacing scheme.

The assessment of capture was based on the method used in chapter 5. In each atrium, electrograms were computed at four nodes located distantly from the septal pacing site, two nodes being placed on the posterior atrial side, and two nodes on the anterior one (Figure 6.3, panel A). During rapid pacing, a node was considered to be entrained if over at least five consecutive beats the measured cycle length was within  $\pm 3 \text{ ms}$  of the PCL. In each atrium separately, capture was considered effective if at least three out of four nodes were entrained. This capture criterion combined with the node placement ensured the detection of spatially consistent capture episodes of the atrium under study. Bilateral capture from the septum was considered to be achieved when both the right atrium (RA) and the left atrium (LA) were simultaneously in a state of capture.

## Slow Pacing Phase

As was shown in chapter 5, single site rapid pacing of the septal area could not reliably lead to SAF termination, because of fibrillating spiral waves surviving in areas distant from the septum and sustained by the rapid stimulation [139]. In both experimental and computer studies, perpetuation of AF has been shown to be promoted by short cardiac wavelengths, the latter being computed as the product of CV and effective refractory period (ERP) [86, 91, 212]. Based on these considerations, it was hypothesized that a second phase with paced waves at longer PCLs, i.e. with wavelengths prolonged through restitution adaptation, could eliminate this fibrillating residue and leave the tissue free from AF. The PCL parameters of the slow pacing phase were determined based on preliminary observations. After testing various slow PCLs, the value of  $180\% \text{AFCL}_{\text{mean}}$  was selected as the optimal value. It was the shortest PCL provoking sufficient wavelength lengthening to suppress fibrillating activity and lead to complete capture of the whole atrial tissue. A detailed analysis of the restitution properties of the cellular model used in this study was performed in a 1-D cable and is presented in the

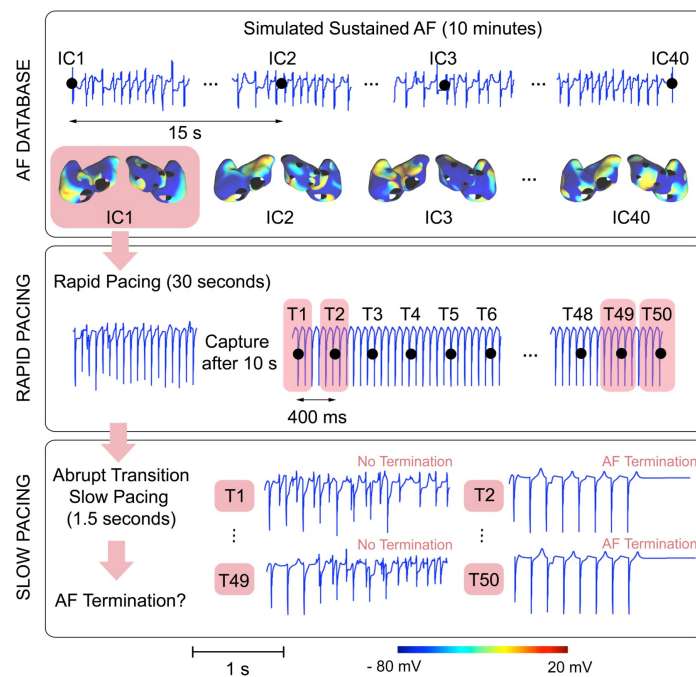


**Figure 6.2:** Study protocol for the testing of the septal pacing algorithm. 1. Creation of a database of AF initial conditions by selecting 40 transmembrane potential maps at 15 s interval from the 10 minutes of sustained AF. The subsequent steps are applied to each initial condition separately (IC1 to IC40). 2. Rapid pacing phase from the septal area during 10 to 30 s: capture is achieved after 10 s and 50 transmembrane potential maps are selected at 400 ms interval after 10 s of septal rapid pacing and will serve as initial conditions for the transition to the slow pacing phase (T1 to T50). 3. Abrupt transition to a slow pacing phase during 1.5 s and assessment of AF termination for T1 to T50. Electrograms were recorded in the septal area.

panel B of Figure 6.1. Switching abruptly from a rapid PCL of 65%  $AFCL_{mean}$  to a slow PCL of 180%  $AFCL_{mean}$  increases the ERP value from 60 ms to 127 ms, while the CV is increased from 60 cm/s to 72 cm/s. As a result, the wavelength of the paced waves is lengthened by 5.5 cm (from 3.6 cm to 9.1 cm) after the transition towards the slow PCL. A potential problem was that the abrupt transition from the rapid PCL to 180%  $AFCL_{mean}$  resulted first in a long pause without electrical activity in most parts of the atrial tissue during which it was possible for residual reentries to reinitiate AF from the appendages. To avoid this problem, the transition was smoothed in a stepwise manner and the slow pacing phase at 180%  $AFCL_{mean}$  was preceded by one single pacing pulse at an interval of 130%  $AFCL_{mean}$ .

### Evaluation of the Septal Pacing Algorithm Using the AF Database

The study protocol for the evaluation of the septal pacing algorithm is presented in Figure 6.2. For each initial condition of the SAF database (IC1 to IC40), the rapid pacing phase was applied during a variable period of 10 to 30 s, followed by an abrupt transition to the slow pacing phase of 1.5 s duration. The transition from rapid to slow pacing was tested at 50 different time instants (T1 to T50) taken 10 to 30 s after the start of the rapid pacing phase with 400 ms increments. At the end of the slow pacing phase, the atrial tissue was allowed to evolve for another 0.5 s to assess SAF termination. For each initial condition IC1 to IC40, the SAF termination success rate was therefore computed as an

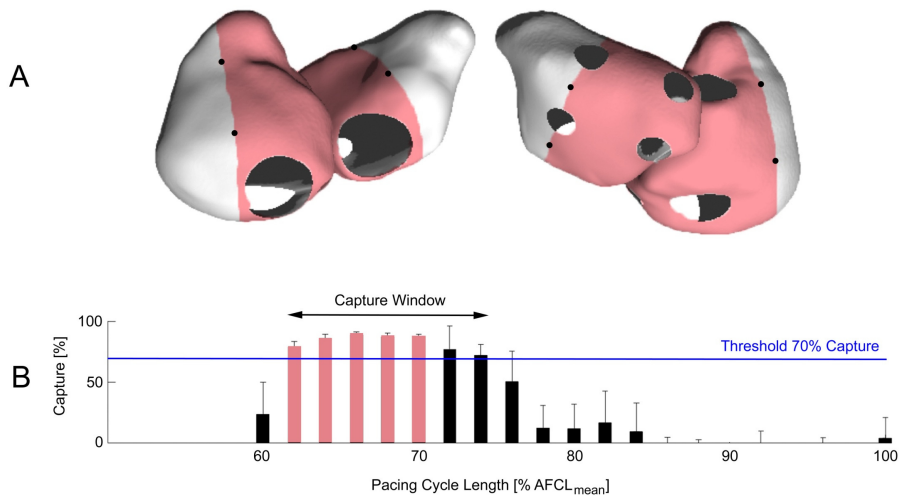


**Figure 6.3:** Capture window for septal pacing. (A) Assessment of capture induced by septal pacing: four electrodes are placed in the RA and the LA (black dots) corresponding to the area of capture represented in red. (B) Capture window for septal pacing. PCL tested were in the range 50-100%  $AFCL_{mean}$  with 2% increments. Results were averaged on the 40 elements of the AF database (IC1 to IC40). The rectangles highlighted in red represent the 5 PCL values having a standard deviation of less than 5% on the mean percentage of capture, and therefore selected for the testing of the rapid septal pacing phase (62%, 64%, 66%, 68% and 70%  $AFCL_{mean}$ ).



average on T1 to T50.

SAF termination success rates obtained with the proposed septal algorithm (rapid pacing phase followed by an abrupt transition to the slow pacing phase) were compared to results obtained when applying the rapid septal pacing phase only to terminate SAF. Comparisons were made using Wilcoxon's rank sum test.

### **Analysis of the Septal Capture Pattern**

After 10 s of rapid pacing, capture was considered stable, meaning that a periodic pattern was observed, with a large portion of atrial tissue being controlled by the PCL (except for the reentrant wavelets still present in areas distant from the septum). This capture pattern could occasionally involve anchored waves rotating periodically around anatomical obstacles. We hypothesized that the presence of these anchored waves could reduce the SAF termination rates by sending wavelets back to the stimulation site during the transition between rapid and slow pacing. To test this hypothesis, for each capture pattern obtained after 10 s of rapid pacing of one of the initial conditions (IC1 to IC40) of the SAF database, the number of anchored waves was documented as well as their location around the nine major anatomical obstacles: tricuspid valve (TV), superior and inferior vena cava (SVC and IVC), coronary sinus (CS), mitral valve (MV), superior right and left pulmonary veins (RSPV and LSPV), and inferior right and left pulmonary veins (RIPV and LIPV). The impact of the number of anchored waves (independently of their anatomical location) on the SAF termination rate was computed for each SAF initial condition shown in Figure 6.2 (IC1 to IC40), and comparisons were made using Wilcoxon's rank sum test. Finally, further statistical tests were conducted within the analysis of variance (ANOVA) framework to determine specific anatomical locations of anchored waves significantly impacting subsequent termination rates. For each of these analyses, the case of rapid pacing only was systematically compared to the proposed pacing sequence combining rapid and slow pacing

## **6.3 Results**

### **6.3.1 Capture Window for Septal Rapid Pacing**

The lower panel of Figure 6.3 shows the capture window obtained for septal rapid pacing. For an average  $AFCL_{\text{mean}}=99.76 \pm 25.20$  ms, the capture window was 62-74%  $AFCL_{\text{mean}}$ . Within this capture window, five PCL values were selected for the testing of the rapid pacing phase: 62%, 64%, 66%, 68%, and 70%  $AFCL_{\text{mean}}$ . These values were either used to test the efficiency of rapid pacing alone to terminate SAF resulting in 200 simulations (5 PCL  $\times$  40 initial conditions), or were combined with PCL values of the slow pacing phase (180%  $AFCL_{\text{mean}}$  pacing preceded by one pacing pulse at 130%  $AFCL_{\text{mean}}$ ), resulting in a total of 10,000 simulations (5 PCL  $\times$  40 initial conditions  $\times$  50 time instants for the transition between rapid and slow pacing).

### 6.3.2 Example of Successful AF Termination

Figure 6.4 presents an example of successful termination. Before pacing was applied, SAF was sustained by multiple reentrant wavelets (from 2 to 12) propagating on the whole atrial surface. Considering a random 10 s segment of freely evolving SAF, an average of  $8.5 \pm 2.5$  wavefronts were observed over the whole atrial surface. After application of the rapid pacing phase at  $64\%$   $AFCL_{\text{mean}}$ , a gradual capture of both atria was visible, starting in this case with a capture in the posterior RA ( $t=2350$  ms), followed by the posterior LA ( $t=3320$  ms: posterior LA and RA captured), and finally by the anterior LA and RA. During this process, pace-induced wavefronts were fast enough to spread in both atria and gradually block AF reentries. In this example, bilateral capture was achieved after 5 s of rapid pacing, with both atria controlled at the rapid PCL, except for some residual reentries in the LA appendage and the RA wall ( $t=9425$  ms). It was also observed that anchored waves around anatomical obstacles could be present during bilateral capture. In this case two anchored waves were present, one around the tricuspid valve, the other around the left superior pulmonary vein. The transition from rapid to slow pacing was applied after 10 s. The first beat of the slow pacing pulse was at  $130\%$   $AFCL_{\text{mean}}$  and a longer period with no electrical activity was observed between the last rapid pacing pulse and the first slow pacing pulse, where the atrial tissue had time to repolarize ( $t=10090$  ms), implying for the next wavefronts a prolongation of APD and an increase in CV, i.e. a lengthening of the wavelength through restitution adaptation. Anchored waves could reenter the atrial tissue after its repolarization but were stopped by the first slow pacing pulse before being able to propagate to the whole atrium. This first slow pacing pulse had a longer APD, leaving less space for the reentrant wavelets to be sustained, and this phenomenon was amplified by the increased CV of the reentries ( $t=10235$  ms: self-annihilation of the residual reentries due to the presence of the first slow pacing wave). In this example, all reentrant waves could be stopped by the first slow pacing pulse ( $t=10320$  ms: repolarization of the first slow pulse after annihilation of all residual reentries) and the second and subsequent slow pacing pulses at  $180\%$   $AFCL_{\text{mean}}$  took control of both atria at a reduced pacing cycle length ( $t=10960$  ms). In other simulations, more than one slow pulse was needed to annihilate all reentrant waves and subsequently control the atria. At this point, slow pacing could be stopped at any moment since fibrillating activity was not present anymore in the tissue. In a physiological situation, the sinoatrial node would now be able to take control of the atria as soon as slow pacing is stopped, in order to restore normal sinus rhythm in the atria.

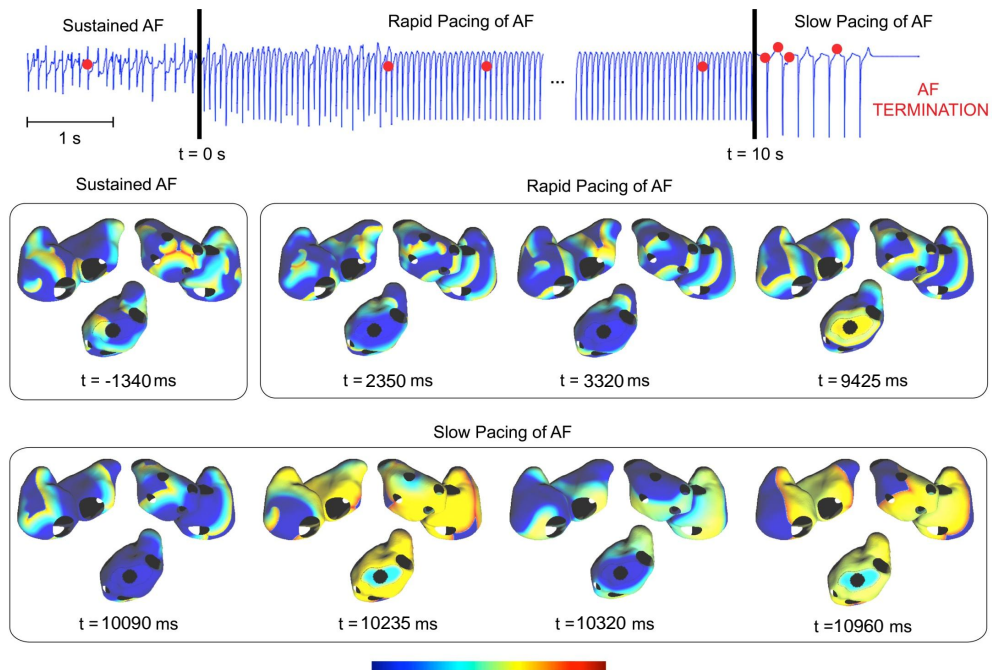
### 6.3.3 Example of Unsuccessful Septal Pacing

Figure 6.5 presents an example in which the septal pacing algorithm did not succeed in terminating SAF when started on different SAF initial conditions while using the same rapid and slow PCL as in Figure 6.4. The establishment of the bilateral capture pattern was similar to what had been observed in Figure 6.4, starting with a progressive control of the anterior LA and posterior RA ( $t=2725$  ms and  $t=3635$  ms). However, the final capture state was different, with a higher number of anchored waves. In this example, five anchored waves were present, located around the TV, the IVC, the MV

and the RIPV and LIPV ( $t=9710$  ms). The abrupt transition from rapid to slow pacing was applied after 10 s. The longer period with no electrical activity between the last rapid pacing pulse and the first slow pacing pulse at  $130\%$   $AFCL_{mean}$ , during which the atrial tissue had time to repolarize, was also observed ( $t=10090$  ms). However, the first slow pacing pulse could take control of the RA only but could not prevent the anchored waves from reentering the atrial tissue in the LA appendage and around the left inferior pulmonary vein ( $t=10220$  ms). During the repolarization of the RA, these reentries gradually invaded the anterior and posterior LA ( $t=10300$  ms: just before the application of the second slow pacing pulse). SAF could then also spread to the RA even in the presence of the  $180\%$   $AFCL_{mean}$  slow pacing, that could no longer capture the atria ( $t=10730$  ms). In such situation, slow pacing should be stopped as it will not be able to capture the activity of the atria due to the faster rate of the reinitiated SAF. The only solution here is to launch again the whole pacing sequence for a supplementary attempt to terminate SAF.

### 6.3.4 Performance of the Septal Pacing Algorithm

SAF termination results are summarized in Table 6.1 for rapid pacing only, as well as for the proposed septal pacing algorithm combining rapid and slow pacing. We found



**Figure 6.4:** Example of application of the septal pacing algorithm with successful AF termination. This example corresponds to IC2 and T1 for a rapid PCL of  $64\%$  of  $AFCL_{mean}$  and a slow PCL consisting of one pacing pulse at  $130\%$   $AFCL_{mean}$  followed by continuous pacing at  $180\%$  of  $AFCL_{mean}$ . Transmembrane potential maps are shown at time instants represented by red dots on the electrogram. Electrograms were recorded in the septal area.

that the combination leading to the highest SAF termination rate of 29% was a rapid pacing at 64%  $AFCL_{mean}$  for 10-30 s followed by an abrupt transition to slow pacing at 130%  $AFCL_{mean}$  for one pacing pulse and then 180%  $AFCL_{mean}$  for 1.5 s. Using a rapid PCL different from 64%  $AFCL_{mean}$  tended to create more complex bilateral capture patterns before the transition to the slow pacing phase, and decreased the average SAF termination rate as the PCL was moved away from the optimum. Compared to the case where only rapid septal pacing was applied, the proposed septal pacing algorithm could in most cases double the SAF termination rate. When considering the average performance of the pacing scheme over the 5 rapid PCLs tested, the addition of the slow pacing phase provided a significant increase of the SAF termination rate from 10.2% to 20.2% ( $p < 0.05$ ).

Histograms of the SAF termination rates considering all rapid PCLs taken together are shown in Figure 6.6, septal rapid pacing only (panel A) and with the proposed pacing sequence with rapid and slow pacing combined (panel B). For both cases, most SAF initial conditions led to an SAF termination rate between 0-20%. However, the proportion of initial conditions resulting in failures was lower when the slow pacing phase was added (88.5% of initial conditions with rapid pacing only compared to 77.5% with rapid and slow pacing combined). Interestingly, an important proportion of initial conditions

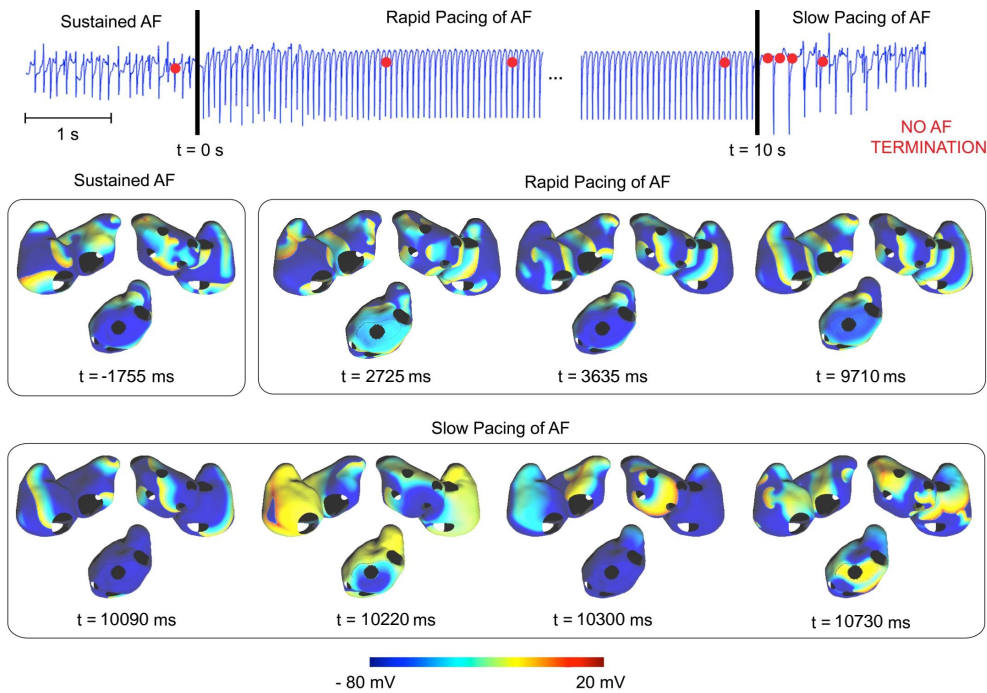


**Figure 6.5:** Example of application of the septal pacing algorithm without AF termination. This example corresponds to IC28 and T1 for a rapid PCL of 64%  $AFCL_{mean}$  and a slow PCL consisting of one pacing pulse at 130%  $AFCL_{mean}$  followed by continuous pacing at 180%  $AFCL_{mean}$ . Transmembrane potential maps are shown at time instants represented by red dots on the electrogram. Electrograms were recorded in the septal area.

led to an SAF termination rate in the range 80-100%, with a higher occurrence when using the complete septal pacing algorithm (7.0% for septal rapid pacing only compared to 15.5% when slow pacing was added). Very few initial conditions led to an SAF termination in the range 20-80%.

	Rapid Pacing Cycle Length [% AFCL <sub>mean</sub> ]					Average 62-70
	62	64	66	68	70	
<b>Rapid Pacing Only</b>	8.8%	21.2%	11.5%	3.4%	6.0%	10.2%
<b>Rapid Pacing + Slow Pacing</b>	20.9%	29.0%	24.2%	15.9%	11.2%	20.2%

**Table 6.1:** AF termination rates for the septal pacing algorithm compared to rapid pacing only.

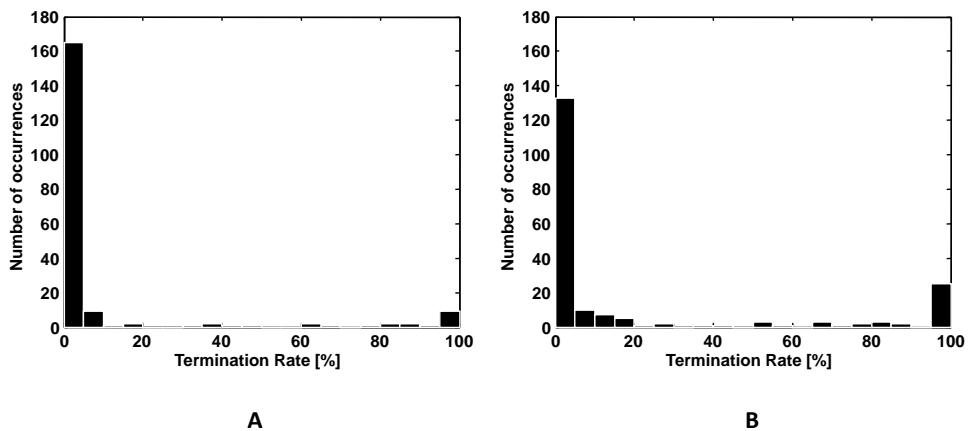


**Figure 6.6:** (A) Histogram of the AF termination rates obtained when applying septal rapid pacing only on the 40 initial conditions of the AF database and the 5 PCLs tested (62%, 64%, 66%, 68%, 70% AFCL<sub>mean</sub>). (B) Histogram of the AF termination rates obtained when applying the whole atrial septal pacing algorithm, including the slow pacing phase.

### 6.3.5 Effect of the Capture Pattern on AF Termination

A detailed inspection of the simulations revealed that the success of the septal pacing algorithm was determined by the configuration of the capture pattern obtained at the end of the rapid pacing phase. The time needed to achieve bilateral capture varied from one simulation to the other, but 10 s was a safe pacing duration to obtain a stabilized bilateral capture pattern in all cases. For the 40 SAF initial conditions and the 5 PCLs tested in the rapid pacing phase ( $N = 200$ ), the number and locations of the anchored waves present in the bilateral capture pattern achieved after 10 s of rapid pacing were documented. Moreover, the influence of capture pattern configurations on subsequent termination rates was also investigated.

### Influence of the number of anchored waves

In a first stage, the number of anchored waves, independently of their anatomical location, and its impact on subsequent termination success rates were investigated. Depending on the simulation, the number of anchored waves ranged between 0 and 8, with an average of  $4.1 \pm 1.4$  during the stabilized capture patterns over the 200 simulations performed. In Figure 6.7, simulations were grouped according to the number of anchored waves present in their capture pattern, and the corresponding average termination rate was computed in order to investigate the influence of the number of anchored waves on termination rates. It was observed that higher termination rates were consistently linked to a low number of anchored waves and *vice versa*. For both pacing configurations (rapid pacing only or rapid pacing combined with slow pacing), termination rates were not significantly different when only 1 or 2 anchored waves could be detected ( $p = 0.58$  and  $p = 0.86$  respectively). However, they started to decrease significantly when three or more anchored waves were present in the capture pattern ( $p = 0.0046$  and  $p = 0.0052$  respectively).

Based on these results, it was attempted to determine, for each pacing configuration, a critical number of anchored waves above which termination success rates would be significantly degraded. The results of this investigation are summarized in Figure 6.8. When only septal rapid pacing is applied (panel A of Figure 6.8), it can be shown that grouping simulations with more than three anchored waves and computing the resulting average termination rates results in a value of  $4.6 \pm 15.4\%$ . This represents a significant decrease compared to the average termination rate of  $11.8 \pm 28.2\%$  observed when grouping simulations with exactly three anchored waves. This significant degradation of termination rates as the number of anchored waves increases can not be observed anymore when comparing the simulations with exactly four anchored waves to the ones with more than four anchored waves. Thus, the critical number of anchored waves when applying septal rapid pacing only is equal to three. In panel B of Figure 6.8, the same analysis was performed for the proposed pacing sequence combining rapid and slow pacing. Here, it can be demonstrated that the critical number of anchored waves is equal to four. Indeed, even with four anchored waves, an average termination rate of  $16.0 \pm 31.5\%$  can still be obtained. However, when more than four anchored waves are present, the termination rates are significantly degraded.

### Influence of the location of anchored waves

Next, we investigated whether the anatomical location of an anchored wave had a significant impact on subsequent termination success rates. First, the percentage of occurrence of anchored waves on each anatomical obstacle was documented as follows: TV 51%, SVC 44.5%, IVC 53%, CS 39.5%, MV 54%, LSPV 45%, LIPV 38.5%, RSPV 36.5%, RIPV 44%. This provided no indication of any preferential site for the anchoring during the rapid pacing phase.

The effect of the locations of anchored waves on the subsequent AF termination rate was evaluated using a 9-way ANOVA, the results of which are summarized in Table

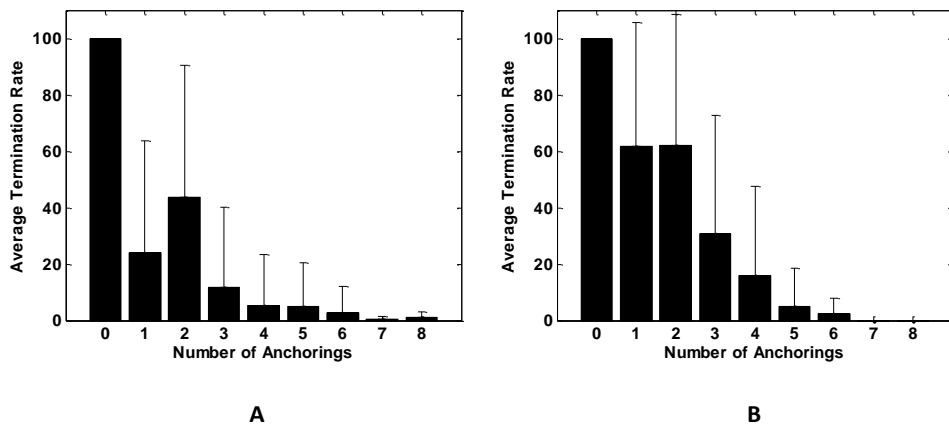


**Figure 6.7:** (A) Impact of the number of anchored waves around anatomical obstacles after 10 s of rapid pacing on the AF termination rate when applying septal rapid pacing only. (B) Impact of the number of anchored waves around anatomical obstacles after 10 s of the rapid pacing phase on the AF termination rate when applying the complete atrial septal algorithm including a combination of both rapid and slow pacing phases.

6.2. In order to keep the computational load tractable, we only considered the impact on termination rates of the 9 main effects, i.e. the 9 anatomical locations (veins or valves) taken independently, as well as the impact of the two-factor interactions, i.e. each of the 36 possible pairs of anatomical locations. Significant effects and interactions are shown in Table 6.2 for both pacing configurations. When rapid pacing only is applied, the anatomical locations significantly impacting termination rates are the CS, the MV and both right PVs. Interestingly, these are the four anatomical obstacles nearest to the septal stimulation site. In addition, significant interactions between anatomical locations with anchored waves were also shown to involve at least one obstacle near the stimulation site. When applying both rapid and slow pacing, results were only slightly different, as a smaller number of anatomical locations was shown to impact termination rates significantly. While right pulmonary veins did not impact termination rates anymore when considered individually (main effect not significant), the critical role of waves anchored around CS and MV was clearly confirmed for this pacing configuration as well.

## 6.4 Discussion

### 6.4.1 Possibility of AF Termination by Septal Pacing

Existing antitachycardia pacing algorithms were designed to terminate atrial tachycardias by delivering rapid pacing bursts or ramps at a single electrode with cycle lengths shorter than the detected arrhythmia [23, 166]. While these methods have been successful at terminating atrial flutter or slower and organized atrial tachycardia [213], it has proved difficult to interpret results from clinical studies evaluating pacing for

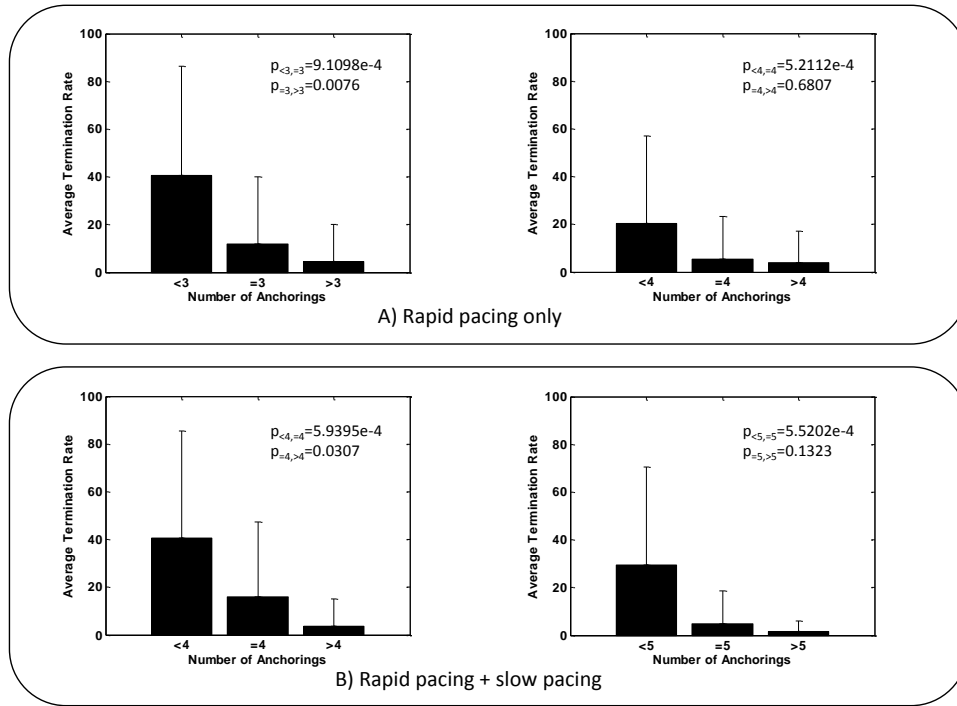


**Figure 6.8:** Assessment of a critical number of anchored waves. (A) Assessment of the number of anchored waves critically impacting subsequent termination rates when applying septal rapid pacing only;  $p$ -values between bins are indicated in each graph. (B) Same as (A) when applying the complete atrial septal algorithm including a combination of both rapid and slow pacing phases.

Rapid Pacing Only		Rapid Pacing + Slow Pacing	
Anchored wave(s)	p-value	Anchored wave(s)	p-value
CS	0.012	CS	0.0001
MV	0.006	MV	0.035
RSPV	0.008	LSPV	0.048
RIPV	0.012		
CS + MV	0.025	CS + MV	0.013
CS + LSPV	0.025	CS + RIPV	0.039
MV + RSPV	0.001	CS + LSPV	0.016
MV + RIPV	0	TV + RIPV	0.021
RIPV + LSPV	0.033		

**Table 6.2:** Locations of anchored waves with significant impact on termination rates as computed with an ANOVA. The effects of anatomical locations and their pairwise interactions on subsequent SAF termination success rates were investigated. Only statistically significant results ( $p < 0.05$ ) are shown.

AF termination and, hence, evidence for treating AF through pacing remains limited [191, 192, 201]. In chapter 5, the systematic study of single site rapid pacing of AF



using the same biophysical model of AF as the one used in the present study indicated that it is possible to obtain local capture of SAF using rapid pacing, but that in general this did not result in SAF termination or in permanent changes in SAF patterns [139]. While the use of low-energy pacing from a single electrode was not conclusive for AF termination, cardioversion with a single high voltage shock could terminate AF reliably, the major side effect being pain experienced by the patient. Based on this observation, Fenton et al. developed a method to terminate AF called far-field antifibrillation pacing, delivering trains of rapid low-energy pacing from field electrodes [195]. The method was tested in isolated canine hearts, showing a termination success rate for AF and atrial flutters of 93% with 13% of the energy needed for cardioversion applied in a single shock. Very recently, similar findings with even better termination rates for AF specifically were found in a rabbit model [197]. It is not sure however whether the energy of such stimulation bursts would be below the threshold of pain, as the cumulative effect of subsequent shocks could be subjectively perceived as more painful. The method proposed here uses the same energy as antitachycardia pacing, with a stimulation of the whole septal area (4.36 cm<sup>2</sup>). This large stimulation site was voluntarily chosen to simulate an ideal pacing device placed in the septum; a similar stimulation pattern remains to be implemented and tested experimentally, for instance by means of a ring-shaped stimulation device encompassing the septal area. As such, this approach lies between a single electrode rapid pacing for which almost no AF termination could be achieved and the approach proposed by Fenton et al. [195]. The multi-stage septal pacing scheme presented in this study is the first algorithm leading to SAF termination in the biophysical model, with a termination rate of up to 29%.

### 6.4.2 Rapid Pacing Phase

The first phase of the proposed septal pacing scheme aimed at capturing atrial electrical activity through rapid pacing in order to facilitate the installation of the subsequent slow pacing. During this rapid pacing phase, pace-induced wavefronts were injected into the septal area at a cycle length shorter than the one of the fibrillating wavelets in order to progressively move SAF activity away from the stimulation site. It was observed that in most cases atrial capture could be obtained in less than 10 s. The resulting capture patterns were characterized by a periodic activity at the pacing cycle length in a major portion of atrial tissue. The possibility of creating an area of local capture of the atrial tissue by rapid pacing of AF was first demonstrated in animals by Alessie et al. [161]. In the present study, entrained waves could either propagate from the septum to appendages, or be anchored on anatomical obstacles and rotate periodically around them. The observed capture patterns remained stable as long as rapid pacing was maintained. This was also valid for the anchored waves, which stayed anchored around their specific anatomical obstacle even if rapid pacing was prolonged. Results showed that a PCL of 64% AFCL<sub>mean</sub> was optimal to take control of electrical activity during the rapid pacing phase. Interestingly, this PCL corresponds to the 5<sup>th</sup> percentile of the AFCL histogram, which was used by Duytschaever et al. to obtain an approximated value of the excitable gap [214]. Therefore, the optimal way to control atria during the rapid pacing

phase is to stimulate at a PCL near the lower limit of the excitable gap. Finally, it can be seen in Table 6.1 that rapid pacing only can already reach termination success rates of up to 21.2%, with an average of 10.2%. This could seem in opposition to numerous publications stating that rapid pacing cannot terminate AF at all. However, it must be kept in mind that ideal septal stimulation was considered in this study, and not single site pacing. This difference in the stimulation protocol can certainly account for these unexpectedly high termination rates. In chapter 5, using single site pacing and the same biophysical model as here, no termination could be observed when pacing in the septal area.

### 6.4.3 Slow Pacing Phase

The second phase of the proposed pacing scheme involved a transition from rapid pacing to slow pacing at a PCL longer than the measured AFCL. The rationale behind this procedure is to take advantage of the brutal wavelength lengthening due to restitution adaptation after PCL increase. Rensma et al. demonstrated in chronically instrumented conscious dogs that fibrillating phenomena occur at wavelengths shorter than a critical value of 7.8 cm [86]. The necessity of short wavelengths to ensure AF perpetuation was later confirmed in a computer study using the same model of multiple wavelets as in the present work [91]. Consequently, wavelength lengthening can serve as a mechanism to eliminate residual fibrillation preventing AF termination during rapid pacing alone. In the proposed pacing scheme, once sufficient capture is obtained by rapid pacing, the abrupt transition towards slow pacing provokes an immediate increase of both APD and CV via restitution adaptation within a time window shorter than 500 ms. As a result, the wavelength of the paced waves is shifted from 3.6 cm to 9.1 cm, in turn creating wavefronts less prone to reentrant phenomena. These extensive depolarizing wavefronts could therefore take control of a larger area in the atria, leaving less space for the remaining fibrillating wavelets and forcing their annihilation. During the slow pacing phase, the train of pacing pulses at 180%  $AFCL_{\text{mean}}$  was preceded by one single pacing pulse at 130%  $AFCL_{\text{mean}}$ . The role of this stepwise transition was to help install the slow pacing in a more robust way. Indeed, it was observed that a direct transition towards slow pacing at 180%  $AFCL_{\text{mean}}$  permitted SAF reinitiation in some cases since the first long pause following the last rapid pacing pulse gave enough time for reentrant waves to invade the septal area. Alternatively, a direct transition towards the slow pacing phase at 130%  $AFCL_{\text{mean}}$  tended to provoke a better suppression of reentrant waves after the application of the first slow pacing pulse due to a shorter pause, but the subsequent pulses were too close to allow for a full repolarization of the atrial tissue and showed a tendency to reinitiate SAF. Therefore the proposed stepwise transition was a good trade-off to avoid SAF reinitiation both during the transition from rapid to slow pacing and during slow pacing. To our knowledge, this is the first time that such a combination of rapid and slow pacing is proposed as a therapeutic solution to AF. Compared to rapid pacing only, the average SAF termination rate obtained by the proposed pacing scheme was doubled. Furthermore, when only rapid pacing was applied, the SAF termination rate showed a substantial drop when pacing at a suboptimal PCL, while the addition of

the slow pacing phase made the overall procedure less dependent on the choice of the rapid PCL, as shown in Table 6.1. Indeed, SAF termination rates in the range 20-30% were obtained even when the rapid PCL selected for the first phase differed from the optimal PCL of 64% AFCL<sub>mean</sub> (except for PCLs of 68 and 70% AFCL<sub>mean</sub>).

#### 6.4.4 Practical Aspects of Septal Pacing

Pacing from the septum offers many advantages from a practical point of view. The strategic anatomical location of the septal area provides a pacing solution offering symmetric propagation on both atria while pacing from a single site. Pacing strategies involving the stimulation of the septal area have proven to be feasible [206], and have been widely tested in the framework of AF prevention, although leading to mixed conclusions [207, 208, 209, 210, 211]. However, the ability of septal pacing for suppressing ongoing AF episodes remains to be more fully addressed [199]. In our previous systematic study of single site rapid pacing of SAF in a biophysical model of human atria, the septum was the only pacing site that yielded sporadic capture episodes in both atria simultaneously [139]. However, using only a single septal electrode, it was difficult to maintain this capture and no termination could be observed. In the present study, a rapid pacing of the whole septal area led to a more synchronous depolarization of both atria and to the possibility of observing SAF termination. The key feature of the septal pacing presented here is that a greater amount of current was injected in the tissue at each pacing pulse, and in a more homogeneous way, than with single or multiple electrodes. This septal area stimulation provided more uniform depolarization patterns linked to a higher effectiveness in blocking SAF reentries. The delivery of the septal stimulus in this model study was ideal and the results obtained can be seen as a theoretical limit representing the best performance achievable. The step towards a practical version of the proposed pacing scheme requires the design of an electrode configuration reproducing the depolarization pattern offered by the ideal septal pacing used throughout this study. Future work will be devoted to finding a suitable electrode design.

#### 6.4.5 Importance of Capture Patterns

The advantage of the modeling approach adopted in this work is that the temporal and spatial evolution of depolarization waves and reentries on the whole atrial surface can be observed in detail through inspection of transmembrane potential maps during the whole AF septal pacing procedure. Such analysis could highlight the importance of the capture patterns created by rapid pacing on the subsequent SAF termination rates.

In particular, the number of anchored waves present in the capture pattern at the end of the rapid pacing phase was shown to have a significant effect on the ability to terminate SAF: a low number of anchored waves was correlated to a high SAF termination rate and *vice versa*. Most importantly, it was possible to demonstrate that compared to a simple rapid pacing sequence, the proposed septal pacing algorithm showed more robustness with respect to the number of anchored waves present at the end of the rapid pacing phase. Indeed, the critical number of anchored waves above which results were

strongly degraded was shown to be higher when adding the slow pacing phase. This increased robustness can be explained by the presence of the first slow pacing pulse at  $130\% \text{ AFCL}_{\text{mean}}$  that helped blocking anchored waves trying to propagate back to the stimulation site once rapid pacing was stopped.

The importance of the anatomical location of anchored waves could also be demonstrated, with anchored waves nearer to the stimulation site having significant impact on subsequent termination success. Once again, the proposed pacing sequence compared to a mere rapid pacing was more robust with respect to certain anatomical locations such as the pulmonary veins.

In the light of these results, it would be of great interest to actively optimize the capture patterns during the rapid pacing phase, for instance by minimizing the number of anchored waves before applying the transition towards the slow pacing phase. Several studies have explored the phenomenon of anchored spiral waves and how to unpin these waves by means of external pulsation trains [215]. Such methods could be included in the proposed pacing scheme in order to optimize overall SAF termination success.

#### 6.4.6 Study Limitations

The biophysical model used in this study was based on a three-dimensional monolayer surface and did not take into account anatomical details such as Bachman's bundle, pectinate muscles or crista terminalis. Moreover, the tissue had homogeneous properties and did not include fibrosis or anisotropy. In this sense, the model corresponds to a patient with electrical remodeling but no structural remodeling, and is therefore a model of recent chronic AF. These simplifications are part of the trade-off between model accuracy and computational load needed to perform large scale evaluations such as the ones presented here. For instance, a similar approach using the same model has been successfully used in a previous study for the simulation of different ablation procedures, showing that ablation outcomes in the model were not significantly different from clinical experience in humans [113]. Finally, although values of CV and APD are within values reported for the human atria, AFCL values in the model are slightly lower than human responses, where AFCL values of 100 ms are only rarely measured. Throughout this study, the activity from the sinoatrial node was not simulated since it was considered silent due to overdrive suppression. It is a reasonable approximation to hypothesize that during SAF or rapid pacing the contribution of sinus rhythm to the global electrical activity is negligible, since the area of the sinoatrial node is most of the time in a refractory state. However, during the slow pacing phase, sinoatrial node activity could occasionally interact with the pacing stimulus, possibly disturbing it. Nevertheless, the slow pacing rate is still several times faster than the discharge rate of the sinoatrial node and such interferences are relatively unlikely.

Finally, it is important to mention that the proposed algorithm was specifically designed for patients with early persistent AF, and not for patients with long-standing persistent or permanent AF. Indeed, it was shown in both animals and humans that restitution properties are modified during late chronification of AF, so that restitution curves

are progressively flattened [92, 116]. These changes are likely to alter the ability of the proposed algorithm to terminate AF, because the wavelength lengthening supposed to occur during the transition to slow pacing would not be possible in the case of a flat restitution curve. Thus, the proposed pacing solution will only express its full potential when applied during early stages of AF chronification. This remark validates our choice to focus on a model of recent chronic AF.

### 6.4.7 Clinical Implications

The model-based results obtained in this study suggest that a pacing protocol combining rapid and slow pacing in a sequential way from the interatrial septal area could provide a new therapy to terminate ongoing AF episodes by means of low-energy stimulation. This is the first time that such a multi-stage septal pacing sequence for the treatment of AF is proposed and tested. The procedure appears to be more robust and efficient in terminating AF episodes than currently used rapid pacing strategies. Such a pacing therapy could represent an alternative to drugs and catheter-based ablation, and could easily be implemented in patients who already have an indication for pacing. The interesting property of the proposed pacing scheme is its short duration (about 30 s in total) and its reproducibility. Therefore the whole procedure could be repeated as many times as needed until SAF termination occurs. In this perspective, the SAF termination rates of up to 29% obtained in this model-based study for a single run of the pacing sequence are encouraging. Even if the termination rates of the pacing scheme drop to lower values when tested in real electrophysiological settings, the effective AF termination ability of the protocol would be increased by its repeatability.

## 6.5 Conclusion

In this chapter, a novel atrial septal pacing algorithm was specifically designed for AF termination, and was tested in a model-based study leading to AF termination rates of up to 29% when optimal pacing cycle lengths were considered. The systematic analysis framework developed in chapter 5 could be used to determine which pacing cycle lengths were the most efficient at controlling atrial electrical activity for each phase of the pacing protocol.

Innovations compared with previous pacing protocols for AF termination were the selection of a septal stimulation site, as well as the combination of a rapid pacing and a slow pacing in a sequential way. The proposed multi-stage pacing approach could suppress AF reentries in a more robust way than classical single site rapid pacing. Experimental studies are needed to determine whether similar termination mechanisms and rates would be observed in animals and humans, and for which types of AF populations the procedure might be most effective.



# Measures of Atrial Fibrillation Organization for Improved Patient Management

---

# 7

## 7.1 Introduction

In this chapter, novel measures of AF organization are presented and used on real surface ECG signals to optimize AF management. After a brief summary of past developments in AF complexity quantification, a new analysis framework based on advanced signal processing methods is presented in detail and proposed as an automatic diagnostic tool to discriminate between persistent and permanent AF and therefore to better orient therapeutic decisions.

### 7.1.1 Quantifying Atrial Fibrillation Complexity: a State of the Art

Atrial fibrillation is known to be a polymorphic disease whose dynamical complexity and electrophysiologic properties strongly depend on its state of development, a longer AF often presenting higher levels of disorganization and alteration in electrical activity [92, 216]. As a result, AF was progressively considered as a continuous spectrum of dynamical phenomena with different levels of complexity. This evolutive nature of AF led researchers to propose various classifications of its organization based on electrophysiological measurements. First, Wells and colleagues performed bipolar EGM measurements of the human RA and observed the morphology, polarity and beat-to-beat cycle length of the acquired signals [73]. They found that AF signals could be classified in four different classes of increasing complexity, but no statistical difference was found between the four types of AF with regard to disease state. Moreover, two measurements made on the same patient at different time instants could lead to a classification in a different AF type. These results suggest that, although interesting, this complexity measure

was somehow not robust enough, maybe because observing only one or two bipolar signals in the RA provided a measure of dynamics complexity that was too local. A more global classification of AF complexity was proposed by Konings and colleagues, during high-density mapping of AF in humans [74]. In this study, fibrillating wavefronts propagating on the RA free wall could be observed by means of a spoon-shaped electrode of 244 unipolar leads. Three AF types of increasing complexity were defined according to the number of AF wavelets detected on the RA and their dynamical patterns. This classification soon became a reference one and was used in many electrophysiological studies to depict the level of AF complexity under observation.

In parallel, numerous methods based on basic or advanced signal processing techniques and dedicated to the quantification of AF organization emerged from the biomedical engineering field, offering electrophysiologists new ways to understand the underlying dynamics of AF [217]. Linear methods were designed to exploit relationships between atrial recordings in both the time and the frequency domain. Spatial correlation estimates were first used to show that AF was spatially ordered, but with a degree of correlation decreasing with distance between measurement points [216, 218, 219]. Temporal and spatial phase analyses of ECG atrial waveforms were then proposed to quantify intracardiac organization, leading to the successful distinction of atrial flutter from highly organized AF sequences [220, 221, 222]. On the other hand, frequency-domain analyses provided a simple and powerful approach to explore AF activity, and several techniques were rapidly derived to depict its dynamics and measure its organization. Fourier analysis was used to extract dominant frequencies (DF) of AF activity, and 3D DF maps were constructed by extracting DFs from each electrode of epicardial mapping recordings separately. Such techniques opened the way to global analyses of AF spectral activity, and could demonstrate that AF was not a random phenomenon, but was characterized by spatial inhomogeneities in AF spectrum [223, 224] as well as differences in oscillatory properties for AFs at different stages [225, 226]. Magnitude square coherence was used to quantify the phase consistency between two cardiac signals, therefore returning a measure of stability of cardiac activity [227, 228, 229]. Two indices computed from power spectrum analysis were also proposed to describe specifically the degree of organization within AF: a regularity index (RI) was defined as the ratio of the area under the dominant peak in the power spectrum to the total area [230], while the organization index (OI) was computed as the sum of the areas under the dominant peak and its harmonic divided by the total area [231, 232]. This family of indices was successfully used to describe variations of AF spatiotemporal disorganization due to left atrial dilatation [233], and could also help to better understand the impact of therapies such as defibrillation, low-energy pacing, catheter ablation or drugs [189, 232, 234, 235, 236]. Finally, other linear measures of AF organization were proposed based on principal component analysis [237] and on the linear prediction error between two atrial recordings [238]. The latter technique proved to be efficient for distinguishing different levels of AF organization in the presence of noise.

Non-linear methods for AF organization quantification were also investigated, as the possibly chaotic nature of fibrillation was questioned early [239]. It was first demonstrated in 1995 that basic measures from chaos theory could already detect non-linear



interactions in AF signals [240]. Then, numerous other non-linear techniques were specifically proposed for the analysis of cardiac arrhythmias. Trajectory analysis in reconstructed phase space was used to better describe fibrillating spiral dynamics [133]. Methods based on wave morphology analysis [241] or recurrence plots [242] were designed to track periodicities in AF signals, and could distinguish AF of different types. Finally, various measures were based on entropy computation. Approximate and sample entropies were developed to quantify the degree of repetitiveness of a physiological signal [243]. The sample entropy was then extensively used as an organization measure to study the complexity of atrial electrical activity during both AF onset and spontaneous termination [120]. Similarly, a regularity index based on corrected conditional entropies [244] and a synchronization index computed from Shannon entropy [245] were both used to discriminate between different types of AF.

The methods described above coupled with the progressive improvements in electrophysiological recordings accuracy contributed to shed new lights on the complexity and subtleties of AF dynamics. In particular, the organization level of electrical activity during ongoing AF proved to be even less predictable than foreseen, as it could vary suddenly in a single AF episode. Indeed, it was first shown in 1992 and confirmed later that transient linking of fibrillating wavefronts occurred during AF in humans, with a related decrease of AF rate [246, 247]. Such short and transient episodes of organized AF were later observed during monophasic action potential measurements, endocardial mapping and ECG recordings in humans, as well as through wide bipolar electrodes in dogs [229, 232, 247, 248, 249]. The duration of these short organized AF sequences ranged between 1 and 5 seconds [232, 246, 249]. Moreover, changes in AF complexity were also shown to be determinant during onset and termination of AF episodes, as AF organization tended to decrease immediately after AF onset and increase progressively before AF spontaneous termination [126, 127, 188, 250]. These results tend to suggest that time segments with higher AF organization may provide a favorable window for its termination [251]. Indeed, it was proposed that the efficacy of both atrial defibrillation and burst pace termination could be improved when shocks or bursts were applied during episodes of high AF organization [189, 232], and that atrial defibrillation outcome could be predicted by non-linear organization measures [252]. Similarly, it was shown that AF cycle length and OI could be used as a quantitative tool for monitoring substrate changes during ablation of ongoing AF, with longer cycle length and higher OI corresponding to progressive elimination of fibrillating activity [144, 234]. Taken together, these studies confirm that optimized measures of organization can reveal new aspects of cardiac arrhythmias such as AF, and show great promise for future monitoring and therapeutic tools.

### 7.1.2 Motivation of the Proposed Study

It is now well known that the presence of AF in atrial tissue tends to provoke electrical and structural remodeling of its substrate, which will in turn modify the dynamical features of AF and promote its long-term perpetuation [92, 103, 253, 254]. Due to this evolutive nature, AF was classified by clinicians according to its state of development

[1, 2, 3]. AF is called paroxysmal or acute when its duration is shorter than seven days and when it returns spontaneously towards normal sinus rhythm. When it becomes sustained beyond seven days due to remodeling, and is not likely to spontaneously self-terminate anymore, the arrhythmia is called persistent. Finally, AF is termed permanent when cardioversion attempts are not worth trying anymore because the arrhythmia is now definitively installed. Chronic AF is used to depict recurrent and long-lasting AF, which can be considered as encompassing both persistent and permanent AF.

For each stage of the arrhythmia, standard management guidelines were defined [1, 2, 3]. Of particular interest is the management of non-terminating AF episodes, i.e. the management of patients with AF lasting many weeks (Figure 7.1). For this category of patients, initial therapy may be anticoagulation and rate control while the long-term goal, if AF is persistent and not yet in a permanent state, is to restore sinus rhythm especially when the presence of AF implies disabling symptoms for the patient (Figure 7.1, Panel (A)). If permanent AF has been diagnosed, cardioversion is not considered and anticoagulation and rate control is the only indicated treatment (Figure 7.1, Panel (B)). In this context, it becomes essential to know accurately, for a given patient, the degree of chronification of the arrhythmia, because it will provide valuable information about the future effectiveness of a potential cardioversion or ablation procedure, and could even directly discard such interventions in case of a too developed AF. Indeed, the decision of entering a long therapy process or a ablation procedure for normal rhythm restoration may have a significant impact on the patient's quality of life, as well as on health expenditures. In other words, being able to discriminate reliably between persistent and permanent AF before any cardioversion attempt would directly improve patient management as cardioversion options could be considered appropriately in the case of a diagnosed persistent AF, and alternatively substantial cost savings could be made through the bypass of the whole cardioversion procedure in the case of a permanent AF.

AF management is always a difficult task, especially when patient history has not been documented correctly or sufficiently. In such situations, it appears difficult for practitioners to clearly evaluate the degree of development of the arrhythmia and classify it as persistent or permanent. Thus, it would be of critical importance to benefit from an automatic diagnostic tool able to make this distinction directly based on dynamical features of AF electrical activity. So far, many of the methods mentioned in the last section were proposed to discriminate between paroxysmal AF and chronic AF. Indeed, these two AF categories could be successfully distinguished by means of activation mapping [255], spatial correlation mapping [216], DF mapping [225, 256], linear prediction error analysis [238], wave similarity mapping [257], entropy-based analysis [258, 259], AFCL analysis [260] and ECG F-wave analysis [261]. However, to our knowledge, no method has been proposed to distinguish persistent from permanent AF, although such a method would be of clinical interest. In the present study, a multivariate frequency analysis framework is proposed to develop AF organization indices based on the combined analysis of multiple surface ECG leads. These measures were used to classify persistent and permanent AF signals.

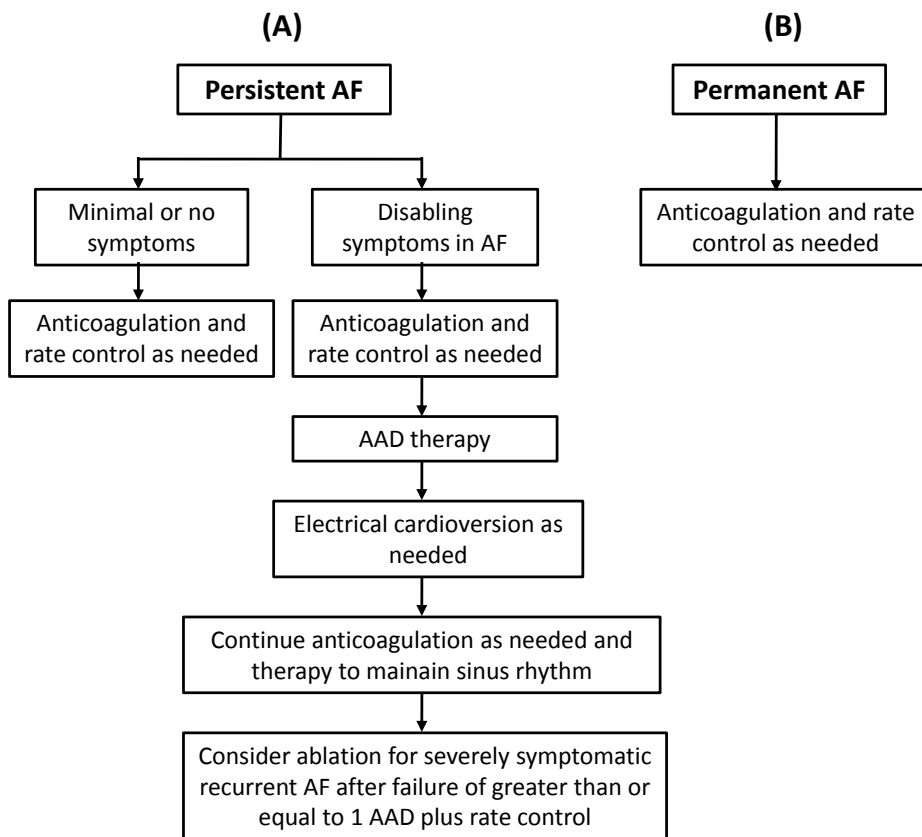


**Figure 7.1:** Pharmacological management of patients with (A) persistent AF or (B) permanent AF. AAD indicates antiarrhythmic drug. Modified from [1].

## 7.2 Clinical Electrocardiogram Database and Data Preprocessing

A clinical ECG database was created in collaboration with the cardiology department of the CHUV (Centre Hospitalier Universitaire Vaudois). Standard ECG recordings of 5 minutes duration were acquired in patients with either persistent AF ( $N = 20$ ) or permanent AF ( $N = 33$ ) as diagnosed based on their known clinical history. Patients with multiple pathologies leading to an unclear AF classification were avoided. Signals were recorded and stored using a commercial system (CardioLaptop<sup>®</sup>, AT-110, SCHILLER). The acquisition system used electrocardiographic filtering (0.05 to 150 Hz), a dynamic range of  $\pm 10$  mV AC (resolution of  $5 \mu\text{V}$ ) and a sampling rate of 500 Hz. The following preprocessing was performed on each ECG lead of each acquired signal to prepare it for further analysis:

- Ventricular complexes were detected and subtracted following the single beat cancellation method described in [262].

- Resulting signals of atrial activity were downsampled to 50 Hz.
- High-pass filtering was applied using a digital Butterworth filter with a 3 Hz cut-off frequency.
- To get rid of any residual artifacts, segments of 10 seconds were truncated at the beginning and at the end of each recording.

The resulting preprocessed signals were then used for AF organization assessment.

### 7.3 Multivariate Analysis of Atrial Fibrillation Organization

The proposed approach to quantify AF organization based on a standard ECG recording is composed of distinct steps which will be described in detail in the sections below. First, a multivariate frequency analysis extracts oscillatory features from multiple ECG electrodes by means of the so-called spectral envelope method, and organization measures are then computed on the resulting spectrum to assess AF complexity. Finally, a classification procedure is performed to distinguish persistent from permanent AF signals. In Figure 7.2, a block diagram summarizes the whole analysis procedure.

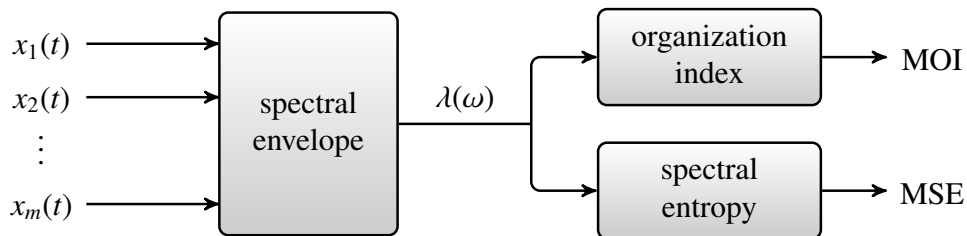


**Figure 7.2:** Block diagram of the multivariate analysis framework. In this scheme, the different parts of the proposed method are illustrated. First, several ECG leads are selected and analyzed collectively by means of the spectral envelope method to obtain a multivariate spectrum. Then, organization measures such as the organization index or the spectral entropy are computed on the spectral envelope.

#### 7.3.1 Multivariate Spectral Analysis: the Spectral Envelope

The spectral envelope was first developed to explore the periodic nature of categorical time series, and can be described as a frequency-based, principal component technique applied to multivariate time series [263]. The basic idea is to assign numerical values to each category of the time series under study and then perform a spectral analysis of the resulting discrete valued signal. Furthermore, the method was extended to deal directly with real-valued time series [264]. More generally, the spectral envelope can be used to run multivariate spectral analysis, as several variables of a multidimensional signal describing the same phenomenon can be processed by the method in order to detect and emphasize the periodic components common to them. This type of analysis has already been used successfully in the field of industrial data to detect plant-wide oscillations [265]. Thus, such approach seems to be particularly well suited for detecting spectral

components in multiple lead systems such as ECG recordings, where cardiac oscillations are recorded by several surface electrodes simultaneously but are at the same time heavily altered by substantial measurement noise. The definition and implementation of the spectral envelope method as well as practical examples are exposed below.

### Definition of the Spectral Envelope

Let

$$\mathbf{x}(t) = \begin{bmatrix} x_1(t) \\ x_2(t) \\ \vdots \\ x_m(t) \end{bmatrix} \quad t = 0, \pm 1, \pm 2, \dots \quad (7.1)$$

be a multivariate, vector-valued time series on  $\mathfrak{R}^m$ . Its covariance matrix is  $\mathbf{V}_x = E[\mathbf{x}\mathbf{x}^T]$ , assuming that  $E[\mathbf{x}] = 0$  and that  $^T$  is the transpose operator, and its associated power spectral density (PSD) is denoted by  $\mathbf{P}_x(\omega)$ , with  $\omega$  representing normalized frequency and  $-1/2 < \omega \leq 1/2$ . Let  $g(t, \boldsymbol{\beta}) = \boldsymbol{\beta}^H \mathbf{x}(t)$  be a scaled time series from  $\mathfrak{R}^m$  to  $\mathfrak{R}$  or, in other words, a linear combination of the rows of  $\mathbf{x}(t)$ .  $\boldsymbol{\beta}$  is a  $m \times 1$  real or complex column vector, and  $^H$  stands for the conjugate transpose operator. The variance of  $g(t, \boldsymbol{\beta})$  can be expressed as  $V_g(\boldsymbol{\beta}) = \boldsymbol{\beta}^H \mathbf{V}_x \boldsymbol{\beta}$ , and the expression of its PSD is  $P_g(\omega, \boldsymbol{\beta}) = \boldsymbol{\beta}^H \mathbf{P}_x(\omega) \boldsymbol{\beta}$ . The spectral envelope  $\lambda(\omega)$  of  $\mathbf{x}$  is defined as:

$$\lambda(\omega) = \sup_{\boldsymbol{\beta} \neq 0} \left\{ \frac{P_g(\omega, \boldsymbol{\beta})}{V_g(\boldsymbol{\beta})} \right\} = \sup_{\boldsymbol{\beta} \neq 0} \left\{ \frac{\boldsymbol{\beta}^H \mathbf{P}_x(\omega) \boldsymbol{\beta}}{\boldsymbol{\beta}^H \mathbf{V}_x \boldsymbol{\beta}} \right\} \quad -1/2 < \omega \leq 1/2 \quad (7.2)$$

The quantity  $\lambda(\omega)$  can be interpreted as follows. It represents the largest portion of power (or variance) that can be obtained at the frequency  $\omega$  for any scaled series  $g(t, \boldsymbol{\beta})$ . The scaling vector associated with  $\lambda(\omega)$  is denoted by  $\boldsymbol{\beta}(\omega)$  and is called the optimal scaling vector at frequency  $\omega$ . Therefore, this optimal scaling vector is not necessary the same for all  $\omega$ . Throughout this work, it was decided to constrain  $\boldsymbol{\beta}$  to  $\boldsymbol{\beta}^H \mathbf{V}_x \boldsymbol{\beta} = 1$ , so that the scaled series  $g(t, \boldsymbol{\beta})$  has a unit variance. Doing so, it ensured that (7.2) had a unique solution, and that the magnitude of the elements of  $\boldsymbol{\beta}(\omega)$  were easily comparable. The name of "spectral envelope" is appropriate since  $\lambda(\omega)$  "envelopes" the standardized spectrum of any scaled processes. Indeed, given any  $\boldsymbol{\beta}$  normalized so that  $g(t, \boldsymbol{\beta})$  has a unit power,  $P_g(\omega, \boldsymbol{\beta}) \leq \lambda(\omega)$ , with equality if and only if  $\boldsymbol{\beta}$  is colinear to  $\boldsymbol{\beta}(\omega)$  [263].

Considering the optimal scaling vector  $\boldsymbol{\beta}(\omega)$ , (7.2) can be rewritten as

$$\lambda(\omega) \mathbf{V}_x \boldsymbol{\beta}(\omega) = \mathbf{P}_x(\omega) \boldsymbol{\beta}(\omega) \quad (7.3)$$

This new formulation is a generalized eigenvalue problem. Thus,  $\lambda(\omega)$  is the largest eigenvalue of  $\mathbf{P}_x(\omega)$  in the metric of  $\mathbf{V}_x$ , i.e.  $\lambda(\omega)$  is the largest eigenvalue associated with the determinant equation:

$$|\mathbf{P}_x(\omega) - \lambda(\omega) \mathbf{V}_x| = 0 \quad (7.4)$$

and  $\boldsymbol{\beta}(\omega)$  is the corresponding eigenvector satisfying (7.3).

The spectral envelope method can be useful to detect and emphasize spectral components present simultaneously in several measurement channels altered by noise. The following example proposed in [266] illustrates this situation. Let us assume that the measurement channels are modeled by  $m$  univariate time series  $x_i(t)$ ,  $1 \leq i \leq m$ ,  $-\infty < t < \infty$ , and that they share a common signal of interest  $s(t)$  perturbed by independent identically distributed noise, i.e.  $x_i(t) = s(t) + \varepsilon_i(t)$ . The power spectrum of each channel will be  $P_{x_i}(\omega) = P_s(\omega) + \sigma_\varepsilon^2$ . It is interesting to note that the power spectrum of a simple linear combination of  $\{x_i(t)\}$  such as  $\bar{x}(t) = m^{-1} \sum_{i=1}^m x_i(t)$  will read  $P_{\bar{x}}(\omega) = P_s(\omega) + m^{-1} \sigma_\varepsilon^2$ . The signal to noise ratio of  $\bar{x}(t)$  has increased by a factor of  $m$  compared to the individual  $x_i(t)$ . This simple example suggests that the scaling procedure performed by the spectral envelope computation will tend to enhance periodic signatures common to several input variables and attenuate noise. Moreover, the spectral envelope method will systematically select for each frequency  $\omega$  the optimal linear combination maximizing spectral component enhancement. Thus, the proposed technique appears particularly suitable for clinical electrophysiological measurements such as surface ECG recordings.

### Estimation of the Spectral Envelope

This section describes in more practical detail how the spectral envelope method was implemented in this work. The multivariate input signal to be analyzed is a  $m \times n$  matrix of  $m$  variables and  $n$  samples, i.e.  $[\mathbf{x}(0), \mathbf{x}(1), \dots, \mathbf{x}(n-1)] \in \mathfrak{X}^{m \times n}$ . Data were first normalized to make spectral envelopes between different signal sets more interpretable. The first step was to calculate the periodogram of the normalized matrix as an estimate of  $\mathbf{P}_\mathbf{x}(\omega)$ :

$$\hat{\mathbf{I}}_n(\omega) = \frac{1}{n} \left[ \sum_{i=1}^{n-1} \mathbf{x}(t) e^{-j2\pi i t \omega} \right] \left[ \sum_{i=1}^{n-1} \mathbf{x}(t) e^{-j2\pi i t \omega} \right]^H \quad -1/2 < \omega \leq 1/2 \quad (7.5)$$

The continuous expression of (7.5) was implemented using the discrete Fourier transformation, translating into the following formulation:

$$\hat{\mathbf{I}}_n(\omega_k) = \frac{1}{n} \left[ \sum_{i=1}^{n-1} \mathbf{x}(t) e^{-j2\pi i t \omega_k} \right] \left[ \sum_{i=1}^{n-1} \mathbf{x}(t) e^{-j2\pi i t \omega_k} \right]^H \quad (7.6)$$

with  $\omega_k = k/n$ , for  $k = 1, \dots, [n/2]$ , being the harmonic (or Fourier) frequencies. However, the periodogram expressed in (7.6) is not a consistent estimator of the PSD [267]. To overcome this, periodogram averaging or smoothing can be used [268, 269]. In the present work, a smoothing technique consisting of a symmetric moving average of the periodogram was applied as suggested in [269]. The periodogram estimate then becomes

$$\hat{\mathbf{P}}_\mathbf{x}(\omega_k) = \sum_{q=-d}^d h_q \hat{\mathbf{I}}_n(\omega_{k+q}) \quad (7.7)$$

where the smoothing weights  $\{h_q\}$  are symmetric ( $h_q = h_{-q}$ ) and  $\sum_{q=-d}^d h_q = 1$ . The parameter  $d$  is chosen to obtain a desired degree of smoothness. Large values of  $d$  will

lead to smoother estimates, but a trade-off has to be made in order to avoid leakage, i.e. significant peaks being smoothed away. For  $\hat{\mathbf{P}}_{\mathbf{x}}(\omega_k)$  to be consistent, the weights must satisfy  $\sum h_q^2 \rightarrow 0$  as  $d \rightarrow \infty$ , but  $d/n \rightarrow 0$  as  $n \rightarrow \infty$ . In this work, the set of weights  $\{h_q\}$  for periodogram smoothing was chosen similarly as in [265]:

$$h_q = \frac{d - |q| + 1}{(d + 1)^2} \quad |q| = 1, 2, \dots, d \quad (7.8)$$

and a default value of  $d = 2$  was used throughout the different computations of the study.

The periodogram estimate  $\hat{\mathbf{P}}_{\mathbf{x}}(\omega_k)$  can then be used together with the sample estimate of the covariance matrix  $\hat{\mathbf{V}}_{\mathbf{x}}$  to estimate the spectral envelope defined in (7.2):

$$\hat{\lambda}(\omega_k) = \sup_{\boldsymbol{\beta} \neq \mathbf{0}} \left\{ \frac{\boldsymbol{\beta}^H \hat{\mathbf{P}}_{\mathbf{x}}(\omega_k) \boldsymbol{\beta}}{\boldsymbol{\beta}^H \hat{\mathbf{V}}_{\mathbf{x}} \boldsymbol{\beta}} \right\} \quad (7.9)$$

The estimate of  $\boldsymbol{\beta}(\omega)$  at the Fourier frequencies is denoted by  $\hat{\boldsymbol{\beta}}(\omega_k)$ , and the constraint  $\hat{\boldsymbol{\beta}}(\omega_k)^H \hat{\mathbf{V}}_{\mathbf{x}} \hat{\boldsymbol{\beta}}(\omega_k) = 1$  was enforced as mentioned above. One obtains  $\hat{\lambda}(\omega_k)$  as the largest eigenvalue of the matrix  $\hat{\mathbf{H}}(\omega_k)$  defined by

$$\hat{\mathbf{H}}(\omega_k) = \hat{\mathbf{V}}_{\mathbf{x}}^{-\frac{1}{2}} \hat{\mathbf{P}}_{\mathbf{x}}(\omega_k) \hat{\mathbf{V}}_{\mathbf{x}}^{-\frac{1}{2}} \quad (7.10)$$

The optimal scaling vector  $\hat{\boldsymbol{\beta}}(\omega_k)$  was computed as  $\hat{\boldsymbol{\beta}}(\omega_k) = \hat{\mathbf{V}}_{\mathbf{x}}^{-\frac{1}{2}} \hat{\boldsymbol{\beta}}_0(\omega_k)$ , where  $\hat{\boldsymbol{\beta}}_0(\omega_k)$  is the eigenvector of  $\hat{\mathbf{H}}(\omega_k)$  associated with  $\hat{\lambda}(\omega_k)$ .

### Example on Synthetic Signals

In the following example based on synthetic signals, interesting properties of the spectral envelope method and its superiority over simple PSD averages for the detection of common oscillations in a noisy environment are demonstrated. A set of three univariate time series sharing three noisy periodic components (normalized frequencies of  $\omega_1 = 0.1$ ,  $\omega_2 = 0.15$ ,  $\omega_3 = 0.2$ ) and altered by normally distributed white noise  $\varepsilon_i(t)$ ,  $i = 1, 2, 3$ , is first created:

$$x_1(t) = \cos(2\pi\omega_1 t) + 0.5 \cos(2\pi\omega_2 t + \pi/4) + 0.5 \cos(2\pi\omega_3 t - \pi/2) + \varepsilon_1(t) \quad (7.11a)$$

$$x_2(t) = \cos(2\pi\omega_1 t) + 0.8 \cos(2\pi\omega_2 t + \pi/4) + \varepsilon_2(t) \quad (7.11b)$$

$$x_3(t) = 0.7 \cos(2\pi\omega_1 t) + 0.5 \cos(2\pi\omega_2 t + \pi/4) + \cos(2\pi\omega_3 t - \pi/2) + \varepsilon_3(t) \quad (7.11c)$$

In these time series,  $t = 1, \dots, 256$ . The white Gaussian noise  $\varepsilon_1(t)$  has unit variance, while  $\varepsilon_2(t)$  and  $\varepsilon_3(t)$  have variances of 4 and 9 respectively. Each signal contains at least two of the periodic components and the amplitude of each oscillation varies from one signal to another. The PSD of each signal was computed individually using the same smoothing procedure as for spectral envelope computation, and averaged for purposes of comparison with the spectral envelope applied directly to the three input variables. The results of these simulations are shown in Figure 7.3. First, it can be observed that

individual PSDs indeed contain the oscillations at frequencies  $\omega_1$  to  $\omega_3$ , but also display several spurious frequency peaks induced by noise, especially for the signals  $x_2(t)$  and  $x_3(t)$  for which the background noise is so strong that some peaks of interest are hardly visible. Even when computing the average PSD of the three signals, these interferences remain important. In particular, a peak at  $\omega = 0.33$  shows a higher amplitude than the  $\omega_2$  component, although the latter was present in each of the three input signals. As a result, a crude average of PSDs would not be able to detect the common oscillatory components in this particular case. Inversely, the spectral envelope of the input variables clearly emphasizes the frequency peaks  $\omega_1$  to  $\omega_3$ , while all other spurious frequency peaks are systematically attenuated compared to those of the average PSD. Thus, this example shows that the spectral envelope, due to the optimal scaling of the input signals, is better than a simple PSD average for the detection of common oscillations and is especially suitable for the analysis of noise-corrupted data. In a past study, the superiority of the spectral envelope over spectral principal component analysis [270] was demonstrated in the same context [265].

### **Spectral Envelope Computation on the ECG Database**

The ECG database used in this study contains continuous recordings of 5 minutes duration, resulting in long AF episodes. In order to best investigate the properties of AF organization, an appropriate time-scale for AF complexity analysis must be determined. Past studies performing such analyses on various types of AF used different segment lengths, but converging evidence suggests that considering AF segments of 8 s to 10 s can reveal important features of AF organization [255, 256, 271]. In the present work, it was therefore decided for each ECG recording to compute spectral envelopes on successive segments of 10 s with an overlap of 5 s between two adjacent segments. The spectral envelopes computed over the 5 minutes segment with discarded first and last 10 seconds were then averaged to give a global value for the ECG recording. Univariate PSDs that were used throughout this study for comparison with the multivariate case were computed following the same protocol. It was observed that such a procedure tended to optimize the smoothness of the resulting spectra for further calculations of organization indices.

An example of spectral envelope applied to a typical ECG recording of AF is shown in Figure 7.4, using the computation procedure detailed above. Precordial leads V1 and V6 were used as input variables for the spectral envelope, and their respective PSDs were also computed and are shown for comparison purpose. When looking at the individual PSDs, it appears that a common periodic component at 6.5 Hz can be observed on both ECG electrodes, but at a lower power on electrode V6. The first harmonic of this frequency peak is also visible at 13 Hz on both leads, although not strikingly apparent. At the same time, other frequency peaks are present on one or the other electrode, but are not common to both. For instance, the 7.5 Hz oscillation visible on electrode V1 cannot be found on electrode V6. Similarly, a spectral component at 4.7 Hz on lead V6 is almost as powerful as the 6.5 Hz frequency of interest, but cannot be distinguished properly on lead V1.



The result of applying the spectral envelope method to leads V1 and V6 is shown in the panel (C) of Figure 7.4. Here again, the ability of the spectral envelope to detect and amplify common oscillations while attenuating noise and non-shared spectral features is well illustrated in this real-life example. First, the common frequency of 6.5 Hz is significantly amplified, as its second and even third harmonics (19.5 Hz) become clearly visible (indicated by vertical arrows). At the same time, the frequency peaks that were not common to both electrodes, although present, are strongly attenuated. Thus, the spectral envelope proves useful for the investigation of non-invasive physiological recordings such as ECG. In particular, analyzing spatially distant ECG leads like V1 and V6 is of special interest, since the spectral envelope will emphasize global oscillatory properties observable on the whole atrial surface more than local phenomena. Such information is highly relevant for global AF organization analysis.

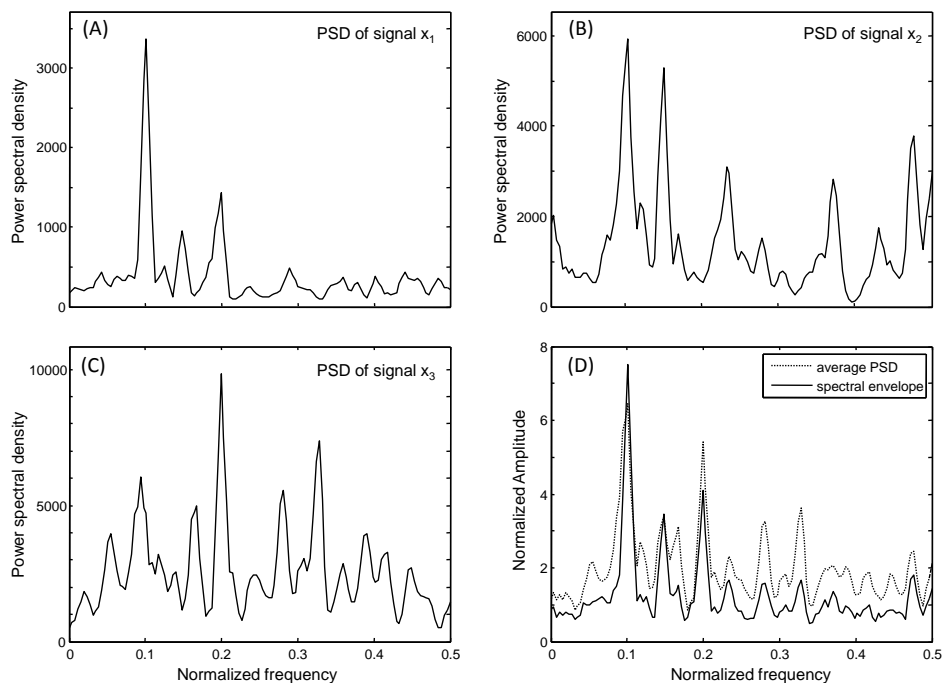


**Figure 7.3:** Detection of common oscillations in a noisy environment. Panels (A) to (C) show the individual PSDs of the synthetic signals of system (7.11). Panel (D) shows the comparison between the average PSD and the spectral envelope of the input signals. Amplitudes were normalized by the total power for comparison purpose.

### 7.3.2 Two measures of Atrial Fibrillation Organization

Once a spectral envelope has been estimated from a group of ECG electrodes, measures of complexity can be designed to assess the global level of AF organization (Figure 7.2). In this work, two measures of AF organization were tested and are presented below.

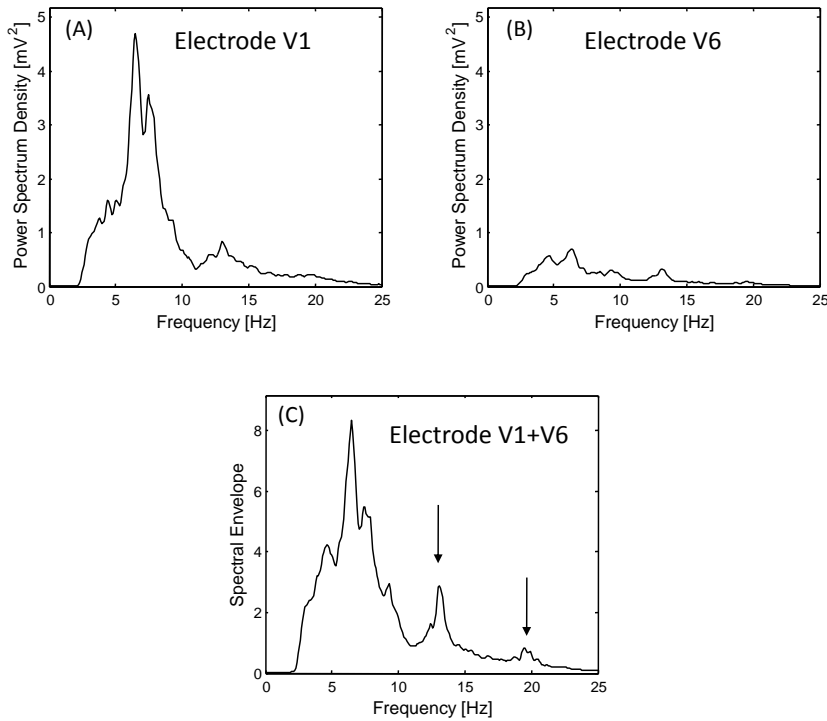


**Figure 7.4:** Spectral envelope of an ECG recording of AF. Panels (A) and (B) show the individual PSDs of leads V1 and V6. Panel (C) shows the spectral envelope obtained with V1 and V6 as input variables. The second and third harmonics of the common frequency component are indicated by vertical arrows.

### Multivariate Organization Index

The first method, originally called organization index (OI), was developed by Everett and colleagues to assess spatiotemporal organization of AF [231, 232]. The initial version of the algorithm was as follows: a univariate spectrum is first computed and its maximum peak is detected and considered as the dominant atrial frequency. Then, the areas under the maximum peak and three of its harmonic peaks are calculated over a 1 Hz window. The OI is defined as the ratio of the area under these four peaks to the total spectrum area. In the present study, we used the multivariate frequency analysis framework presented in the last section to derive a multivariate organization index (MOI) by simply computing the OI on the spectral envelope. Compared to the original algorithm, it was also decided to give more freedom to the different parameters of the measure:

- Instead of taking the maximum frequency peak and its three harmonics for area computation, the MOI algorithm looked for the  $N_p$  highest peaks of the spectrum regardless of their location, the only constraint being that two detected peaks had to be distant from each other by at least 0.5 Hz. The latter constraint ensured that each peak represented a distinct physiological oscillation. The number of peaks  $N_p$  was left as a variable parameter for feature selection.

- The bandwidth ( $BW$ ) parameter was defined as the length (in Hz) of the window encompassing each detected peak to define the integration bounds. Different values of this parameter were also considered during feature selection (see section 7.3.3).

The ratio of the area under the  $N_p$  peaks to the total spectral area was then computed to give a MOI value. The general mechanism behind this measure is the following: when common oscillations between observed leads are predominant, the spectral envelope tends to emphasize their corresponding frequency peaks compared to the rest of the spectrum. As a result, the MOI is boosted. Inversely, heterogeneous frequencies create numerous frequency peaks in the spectral envelope, and decrease the MOI.

### Multivariate Spectral Entropy

The second measure proposed is based on the concept of spectral entropy (SE) [272]. To compute SE, the PSD must be first computed and normalized, in order to make it equivalent to a probability mass function. Then, the Shannon's entropy is computed on this normalized PSD to give an estimate of the SE of the process:

$$SE = - \sum_f p_f \log_2(p_f) \quad (7.12)$$

where  $p_f$  is the normalized PSD value at frequency  $f$ .

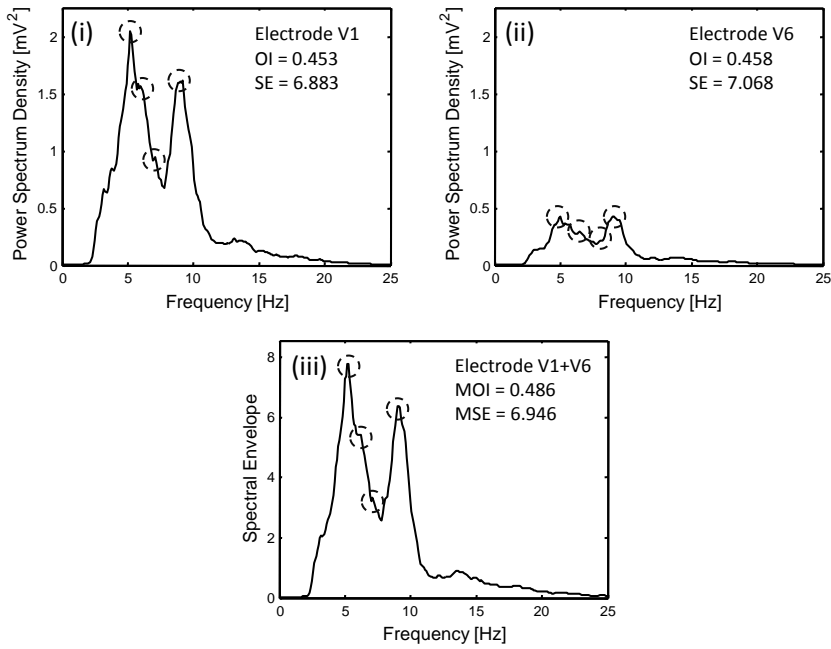
Randomly distributed noise typically shows a relatively flat spectrum and a high entropy value, whereas isolated oscillations such as sinusoids present sharp frequency peaks and therefore give low entropy values. As a result, the SE can be considered as a measure of the flatness of a spectrum. The multivariate spectral entropy (MSE) is defined as the measure obtained by computing the SE on a spectral envelope.

### Application to the ECG database

In order to illustrate the behavior of the proposed measures, two examples of MOI and MSE computations on real ECG signals presenting different levels of AF organization are shown in Figure 7.5 together with their corresponding univariate measures. Spectral envelopes were computed on ECG leads V1 and V6. OI/MOI parameter  $BW$  was set to 1 Hz and  $N_p$  to 4 for both examples in order to provide proper comparisons between each case.

The first ECG signal (signal A of Figure 7.5) is a typical example of organized activity, in which common oscillations are observed on distinct ECG leads. Indeed, electrodes V1 and V6 present a relatively similar spectral content (leading to comparable OI values), with two dominant frequency components at 5 Hz and 9 Hz. As in previous examples, the spectral envelope of leads V1 and V6 detects these shared frequencies, filtering other components of lesser interest. As a result, the MOI computation returns a higher value than the corresponding univariate measures, indicating global organization.

## (1) Signal A



## (2) Signal B

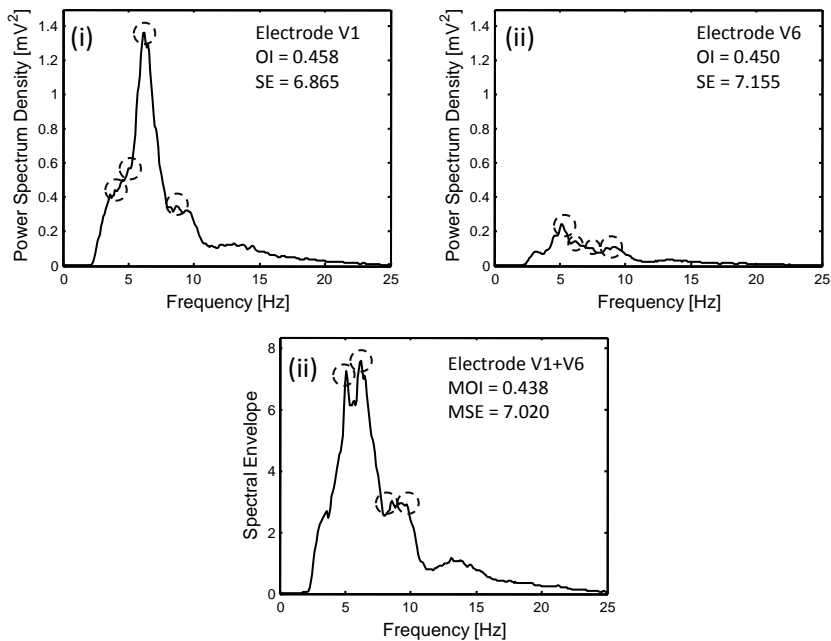


**Figure 7.5:** Examples of MOI and MSE measures on ECG signals. (1) Signal A: example of an AF signal with globally homogeneous oscillations. PSDs and univariate OI and SE are given in (i) and (ii), while multivariate measures are shown with spectral envelope in (iii). Dashed circles indicate the location of spectral peaks used for OI/MOI computation. (2) Same as (1) with a signal with spatially heterogeneous spectral content.

As opposed to the first example, signal B of Figure 7.5 is characterized by a spatially heterogeneous spectral activity, since the frequencies observed are different from one electrode to another. Indeed, a dominant oscillation at 6.1 Hz can be observed on lead V1, while the main frequency peak of lead V6 is at 5.1 Hz. The corresponding spectral envelope makes this difference even more obvious. Interestingly, both peaks are present in the spectral envelope with equal importance, even though they were measured at very different intensities in their respective PSDs (panels (i)-(ii)). This example shows that the spectral envelope can detect multiple frequencies from multiple input variables, regardless of individual importance. Thus, the resulting multivariate spectrum summarizes the mixed spectral content of leads V1 and V6, and presents several peaks of similar predominances as well as a wider spectral content. As a consequence, the MOI computed on signal B returns a lower value than the one obtained for the organized signal A. Similarly, the MSE value of signal B is higher than the MSE of signal A, indicating a less predictable oscillatory activity.

### 7.3.3 Feature Selection and Classification

In order to test the ability of both MOI and MSE measures to discriminate between persistent and permanent AF signals and to compare the multivariate and univariate approaches, a systematic classification using a leave-one-out cross-validation across patients was performed based on an extensive set of features:

- ECG leads combinations: Several combinations of ECG leads were tested as input variables for the multivariate organization measures. First, all possible pairs of precordial leads (V1 to V6) were considered. In addition, the following combinations were also tested: {V1,V2,V3}, {V4,V5,V6}, {V1,V2,V5,V6}, {V1,V2,V3,V4,V5,V6}. This resulted in a set of 19 different configurations. For the computation of univariate OI and SE, the 6 precordial ECG leads V1 to V6 were tested.
- MOI/OI parameters: the number of peaks  $N_p$  to be detected during MOI/OI computation was varied between 2 and 5, while the following values were tested for the bandwidth parameter: {0.5, 1, 1.5, 2} Hz. These values were determined after extensive empirical testing during which it was observed that further increasing or decreasing parameter values could not improve results. Thus, 16 parameter configurations were investigated.

Thus, for each patient, 304 parameter configurations were systematically tested for the multivariate measures and 96 for the univariate measures. For each of these configurations, quadratic discriminant analysis (QDA) [273] was run to classify signals as persistent or permanent AF. Classification performance was assessed with leave-one-out cross-validation and using receiver-operating characteristic analysis [274]. Correct classification and predictive values (also called precision rates) for each type of AF were documented for the five best configurations of features [275], and the multivariate and univariate approaches were compared in terms of these performance scores. In addition, Wilcoxon rank-sum tests were conducted on each feature retained in this classification ranking to assess its individual statistical power for the discrimination between AF types

(5% significance level). Finally, the whole classification procedure was conducted using all possible combinations of 2 or 3 features.

## 7.4 Results

### 7.4.1 Two-Feature Classification Results

Using the database presented in section 7.2, the performance of the methods for classification of AF feature pairs are presented in Table 7.1 and in Figure 7.6. For the multivariate case, discrimination between persistent and permanent AF could be performed with classification accuracies of up to 84.9% with a combination of MOI and MSE measures. The optimal classification is represented in Figure 7.6(A). Persistent AF signals were well clustered in a range of MOI-MSE values that could be effectively delineated by a quadratic classifier. Permanent AF signals were more diffused and occasionally presented a large variability in their organization as measured by the MOI and MSE, although most of them showed lower MOI values than the persistent AF signals. Furthermore, the predictive value for permanent AF was 93.1%. This valuable result suggests that the method proved to be very precise when diagnosing an advanced AF development. When looking at the features retained for classification in the optimal configurations of Table 7.1(A), several observations can be made. First, the optimal feature pairs were either combinations of MOI and MSE measures or pairs of MOI measures. The optimal MOI parameter configuration was very stable, as the five best classifications all used values of  $BW = 1$  Hz and  $N_p = 5$ . Furthermore, the ECG electrodes providing the best results when considered as input variables were mainly combinations of the three most lateral leads, V4 to V6. The features selected for classification in the five best configurations were also investigated individually by means of statistical tests to assess their discriminative power in the classification task considered, as shown in Table 7.2. Among all features, only one could provide a statistically significant separation between persistent and permanent AF, namely the MOI measure applied to ECG electrodes V5 and V6. With this feature, the medians obtained for persistent and permanent AF were 0.545 and 0.511 respectively with relatively small variabilities, indicating that AF organization was degraded in permanent AF compared to persistent AF. The other MOI features could not distinguish alone persistent from permanent AF with statistical significance, although they pointed towards persistent AF being more organized than permanent AF. This tendency could not be found consistently in all MSE features, because their respective ranges were clearly overlapping due to a strong variability.

Using univariate organization measures did not result in a clear discrimination between persistent and permanent AF. Classification scores did not exceed 66.0%, with a maximal predictive value for permanent AF of 71.9%. As shown in Figure 7.6(B), signals from different AF classes were not clearly separated, and both classes were characterized by high variability. Optimal features configurations always involved a combination of SE and OI measures with different ECG electrodes, but it was difficult to find any tendency in the selection of OI parameters, as their combination changed from one

classification to another. Finally, none of the univariate features considered alone could distinguish persistent AF from permanent AF in a significant manner (not shown).

**(A) Multivariate Approach**

	Feature #1	Feature #2	BW	NBP	Correct Classif. Rate	Permanent AF P.V.	Persistent AF P.V.
1.	MOI(V5, V6)	MSE(V4, V6)	1	5	84.9%	93.1%	75.0%
2.	MOI(V5, V6)	MOI(V4, V5)	1	5	81.1%	92.6%	69.2%
3.	MOI(V5, V6)	MSE(V4, V5)	1	5	81.1%	87.1%	72.7%
4.	MOI(V5, V6)	MOI(V4, V6)	1	5	79.3%	86.7%	69.6%
5.	MOI(V5, V6)	MOI(V3, V5)	1	5	79.3%	86.7%	69.6%

**(B) Univariate Approach**

	Feature #1	Feature #2	BW	NBP	Correct Classif. Rate	Permanent AF P.V.	Persistent AF P.V.
1.	SE(V1)	OI(V4)	1.5	5	66.0%	71.4%	55.6%
2.	SE(V1)	OI(V4)	2	4	64.2%	71.9%	52.4%
3.	SE(V1)	OI(V5)	2	2	62.3%	71.0%	50.0%
4.	SE(V3)	OI(V4)	2	5	62.3%	71.0%	50.0%
5.	SE(V1)	OI(V3)	1	5	60.4%	70.0%	47.8%

**Table 7.1:** Two-feature classification results. (A) Five best configurations of features and parameters to classify AF signals using the two-feature multivariate approach. ECG electrodes taken as inputs are shown in brackets. Correct classification rates and predictive values for permanent and persistent AF are specified. (B) Same as (A) for the univariate approach.

Feature	Persistent AF (median $\pm$ mad)	Permanent AF (median $\pm$ mad)	p-value
MOI(V5, V6)	0.545 $\pm$ 0.015	0.511 $\pm$ 0.024	p = 0.0054
MOI(V1, V2, V5, V6)	0.551 $\pm$ 0.039	0.527 $\pm$ 0.025	p = 0.1834
MOI(V4, V6)	0.540 $\pm$ 0.029	0.530 $\pm$ 0.021	p = 0.2914
MOI(V3, V5)	0.561 $\pm$ 0.041	0.540 $\pm$ 0.044	p = 0.3541
MSE(V4, V6)	6.986 $\pm$ 0.085	6.956 $\pm$ 0.120	p = 0.5509
MOI(V4, V5)	0.530 $\pm$ 0.022	0.526 $\pm$ 0.029	p = 0.6010
MOI(V1, V6)	0.554 $\pm$ 0.034	0.545 $\pm$ 0.021	p = 0.6398
MSE(V2, V3)	6.895 $\pm$ 0.121	6.910 $\pm$ 0.114	p = 0.6797
MSE(V4, V5)	6.959 $\pm$ 0.106	6.955 $\pm$ 0.111	p = 0.7205

**Table 7.2:** Multivariate features statistics. This table shows the list of multivariate features selected for classification in the five best configurations shown in Table 7.1(A) and 7.3(A). For each feature, the median and median absolute deviation (MAD) values are shown for each condition (persistent AF or permanent AF), with the corresponding statistical power expressed as a p-value.

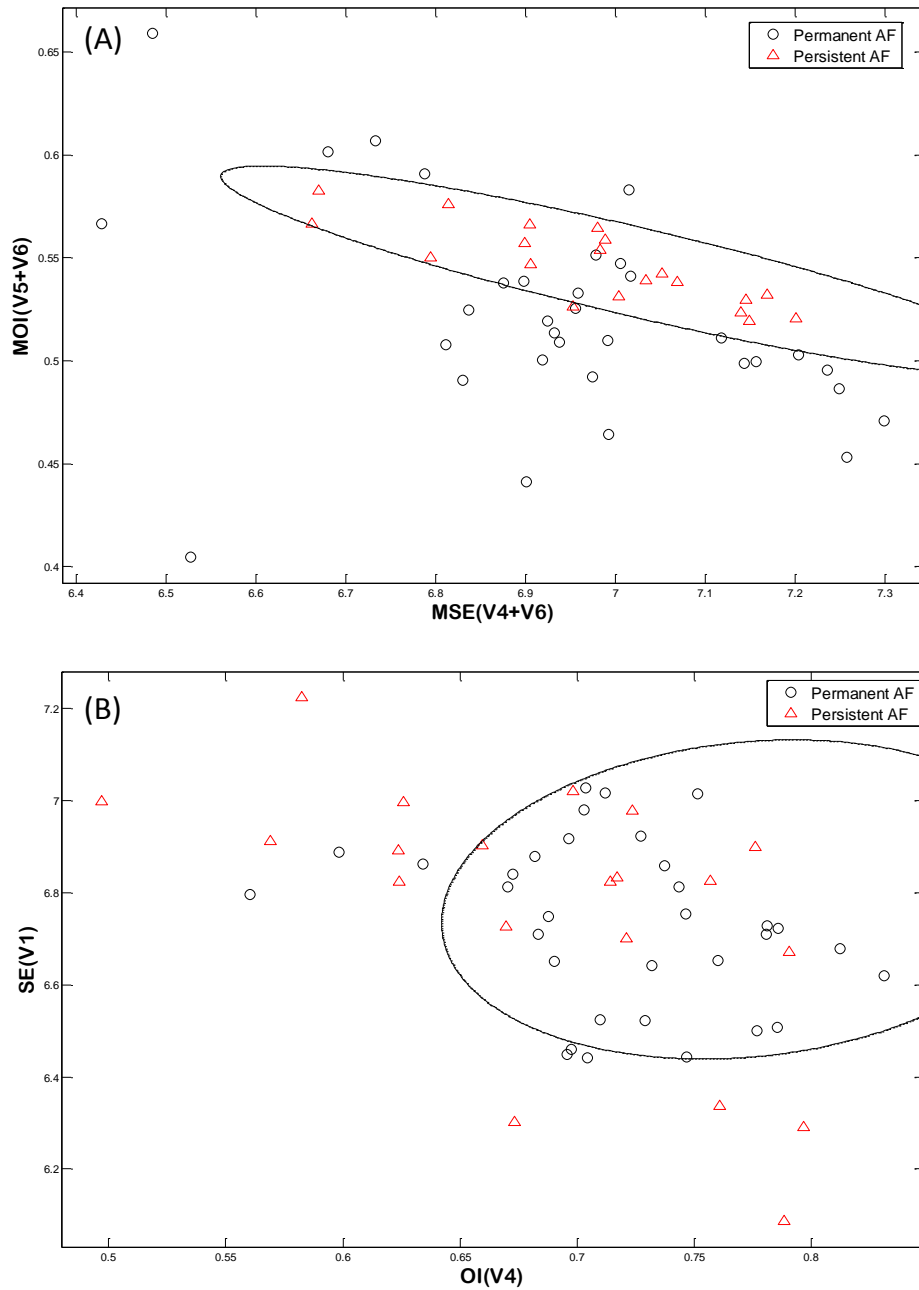


**Figure 7.6:** Two-feature classification of persistent and permanent AF signals. (A) Two-feature classification example obtained for the best multivariate configuration of Table 7.1(A). The continuous black line indicates the discrimination boundaries computed by a quadratic classifier trained on the whole dataset. (B) Same as (A) for the best univariate configuration of table 7.1(B).



### 7.4.2 Three-Feature Classification Results

Classification results using a combination of three features are presented in Table 7.3, as well as in Figures 7.7 and 7.8, and show that slight improvements can be obtained in classification accuracy compared to two-feature classification. For the multivariate approach, correct classification rates could be increased up to 88.7%, and predictive values for permanent AF and persistent AF reached values of 96.6% and 81.0% respectively. As shown in Figure 7.7, AF signals of different classes were relatively well separated, following the same patterns as in the two-feature case. Selected parameters  $BW$  and  $N_p$  for the MOI methods were similar as for two-feature classification, and showed the same stability. The ECG electrodes retained as optimal input variables were also comparable to those of the two-feature case. Interestingly, for the third input feature, a global and symmetric electrode combination ( $\{V1, V2, V5, V6\}$  in two cases and  $\{V1, V6\}$  in two other configurations) was preferentially added to the electrodes already selected in the two-feature case. These newly selected features were not able, when considered alone, to discriminate between persistent AF and permanent AF with statistical significance (Table 7.2).

The three-feature classification scheme using the univariate approach only slightly increased correct classification rates to 67.9%. However, several interesting improvements were observed. First, the predictive value for permanent AF was boosted to 78.6%, which represents a 10% increase compared to the two-feature case. Moreover, the selected parameters for OI computation were much more stable, with a preferential configuration of  $BW = 0.5$  Hz and  $N_p = 4$ . Finally, input features could be either combinations of OI and SE or sets of OI measures only. Despite these significant improvements, clear separation between persistent and permanent AF signals remained a difficult task when using the univariate approach, as is shown in Figure 7.8.

## 7.5 Discussion

In this work, a combination of advanced spectral analysis and standard AF organization measures (i.e. OI and SE) was used to explore new dynamical aspects of AF (Figure 7.2). The spectral envelope is a principal component technique for multidimensional spectral analysis that was already used to analyze genetic and industrial data [265, 269]. For the first time, in this study, this method was applied to AF signals, and showed its numerous advantages for the analysis of oscillatory phenomena in biomedical signal processing. Concerning the proposed implementation of the OI, slight differences with respect to its original version were introduced: instead of considering the DF peak of AF activity and its harmonics for area computation, it was decided to take into account the highest peaks in the power spectrum, regardless of their relative frequency locations. Following this procedure, several components at different frequencies could be considered in the OI computation. Thus, it was possible to assess the global organization of AF activity in the presence of multiple competing oscillations, as it would be the case with a multiple wavelet AF [96, 97].

**(A) Multivariate Approach**

	Feature #1	Feature #2	Feature #3	BW	NBP	Correct Classif. Rate	Permanent AF P.V.	Persistent AF P.V.
1.	MOI(V5, V6)	MSE(V4, V6)	MOI(V1, V2, V5, V6)	1	5	88.7%	96.6%	79.2%
2.	MOI(V5, V6)	MSE(V4, V5)	MOI(V1, V2, V5, V6)	1	5	86.8%	90.6%	81.0%
3.	MOI(V5, V6)	MSE(V4, V5)	MOI(V1, V6)	1	5	86.8%	90.6%	81.0%
4.	MOI(V5, V6)	MSE(V4, V6)	MSE(V2, V3)	1	5	86.8%	90.6%	81.0%
5.	MOI(V5, V6)	MSE(V4, V6)	MOI(V1, V6)	1	5	84.9%	90.3%	77.3%

**(B) Univariate Approach**

	Feature #1	Feature #2	Feature #3	BW	NBP	Correct Classif. Rate	Permanent AF P.V.	Persistent AF P.V.
1.	OI(V2)	OI(V4)	OI(V6)	0.5	4	67.9%	78.6%	56.0%
2.	OI(V2)	OI(V4)	SE(V4)	0.5	4	67.9%	78.6%	56.0%
3.	OI(V2)	OI(V4)	OI(V5)	0.5	4	66.0%	75.9%	54.2%
4.	OI(V1)	OI(V4)	SE(V3)	0.5	4	64.2%	73.3%	52.2%
5.	OI(V2)	OI(V4)	OI(V5)	0.5	3	64.2%	75.0%	52.0%

**Table 7.3:** Three-feature classification results. (A) Five best configurations of features and parameters to classify AF signals using the three-feature multivariate approach. ECG electrodes taken as inputs are shown in brackets. Correct classification rates and predictive values for permanent and persistent AF are specified. (B) Same as (A) for the univariate approach.

### 7.5.1 A Discriminative Measure of Atrial Fibrillation Chronification

To our knowledge, this study is the first to propose an analysis framework providing reliable and automatic discrimination between persistent and permanent AF signals from patient without previously known AF history. The results suggest that the transition from a persistent AF towards a permanent AF is characterized by a decrease in global AF organization that can be detected by the proposed multivariate measures. This finding is supported by previous studies pointing to the same increase in disorganization when evolving from a paroxysmal AF to a persistent or chronic AF [216, 225, 259]. Considered together, these results confirm the existence of a continuous spectrum of increasing AF disorganization as AF chronification progresses. Similar ideas were proposed early when the self-sustained and evolving nature of AF was first demonstrated [92]. However, it can be argued that the difference between persistent and permanent AF is more subtle and difficult to quantify than the changes occurring between an acute and a chronic AF state. Indeed, electrical and structural remodeling of atrial tissue are the first manifestations of AF chronification, and these massive substrate changes are known to modify AF properties dramatically [46, 254]. Therefore, differences in AF dynamics between acute AF and chronic AF are likely to provoke changes easy to observe in underlying AF organization. In comparison, the gradual process leading AF from a persistent to a permanent state is certainly more difficult to describe and quantify, as it is probably due to a strengthening of already existing remodeling processes, and not by

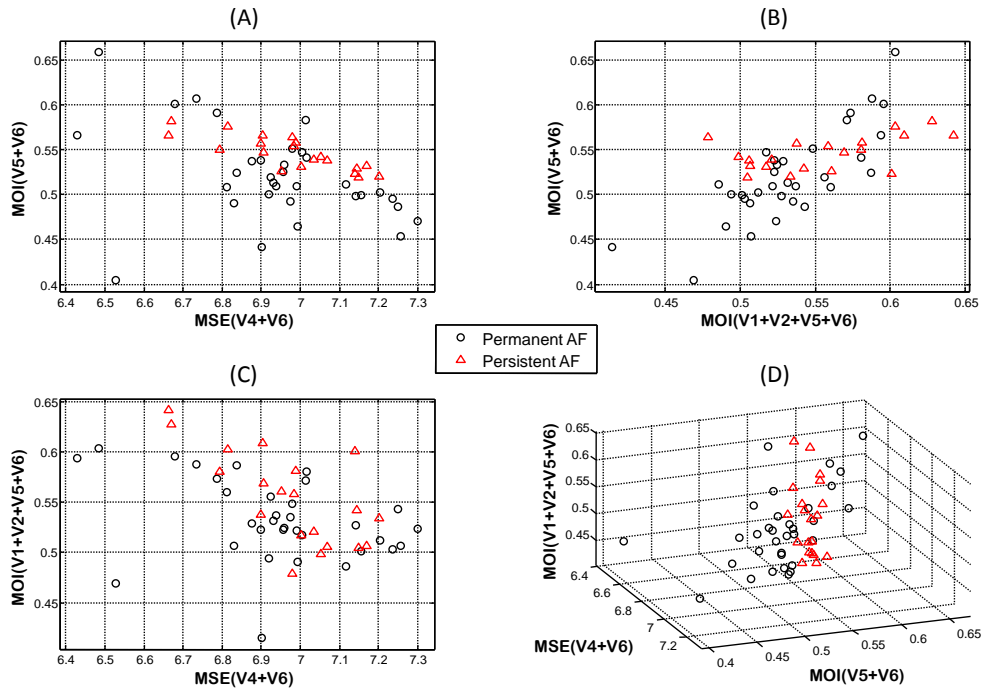


**Figure 7.7:** Multivariate three-feature classification of persistent and permanent AF signals obtained for the best configuration of Table 7.3(A). Two-feature projections of each possible pair of features are shown in panels (A)-(C), and the three-feature visualization is shown in panel (D).

the occurrence of totally different dynamical phenomena. For this reason, the changes in AF organization that we targeted in this study were difficult to measure.

Among all features tested to discriminate between persistent and permanent AF, only one could demonstrate a significant decrease in AF organization during transition to permanent AF. The most sensitive multivariate measure was the MOI, with all related features showing a tendency towards more disorganized permanent AF, but only combinations of MSE and MOI features during two-feature or three-feature classification could clearly distinguish both classes of AF. MSE features considered alone could not provide accurate discrimination due to their high variability, but were systematically selected combined with MOI features for the configurations providing the best classification scores. Possibly, MOI and MSE measures could be complementary for the description of the underlying global organization of AF.

### 7.5.2 Advantages of the Multivariate Approach

It is also interesting to consider the improvements brought by the multivariate approach compared to its univariate counterpart. First, the multivariate framework resulted in a high stability and interpretability of selected features compared to the univariate

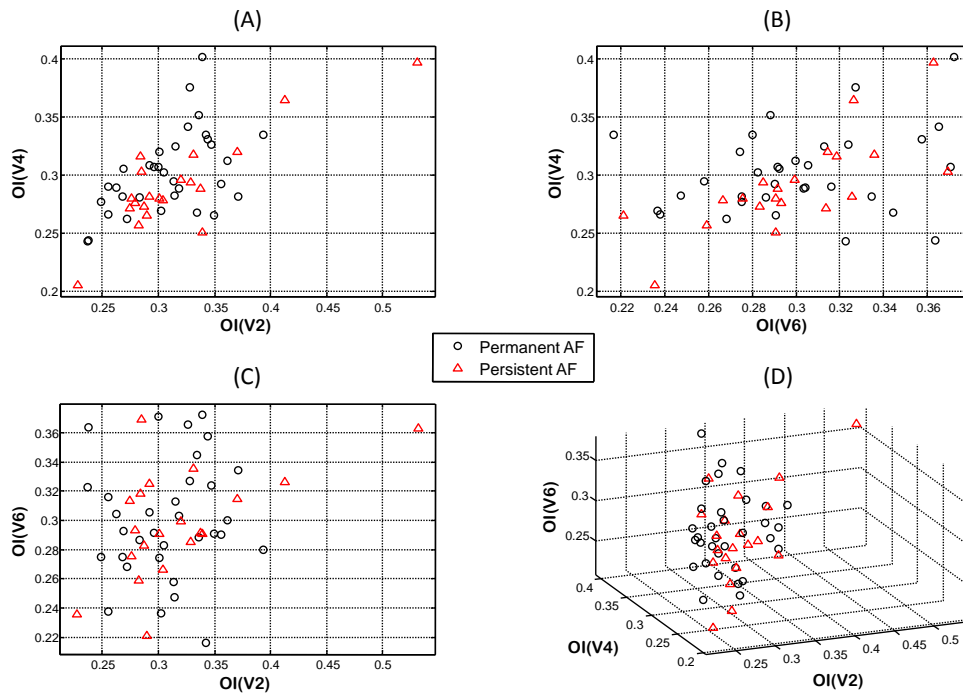


**Figure 7.8:** Univariate three-feature classification of persistent and permanent AF signals obtained for the best configuration of Table 7.3(B). Two-feature projections of each possible pair of features are shown in panels (A)–(C), and the three-feature visualization is shown in panel (D).

approach. Indeed, the optimal MOI parameters were always the same for each configuration of two-feature and three-feature classifications. On the contrary, optimal OI parameters were variable, making any interpretation or comparison more difficult. It would be thus easier to design an automatic tool based on the multivariate approach, since the values of  $BW = 1$  Hz and  $N_p = 5$  could be fixed *a priori*. Furthermore, the multivariate approach was superior in terms of classification performance. For the univariate approach, only three-feature classification could provide stable parameters, although predictive values and correct classification rates remained relatively low. In comparison, two-feature classification using multivariate features was already satisfactory with high accuracy and stable parameters, so that three-feature classification only provided small improvements. Once again, it would be much more practical to setup a classification scheme based on multivariate features, since the number of parameters and features to choose would be significantly minimized.

As mentioned above, the spectral envelope method was used for the first time in this study to investigate ECG signals of atrial arrhythmias. In the light of the results, the valuable properties of the method consisting in detecting common oscillations between ECG leads while removing non-shared spectral content such as noise or irrelevant oscillations have proved very useful and innovative for AF analysis. Applying spectral envelope on

ECG electrodes and measuring OI/SE on its output implies that the resulting measures are quantifying spectral homogeneity between different leads of the ECG, i.e. global spatiotemporal organization.

A highly interesting finding in this study is the set of ECG precordial electrodes selected by the multivariate classification schemes. Indeed, most of the combinations of ECG leads selected as optimal features were lateral left electrodes, i.e. combinations of leads V4 to V6 (Table 7.1(A)). Historically, it has been widely accepted that lead V1 reflects best the right atrial fibrillatory activity hidden in the ECG signal, the other leads presenting other components of the cardiac signal such as ventricular activity [276, 277]. However, two recent studies aiming at precisely determining the contribution of left and right atrial activity to standard and non-standard ECG leads strongly challenged this theory [278, 279]. A first study used standard ECG leads V1 and V2, and added posterior leads V7, V8 and V9, to assess the contribution of AF oscillations at these locations of the body surface [278]. V1 was found to be strongly correlated to RA activity, as predicted by past studies. However, it was also found that LA fibrillatory activity was observable in posterior lead V9. The study of Platonov and colleagues went even further, reproducing the same analysis with the standard ECG system on two unique clinical cases of AT confined to the left atrium [279]. This particular situation created a massive interatrial frequency gradient, and precise analysis of the contribution of atrial activity on each ECG lead could be conducted. It was found that the electrodes V1, V2, V5 and V6 reflected both RA and LA activity, with V5 and V6 better emphasizing the oscillatory activity of the LA. V3 and V4 were shown to contain RA activity exclusively. Thus, these studies demonstrate that precordial ECG leads not only provide information about RA activity, but also contain oscillatory components of the LA, especially in lateral precordial leads. They also suggest that, in surface ECG signals, AF activity is more difficult to detect than the ATs presented in [279], because AF involves oscillations of smaller amplitudes than AT. This observation could explain why Petrutiu and colleagues did not detect LA activity in V1, while Platonov and colleagues did.

In our study, the pairs of lateral ECG leads V4 to V6 selected as optimal features (Table 7.1(A)) were combined and processed by the spectral envelope. This computation resulted in a multivariate spectrum containing relevant oscillatory components common to the neighboring leads. Based on the findings of [279], it can be argued that in our case AF spectral activity stemming from the LA and hidden in lateral precordial electrodes was emphasized by the spectral envelope and helped discriminating between persistent and permanent AF. The additional electrode combinations retained by the multivariate three-feature classification ( $\{V1, V2, V5, V6\}$  and  $\{V1, V6\}$ ) give further information about the global activity of both RA and LA, as was suggested in [279]. Furthermore, a MOI measure applied to V5 and V6 demonstrated a significant decrease in AF organization when AF becomes permanent (Table 7.2). Thus, it could be speculated that late-stage chronification of AF is characterized by a global decrease in AF organization due to dynamical changes localized in LA fibrillatory activity. Moreover, these dynamical changes may be provoked by an alteration in LA substrate such as LA dilation or fibrosis, which is known to be associated with AF sustainability and increased risks of strokes [280]. This hypothesis is supported by a recent study of chronic AF ablation,

in which patients undergoing successful maze procedures (i.e. patients with persistent AF) were compared to those with unsuccessful ablations (i.e. patients with permanent AF) in terms of their respective atrial substrates [281]. Patients with unsuccessful maze procedures showed advanced LA fibrosis and larger LA dimensions than patients with successful ablation outcomes. Interestingly, there was no difference in RA properties between groups. Thus, according to this ablation study, patients with permanent AF could be distinguished from patients with persistent AF on the basis of LA pathological features only. Moreover, it was shown in past literature that the spatial distribution of fibrosis over the atrial surface has a direct influence on subsequent AF wave dynamics [282]. Based on these studies, we propose that the transition from persistent AF to permanent AF caused by LA substrate degradation results in modifications of LA fibrillating patterns, and that these dynamical changes can be detected non-invasively by the multivariate analysis framework we described in the present work.

The superiority of analyzing combined ECG electrodes with multivariate methods becomes evident in the above results, as the univariate approach showed poor classification performances and could not deliver any interpretation about the underlying physiological phenomenon. The multivariate framework proposed in this study may be of interest for numerous fields of cardiovascular research from fundamental research to therapy testing, since it provides advanced spectral analysis performed non-invasively by means of standard surface ECG recordings.

### 7.5.3 Clinical Implications

The multivariate measures of AF organization may be used in clinical settings as a diagnostic tool to optimize patient management and consider optimal cardioversion options. Indeed, anticipating the probability of success of a cardioversion procedure on a case-by-case basis would greatly help both clinicians and patients in their decision making. On one side, clinicians would be assisted in their diagnosis based on patient history by an objective measure quantifying the degree of chronification of the diagnosed arrhythmia from a simple surface ECG recording. On the other side, the detection of a permanent AF could help patients and clinicians to take the decision of avoiding a long and sometimes heavy treatment, e.g. drug therapy or ablative procedures. Such decision could potentially increase the quality of life of the patient and also allow substantial cost savings. To realize such a diagnostic tool, the proposed measures will have to ensure highly reliable diagnostic power. The very high prediction values for permanent AF obtained in this study are encouraging results towards a practical implementation for clinical settings, but further developments will be needed to determine optimal features combinations that would be robust in the case of larger database and higher inter-patients variability.

## 7.6 Conclusion

In this chapter, multivariate spectral analysis and complexity measures were combined to develop an automatic method able to describe subtle changes in AF organization as measured by non-invasive ECG recordings. Accurate discrimination between persistent and permanent AF was made possible, and potential applications in clinical settings to optimize patient management were demonstrated. More generally, this analysis framework may be of valuable importance for the field of cardiovascular research, as it provides an innovative monitoring tool based on standard recording systems.

Nowadays, it is more and more obvious that the clinical world can strongly benefit from the active contribution of engineering sciences and technology. This signal processing development is a striking demonstration of how clinicians and engineers can interact and work hand in hand towards a common objective, namely helping both patients and practitioners by improving current healthcare systems.





# 8

## Conclusion

---

Nowadays, many developments in life sciences are characterized by continuous interactions between medicine, biology and engineering. Especially, the importance of the contributions from the engineering field is progressively growing, as computer-guided medical instrumentation and monitoring devices become essential for the clinical world, and therapies improvements are often proportional to technology developments. In this context, the activities of clinicians, biologists and scientists appear strongly interrelated, and the boundaries between each respective area become blurred. This multidisciplinary approach is at the core of the philosophy of the Lausanne Heart Group, whose objective is to bring together engineering and medicine. Each project supported by this research team combines the different approaches mentioned above in order to tackle the problem of cardiac arrhythmias with innovative points of view. The multifaceted approach of the Lausanne Heart Group already proved fruitful for the investigation of atrial fibrillation and the development of dedicated therapeutic strategies, and is reflected in the present dissertation.

A major part of the developments of therapeutic strategies for AF presented in this work are based on a computer model of human atria. Adopting a modeling approach presents several advantages compared to experimental approaches. First, the investigator using computer models can get rid of systematic animal experiments. The ethical impact of such consideration is obvious, as methods and therapies can be tested and optimized *ad libitum* in the computer modeling framework before starting potential preclinical studies, therefore avoiding massive animal experiments. But economical advantages can also be mentioned, because running long-term animal experiments is a very complicated and expensive process, whereas computer simulations only requires investments in the development phase and limited maintenance costs. The other advantage of computer modeling is unlimited access to any variable of interest and repeatability of experiments under controlled conditions. Of course, models are by definition simplified descriptions of reality, but they represent an appropriate framework for therapy development before extensive validation in animal and human clinical trials.

The biophysical model of human atria used in this dissertation was developed in our

group during more than a decade, and was the object of several PhD theses [38, 40, 41]. Thus, the present work must be considered in the continuation of these past developments. Since the model was developed and validated in previous works, it could be then used for extensive therapy testing. Optimization of AF ablation strategies using the model was already investigated in a previous project, but only few observations were made in the field of low-electrical stimulation of AF [41]. Moreover, this previous contribution demonstrated that the biophysical model was ready to be used as a standard tool to investigate new therapies. For these reasons, the present work focused mainly on the development of a therapeutic pacing solution specifically dedicated to the treatment of AF. Overall, the goal of the project was to take the available computer model to a practical level, and search for implementable therapeutic solutions. Following this line, several properties of AF pacing were determined, and a novel pacing protocol for automatic AF termination was designed and tested, opening the way to experimental validation studies.

In the last chapter of this dissertation, advanced signal processing methods were applied to real cardiac signals. This approach differs from the modeling framework mentioned above, and can be related to other past PhD theses conducted within the Lausanne Heart Group [283, 284]. For this particular study, the goal was to develop new signal processing methods and transfer them from signal processing research to applied biomedical engineering. Once again, beside the significant amount of mathematical and computational developments required to implement accurate methods for AF classification, the real long-term goal of the project is the development of monitoring and automatized diagnostic tools. The encouraging results presented in this dissertation demonstrate that the selected approach can be fruitful. Finally, it should be mentioned that this work required extensive collaboration with cardiologists, and for this reason the clinical component of the Lausanne Heart Group was essential for the success of this study.

In the sections below, a summary of achievements as well as potential future works suggested by the results are listed. When looking globally at the outcomes of this work, it becomes clear that the leitmotiv of this thesis was to adopt a practical approach when developing therapeutic strategies, as engineers do by nature. Each time a method was explored and tested, it was systematically attempted to translate it into concrete schemes and propose practical implementations potentially leading to realistic solutions. Only this kind of approach will help merging together the resources and needs of fundamental research, private industry and clinical centers, and thereby taking healthcare systems to the next level.

## **8.1 Summary of Achievements**

The major achievements of this dissertation are summarized below.

### **A Dynamical Study of AF Spontaneous Termination Processes**

AF spontaneous termination is difficult to observe in real situations due to its transient and unpredictable nature. Using our biophysical model, it was possible to conduct a detailed analysis of several AF dynamical parameters during the seconds preceding this termination process. First, a database of simulations of AF spontaneous termination was created, taking into account models of AF dynamics with different complexity levels (paroxysmal AF vs. recent chronic AF). Different termination processes between models could be described and compared with the existing literature. For the model of paroxysmal AF, spatial and temporal AF patterns prior to termination could be described in detail, and critical value of basic dynamical properties such as *AFCL* were proposed as potential triggers for termination occurrence.

A better understanding of AF spontaneous termination processes may be of value for the field of AF therapy research. Indeed, understanding a natural phenomenon can be the first step of therapeutic developments aiming at reproducing this particular natural process. Such biomimetic solutions may represent the future of AF therapies.

### **Rapid Pacing of AF: Optimization of Parameters and Effects of Atrial Substrate**

Overdrive pacing has been shown to entrain successfully the electrical activity of basic ATs, leading to termination of the underlying arrhythmias. However, its efficacy cannot be clearly demonstrated in the case of AF, although this protocol might be promising. Using our biophysical model, a systematic study was designed in order to understand the importance of pacing cycle length, pacing location and atrial tissue properties on the ability to capture AF by rapid pacing. In addition to the massive amount of simulations needed for the statistical description of this study, a complete analysis framework designed for the assessment of AF capture by rapid pacing had to be conceptualized. First, an automatic system to assess the local capture of a portion of atrial tissue was developed in the biophysical model. Once capture could be reliably detected, quantitative measures of its quality were developed to assess both temporal and spatial aspects of AF capture by pacing. Based on these tools, pacing parameters such pacing cycle length or pacing location could be explored in a systematic manner, and optimal combinations for AF capture could be determined. The ability to capture AF was also shown to depend on the atrial substrate as characterized by an estimate of its wavelength, a better capture being achieved at shorter wavelengths.

These results have several implications. First, they show that patients may respond differently to pacing therapies according to their intrinsic atrial tissue properties. However, simple measures of tissue wavelength can provide valuable information about the future response of a specific patient to rapid pacing sequences. Moreover, the results emphasized some limitations of current rapid pacing protocols, and suggested pacing sites and cycle lengths that would be optimal for AF capture. Considered together, these observations are of crucial importance for future developments in AF therapy by low-energy stimulation.

### **A Multi-Stage Pacing Scheme for Automatic AF Termination**

Based on the results of the systematic analysis of AF rapid pacing, a multi-stage pacing scheme for AF termination was designed and implemented in the biophysical model. The atrial septal area was selected as a strategic pacing location, and an abrupt transition between rapid and slow pacing phases was introduced in the protocol to increase AF extinction probability. Pacing cycle lengths of both phases were optimized and termination rates were computed for several configurations to derive statistical performance evaluation. The obtained termination success rates were promising, and potential decreases in performance when applying the protocol in real experimental settings could be compensated by the high repeatability of the procedure. Moreover, the concepts of capture pattern during rapid pacing as well as wavelength lengthening were introduced as crucial elements for AF termination efficacy and as possible directions for future optimization. The proposed pacing scheme was compared to current pacing protocols such as rapid pacing, and showed great promise as a potential therapeutic solution for the treatment of AF in patients with implantable pacemakers.

### **A multivariate Analysis Framework for AF Organization Assessment**

In this study, a database of real surface ECG signals was used to assess the differences in AF complexity between persistent and permanent AF. Measures of organization based on multivariate spectral analysis were developed to evaluate the spatiotemporal organization of AF based on the spectral information of multiple surface ECG electrodes. In particular, the spectral envelope method was used for the first time in the field of cardiac arrhythmia, demonstrating interesting abilities to extract oscillatory information of interest from combined ECG electrodes. The organization measures provided accurate classification of persistent and permanent AF, and optimal selected features showed that changes in LA dynamical properties were determinant during late stage AF chronification, agreeing with recent clinical and experimental findings. These developments may be the basis for the conception of automatic diagnostic tools assisting clinicians during the management of patients with AF.

## **8.2 Perspectives**

The results presented in this dissertation must be considered in the continuation of a series of projects conducted within the Lausanne Heart Group. As such, this work also suggests numerous lines of research for future investigations perpetuating the activity of the group.

### **From Simple to Complex Models**

When used as a first approach, a biophysical model should be made as simple as possible to provide clear explanations with a minimum number of arbitrary parameters,

but still with a sufficient level of complexity to capture the essential features needed to understand the phenomena under investigation. This trade-off was carefully considered during this dissertation, as the models used were designed in such a way that realistic AF could be simulated with a relatively small number of parameters and in a reasonable time. Thanks to this simplicity, the models made it possible to run systematic analyzes involving a very large number of simulations, and provided precise descriptions of the basic mechanisms in action.

In order to improve and extend these initial findings, a next step would be to make models more complex to include more details about the mechanisms already described. Indeed, with the increasing computational power of today's computers, it will be feasible to simulate the protocols developed in the previous chapters on more complex models that would approximate reality even more closely. Possible refinements of the models include:

- **Tissue thickness:** adding a third dimension to the atrial tissue would make AF wavelet dynamics slightly more complex, as fibrillating spirals would be allowed to evolve in the thickness of the tissue, creating vortex-like patterns. Whether this small additional dimension can really change the overall AF dynamics is still a matter of debate, because the thickness of atrial walls is known to be small compared to ventricles. Nevertheless, comparing these supplementary simulations to the results obtained in the present dissertation would be an interesting starting point for discussions.
- **Additional anatomical structures:** a clear limitation of the presented models is the absence of some influencing anatomical structures such as Bachmann's bundle, pectinate muscles, or crista terminalis. Adding these essential structures could give rise to new interactions between AF wavefronts, particularly for interatrial conduction.
- **Fibers anisotropy:** the models of atrial tissue used in our studies had homogeneous properties and did not include anisotropy. Changing these properties and adding fibers anisotropy would alterate wavefronts propagation patterns, and could for instance modify the reactions of the modeled atrial tissue to electrical stimulation.
- **Structural remodeling:** atrial tissue alterations reflected by structural remodeling were not considered in this dissertation. In order to simulate long-lasting chronic AF, it would be crucial to add structural heterogeneities such as fibrosis, heterogeneities in specific ionic concentrations or gradients in APD.

These modifications were already implemented in our biophysical model in past studies [40, 69], and could be added incrementally to assess the specific effect of each additional element. This step-by-step approach will hopefully lead to a more and more realistic description of AF as observed by our biophysical model.

## From Simulations to Reality

One of the strengths of a fruitful modeling approach is to formulate innovative hypotheses that could be tested experimentally. The model-based studies performed in chapters 4 to 6 provided several suggestions for experimental validations. During the study of AF spontaneous termination of chapter 4, the following proposals for further investigations were made:

- **Optimizing the design of clinical studies:** the first hypothesis to validate is that AF spontaneous termination mechanisms may be very different depending on the stage of the arrhythmia. To test that proposition, clinical studies should be run with special care when selecting patient populations to compare. Indeed, patients with paroxysmal AF should be distinguished from patients with chronic AF. Such procedure may help uncovering termination mechanisms specific to each AF type.
- **High-density mapping studies:** in order to assess the presence of a lateralization process of fibrillating activity prior to termination, it would be interesting to perform bi-atrial mapping studies with high spatial resolution and analyze these recordings by means of advanced signal processing methods such as phase singularity tracking. Doing so, the trajectories of AF reentries could be described over time and spatial patterns prior to spontaneous termination could be assessed precisely, in order to confirm or reject the observations made in our model.
- **Analysis of population dynamics:** it was suggested in section 4.4.4 that considering portions of excited and non-excited atrial tissue as interacting populations of predators and preys may help uncovering unknown processes of AF dynamics related to spontaneous termination. In particular, such analyses could point out whether parameters such as  $AFCL$  or  $\#WF$  could act as predictors of AF termination.

The investigations of chapter 5 and 6 on low-energy pacing of AF also led to the following testable concepts:

- **Measures of AF capture ability:** experimental measurements could be performed either on animals or humans, in order to test the hypothesis that an approximation of the atrial tissue wavelength may give information about the subsequent ability to capture AF by rapid pacing (chapter 5). Simple S1-S2 protocols would easily provide values of APD and CV, and approximated wavelength measures could be derived, and tested as potential predictors of AF capture ability by rapid pacing. Ideally, populations of patients with either large or short tissue wavelengths should be compared during rapid pacing of AF and quantitative capture assessment.
- **Validation of the septum pacing protocol:** the septal pacing scheme for AF termination proposed in chapter 6 is now the object of preclinical studies on animals, with the collaboration of our industrial partner. During these tests, the different pacing parameters optimized in the model will be adapted to experimental settings, and AF termination abilities will be assessed. Ideally, a cross-talk between electrophysiologists and modeling engineers will be established in order to better understand potential issues raised during experiments with the help of additional simulations, and to eventually tune the current algorithm for its realistic imple-

mentation. Overall, the goal of this study is to assess the feasibility of a concrete solution that could be integrated in human patients with implantable pacemakers.

### **From Signal Processing to Monitoring and Diagnostic Tools**

The measures of AF organization presented in chapter 7 certainly represent potential methods for discriminating between different types of AF, and thereby helping clinicians in their daily activity. However, further improvements and investigations will be required to finally develop a robust and automatic diagnostic tool. First, it will be necessary to test the methods on a larger database of patients with permanent and persistent AF, in order to verify that the accuracy of the measures remains high and robust against occasionally large inter-patient variability. Furthermore, ECG leads combinations providing the optimal features for the considered classification task must be determined more precisely in order to select them and avoid the extensive exploration of parameters performed in this study. So far, the results obtained clearly suggest that electrodes reflecting the activity of the LA should be favoured, but further tests on larger datasets will be needed to verify this hypothesis.

The proposed multivariate organization measures could also be used for other purposes related to AF analysis. The same classifier could be applied to other discrimination tasks, such as the differentiation between acute and chronic AF, the prediction of electrical or pharmacological cardioversion outcomes, or the prediction of AF recurrence. All these functionalities could be concentrated in a polyvalent and automatic ECG-based system that would provide significant support to clinicians during their diagnosis and decision making.

Another application of the organization measures would consist in a monitoring tool for AF ablation procedure. Surface ECG leads as well as intracardiac signals could be processed by the algorithm continuously, which in turn would provide a real-time assessment of atrial organization. In this context, a sudden increase in the estimated organization could indicate successful extinction of fibrillating activity, and decisions whether to stop or continue the ablation procedure could be optimized based on this quantitative measure. Clearly, the analysis framework proposed in chapter 7 cannot be restricted to the presented classification task, and future studies will hopefully reveal the full potential of the methods and their potential contributions to the clinical world.





# Bibliography

---

- [1] V. Fuster, L. E. Rydén, D. S. Cannom, H. J. Crijns, A. B. Curtis, K. A. Ellenbogen, J. L. Halperin, J.-Y. L. Heuzey, G. N. Kay, J. E. Lowe, S. B. Olsson, E. N. Prystowsky, J. L. Tamargo, and S. Wann, “ACC/AHA/ESC 2006 guidelines for the management of patients with atrial fibrillation—executive summary: a report of the American College of Cardiology/American Heart Association Task Force on Practice Guidelines and the European Society of Cardiology Committee for Practice Guidelines (Writing Committee to Revise the 2001 Guidelines for the Management of Patients With Atrial Fibrillation) Developed in Collaboration With the European Heart Rhythm Association and the Heart Rhythm Society.” *J Am Coll Cardiol*, vol. 48, no. 4, pp. 854–906, Aug 2006.
- [2] L. S. Wann, A. B. Curtis, C. T. January, K. A. Ellenbogen, J. E. Lowe, N. A. M. Estes, R. L. Page, M. D. Ezekowitz, D. J. Slotwiner, W. M. Jackman, W. G. Stevenson, and C. M. Tracy, “2011 ACCF/AHA/HRS Focused Update on the Management of Patients With Atrial Fibrillation (Updating the 2006 Guideline): A Report of the American College of Cardiology Foundation/American Heart Association Task Force on Practice Guidelines.” *Circulation*, Dec 2010. [Online]. Available: <http://dx.doi.org/10.1161/CIR.0b013e3181fa3cf4>
- [3] A. J. Camm, P. Kirchhof, G. Y. H. Lip, U. Schotten, I. Savelieva, S. Ernst, I. C. V. Gelder, N. Al-Attar, G. Hindricks, B. Prendergast, H. Heidbuchel, O. Alfieri, A. Angelini, D. Atar, P. Colonna, R. D. Caterina, J. D. Sutter, A. Goette, B. Gorenek, M. Haldal, S. H. Hohloser, P. Kolh, J.-Y. L. Heuzey, P. Ponikowski, and F. H. Rutten, “Guidelines for the management of atrial fibrillation: the Task Force for the Management of Atrial Fibrillation of the European Society of Cardiology (ESC).” *Eur Heart J*, vol. 31, no. 19, pp. 2369–2429, Oct 2010. [Online]. Available: <http://dx.doi.org/10.1093/eurheartj/ehq278>
- [4] F. Jung and J. P. DiMarco, “Treatment strategies for atrial fibrillation.” *Am J Med*, vol. 104, no. 3, pp. 272–286, Mar 1998.
- [5] G. Thrall, D. Lane, D. Carroll, and G. Y. H. Lip, “Quality of life in patients with atrial fibrillation: a systematic review.” *Am J Med*, vol. 119, no. 5, pp. 448.e1–448.19, May 2006. [Online]. Available: <http://dx.doi.org/10.1016/j.amjmed.2005.10.057>
- [6] E. J. Benjamin, P. A. Wolf, R. B. D’Agostino, H. Silbershatz, W. B. Kannel, and D. Levy, “Impact of atrial fibrillation on the risk of death: the Framingham Heart Study.” *Circulation*, vol. 98, no. 10, pp. 946–952, Sep 1998.
- [7] Y. Miyasaka, M. E. Barnes, B. J. Gersh, S. S. Cha, K. R. Bailey, W. P. Abhayaratna, J. B. Seward, and T. S. M. Tsang, “Secular trends in incidence of atrial fibrillation in

- Olmsted County, Minnesota, 1980 to 2000, and implications on the projections for future prevalence." *Circulation*, vol. 114, no. 2, pp. 119–125, Jul 2006. [Online]. Available: <http://dx.doi.org/10.1161/CIRCULATIONAHA.105.595140>
- [8] J. S. Steinberg, "Atrial fibrillation: an emerging epidemic?" *Heart*, vol. 90, no. 3, pp. 239–240, Mar 2004.
- [9] G. Y. H. Lip and H.-F. Tse, "Management of atrial fibrillation." *Lancet*, vol. 370, no. 9587, pp. 604–618, Aug 2007. [Online]. Available: [http://dx.doi.org/10.1016/S0140-6736\(07\)61300-2](http://dx.doi.org/10.1016/S0140-6736(07)61300-2)
- [10] B. Brendorp, O. Pedersen, C. Torp-Pedersen, N. Sahebzadah, and L. Køber, "A benefit-risk assessment of class III antiarrhythmic agents." *Drug Saf*, vol. 25, no. 12, pp. 847–865, 2002.
- [11] U. Ravens, "Antiarrhythmic therapy in atrial fibrillation." *Pharmacol Ther*, vol. 128, no. 1, pp. 129–145, Oct 2010. [Online]. Available: <http://dx.doi.org/10.1016/j.pharmthera.2010.06.004>
- [12] I. Nault, S. Miyazaki, A. Forclaz, M. Wright, A. Jadidi, P. Jaïs, M. Hocini, and M. Haïssaguerre, "Drugs vs. ablation for the treatment of atrial fibrillation: the evidence supporting catheter ablation." *Eur Heart J*, vol. 31, no. 9, pp. 1046–1054, May 2010. [Online]. Available: <http://dx.doi.org/10.1093/eurheartj/ehq079>
- [13] S. Nattel, "Newer developments in the management of atrial fibrillation." *Am Heart J*, vol. 130, no. 5, pp. 1094–1106, Nov 1995.
- [14] M. C. Sanguinetti and M. Tristani-Firouzi, "hERG potassium channels and cardiac arrhythmia." *Nature*, vol. 440, no. 7083, pp. 463–469, Mar 2006. [Online]. Available: <http://dx.doi.org/10.1038/nature04710>
- [15] S. Krishnamoorthy and G. Y. H. Lip, "How safe is the antiarrhythmic drug therapy in atrial fibrillation?" *Europace*, vol. 11, no. 7, pp. 837–839, Jul 2009. [Online]. Available: <http://dx.doi.org/10.1093/europace/eup170>
- [16] S. Levy and J. Camm, "An implantable atrial defibrillator. An impossible dream?" *Circulation*, vol. 87, no. 5, pp. 1769–1771, May 1993.
- [17] J. Koebe and P. Kirchhof, "Novel non-pharmacological approaches for antiarrhythmic therapy of atrial fibrillation." *Europace*, vol. 10, no. 4, pp. 433–437, Apr 2008. [Online]. Available: <http://dx.doi.org/10.1093/europace/eun058>
- [18] T. Yamashita, "Is catheter ablation a mature fruit for treatment of atrial fibrillation?—is catheter ablation established as a treatment option of atrial fibrillation? (Con)." *Circ J*, vol. 74, no. 9, pp. 1978–1982, 2010.
- [19] K. Satomi, "Electrophysiological characteristics of atrial tachycardia after pulmonary vein isolation of atrial fibrillation." *Circ J*, vol. 74, no. 6, pp. 1051–1058, May 2010.
- [20] A. N. Shah, S. Mittal, T. C. Sichrovsky, D. Cotiga, A. Arshad, K. Maleki, W. J. Pierce, and J. S. Steinberg, "Long-term outcome following successful pulmonary vein isolation: pattern and prediction of very late recurrence." *J Cardiovasc Electrophysiol*, vol. 19, no. 7, pp. 661–667, Jul 2008. [Online]. Available: <http://dx.doi.org/10.1111/j.1540-8167.2008.01101.x>

- [21] E. M. Balk, A. C. Garlitski, A. A. Alsheikh-Ali, T. Terasawa, M. Chung, and S. Ip, "Predictors of atrial fibrillation recurrence after radiofrequency catheter ablation: a systematic review." *J Cardiovasc Electrophysiol*, vol. 21, no. 11, pp. 1208–1216, Nov 2010. [Online]. Available: <http://dx.doi.org/10.1111/j.1540-8167.2010.01798.x>
- [22] A. R. J. Mitchell and N. Sulke, "How do atrial pacing algorithms prevent atrial arrhythmias?" *Europace*, vol. 6, no. 4, pp. 351–362, Jul 2004. [Online]. Available: <http://dx.doi.org/10.1016/j.eupc.2004.03.005>
- [23] K. A. Ellenbogen, "Pacing therapy for prevention of atrial fibrillation." *Heart Rhythm*, vol. 4, no. 3 Suppl, pp. S84–S87, Mar 2007. [Online]. Available: <http://dx.doi.org/10.1016/j.hrthm.2006.12.005>
- [24] A. M. Gillis, M. Morck, D. V. Exner, R. S. Sheldon, H. J. Duff, B. L. Mitchell, and G. D. Wyse, "Impact of atrial antitachycardia pacing and atrial pace prevention therapies on atrial fibrillation burden over long-term follow-up." *Europace*, May 2009. [Online]. Available: <http://dx.doi.org/10.1093/europace/eup115>
- [25] A. R. J. Mitchell, P. A. R. Spurrell, L. Cheadle, and N. Sulke, "Effect of atrial antitachycardia pacing treatments in patients with an atrial defibrillator: randomised study comparing subthreshold and nominal pacing outputs." *Heart*, vol. 87, no. 5, pp. 433–437, May 2002.
- [26] S. Nattel and L. Carlsson, "Innovative approaches to anti-arrhythmic drug therapy." *Nat Rev Drug Discov*, vol. 5, no. 12, pp. 1034–1049, Dec 2006. [Online]. Available: <http://dx.doi.org/10.1038/nrd2112>
- [27] J. P. Morrow and J. A. Reiffel, "Drug therapy for atrial fibrillation: what will its role be in the era of increasing use of catheter ablation?" *Pacing Clin Electrophysiol*, vol. 32, no. 1, pp. 108–118, Jan 2009. [Online]. Available: <http://dx.doi.org/10.1111/j.1540-8159.2009.02184.x>
- [28] H. Ahmed, P. Neuzil, J. Skoda, A. D'Avila, D. M. Donaldson, M. C. Laragy, and V. Y. Reddy, "The permanency of pulmonary vein isolation using a balloon cryoablation catheter." *J Cardiovasc Electrophysiol*, vol. 21, no. 7, pp. 731–737, Jul 2010. [Online]. Available: <http://dx.doi.org/10.1111/j.1540-8167.2009.01703.x>
- [29] O. M. Wazni, N. F. Marrouche, D. O. Martin, A. Verma, M. Bhargava, W. Saliba, D. Bash, R. Schweikert, J. Brachmann, J. Gunther, K. Gutleben, E. Pisanò, D. Potenza, R. Fanelli, A. Raviele, S. Themistoclakis, A. Rossillo, A. Bonso, and A. Natale, "Radiofrequency ablation vs antiarrhythmic drugs as first-line treatment of symptomatic atrial fibrillation: a randomized trial." *JAMA*, vol. 293, no. 21, pp. 2634–2640, Jun 2005. [Online]. Available: <http://dx.doi.org/10.1001/jama.293.21.2634>
- [30] L. Kappenberger, "Arrhythmia: a therapeutic dilemma," in *Computer Simulation and Experimental Assessment of Cardiac Electrophysiology*, N. Virag, O. Blanc, and L. Kappenberger, Eds. Futura Publishing, Armonk, New York, 2001, pp. 185–188.
- [31] A. Nygren, C. Fiset, L. Firek, J. W. Clark, D. S. Lindblad, R. B. Clark, and W. R. Giles, "Mathematical model of an adult human atrial cell: the role of K<sup>+</sup> currents in repolarization." *Circ Res*, vol. 82, no. 1, pp. 63–81, 1998.
- [32] D. Harrild and C. Henriquez, "A computer model of normal conduction in the human atria." *Circ Res*, vol. 87, no. 7, pp. E25–E36, Sep 2000.

- [33] C. W. Zemlin, "A realistic and efficient model of excitation propagation in the human atria," in *Computer Simulation and Experimental Assessment of Cardiac Electrophysiology*, N. Virag, O. Blanc, and L. Kappenberger, Eds. Futura Publishing, Armonk, New York, 2001, pp. 29–34.
- [34] E. J. Vigmond, R. Ruckdeschel, and N. Trayanova, "Reentry in a morphologically realistic atrial model." *J Cardiovasc Electrophysiol*, vol. 12, no. 9, pp. 1046–1054, Sep 2001.
- [35] N. Virag, V. Jacquemet, C. S. Henriquez, S. Zozor, O. Blanc, J.-M. Vesin, E. Pruvot, and L. Kappenberger, "Study of atrial arrhythmias in a computer model based on magnetic resonance images of human atria." *Chaos*, vol. 12, no. 3, pp. 754–763, Sep 2002. [Online]. Available: <http://dx.doi.org/10.1063/1.1483935>
- [36] M. Reumann, J. Bohnert, G. Seemann, B. Osswald, and O. Dossel, "Preventive Ablation Strategies in a Biophysical Model of Atrial Fibrillation Based on Realistic Anatomical Data," vol. 55, no. 2, pp. 399–406, 2008.
- [37] L. Dang, N. Virag, Z. Ihara, V. Jacquemet, J. M. Vesin, J. Schlaepfer, P. Ruchat, and L. Kappenberger, "Evaluation of ablation patterns using a biophysical model of atrial fibrillation." *Ann Biomed Eng*, vol. 33, no. 4, pp. 465–474, Apr 2005.
- [38] O. Blanc, "A computer model of human atrial arrhythmia." Ph.D. dissertation, Swiss Federal Institute of Technology, 2002.
- [39] S. Zozor, O. Blanc, V. Jacquemet, N. Virag, J.-M. Vesin, E. Pruvot, L. Kappenberger, and C. Henriquez, "A numerical scheme for modeling wavefront propagation on a monolayer of arbitrary geometry." *IEEE Trans Biomed Eng*, vol. 50, no. 4, pp. 412–420, Apr 2003. [Online]. Available: <http://dx.doi.org/10.1109/TBME.2003.809505>
- [40] V. Jacquemet, "A biophysical model of atrial fibrillation and electrograms : formulation, validation and applications." Ph.D. dissertation, Swiss Federal Institute of Technology, 2004.
- [41] L. Dang, "An investigation into therapies for atrial arrhythmias using a biophysical model of the human atria." Ph.D. dissertation, Swiss Federal Institute of Technology, 2005.
- [42] G. K. Moe, W. C. Rheinboldt, and J. A. Abildskov, "A computer model of atrial fibrillation." *Am Heart J*, vol. 67, pp. 200–220, Feb 1964.
- [43] Y. E. Earm and D. Noble, "A model of the single atrial cell: relation between calcium current and calcium release." *Proc R Soc Lond B Biol Sci*, vol. 240, no. 1297, pp. 83–96, May 1990.
- [44] D. S. Lindblad, C. R. Murphey, J. W. Clark, and W. R. Giles, "A model of the action potential and underlying membrane currents in a rabbit atrial cell." *Am J Physiol*, vol. 271, no. 4 Pt 2, pp. H1666–H1696, Oct 1996.
- [45] M. Courtemanche, R. J. Ramirez, and S. Nattel, "Ionic mechanisms underlying human atrial action potential properties: insights from a mathematical model." *Am J Physiol*, vol. 275, no. 1 Pt 2, pp. H301–H321, Jul 1998.
- [46] M. Courtemanche, R. Ramirez, and S. Nattel, "Ionic targets for drug therapy and atrial fibrillation-induced electrical remodeling: insights from a mathematical model." *Cardiovasc Res*, vol. 42, no. 2, pp. 477–489, May 1999.

- [47] R. J. Ramirez, S. Nattel, and M. Courtemanche, "Mathematical analysis of canine atrial action potentials: rate, regional factors, and electrical remodeling." *Am J Physiol Heart Circ Physiol*, vol. 279, no. 4, pp. H1767–H1785, Oct 2000.
- [48] V. Jacquemet, L. Kappenberger, and C. Henriquez, "Modeling Atrial Arrhythmias: Impact on Clinical Diagnosis and Therapies," *Biomedical Engineering, IEEE Reviews in*, vol. 1, pp. 94–114, 2008.
- [49] C. S. Henriquez and A. A. Papazoglou, "Using computer models to understand the roles of tissue structure and membrane dynamics in arrhythmogenesis." *Proc IEEE*, vol. 84, no. 3, pp. 334–354, 1996.
- [50] B. Alberts, A. Johnson, J. Lewis, M. Raff, K. Roberts, and P. Walter, *Molecular Biology of the Cell*. Garland Science, 2002.
- [51] J. Jalife, M. Delmar, J. Davidenko, and J. Anumonwo, *Basic Cardiac Electrophysiology for the Clinician*. Futura, 1999.
- [52] S. Nattel, "New ideas about atrial fibrillation 50 years on." *Nature*, vol. 415, no. 6868, pp. 219–226, Jan 2002. [Online]. Available: <http://dx.doi.org/10.1038/415219a>
- [53] F. Bode, M. Kilborn, P. Karasik, and M. R. Franz, "The repolarization-excitability relationship in the human right atrium is unaffected by cycle length, recording site and prior arrhythmias." *J Am Coll Cardiol*, vol. 37, no. 3, pp. 920–925, Mar 2001.
- [54] F. Xie, Z. Qu, A. Garfinkel, and J. N. Weiss, "Electrical refractory period restitution and spiral wave reentry in simulated cardiac tissue." *Am J Physiol Heart Circ Physiol*, vol. 283, no. 1, pp. H448–H460, Jul 2002. [Online]. Available: <http://dx.doi.org/10.1152/ajpheart.00898.2001>
- [55] Z. Qu, J. Kil, F. Xie, A. Garfinkel, and J. N. Weiss, "Scroll wave dynamics in a three-dimensional cardiac tissue model: roles of restitution, thickness, and fiber rotation." *Biophys J*, vol. 78, no. 6, pp. 2761–2775, Jun 2000. [Online]. Available: [http://dx.doi.org/10.1016/S0006-3495\(00\)76821-4](http://dx.doi.org/10.1016/S0006-3495(00)76821-4)
- [56] B.-S. Kim, Y.-H. Kim, G.-S. Hwang, H.-N. Pak, S. C. Lee, W. J. Shim, D. J. Oh, and Y. M. Ro, "Action potential duration restitution kinetics in human atrial fibrillation." *J Am Coll Cardiol*, vol. 39, no. 8, pp. 1329–1336, Apr 2002.
- [57] A. L. Hodgkin and A. F. Huxley, "A quantitative description of membrane current and its application to conduction and excitation in nerve." *J Physiol*, vol. 117, no. 4, pp. 500–544, Aug 1952.
- [58] G. W. Beeler and H. Reuter, "Reconstruction of the action potential of ventricular myocardial fibres." *J Physiol*, vol. 268, no. 1, pp. 177–210, Jun 1977.
- [59] D. DiFrancesco and D. Noble, "A model of cardiac electrical activity incorporating ionic pumps and concentration changes." *Philos Trans R Soc Lond B Biol Sci*, vol. 307, no. 1133, pp. 353–398, Jan 1985.
- [60] C. H. Luo and Y. Rudy, "A model of the ventricular cardiac action potential. Depolarization, repolarization, and their interaction." *Circ Res*, vol. 68, no. 6, pp. 1501–1526, Jun 1991.

- [61] C. Luo and Y. Rudy, "A dynamic model of the cardiac ventricular action potential. I. Simulations of ionic currents and concentration changes." *Circ Res*, vol. 74, no. 6, pp. 1071–1096, Jun 1994.
- [62] Z. Qu, J. N. Weiss, and A. Garfinkel, "From local to global spatiotemporal chaos in a cardiac tissue model." *Phys Rev E Stat Phys Plasmas Fluids Relat Interdiscip Topics*, vol. 61, no. 1, pp. 727–732, Jan 2000.
- [63] C. S. Henriquez, "Simulating the electrical behavior of cardiac tissue using the bidomain model." *Crit Rev Biomed Eng*, vol. 21, no. 1, pp. 1–77, 1993.
- [64] V. A. Holden and V. A. Panfilov, "Modeling propagation in excitable media," in *Computational Biology of the Heart*, A. Panfilov and A. Holden, Eds. John Wiley & Son, 1997, pp. 217–233.
- [65] H. I. Saleheen and K. T. Ng, "A new three-dimensional finite-difference bidomain formulation for inhomogeneous anisotropic cardiac tissues." *IEEE Trans Biomed Eng*, vol. 45, no. 1, pp. 15–25, Jan 1998.
- [66] J. P. Keener and K. Bogar, "A numerical method for the solution of the bidomain equations in cardiac tissue." *Chaos*, vol. 8, no. 1, pp. 234–241, Mar 1998. [Online]. Available: <http://dx.doi.org/10.1063/1.166300>
- [67] V. Jacquemet, L. Kappenberger, and C. Henriquez, "Modeling Atrial Arrhythmias: Impact on Clinical Diagnosis and Therapies," *Biomedical Engineering, IEEE Reviews in*, vol. 1, pp. 94–114, 2008.
- [68] A. T. Winfree, "Rotors, fibrillation and dimensionality," in *Computational Biology of the Heart*, A. Panfilov and A. Holden, Eds. John Wiley & Sons, 1997, pp. 101–135.
- [69] V. Jacquemet, N. Virag, Z. Ihara, L. Dang, O. Blanc, S. Zozor, J.-M. Vesin, L. Kappenberger, and C. Henriquez, "Study of unipolar electrogram morphology in a computer model of atrial fibrillation." *J Cardiovasc Electrophysiol*, vol. 14, no. 10 Suppl, pp. S172–S179, Oct 2003.
- [70] A. van Oosterom and V. Jacquemet, "Genesis of the P wave: atrial signals as generated by the equivalent double layer source model." *Europace*, vol. 7 Suppl 2, pp. 21–29, Sep 2005. [Online]. Available: <http://dx.doi.org/10.1016/j.eupc.2005.05.001>
- [71] V. Jacquemet, A. van Oosterom, J.-M. Vesin, and L. Kappenberger, "Analysis of electrocardiograms during atrial fibrillation. A biophysical model approach." *IEEE Eng Med Biol Mag*, vol. 25, no. 6, pp. 79–88, 2006.
- [72] J. W. Kirklin and B. G. Barret-Boyes, "Anatomy, dimensions, and terminology," in *Cardiac Surgery*. Churchill Livingstone, New York, 1990, pp. 3–60.
- [73] J. L. Wells, R. B. Karp, N. T. Kouchoukos, W. A. MacLean, T. N. James, and A. L. Waldo, "Characterization of atrial fibrillation in man: studies following open heart surgery." *Pacing Clin Electrophysiol*, vol. 1, no. 4, pp. 426–438, Oct 1978.
- [74] K. T. Konings, C. J. Kirchhof, J. R. Smeets, H. J. Wellens, O. C. Penn, and M. A. Allesie, "High-density mapping of electrically induced atrial fibrillation in humans." *Circulation*, vol. 89, no. 4, pp. 1665–1680, Apr 1994.

- [75] R. Coronel, "Myths, metaphors, and mathematical models." *Heart Rhythm*, vol. 4, no. 8, pp. 1046–1047, Aug 2007. [Online]. Available: <http://dx.doi.org/10.1016/j.hrthm.2007.05.015>
- [76] L. Sörnmo and P. Laguna, *Bioelectrical Signal Processing in Cardiac and Neurological Applications*. Elsevier Academic Press, 2005.
- [77] J. L. Cox, T. E. Canavan, R. B. Schuessler, M. E. Cain, B. D. Lindsay, C. Stone, P. K. Smith, P. B. Corr, and J. P. Boineau, "The surgical treatment of atrial fibrillation. II. Intraoperative electrophysiologic mapping and description of the electrophysiologic basis of atrial flutter and atrial fibrillation." *J Thorac Cardiovasc Surg*, vol. 101, no. 3, pp. 406–426, Mar 1991.
- [78] A. Vulpian, "Note sur les effets de la faradisation directe des ventricules du coeur chez les chiens," *Archive de physiologie normale et pathologique*, vol. 6, p. 975, 1874.
- [79] J. McMichael, "History of atrial fibrillation 1628-1819 harvey - de senac - laënnec." *Br Heart J*, vol. 48, no. 3, pp. 193–197, Sep 1982.
- [80] K. M. Flegel, "From delirium cordis to atrial fibrillation: historical development of a disease concept." *Ann Intern Med*, vol. 122, no. 11, pp. 867–873, Jun 1995.
- [81] W. Einthoven, "Le télécardiogramme," *Archives internationales de physiologie*, vol. 4, pp. 132–164, 1906.
- [82] C. J. Rothberger and H. Winterberg, "Vorhofflimmern und Arrhythmia perpetua." *Wiener klinische Wochenschrift*, vol. 22, pp. 839–844, 1909.
- [83] C. Rothberger and H. Winterberg, "Über Vorhofflimmern und Vorhofflattern." *Pflüger's Archiv für die gesamte Physiologie des Menschen und der Tiere*, vol. 160, pp. 42–90, 1915.
- [84] T. Lewis, A. N. Drury, and H. A. Bulger, "Observations upon flutter and fibrillation II. The nature of auricular flutter." *Heart*, vol. 7, pp. 191–233, 1920.
- [85] M. A. Allesie, F. I. Bonke, and F. J. Schopman, "Circus movement in rabbit atrial muscle as a mechanism of tachycardia. III. The "leading circle" concept: a new model of circus movement in cardiac tissue without the involvement of an anatomical obstacle." *Circ Res*, vol. 41, no. 1, pp. 9–18, Jul 1977.
- [86] P. L. Rensma, M. A. Allesie, W. J. Lammers, F. I. Bonke, and M. J. Schalij, "Length of excitation wave and susceptibility to reentrant atrial arrhythmias in normal conscious dogs." *Circ Res*, vol. 62, no. 2, pp. 395–410, Feb 1988.
- [87] M. Haïssaguerre, P. Jaïs, D. C. Shah, A. Takahashi, M. Hocini, G. Quiniou, S. Garrigue, A. L. Mouroux, P. L. Métayer, and J. Clémenty, "Spontaneous initiation of atrial fibrillation by ectopic beats originating in the pulmonary veins." *N Engl J Med*, vol. 339, no. 10, pp. 659–666, Sep 1998.
- [88] R. Mandapati, A. Skanes, J. Chen, O. Berenfeld, and J. Jalife, "Stable microreentrant sources as a mechanism of atrial fibrillation in the isolated sheep heart." *Circulation*, vol. 101, no. 2, pp. 194–199, Jan 2000.

- [89] M. J. Janse, "Focus, reentry, or "focal" reentry?" *Am J Physiol Heart Circ Physiol*, vol. 292, no. 6, pp. H2561–H2562, Jun 2007. [Online]. Available: <http://dx.doi.org/10.1152/ajpheart.00167.2007>
- [90] M. Haissaguerre, K.-T. Lim, V. Jacquemet, M. Rotter, L. Dang, M. Hocini, S. Matsuo, S. Knecht, P. Jaïs, and N. Virag, "Atrial fibrillatory cycle length: computer simulation and potential clinical importance." *Europace*, vol. 9 Suppl 6, pp. vi64–vi70, Nov 2007. [Online]. Available: <http://dx.doi.org/10.1093/europace/eum208>
- [91] V. Jacquemet, N. Virag, and L. Kappenberger, "Wavelength and vulnerability to atrial fibrillation: Insights from a computer model of human atria." *Europace*, vol. 7 Suppl 2, pp. 83–92, Sep 2005. [Online]. Available: <http://dx.doi.org/10.1016/j.eupc.2005.03.017>
- [92] M. C. Wijffels, C. J. Kirchhof, R. Dorland, and M. A. Allesie, "Atrial fibrillation begets atrial fibrillation. A study in awake chronically instrumented goats." *Circulation*, vol. 92, no. 7, pp. 1954–1968, Oct 1995.
- [93] M. Brignole, C. Menozzi, B. Sartore, M. Barra, and I. Monducci, "The use of atrial pacing to induce atrial fibrillation and flutter." *Int J Cardiol*, vol. 12, no. 1, pp. 45–54, Jul 1986.
- [94] A. S. Manolis, J. Cameron, T. Deering, E. H. Han, and N. A. Estes, "Sensitivity and specificity of programmed atrial stimulation for induction of supraventricular tachycardias." *Clin Cardiol*, vol. 11, no. 5, pp. 307–310, May 1988.
- [95] R. B. Krol, S. Saksena, A. Prakash, I. Giorgberidze, and P. Mathew, "Prospective clinical evaluation of a programmed atrial stimulation protocol for induction of sustained atrial fibrillation and flutter." *J Interv Card Electrophysiol*, vol. 3, no. 1, pp. 19–25, Mar 1999.
- [96] G. K. Moe, "On the multiple wavelet hypothesis of atrial fibrillation." *Arch. Int. Pharmacodyn. Ther.*, vol. 140, pp. 183–188, 1962.
- [97] M. A. Allesie, W. J. E. P. Lammers, and J. H. F. I. M. Bonke, "Experimental evaluation of Moe's multiple wavelet hypothesis of atrial fibrillation," in *Cardiac Arrhythmias*, D. P. Zipes and J. Jalife, Eds. Grune & Stratton, 1985, pp. 265–276.
- [98] M. A. Allesie, K. Konings, C. J. Kirchhof, and M. Wijffels, "Electrophysiologic mechanisms of perpetuation of atrial fibrillation." *Am J Cardiol*, vol. 77, no. 3, pp. 10A–23A, Jan 1996.
- [99] A. Kourliouros, I. Savelieva, A. Kiotsekoglou, M. Jahangiri, and J. Camm, "Current concepts in the pathogenesis of atrial fibrillation." *Am Heart J*, vol. 157, no. 2, pp. 243–252, Feb 2009. [Online]. Available: <http://dx.doi.org/10.1016/j.ahj.2008.10.009>
- [100] A. Vinet, D. R. Chialvo, D. C. Michaels, and J. Jalife, "Nonlinear dynamics of rate-dependent activation in models of single cardiac cells." *Circ Res*, vol. 67, no. 6, pp. 1510–1524, Dec 1990.
- [101] Z. Qu, J. N. Weiss, and A. Garfinkel, "Cardiac electrical restitution properties and stability of reentrant spiral waves: a simulation study." *Am J Physiol*, vol. 276, no. 1 Pt 2, pp. H269–H283, Jan 1999.
- [102] K. U. Thiedemann and V. J. Ferrans, "Left atrial ultrastructure in mitral valvular disease." *Am J Pathol*, vol. 89, no. 3, pp. 575–604, Dec 1977.



- [103] C. A. Morillo, G. J. Klein, D. L. Jones, and C. M. Guiraudon, "Chronic rapid atrial pacing. Structural, functional, and electrophysiological characteristics of a new model of sustained atrial fibrillation." *Circulation*, vol. 91, no. 5, pp. 1588–1595, Mar 1995.
- [104] J. Kneller, R. Zou, E. J. Vigmond, Z. Wang, L. J. Leon, and S. Nattel, "Cholinergic atrial fibrillation in a computer model of a two-dimensional sheet of canine atrial cells with realistic ionic properties." *Circ Res*, vol. 90, no. 9, pp. E73–E87, May 2002.
- [105] G. Mariscalco, K. G. Engström, S. Ferrarese, G. Cozzi, V. D. Bruno, F. Sessa, and A. Sala, "Relationship between atrial histopathology and atrial fibrillation after coronary bypass surgery." *J Thorac Cardiovasc Surg*, vol. 131, no. 6, pp. 1364–1372, Jun 2006. [Online]. Available: <http://dx.doi.org/10.1016/j.jtcvs.2006.01.040>
- [106] M. K. Chung, D. O. Martin, D. Sprecher, O. Wazni, A. Kanderian, C. A. Carnes, J. A. Bauer, P. J. Tchou, M. J. Niebauer, A. Natale, and D. R. V. Wagoner, "C-reactive protein elevation in patients with atrial arrhythmias: inflammatory mechanisms and persistence of atrial fibrillation." *Circulation*, vol. 104, no. 24, pp. 2886–2891, Dec 2001.
- [107] S. N. Psychari, T. S. Apostolou, L. Sinos, E. Hamodraka, G. Liakos, and D. T. Kremastinos, "Relation of elevated C-reactive protein and interleukin-6 levels to left atrial size and duration of episodes in patients with atrial fibrillation." *Am J Cardiol*, vol. 95, no. 6, pp. 764–767, Mar 2005. [Online]. Available: <http://dx.doi.org/10.1016/j.amjcard.2004.11.032>
- [108] D. Li, L. Zhang, J. Kneller, and S. Nattel, "Potential ionic mechanism for repolarization differences between canine right and left atrium." *Circ Res*, vol. 88, no. 11, pp. 1168–1175, Jun 2001.
- [109] Z. Qu, A. Garfinkel, P. S. Chen, and J. N. Weiss, "Mechanisms of discordant alternans and induction of reentry in simulated cardiac tissue." *Circulation*, vol. 102, no. 14, pp. 1664–1670, Oct 2000.
- [110] M. A. Allesie, P. L. Rensma, and J. Brugada, "Pathophysiology of atrial fibrillation," in *Cardiac Electrophysiology: From Cell to Bedside*, D. P. Zipes and J. Jalife, Eds. W. B. Saunders, Philadelphia, 1995, pp. 548–559.
- [111] M. Mansour, R. Mandapati, O. Berenfeld, J. Chen, F. H. Samie, and J. Jalife, "Left-to-right gradient of atrial frequencies during acute atrial fibrillation in the isolated sheep heart." *Circulation*, vol. 103, no. 21, pp. 2631–2636, May 2001.
- [112] H. Shao, K. J. Sampson, J. B. Pormann, D. J. Rose, and C. S. Henriquez, "A resistor interpretation of general anisotropic cardiac tissue." *Math Biosci*, vol. 187, no. 2, pp. 155–174, Feb 2004.
- [113] P. Ruchat, L. Dang, J. Schlaepfer, N. Virag, L. K. von Segesser, and L. Kappenberger, "Use of a biophysical model of atrial fibrillation in the interpretation of the outcome of surgical ablation procedures." *Eur J Cardiothorac Surg*, vol. 32, no. 1, pp. 90–95, Jul 2007. [Online]. Available: <http://dx.doi.org/10.1016/j.ejcts.2007.02.031>
- [114] G. T. Lines, M. C. MacLachlan, S. Linge, and A. Tveito, "Synchronizing computer simulations with measurement data for a case of atrial flutter." *Ann Biomed Eng*, vol. 37, no. 7, pp. 1287–1293, Jul 2009. [Online]. Available: <http://dx.doi.org/10.1007/s10439-009-9692-3>

- [115] E. Cherry, F. Fenton, H. M. Hastings, F. Xie, A. Garfinkel, J. N. Weiss, and S. J. Evans, "The role of decreased conduction velocity in the initiation and maintenance of atrial fibrillation in a computer model of human atria," *Pacing and Clinical Electrophysiology*, vol. 25, no. 4 (Part II, Abstract Suppl.), p. 538, 2002.
- [116] S. M. Narayan, D. Kazi, D. E. Krummen, and W.-J. Rappel, "Repolarization and activation restitution near human pulmonary veins and atrial fibrillation initiation: a mechanism for the initiation of atrial fibrillation by premature beats." *J Am Coll Cardiol*, vol. 52, no. 15, pp. 1222–1230, Oct 2008. [Online]. Available: <http://dx.doi.org/10.1016/j.jacc.2008.07.012>
- [117] L. Uldry, N. Virag, V. Jacquemet, J.-M. Vesin, and L. Kappenberger, "Spontaneous termination of atrial fibrillation: study of the effect of atrial geometry in a biophysical model." *Conf Proc IEEE Eng Med Biol Soc*, vol. 2009, pp. 4504–4507, 2009. [Online]. Available: <http://dx.doi.org/10.1109/IEMBS.2009.5334111>
- [118] L. Uldry, N. Virag, J.-M. Vesin, and L. Kappenberger, "Effect of atrial fibrillation dynamics on the mechanisms of spontaneous termination." *Heart Rhythm*, vol. 7, no. 5, Supplement (May2010), p. S350, 2010.
- [119] S. Vaisrub, "Spontaneous reversion to normal sinus rhythm in a case of auricular fibrillation of long standing." *Can Med Assoc J*, vol. 63, no. 6, pp. 599–600, Dec 1950.
- [120] R. Alcaraz and J. J. Rieta, "Non-invasive organization variation assessment in the onset and termination of paroxysmal atrial fibrillation." *Comput Methods Programs Biomed*, vol. 93, no. 2, pp. 148–154, Feb 2009. [Online]. Available: <http://dx.doi.org/10.1016/j.cmpb.2008.09.001>
- [121] S. Petrutiu, A. V. Sahakian, and S. Swiryn, "Abrupt changes in fibrillatory wave characteristics at the termination of paroxysmal atrial fibrillation in humans." *Europace*, vol. 9, no. 7, pp. 466–470, Jul 2007. [Online]. Available: <http://dx.doi.org/10.1093/europace/eum096>
- [122] G. Ndrepepa, S. Weber, M. R. Karch, M. A. E. Schneider, J. Schreieck, A. Schömig, and C. Schmitt, "Electrophysiologic characteristics of the spontaneous onset and termination of atrial fibrillation." *Am J Cardiol*, vol. 90, no. 11, pp. 1215–1220, Dec 2002.
- [123] H. J. Sih, K. M. Ropella, S. Swiryn, E. P. Gerstenfeld, and A. V. Sahakian, "Observations from intraatrial recordings on the termination of electrically induced atrial fibrillation in humans." *Pacing Clin Electrophysiol*, vol. 17, no. 7, pp. 1231–1242, Jul 1994.
- [124] A. Fujiki, M. Sakabe, K. Nishida, K. Mizumaki, and H. Inoue, "Role of fibrillation cycle length in spontaneous and drug-induced termination of human atrial fibrillation." *Circ J*, vol. 67, no. 5, pp. 391–395, May 2003.
- [125] A. Capucci, M. Biffi, G. Boriani, F. Ravelli, G. Nollo, P. Sabbatani, C. Orsi, and B. Magnani, "Dynamic electrophysiological behavior of human atria during paroxysmal atrial fibrillation." *Circulation*, vol. 92, no. 5, pp. 1193–1202, Sep 1995.
- [126] S. Shimizu, M. Osaka, H. Saitoh, H. Atarashi, and T. Takano, "Quantitative analysis of termination of vagally induced canine atrial fibrillation by mutual information." *Jpn Circ J*, vol. 65, no. 2, pp. 111–116, Feb 2001.

- [127] R. Alcaraz and J. J. Rieta, "Sample entropy of the main atrial wave predicts spontaneous termination of paroxysmal atrial fibrillation." *Med Eng Phys*, vol. 31, no. 8, pp. 917–922, Oct 2009. [Online]. Available: <http://dx.doi.org/10.1016/j.medengphy.2009.05.002>
- [128] F. Nilsson, M. Stridh, A. Bollmann, and L. Sörnmo, "Predicting spontaneous termination of atrial fibrillation using the surface ECG." *Med Eng Phys*, vol. 28, no. 8, pp. 802–808, Oct 2006. [Online]. Available: <http://dx.doi.org/10.1016/j.medengphy.2005.11.010>
- [129] M. A. Bennett and B. L. Pentecost, "The pattern of onset and spontaneous cessation of atrial fibrillation in man." *Circulation*, vol. 41, no. 6, pp. 981–988, Jun 1970.
- [130] L. H. Frame and M. B. Simson, "Oscillations of conduction, action potential duration, and refractoriness. A mechanism for spontaneous termination of reentrant tachycardias." *Circulation*, vol. 78, no. 5 Pt 1, pp. 1277–1287, Nov 1988.
- [131] C. Cabo, A. M. Pertsov, W. T. Baxter, J. M. Davidenko, R. A. Gray, and J. Jalife, "Wave-front curvature as a cause of slow conduction and block in isolated cardiac muscle." *Circ Res*, vol. 75, no. 6, pp. 1014–1028, Dec 1994.
- [132] T. Ikeda, T. Uchida, D. Hough, J. J. Lee, M. C. Fishbein, W. J. Mandel, P. S. Chen, and H. S. Karagueuzian, "Mechanism of spontaneous termination of functional reentry in isolated canine right atrium. Evidence for the presence of an excitable but nonexcited core." *Circulation*, vol. 94, no. 8, pp. 1962–1973, Oct 1996.
- [133] R. A. Gray, A. M. Pertsov, and J. Jalife, "Spatial and temporal organization during cardiac fibrillation." *Nature*, vol. 392, no. 6671, pp. 75–78, Mar 1998. [Online]. Available: <http://dx.doi.org/10.1038/32164>
- [134] M. C. Wijffels, R. Dorland, F. Mast, and M. A. Allesie, "Widening of the excitable gap during pharmacological cardioversion of atrial fibrillation in the goat: effects of cibenzoline, hydroquinidine, flecainide, and d-sotalol." *Circulation*, vol. 102, no. 2, pp. 260–267, Jul 2000.
- [135] J. Kneller, J. Kalifa, R. Zou, A. V. Zaitsev, M. Warren, O. Berenfeld, E. J. Vigmond, L. J. Leon, S. Nattel, and J. Jalife, "Mechanisms of atrial fibrillation termination by pure sodium channel blockade in an ionically-realistic mathematical model." *Circ Res*, vol. 96, no. 5, pp. e35–e47, Mar 2005. [Online]. Available: <http://dx.doi.org/10.1161/01.RES.0000160709.49633.2b>
- [136] P. Comtois, M. Sakabe, E. J. Vigmond, M. Munoz, A. Texier, A. Shiroshita-Takeshita, and S. Nattel, "Mechanisms of atrial fibrillation termination by rapidly unbinding Na<sup>+</sup> channel blockers: insights from mathematical models and experimental correlates." *Am J Physiol Heart Circ Physiol*, vol. 295, no. 4, pp. H1489–H1504, Oct 2008. [Online]. Available: <http://dx.doi.org/10.1152/ajpheart.01054.2007>
- [137] J. Jalife, O. Berenfeld, and M. Mansour, "Mother rotors and fibrillatory conduction: a mechanism of atrial fibrillation." *Cardiovasc Res*, vol. 54, no. 2, pp. 204–216, May 2002.
- [138] Z. Qu, "Critical mass hypothesis revisited: role of dynamical wave stability in spontaneous termination of cardiac fibrillation." *Am J Physiol Heart Circ Physiol*, vol. 290, no. 1, pp. H255–H263, Jan 2006. [Online]. Available: <http://dx.doi.org/10.1152/ajpheart.00668.2005>

- [139] L. Uldry, N. Virag, V. Jacquemet, J.-M. Vesin, and L. Kappenberger, "Optimizing local capture of atrial fibrillation by rapid pacing: study of the influence of tissue dynamics." *Ann Biomed Eng*, vol. 38, no. 12, pp. 3664–3673, Dec 2010. [Online]. Available: <http://dx.doi.org/10.1007/s10439-010-0122-3>
- [140] S. M. Narayan, M. R. Franz, P. Clopton, E. J. Pruvot, and D. E. Krummen, "Repolarization alternans reveals vulnerability to human atrial fibrillation." *Circulation*, vol. 123, no. 25, pp. 2922–2930, Jun 2011. [Online]. Available: <http://dx.doi.org/10.1161/CIRCULATIONAHA.110.977827>
- [141] H. J. Sih, D. P. Zipes, E. J. Berbari, D. E. Adams, and J. E. Olgin, "Differences in organization between acute and chronic atrial fibrillation in dogs." *J Am Coll Cardiol*, vol. 36, no. 3, pp. 924–931, Sep 2000.
- [142] K. Agladze, M. W. Kay, V. Krinsky, and N. Sarvazyan, "Interaction between spiral and paced waves in cardiac tissue." *Am J Physiol Heart Circ Physiol*, vol. 293, no. 1, pp. H503–H513, Jul 2007. [Online]. Available: <http://dx.doi.org/10.1152/ajpheart.01060.2006>
- [143] W. E. Garrey, "The nature of fibrillatory contraction of the heart: its relation to tissue mass and form." *Am J Physiol*, vol. 33, pp. 397–414, 1914.
- [144] M. Haïssaguerre, P. Sanders, M. Hocini, L.-F. Hsu, D. C. Shah, C. Scavée, Y. Takahashi, M. Rotter, J.-L. Pasquié, S. Garrigue, J. Clémenty, and P. Jaïs, "Changes in atrial fibrillation cycle length and inducibility during catheter ablation and their relation to outcome." *Circulation*, vol. 109, no. 24, pp. 3007–3013, Jun 2004. [Online]. Available: <http://dx.doi.org/10.1161/01.CIR.0000130645.95357.97>
- [145] M. A. Bray, S. F. Lin, R. R. Aliev, B. J. Roth, and J. P. Wikswo, "Experimental and theoretical analysis of phase singularity dynamics in cardiac tissue." *J Cardiovasc Electrophysiol*, vol. 12, no. 6, pp. 716–722, Jun 2001.
- [146] R. Zou, J. Kneller, L. J. Leon, and S. Nattel, "Development of a computer algorithm for the detection of phase singularities and initial application to analyze simulations of atrial fibrillation." *Chaos*, vol. 12, no. 3, pp. 764–778, Sep 2002. [Online]. Available: <http://dx.doi.org/10.1063/1.1497505>
- [147] D. Geberth and M. T. Hütt, "Predicting the distribution of spiral waves from cell properties in a developmental-path model of Dictyostelium pattern formation." *PLoS Comput Biol*, vol. 5, no. 7, p. e1000422, Jul 2009. [Online]. Available: <http://dx.doi.org/10.1371/journal.pcbi.1000422>
- [148] J. M. Drake and B. D. Griffen, "Early warning signals of extinction in deteriorating environments." *Nature*, vol. 467, no. 7314, pp. 456–459, Sep 2010. [Online]. Available: <http://dx.doi.org/10.1038/nature09389>
- [149] N. F. Otani, A. Mo, S. Mannava, F. H. Fenton, E. M. Cherry, S. Luther, and R. F. Gilmour, "Characterization of multiple spiral wave dynamics as a stochastic predator-prey system." *Phys Rev E Stat Nonlin Soft Matter Phys*, vol. 78, no. 2 Pt 1, p. 021913, Aug 2008.
- [150] L. A. Geddes, "Historical highlights in cardiac pacing." *IEEE Eng Med Biol Mag*, vol. 9, no. 2, pp. 12–18, 1990. [Online]. Available: <http://dx.doi.org/10.1109/51.57859>
- [151] F. Steiner, "Ueber die Electropunctur des Herzens als Wiederbelebungs mittel in der Chloroformsyncope." *Archiv. Klin. Chir.*, vol. 12, pp. 748–790, 1871.

- [152] T. Greene, "On death from chloroform; its prevention by galvanism." *Brit. Med.*, vol. 1, pp. 551–553, 1872.
- [153] A. A. Hyman, "Resuscitation of the stopped heart by intracardial therapy." *Arch. Inc. Med.*, vol. 50, pp. 289–308, 1932.
- [154] P. M. Zoll, A. J. Linenthal, W. Gibson, M. H. Paul, and L. R. Norman, "Termination of ventricular fibrillation in man by externally applied electric countershock." *N Engl J Med*, vol. 254, no. 16, pp. 727–732, Apr 1956.
- [155] V. Parsonnet, "Permanent transvenous pacing in 1962." *Pacing Clin Electrophysiol*, vol. 1, no. 2, pp. 265–268, Apr 1978.
- [156] W. M. Chardack, A. A. Gage, and W. Greatbatch, "A transistorized, self-contained, implantable pacemaker for the long-term correction of complete heart block." *Surgery*, vol. 48, pp. 643–654, Oct 1960.
- [157] R. A. Cooper, C. A. Alferness, W. M. Smith, and R. E. Ideker, "Internal cardioversion of atrial fibrillation in sheep." *Circulation*, vol. 87, no. 5, pp. 1673–1686, May 1993.
- [158] A. L. Waldo, W. A. MacLean, R. B. Karp, N. T. Kouchoukos, and T. N. James, "Entrainment and interruption of atrial flutter with atrial pacing: studies in man following open heart surgery." *Circulation*, vol. 56, no. 5, pp. 737–745, Nov 1977.
- [159] J. D. Fisher, S. G. Kim, J. A. Matos, and L. E. Waspe, "Pacing for ventricular tachycardia." *Pacing Clin Electrophysiol*, vol. 7, no. 6 Pt 2, pp. 1278–1290, Nov 1984.
- [160] D. J. Dossdall and R. E. Ideker, "Intracardiac atrial defibrillation." *Heart Rhythm*, vol. 4, no. 3 Suppl, pp. S51–S56, Mar 2007. [Online]. Available: <http://dx.doi.org/10.1016/j.hrthm.2006.12.030>
- [161] M. Alessie, C. Kirchhof, G. J. Scheffer, F. Chorro, and J. Brugada, "Regional control of atrial fibrillation by rapid pacing in conscious dogs." *Circulation*, vol. 84, no. 4, pp. 1689–1697, Oct 1991.
- [162] C. Kirchhof, F. Chorro, G. J. Scheffer, J. Brugada, K. Konings, Z. Zetelaki, and M. Alessie, "Regional entrainment of atrial fibrillation studied by high-resolution mapping in open-chest dogs." *Circulation*, vol. 88, no. 2, pp. 736–749, Aug 1993.
- [163] J. M. Kalman, J. E. Olgin, M. R. Karch, and M. D. Lesh, "Regional entrainment of atrial fibrillation in man." *J Cardiovasc Electrophysiol*, vol. 7, no. 9, pp. 867–876, Sep 1996.
- [164] C. Pandozi, L. Bianconi, M. Villani, A. Castro, G. Altamura, S. Toscano, A. P. Jesi, G. Gentilucci, F. Ammirati, F. L. Bianco, and M. Santini, "Local capture by atrial pacing in spontaneous chronic atrial fibrillation." *Circulation*, vol. 95, no. 10, pp. 2416–2422, May 1997.
- [165] E. G. Daoud, B. Pariseau, M. Niebauer, F. Bogun, R. Goyal, M. Harvey, K. C. Man, S. A. Strickberger, and F. Morady, "Response of type I atrial fibrillation to atrial pacing in humans." *Circulation*, vol. 94, no. 5, pp. 1036–1040, Sep 1996.
- [166] D. P. Redfearn and R. Yee, "Pacing delivered rate and rhythm control for atrial fibrillation." *Curr Opin Cardiol*, vol. 21, no. 2, pp. 83–87, Mar 2006. [Online]. Available: <http://dx.doi.org/10.1097/01.hco.0000210302.56736.60>

- [167] Y. Guyomar, O. Thomas, C. Marquié, M. Jarwe, D. Klug, S. Kacet, R. Carlioz, A. Ferrier, F. Fossati, S. Guérin, S. Heuls, and P. Graux, "Mechanisms of onset of atrial fibrillation: a multicenter, prospective, pacemaker-based study." *Pacing Clin Electrophysiol*, vol. 26, no. 6, pp. 1336–1341, Jun 2003.
- [168] M. D. Carlson, J. Ip, J. Messenger, S. Beau, S. Kalbfleisch, P. Gervais, D. A. Cameron, A. Duran, J. Val-Mejias, J. Mackall, M. Gold, and A. D. O. P. T. A. Investigators, "A new pacemaker algorithm for the treatment of atrial fibrillation: results of the Atrial Dynamic Overdrive Pacing Trial (ADOPT)." *J Am Coll Cardiol*, vol. 42, no. 4, pp. 627–633, Aug 2003.
- [169] L. Padeletti, H. Pürerfellner, S. W. Adler, T. J. Waller, M. Harvey, L. Horvitz, R. Holbrook, K. Kempen, A. Mugglin, D. A. Hettrick, and W. A. Investigators, "Combined efficacy of atrial septal lead placement and atrial pacing algorithms for prevention of paroxysmal atrial tachyarrhythmia." *J Cardiovasc Electrophysiol*, vol. 14, no. 11, pp. 1189–1195, Nov 2003.
- [170] M. A. Lee, R. Weachter, S. Pollak, M. S. Kremers, A. M. Naik, R. Silverman, J. Tuzi, W. Wang, L. J. Johnson, D. E. Euler, and A. T. T. E. S. T. Investigators, "The effect of atrial pacing therapies on atrial tachyarrhythmia burden and frequency: results of a randomized trial in patients with bradycardia and atrial tachyarrhythmias." *J Am Coll Cardiol*, vol. 41, no. 11, pp. 1926–1932, Jun 2003.
- [171] J.-J. Blanc, L. D. Roy, J. Mansourati, Y. Poezevara, J.-L. Marcon, W. Schoels, F. Hidden-Lucet, C. Barnay, and P. I. P. A. F. Investigators, "Atrial pacing for prevention of atrial fibrillation: assessment of simultaneously implemented algorithms." *Europace*, vol. 6, no. 5, pp. 371–379, Sep 2004.
- [172] H. Pürerfellner, J. H. Ruiter, J. W. M. G. Widdershoven, I. C. V. Gelder, L. Urban, C. J. H. J. Kirchhof, A. Havlicek, L. Kornet, and P. M. O. P. Investigators, "Reduction of atrial tachyarrhythmia episodes during the overdrive pacing period using the post-mode switch overdrive pacing (PMOP) algorithm." *Heart Rhythm*, vol. 3, no. 10, pp. 1164–1171, Oct 2006.
- [173] H. Pürerfellner, L. Urban, G. de Weerd, J. Ruiter, J. Brandt, A. Havlicek, B. Hügl, J. Widdershoven, L. Kornet, and R. Kessels, "Reduction of atrial fibrillation burden by atrial overdrive pacing: experience with an improved algorithm to reduce early recurrences of atrial fibrillation." *Europace*, vol. 11, no. 1, pp. 62–69, Jan 2009. [Online]. Available: <http://dx.doi.org/10.1093/europace/eun294>
- [174] A. J. Camm, N. Sulke, N. Edvardsson, P. Ritter, B. A. Albers, J. H. Ruiter, T. Lewalter, P. A. Capucci, E. Hoffmann, and A. F. T. Investigators, "Conventional and dedicated atrial overdrive pacing for the prevention of paroxysmal atrial fibrillation: the AFTherapy study." *Europace*, vol. 9, no. 12, pp. 1110–1118, Dec 2007.
- [175] H. Ogawa, T. Ishikawa, K. Matsushita, K. Matsumoto, T. Ishigami, T. Sugano, K. Uchino, S. Umemura, S. Sumita, K. Kimura, T. Nakagawa, M. Shimizu, H. Nishikawa, A. Kasai, and Y. Kioka, "Effects of right atrial pacing preference in prevention of paroxysmal atrial fibrillation: Atrial Pacing Preference study (APP study)." *Circ J*, vol. 72, no. 5, pp. 700–704, May 2008.
- [176] M. R. Gold, S. Adler, L. Fauchier, C. Haffajee, J. Ip, W. Kainz, R. Kawasaki, A. Prakash, M. Tábořský, T. Waller, V. Wilson, S. Li, E. Hoffmann, and S. A. F. A. R. I. Investigators,

- “Impact of atrial prevention pacing on atrial fibrillation burden: primary results of the Study of Atrial Fibrillation Reduction (SAFARI) trial.” *Heart Rhythm*, vol. 6, no. 3, pp. 295–301, Mar 2009. [Online]. Available: <http://dx.doi.org/10.1016/j.hrthm.2008.11.033>
- [177] E. N. Simantirakis, E. G. Arkolaki, and P. E. Vardas, “Novel pacing algorithms: do they represent a beneficial proposition for patients, physicians, and the health care system?” *Europace*, vol. 11, no. 10, pp. 1272–1280, Oct 2009. [Online]. Available: <http://dx.doi.org/10.1093/europace/eup204>
- [178] I. Giorgberidze, S. Saksena, L. Mongeon, R. Mehra, R. B. Krol, A. N. Munsif, and P. Mathew, “Effects of high-frequency atrial pacing in atypical atrial flutter and atrial fibrillation.” *J Interv Card Electrophysiol*, vol. 1, no. 2, pp. 111–123, Sep 1997.
- [179] W. Paladino, M. Bahu, B. P. Knight, R. Weiss, J. Sousa, A. Zivin, R. Goyal, E. Daoud, K. C. Man, S. A. Strickberger, and F. Morady, “Failure of single- and multisite high-frequency atrial pacing to terminate atrial fibrillation.” *Am J Cardiol*, vol. 80, no. 2, pp. 226–227, Jul 1997.
- [180] S. W. Adler, C. Wolpert, E. N. Warman, S. K. Musley, J. L. Koehler, and D. E. Euler, “Efficacy of pacing therapies for treating atrial tachyarrhythmias in patients with ventricular arrhythmias receiving a dual-chamber implantable cardioverter defibrillator.” *Circulation*, vol. 104, no. 8, pp. 887–892, Aug 2001.
- [181] C. W. Israel and S. S. Barold, “Can implantable devices detect and pace-terminate atrial fibrillation?” *Pacing Clin Electrophysiol*, vol. 26, no. 10, pp. 1923–1925, Oct 2003.
- [182] M. R. Gold, N. Sulke, D. S. Schwartzman, R. Mehra, D. E. Euler, and W. J. A.-O. Investigators, “Clinical experience with a dual-chamber implantable cardioverter defibrillator to treat atrial tachyarrhythmias.” *J Cardiovasc Electrophysiol*, vol. 12, no. 11, pp. 1247–1253, Nov 2001.
- [183] P. A. Friedman, B. Dijkman, E. N. Warman, H. A. Xia, R. Mehra, M. S. Stanton, and S. C. Hammill, “Atrial therapies reduce atrial arrhythmia burden in defibrillator patients.” *Circulation*, vol. 104, no. 9, pp. 1023–1028, Aug 2001.
- [184] W. Schoels, C. D. Swerdlow, W. Jung, K. M. Stein, K. Seidl, C. J. Haffajee, and W. J. A. Investigators, “Worldwide clinical experience with a new dual-chamber implantable cardioverter defibrillator system.” *J Cardiovasc Electrophysiol*, vol. 12, no. 5, pp. 521–528, May 2001.
- [185] R. Ricci, C. Pignalberi, M. Disertori, A. Capucci, L. Padeletti, G. Botto, S. Toscano, F. Miraglia, A. Grammatico, and M. Santini, “Efficacy of a dual chamber defibrillator with atrial antitachycardia functions in treating spontaneous atrial tachyarrhythmias in patients with life-threatening ventricular tachyarrhythmias.” *Eur Heart J*, vol. 23, no. 18, pp. 1471–1479, Sep 2002.
- [186] A. R. J. Mitchell and N. Sulke, “Does rapid atrial pacing terminate atrial fibrillation? A comparison of laboratory and device termination studies.” *Card Electrophysiol Rev*, vol. 7, no. 4, pp. 352–354, Dec 2003. [Online]. Available: <http://dx.doi.org/10.1023/B:CEPR.0000023137.24735.6b>
- [187] C. Schmitt, G. Ndrepepa, S. Weyerbrock, C. Kolb, and B. Zrenner, “Pseudotermination of intermittent atrial fibrillation by a pacemaker algorithm: antitachycardia pacing without capture miscounted as successful termination of fibrillation episodes.” *Pacing Clin Electrophysiol*, vol. 24, no. 12, pp. 1824–1826, Dec 2001.

- [188] C. W. Israel, J. R. Ehrlich, G. Grönefeld, A. Klesius, T. Lawo, B. Lemke, and S. H. Hohnloser, "Prevalence, characteristics and clinical implications of regular atrial tachyarrhythmias in patients with atrial fibrillation: insights from a study using a new implantable device." *J Am Coll Cardiol*, vol. 38, no. 2, pp. 355–363, Aug 2001.
- [189] T. H. Everett, J. G. Akar, L.-C. Kok, J. R. Moorman, and D. E. Haines, "Use of global atrial fibrillation organization to optimize the success of burst pace termination." *J Am Coll Cardiol*, vol. 40, no. 10, pp. 1831–1840, Nov 2002.
- [190] B. Hügl, C. W. Israel, C. Unterberg, T. Lawo, J. C. Geller, I. M. Kennis, D. E. Euler, J. L. Koehler, D. A. Hettrick, and A. T. V. S. Investigators, "Incremental programming of atrial anti-tachycardia pacing therapies in bradycardia-indicated patients: effects on therapy efficacy and atrial tachyarrhythmia burden." *Europace*, vol. 5, no. 4, pp. 403–409, Oct 2003.
- [191] A. M. Gillis, J. Koehler, M. Morck, R. Mehra, and D. A. Hettrick, "High atrial antitachycardia pacing therapy efficacy is associated with a reduction in atrial tachyarrhythmia burden in a subset of patients with sinus node dysfunction and paroxysmal atrial fibrillation." *Heart Rhythm*, vol. 2, no. 8, pp. 791–796, Aug 2005. [Online]. Available: <http://dx.doi.org/10.1016/j.hrthm.2005.04.027>
- [192] M. Gulizia, S. Mangiameli, S. Orazi, G. Chiarandà, G. Boriani, G. Piccione, N. Di-Giovanni, A. Colletti, C. Puntrello, G. Butera, C. Vasco, I. Vaccaro, G. Scardace, A. Grammatico, P. I. T. A. G. O. R. A. P. Investigation, T. A. G. for Observation, and R. on Atrial arrhythmias) Investigators, "Randomized comparison between Ramp and Burst+ atrial antitachycardia pacing therapies in patients suffering from sinus node disease and atrial fibrillation and implanted with a DDDR device." *Europace*, vol. 8, no. 7, pp. 465–473, Jul 2006.
- [193] L. Mont, R. Ruiz-Granell, J. G. Martínez, J. R. Carmona, M. Fidalgo, E. Cobo, M. Riera, X. Navarro, and P. or Termination (POT) Study Investigators, "Impact of anti-tachycardia pacing on atrial fibrillation burden when added on top of preventive pacing algorithms: results of the prevention or termination (POT) trial." *Europace*, vol. 10, no. 1, pp. 28–34, Jan 2008.
- [194] A. Pumir, V. Nikolski, M. Hörning, A. Isomura, K. Agladze, K. Yoshikawa, R. Gilmour, E. Bodenschatz, and V. Krinsky, "Wave emission from heterogeneities opens a way to controlling chaos in the heart." *Phys Rev Lett*, vol. 99, no. 20, p. 208101, Nov 2007.
- [195] F. H. Fenton, S. Luther, E. M. Cherry, N. F. Otani, V. Krinsky, A. Pumir, E. Bodenschatz, and R. F. Gilmour, "Termination of atrial fibrillation using pulsed low-energy far-field stimulation." *Circulation*, vol. 120, no. 6, pp. 467–476, Aug 2009. [Online]. Available: <http://dx.doi.org/10.1161/CIRCULATIONAHA.108.825091>
- [196] N. Trayanova, "Atrial defibrillation voltage: falling to a new low." *Heart Rhythm*, vol. 8, no. 1, pp. 109–110, Jan 2011. [Online]. Available: <http://dx.doi.org/10.1016/j.hrthm.2010.10.037>
- [197] C. M. Ambrosi, C. M. Ripplinger, I. R. Efimov, and V. V. Fedorov, "Termination of sustained atrial flutter and fibrillation using low-voltage multiple-shock therapy." *Heart Rhythm*, vol. 8, no. 1, pp. 101–108, Jan 2011. [Online]. Available: <http://dx.doi.org/10.1016/j.hrthm.2010.10.018>



- [198] M. Santini, C. Pandozi, G. Altamura, G. Gentilucci, M. Villani, M. C. Scianaro, A. Castro, F. Ammirati, and B. Magris, "Single shock endocavitary low energy intracardiac cardioversion of chronic atrial fibrillation." *J Interv Card Electrophysiol*, vol. 3, no. 1, pp. 45–51, Mar 1999.
- [199] C.-P. Lau, C.-C. Wang, T. Ngarmukos, Y.-H. Kim, C.-W. Kong, R. Omar, C. Sriratanasathavorn, M. Munawar, R. Kam, K. L. Lee, E. O.-Y. Lau, H.-F. Tse, and S. A. F. E. S. S. C. for SAFE Study Group, "A prospective randomized study to assess the efficacy of rate and site of atrial pacing on long-term development of atrial fibrillation." *J Cardiovasc Electrophysiol*, vol. 20, no. 9, pp. 1020–1025, Sep 2009. [Online]. Available: <http://dx.doi.org/10.1111/j.1540-8167.2009.01484.x>
- [200] B. P. Knight, B. J. Gersh, M. D. Carlson, P. A. Friedman, R. L. McNamara, S. A. Strickberger, H. F. Tse, A. L. Waldo, A. H. A. C. on Clinical Cardiology (Subcommittee on Electrocardiography, Arrhythmias), Q. of Care, O. R. I. W. Group, H. R. Society, and A. H. A. W. Group, "Role of permanent pacing to prevent atrial fibrillation: science advisory from the American Heart Association Council on Clinical Cardiology (Subcommittee on Electrocardiography and Arrhythmias) and the Quality of Care and Outcomes Research Interdisciplinary Working Group, in collaboration with the Heart Rhythm Society." *Circulation*, vol. 111, no. 2, pp. 240–243, Jan 2005.
- [201] S. Janko and E. Hoffmann, "Atrial antitachycardia pacing: do we still need to talk about it?" *Europace*, vol. 11, no. 8, pp. 977–979, Aug 2009. [Online]. Available: <http://dx.doi.org/10.1093/europace/eup182>
- [202] L. Uldry, N. Virag, L. Kappenberger, and J.-M. Vesin, "Optimization of antitachycardia pacing protocols applied to atrial fibrillation: insights from a biophysical model." *Conf Proc IEEE Eng Med Biol Soc*, vol. 2009, pp. 3024–3027, 2009. [Online]. Available: <http://dx.doi.org/10.1109/IEMBS.2009.5333296>
- [203] A. Capucci, F. Ravelli, G. Nollo, A. S. Montenero, M. Biffi, and G. Q. Villani, "Capture window in human atrial fibrillation: evidence of an excitable gap." *J Cardiovasc Electrophysiol*, vol. 10, no. 3, pp. 319–327, Mar 1999.
- [204] A. R. R. Misier, W. P. Beukema, H. A. O. Luttikhuis, and R. Willems, "Multisite atrial pacing: an option for atrial fibrillation prevention? Preliminary results of the Dutch Dual-site Right Atrial Pacing for Prevention of Atrial Fibrillation study." *Am J Cardiol*, vol. 86, no. 9A, pp. 20K–24K, Nov 2000.
- [205] J. C. Hansen, R. Latchamsetty, N. Lavi, S. Uppuluri, D. Lafontaine, R. Hastings, and B. Avitall, "High-density biatrial pacing protects against atrial fibrillation by synchronizing left atrial tissue." *J Interv Card Electrophysiol*, vol. 27, no. 2, pp. 81–87, Mar 2010. [Online]. Available: <http://dx.doi.org/10.1007/s10840-009-9453-0>
- [206] W. H. Spencer, D. W. Zhu, T. Markowitz, S. M. Badruddin, and W. A. Zoghbi, "Atrial septal pacing: a method for pacing both atria simultaneously." *Pacing Clin Electrophysiol*, vol. 20, no. 11, pp. 2739–2745, Nov 1997.
- [207] L. Padeletti, A. Michelucci, P. Pieragnoli, A. Colella, and N. Musilli, "Atrial septal pacing: a new approach to prevent atrial fibrillation." *Pacing Clin Electrophysiol*, vol. 27, no. 6 Pt 2, pp. 850–854, Jun 2004. [Online]. Available: <http://dx.doi.org/10.1111/j.1540-8159.2004.00546.x>

- [208] R. Becker, J. C. Senges, A. Bauer, K. D. Schreiner, F. Voss, W. Kuebler, and W. Schoels, "Suppression of atrial fibrillation by multisite and septal pacing in a novel experimental model." *Cardiovasc Res*, vol. 54, no. 2, pp. 476–481, May 2002.
- [209] M. Kale and D. H. Bennett, "Atrial septal pacing in the prevention of paroxysmal atrial fibrillation refractory to antiarrhythmic drugs." *Int J Cardiol*, vol. 82, no. 2, pp. 167–175, Feb 2002.
- [210] J.-S. Hermida, M. Kubala, F.-X. Lescure, J. Delonca, J. Clerc, A. Otmani, G. Jarry, and J.-L. Rey, "Atrial septal pacing to prevent atrial fibrillation in patients with sinus node dysfunction: results of a randomized controlled study." *Am Heart J*, vol. 148, no. 2, pp. 312–317, Aug 2004. [Online]. Available: <http://dx.doi.org/10.1016/j.ahj.2004.03.012>
- [211] N. Hakacova, D. Velimirovic, P. Margitfalvi, R. Hatala, and T. A. Buckingham, "Septal atrial pacing for the prevention of atrial fibrillation." *Europace*, vol. 9, no. 12, pp. 1124–1128, Dec 2007. [Online]. Available: <http://dx.doi.org/10.1093/europace/eum242>
- [212] G. D. Byrd, S. M. Prasad, C. M. Ripplinger, T. R. Cassilly, R. B. Schuessler, J. P. Boineau, and R. J. Damiano, "Importance of geometry and refractory period in sustaining atrial fibrillation: testing the critical mass hypothesis." *Circulation*, vol. 112, no. 9 Suppl, pp. I7–I13, Aug 2005. [Online]. Available: <http://dx.doi.org/10.1161/CIRCULATIONAHA.104.526210>
- [213] S. S. Barold, C. R. Wyndham, L. L. Kappenberger, E. G. Abinader, J. C. Griffin, and M. D. Falkoff, "Implanted atrial pacemakers for paroxysmal atrial flutter. Long-term efficacy." *Ann Intern Med*, vol. 107, no. 2, pp. 144–149, Aug 1987.
- [214] M. Duytschaever, F. Mast, M. Killian, Y. Blaauw, M. Wijffels, and M. Allessie, "Methods for determining the refractory period and excitable gap during persistent atrial fibrillation in the goat." *Circulation*, vol. 104, no. 8, pp. 957–962, Aug 2001.
- [215] M. Tanaka, A. Isomura, M. Hörning, H. Kitahata, K. Agladze, and K. Yoshikawa, "Unpinning of a spiral wave anchored around a circular obstacle by an external wave train: common aspects of a chemical reaction and cardiomyocyte tissue." *Chaos*, vol. 19, no. 4, p. 043114, Dec 2009. [Online]. Available: <http://dx.doi.org/10.1063/1.3263167>
- [216] G. W. Botteron and J. M. Smith, "Quantitative assessment of the spatial organization of atrial fibrillation in the intact human heart." *Circulation*, vol. 93, no. 3, pp. 513–518, Feb 1996.
- [217] A. M. Kim, J. E. Olgin, and T. H. Everett, "Role of atrial substrate and spatiotemporal organization in atrial fibrillation." *Heart Rhythm*, vol. 6, no. 8 Suppl, pp. S1–S7, Aug 2009. [Online]. Available: <http://dx.doi.org/10.1016/j.hrthm.2009.02.010>
- [218] P. V. Bayly, E. E. Johnson, P. D. Wolf, H. S. Greenside, W. M. Smith, and R. E. Ideker, "A quantitative measurement of spatial order in ventricular fibrillation." *J Cardiovasc Electrophysiol*, vol. 4, no. 5, pp. 533–546, Oct 1993.
- [219] G. W. Botteron and J. M. Smith, "A technique for measurement of the extent of spatial organization of atrial activation during atrial fibrillation in the intact human heart." *IEEE Trans Biomed Eng*, vol. 42, no. 6, pp. 579–586, Jun 1995. [Online]. Available: <http://dx.doi.org/10.1109/10.387197>

- [220] S. M. Narayan, G. K. Feld, A. Hassankhani, and V. Bhargava, "Quantifying intracardiac organization of atrial arrhythmias using temporospatial phase of the electrocardiogram." *J Cardiovasc Electrophysiol*, vol. 14, no. 9, pp. 971–981, Sep 2003.
- [221] S. M. Narayan and V. Bhargava, "Temporal and spatial phase analyses of the electrocardiogram stratify intra-atrial and intra-ventricular organization." *IEEE Trans Biomed Eng*, vol. 51, no. 10, pp. 1749–1764, Oct 2004. [Online]. Available: <http://dx.doi.org/10.1109/TBME.2004.827536>
- [222] B. L. Hoppe, A. M. Kahn, G. K. Feld, A. Hassankhani, and S. M. Narayan, "Separating atrial flutter from atrial fibrillation with apparent electrocardiographic organization using dominant and narrow F-wave spectra." *J Am Coll Cardiol*, vol. 46, no. 11, pp. 2079–2087, Dec 2005. [Online]. Available: <http://dx.doi.org/10.1016/j.jacc.2005.08.048>
- [223] O. Berenfeld, R. Mandapati, S. Dixit, A. C. Skanes, J. Chen, M. Mansour, and J. Jalife, "Spatially distributed dominant excitation frequencies reveal hidden organization in atrial fibrillation in the Langendorff-perfused sheep heart." *J Cardiovasc Electrophysiol*, vol. 11, no. 8, pp. 869–879, Aug 2000.
- [224] P. Sanders, O. Berenfeld, M. Hocini, P. Jaïs, R. Vaidyanathan, L.-F. Hsu, S. Garrigue, Y. Takahashi, M. Rotter, F. Sacher, C. Scavée, R. Ploutz-Snyder, J. Jalife, and M. Haïssaguerre, "Spectral analysis identifies sites of high-frequency activity maintaining atrial fibrillation in humans." *Circulation*, vol. 112, no. 6, pp. 789–797, Aug 2005. [Online]. Available: <http://dx.doi.org/10.1161/CIRCULATIONAHA.104.517011>
- [225] R. B. Schuessler, M. W. Kay, S. J. Melby, B. H. Branham, J. P. Boineau, and R. J. Damiano, "Spatial and temporal stability of the dominant frequency of activation in human atrial fibrillation." *J Electrocardiol*, vol. 39, no. 4 Suppl, pp. S7–12, Oct 2006. [Online]. Available: <http://dx.doi.org/10.1016/j.jelectrocard.2006.04.009>
- [226] K. Ryu, J. Sahadevan, C. M. Khrestian, B. S. Stambler, and A. L. Waldo, "Use of fast fourier transform analysis of atrial electrograms for rapid characterization of atrial activation-implications for delineating possible mechanisms of atrial tachyarrhythmias." *J Cardiovasc Electrophysiol*, vol. 17, no. 2, pp. 198–206, Feb 2006. [Online]. Available: <http://dx.doi.org/10.1111/j.1540-8167.2005.00320.x>
- [227] K. M. Ropella, A. V. Sahakian, J. M. Baerman, and S. Swiryn, "The coherence spectrum. A quantitative discriminator of fibrillatory and nonfibrillatory cardiac rhythms." *Circulation*, vol. 80, no. 1, pp. 112–119, Jul 1989.
- [228] H. J. Sih, A. V. Sahakian, C. E. Arentzen, and S. Swiryn, "A frequency domain analysis of spatial organization of epicardial maps." *IEEE Trans Biomed Eng*, vol. 42, no. 7, pp. 718–727, Jul 1995. [Online]. Available: <http://dx.doi.org/10.1109/10.391158>
- [229] E. G. Lovett and K. M. Ropella, "Time-frequency coherence analysis of atrial fibrillation termination during procainamide administration." *Ann Biomed Eng*, vol. 25, no. 6, pp. 975–984, 1997.
- [230] J. Kalifa, K. Tanaka, A. V. Zaitsev, M. Warren, R. Vaidyanathan, D. Auerbach, S. Pandit, K. L. Vikstrom, R. Ploutz-Snyder, A. Talkachou, F. Atriaza, G. Guiraudon, J. Jalife, and O. Berenfeld, "Mechanisms of wave fractionation at boundaries of high-frequency excitation in the posterior left atrium of the isolated sheep heart during atrial fibrillation." *Circulation*, vol. 113, no. 5, pp. 626–633, Feb 2006. [Online]. Available: <http://dx.doi.org/10.1161/CIRCULATIONAHA.105.575340>

- [231] T. H. Everett, L. C. Kok, R. H. Vaughn, J. R. Moorman, and D. E. Haines, "Frequency domain algorithm for quantifying atrial fibrillation organization to increase defibrillation efficacy." *IEEE Trans Biomed Eng*, vol. 48, no. 9, pp. 969–978, Sep 2001.
- [232] T. H. Everett, J. R. Moorman, L. C. Kok, J. G. Akar, and D. E. Haines, "Assessment of global atrial fibrillation organization to optimize timing of atrial defibrillation." *Circulation*, vol. 103, no. 23, pp. 2857–2861, Jun 2001.
- [233] T. H. Everett, S. Verheule, E. E. Wilson, S. Foreman, and J. E. Olgin, "Left atrial dilatation resulting from chronic mitral regurgitation decreases spatiotemporal organization of atrial fibrillation in left atrium." *Am J Physiol Heart Circ Physiol*, vol. 286, no. 6, pp. H2452–H2460, Jun 2004. [Online]. Available: <http://dx.doi.org/10.1152/ajpheart.01032.2003>
- [234] Y. Takahashi, P. Sanders, P. Jaïs, M. Hocini, R. Dubois, M. Rotter, T. Rostock, C. J. Nalliah, F. Sacher, J. Clémenty, and M. Haïssaguerre, "Organization of frequency spectra of atrial fibrillation: relevance to radiofrequency catheter ablation." *J Cardiovasc Electrophysiol*, vol. 17, no. 4, pp. 382–388, Apr 2006. [Online]. Available: <http://dx.doi.org/10.1111/j.1540-8167.2005.00414.x>
- [235] T. H. Everett, E. E. Wilson, and J. E. Olgin, "Effects of atrial fibrillation substrate and spatiotemporal organization on atrial defibrillation thresholds." *Heart Rhythm*, vol. 4, no. 8, pp. 1048–1056, Aug 2007. [Online]. Available: <http://dx.doi.org/10.1016/j.hrthm.2007.03.032>
- [236] J. Tuan, F. Osman, M. Jeilan, S. Kundu, R. Mantravadi, P. J. Stafford, and G. A. Ng, "Increase in organization index predicts atrial fibrillation termination with flecainide post-ablation: spectral analysis of intracardiac electrograms." *Europace*, vol. 12, no. 4, pp. 488–493, Apr 2010. [Online]. Available: <http://dx.doi.org/10.1093/europace/eup405>
- [237] P. Bonizzi, M. de la Salud Guillem, A. M. Climent, J. Millet, V. Zarzoso, F. Castells, and O. Meste, "Noninvasive assessment of the complexity and stationarity of the atrial wavefront patterns during atrial fibrillation." *IEEE Trans Biomed Eng*, vol. 57, no. 9, pp. 2147–2157, Sep 2010. [Online]. Available: <http://dx.doi.org/10.1109/TBME.2010.2052619>
- [238] H. J. Sih, D. P. Zipes, E. J. Berbari, and J. E. Olgin, "A high-temporal resolution algorithm for quantifying organization during atrial fibrillation." *IEEE Trans Biomed Eng*, vol. 46, no. 4, pp. 440–450, Apr 1999.
- [239] D. T. Kaplan and R. J. Cohen, "Is fibrillation chaos?" *Circ Res*, vol. 67, no. 4, pp. 886–892, Oct 1990.
- [240] B. P. Hoekstra, C. G. Diks, M. A. Allesie, and J. DeGoede, "Nonlinear analysis of epicardial atrial electrograms of electrically induced atrial fibrillation in man." *J Cardiovasc Electrophysiol*, vol. 6, no. 6, pp. 419–440, Jun 1995.
- [241] L. Faes, G. Nollo, R. Antolini, F. Gaita, and F. Ravelli, "A method for quantifying atrial fibrillation organization based on wave-morphology similarity." *IEEE Trans Biomed Eng*, vol. 49, no. 12 Pt 2, pp. 1504–1513, Dec 2002. [Online]. Available: <http://dx.doi.org/10.1109/TBME.2002.805472>
- [242] F. Censi, V. Barbaro, P. Bartolini, G. Calcagnini, A. Michelucci, G. F. Gensini, and S. Cerutti, "Recurrent patterns of atrial depolarization during atrial fibrillation assessed by recurrence plot quantification." *Ann Biomed Eng*, vol. 28, no. 1, pp. 61–70, Jan 2000.

- [243] J. S. Richman and J. R. Moorman, "Physiological time-series analysis using approximate entropy and sample entropy." *Am J Physiol Heart Circ Physiol*, vol. 278, no. 6, pp. H2039–H2049, Jun 2000.
- [244] L. T. Mainardi, A. Porta, G. Calcagnini, P. Bartolini, A. Michelucci, and S. Cerutti, "Linear and non-linear analysis of atrial signals and local activation period series during atrial-fibrillation episodes." *Med Biol Eng Comput*, vol. 39, no. 2, pp. 249–254, Mar 2001.
- [245] M. Masè, L. Faes, R. Antolini, M. Scaglione, and F. Ravelli, "Quantification of synchronization during atrial fibrillation by Shannon entropy: validation in patients and computer model of atrial arrhythmias." *Physiol Meas*, vol. 26, no. 6, pp. 911–923, Dec 2005. [Online]. Available: <http://dx.doi.org/10.1088/0967-3334/26/6/003>
- [246] E. P. Gerstenfeld, A. V. Sahakian, and S. Swiryn, "Evidence for transient linking of atrial excitation during atrial fibrillation in humans." *Circulation*, vol. 86, no. 2, pp. 375–382, Aug 1992.
- [247] S. M. Narayan, D. E. Krummen, A. M. Kahn, P. L. Karasik, and M. R. Franz, "Evaluating fluctuations in human atrial fibrillatory cycle length using monophasic action potentials." *Pacing Clin Electrophysiol*, vol. 29, no. 11, pp. 1209–1218, Nov 2006. [Online]. Available: <http://dx.doi.org/10.1111/j.1540-8159.2006.00525.x>
- [248] A. C. Skanes, R. Mandapati, O. Berenfeld, J. M. Davidenko, and J. Jalife, "Spatiotemporal periodicity during atrial fibrillation in the isolated sheep heart." *Circulation*, vol. 98, no. 12, pp. 1236–1248, Sep 1998.
- [249] F. X. Roithinger, A. SippensGroenewegen, M. R. Karch, P. R. Steiner, W. S. Ellis, and M. D. Lesh, "Organized activation during atrial fibrillation in man: endocardial and electrocardiographic manifestations." *J Cardiovasc Electrophysiol*, vol. 9, no. 5, pp. 451–461, May 1998.
- [250] F. Ravelli, M. Masè, M. D. Greco, L. Faes, and M. Disertori, "Deterioration of organization in the first minutes of atrial fibrillation: a beat-to-beat analysis of cycle length and wave similarity." *J Cardiovasc Electrophysiol*, vol. 18, no. 1, pp. 60–65, Jan 2007. [Online]. Available: <http://dx.doi.org/10.1111/j.1540-8167.2006.00620.x>
- [251] J. Billette and M. Lavallée, "Organized atrial fibrillation onset: a propitious intervention window?" *J Cardiovasc Electrophysiol*, vol. 18, no. 1, pp. 66–68, Jan 2007. [Online]. Available: <http://dx.doi.org/10.1111/j.1540-8167.2006.00678.x>
- [252] R. Alcaraz and J. J. Rieta, "A non-invasive method to predict electrical cardioversion outcome of persistent atrial fibrillation." *Med Biol Eng Comput*, vol. 46, no. 7, pp. 625–635, Jul 2008. [Online]. Available: <http://dx.doi.org/10.1007/s11517-008-0348-5>
- [253] J. Eckstein, S. Verheule, N. M. de Groot, N. de Groot, M. Allesie, and U. Schotten, "Mechanisms of perpetuation of atrial fibrillation in chronically dilated atria." *Prog Biophys Mol Biol*, vol. 97, no. 2-3, pp. 435–451, 2008. [Online]. Available: <http://dx.doi.org/10.1016/j.pbiomolbio.2008.02.019>
- [254] C. B. de Vos, R. Pisters, R. Nieuwlaat, M. H. Prins, R. G. Tieleman, R.-J. S. Coelen, A. C. van den Heijkant, M. A. Allesie, and H. J. G. M. Crijns, "Progression from paroxysmal to persistent atrial fibrillation clinical correlates and prognosis." *J Am Coll Cardiol*, vol. 55, no. 8, pp. 725–731, Feb 2010. [Online]. Available: <http://dx.doi.org/10.1016/j.jacc.2009.11.040>

- [255] B. Zrenner, G. Ndrepepa, M. R. Karch, M. A. Schneider, J. Schreieck, A. Schömig, and C. Schmitt, "Electrophysiologic characteristics of paroxysmal and chronic atrial fibrillation in human right atrium." *J Am Coll Cardiol*, vol. 38, no. 4, pp. 1143–1149, Oct 2001.
- [256] M. K. Stiles, A. G. Brooks, P. Kuklik, B. John, H. Dimitri, D. H. Lau, L. Wilson, S. Dhar, R. L. Roberts-Thomson, L. Mackenzie, G. D. Young, and P. Sanders, "High-density mapping of atrial fibrillation in humans: relationship between high-frequency activation and electrogram fractionation." *J Cardiovasc Electrophysiol*, vol. 19, no. 12, pp. 1245–1253, Dec 2008. [Online]. Available: <http://dx.doi.org/10.1111/j.1540-8167.2008.01253.x>
- [257] F. Ravelli, L. Faes, L. Sandrini, F. Gaita, R. Antolini, M. Scaglione, and G. Nollo, "Wave similarity mapping shows the spatiotemporal distribution of fibrillatory wave complexity in the human right atrium during paroxysmal and chronic atrial fibrillation." *J Cardiovasc Electrophysiol*, vol. 16, no. 10, pp. 1071–1076, Oct 2005. [Online]. Available: <http://dx.doi.org/10.1111/j.1540-8167.2005.50008.x>
- [258] R. Cervigón, J. Moreno, R. B. Reilly, J. Millet, J. Pérez-Villacastín, and F. Castells, "Entropy measurements in paroxysmal and persistent atrial fibrillation." *Physiol Meas*, vol. 31, no. 7, pp. 1011–1020, Jul 2010. [Online]. Available: <http://dx.doi.org/10.1088/0967-3334/31/7/010>
- [259] R. Alcaraz and J. J. Rieta, "The application of nonlinear metrics to assess organization differences in short recordings of paroxysmal and persistent atrial fibrillation." *Physiol Meas*, vol. 31, no. 1, pp. 115–130, Jan 2010. [Online]. Available: <http://dx.doi.org/10.1088/0967-3334/31/1/008>
- [260] P. Sanders, C. J. Nalliah, R. Dubois, Y. Takahashi, M. Hocini, M. Rotter, T. Rostock, F. Sacher, L.-F. Hsu, A. Jönsson, M. D. O'Neill, P. Jaïs, and M. Haïssaguerre, "Frequency mapping of the pulmonary veins in paroxysmal versus permanent atrial fibrillation." *J Cardiovasc Electrophysiol*, vol. 17, no. 9, pp. 965–972, Sep 2006. [Online]. Available: <http://dx.doi.org/10.1111/j.1540-8167.2006.00546.x>
- [261] Q. Xi, A. V. Sahakian, T. G. Frohlich, J. Ng, and S. Swiryn, "Relationship between pattern of occurrence of atrial fibrillation and surface electrocardiographic fibrillatory wave characteristics." *Heart Rhythm*, vol. 1, no. 6, pp. 656–663, Dec 2004. [Online]. Available: <http://dx.doi.org/10.1016/j.hrthm.2004.09.010>
- [262] M. Lemay, J.-M. Vesin, A. van Oosterom, V. Jacquemet, and L. Kappenberger, "Cancellation of ventricular activity in the ECG: evaluation of novel and existing methods." *IEEE Trans Biomed Eng*, vol. 54, no. 3, pp. 542–546, Mar 2007. [Online]. Available: <http://dx.doi.org/10.1109/TBME.2006.888835>
- [263] D. S. Stoffer, D. E. Tyler, and A. J. McDougall, "Spectral analysis for categorical time series: scaling and spectral envelope," *Biometrika*, no. 80, pp. 611–622, 1993.
- [264] A. J. McDougall, D. S. Stoffer, and D. E. Tyler, "Optimal transformations and the spectral envelope for real-valued time series," *J Stat Plan Inf*, no. 57, pp. 195–214, 1997.
- [265] H. Jiang, S. Choudhury, and S. L. Shah, "Detection and diagnosis of plant-wide oscillations from industrial data using the spectral envelope method," *J Process Control*, vol. 17, pp. 143–155, 2007.

- [266] D. S. Stoffer, "Detecting common signals in multiple time series using the spectral envelope," *J Am Stat Assoc*, no. 94, pp. 1341–1356, 1999.
- [267] R. H. Shumway, *Applied Statistical Time Series Analysis*. Prentice-Hall, New Jersey, 1988.
- [268] D. R. Brillinger, *Time Series: Data Analysis and Theory*. Holden-Day, San Francisco, 1975.
- [269] D. S. Stoffer, D. E. Tyler, and D. A. Wendt, "The spectral envelope and its applications," *Statistical Science*, vol. 15, no. 3, pp. 224–253, 2000.
- [270] N. F. Thornhill, S. L. Shah, B. Huang, and A. Vishnubhotla, "Spectral principal component analysis of dynamic process data," *Cont Eng Pract*, no. 10, pp. 833–846, 2002.
- [271] R. Alcaraz, F. Sandberg, L. Sörnmo, and J. J. Rieta, "Classification of Paroxysmal and Persistent Atrial Fibrillation in Ambulatory ECG Recordings." *IEEE Trans Biomed Eng*, vol. 58, no. 5, pp. 1441–1449, May 2011. [Online]. Available: <http://dx.doi.org/10.1109/TBME.2011.2112658>
- [272] I. A. Rezek and S. J. Roberts, "Stochastic complexity measures for physiological signal analysis." *IEEE Trans Biomed Eng*, vol. 45, no. 9, pp. 1186–1191, Sep 1998. [Online]. Available: <http://dx.doi.org/10.1109/10.709563>
- [273] G. J. McLachlan, *Discriminant Analysis and Statistical Pattern Recognition*. Wiley Intersciences, 2004.
- [274] K. H. Zou, A. J. O'Malley, and L. Mauri, "Receiver-operating characteristic analysis for evaluating diagnostic tests and predictive models." *Circulation*, vol. 115, no. 5, pp. 654–657, Feb 2007. [Online]. Available: <http://dx.doi.org/10.1161/CIRCULATIONAHA.105.594929>
- [275] D. G. Altman and J. M. Bland, "Diagnostic tests 2: Predictive values." *BMJ*, vol. 309, no. 6947, p. 102, Jul 1994.
- [276] A. Bollmann, N. K. Kanuru, K. K. McTeague, P. F. Walter, D. B. DeLurgio, and J. J. Langberg, "Frequency analysis of human atrial fibrillation using the surface electrocardiogram and its response to ibutilide." *Am J Cardiol*, vol. 81, no. 12, pp. 1439–1445, Jun 1998.
- [277] M. Holm, S. Pehrson, M. Ingemansson, L. Sörnmo, R. Johansson, L. Sandhall, M. Sune-mark, B. Smideberg, C. Olsson, and S. B. Olsson, "Non-invasive assessment of the atrial cycle length during atrial fibrillation in man: introducing, validating and illustrating a new ECG method." *Cardiovasc Res*, vol. 38, no. 1, pp. 69–81, Apr 1998.
- [278] S. Petrutiu, A. V. Sahakian, W. Fisher, and S. Swiryn, "Manifestation of left atrial events and interatrial frequency gradients in the surface electrocardiogram during atrial fibrillation: contributions from posterior leads." *J Cardiovasc Electrophysiol*, vol. 20, no. 11, pp. 1231–1236, Nov 2009. [Online]. Available: <http://dx.doi.org/10.1111/j.1540-8167.2009.01523.x>
- [279] P. G. Platonov, I. Nault, F. Holmqvist, M. Stridh, M. Hocini, and M. Haïssaguerre, "Left Atrial Appendage Activity Translation in the Standard 12-lead ECG." *J Cardiovasc Electrophysiol*, Oct 2010. [Online]. Available: <http://dx.doi.org/10.1111/j.1540-8167.2010.01909.x>

- [280] M. Daccarett, T. J. Badger, N. Akoum, N. S. Burgon, C. Mahnkopf, G. Vergara, E. Kholmovski, C. J. McGann, D. Parker, J. Brachmann, R. S. Macleod, and N. F. Marrouche, "Association of left atrial fibrosis detected by delayed-enhancement magnetic resonance imaging and the risk of stroke in patients with atrial fibrillation." *J Am Coll Cardiol*, vol. 57, no. 7, pp. 831–838, Feb 2011. [Online]. Available: <http://dx.doi.org/10.1016/j.jacc.2010.09.049>
- [281] S. Kainuma, T. Masai, M. Yoshitatsu, S. Miyagawa, T. Yamauchi, K. Takeda, E. Morii, and Y. Sawa, "Advanced left-atrial fibrosis is associated with unsuccessful maze operation for valvular atrial fibrillation." *Eur J Cardiothorac Surg*, Jan 2011. [Online]. Available: <http://dx.doi.org/10.1016/j.ejcts.2010.11.008>
- [282] K. Tanaka, S. Zlochiver, K. L. Vikstrom, M. Yamazaki, J. Moreno, M. Klos, A. V. Zaitsev, R. Vaidyanathan, D. S. Auerbach, S. Landas, G. Guiraudon, J. Jalife, O. Berenfeld, and J. Kalifa, "Spatial distribution of fibrosis governs fibrillation wave dynamics in the posterior left atrium during heart failure." *Circ Res*, vol. 101, no. 8, pp. 839–847, Oct 2007. [Online]. Available: <http://dx.doi.org/10.1161/CIRCRESAHA.107.153858>
- [283] M. Lemay, "Data processing techniques for the characterization of atrial fibrillation." Ph.D. dissertation, Swiss Federal Institute of Technology, 2007.
- [284] Y. Prudat, "Adaptive frequency tracking and application to biomedical signals." Ph.D. dissertation, Swiss Federal Institute of Technology, 2009.



Laurent Uldry

Av. de Bethusy 39  
1012 Lausanne - CH  
Phone: +41 78 801 47 74  
Email: laurent.uldry@epfl.ch

Date of birth: Jan 27, 1983  
(28 year old)  
Nationality: Swiss  
Marital status: Single

## Education

---

- 2008 – 2011** [ÉCOLE POLYTECHNIQUE FÉDÉRALE DE LAUSANNE](#), Switzerland.  
Ph.D. Thesis in Biomedical Signal Processing.  
*Therapeutic strategies for the treatment of atrial fibrillation: new insights from biophysical modeling and signal processing.*
- 2002 – 2007** [ÉCOLE POLYTECHNIQUE FÉDÉRALE DE LAUSANNE](#), Switzerland.  
M.Sc. in Electrical Engineering.
- 1998 – 2002** [COLLÈGE DE L'ABBAYE](#), Saint-Maurice, Switzerland.  
Literary Baccalauréat.

## Academic Experience

---

- 2008 – 2010** [ÉCOLE POLYTECHNIQUE FÉDÉRALE DE LAUSANNE](#).  
Teaching assistant for lab sessions in the course *Biomedical signal processing*.
- 2007 – 2008** [ÉCOLE POLYTECHNIQUE FÉDÉRALE DE LAUSANNE](#).  
Teaching assistant for exercises and lectures in the course *Introduction au traitement des signaux*.

## Work Experience

---

- 2007 – 2008** (1 year) [CENTRE HOSPITALIER UNIVERSITAIRE VAUDOIS \(CHUV\)](#), Service de Radiologie, Lausanne, Switzerland.  
Research assistant in fundamental neurosciences using magnetic resonance imaging (MRI).

## Language

---

French: mother tongue.  
English: fluent.  
German: advanced.  
Spanish: basic.

## Computer Skills

---

- Basic knowledge of C/C++.
- Experience with Matlab, R and Labview.
- Good working knowledge of Microsoft Windows XP/Vista/7 and Office as well as Linux.

## Interests and Activities

---

- Tennis, Badminton, Running.
- Philosophy and essays (Montaigne, Roger Robert, Plato, etc.).

## References

---

Available upon request.



# Patents and Publications

---

## Patents

Inventors: Nathalie Virag, Laurent Uldry, Fred Lindemans, Lukas Kappenberger. *Terminating Tachyarrhythmias*. Application No 12/8286,010. Filed on June 30, 2010 in the United States of America.

Inventors: Nathalie Virag, Laurent Uldry, Fred Lindemans, Lukas Kappenberger. *Terminating Tachyarrhythmias*. Application No 12/533,650. Filed on July 31, 2009 in the United States of America.

## Book Chapters

L. Uldry, N. Virag, J.-M. Vesin, L. Kappenberger. *Studies of Therapeutic Strategies for Atrial Fibrillation Based on a Biophysical Model of the Human Atria*, In: R.C.P. Kerckhoffs (ed.) *Patient Specific Modeling of the Cardiovascular System*, Springer Science+Business Media, 2010.

L. Uldry, C. Duchene, Y. Prudat, M.M. Murray, J.-M. Vesin. *Adaptive tracking of EEG components* In: Naït-Ali A (ed) *Advanced Biosignal Processing*, Springer, 2009.

## Journal Papers

A. Forclaz, S. M. Narayan, D. Scherr, N. Linton, A. S. Jadidi, I. Nault, L. Rivard, S. Miyazaki, L. Uldry, M. Wright, A. J. Shah, X. Liu, O. Xhaet, N. Derval, S. Knecht, F. Sacher, P. Jaïs, M. Hocini, M. Haïssaguerre. *Early Temporal and Spatial Regularization of Persistent Atrial Fibrillation Predicts Termination and Arrhythmia-Free Outcome*, Heart Rhythm (2011), accepted.

L. Uldry, N. Virag, F. Lindemans, J.-M. Vesin, L. Kappenberger. *A Novel Atrial Septal Pacing Algorithm for the Termination of Atrial Fibrillation*, Cardiovascular Research (2011), submitted.

L. Uldry, J. Van Zaen, J.-M. Vesin, L. Kappenberger. *Non-Invasive Measures of Spatiotemporal Organization Differentiate Persistent From Permanent Atrial Fibrillation*, European Heart Journal (2011), submitted.

L. Uldry, N. Virag, J.-M. Vesin, L. Kappenberger. *Dynamics of Atrial Fibrillation during Spontaneous Termination: A Biophysical Modeling study*, Medical and Biological Engineering and Computing (2011), submitted.

L. Uldry, N. Virag, J.-M. Vesin, L. Kappenberger. *Optimizing local capture of atrial fibrillation: a model based study of the influence of tissue dynamics on the outcome of rapid pacing*, Annals of Biomedical engineering (2010) Volume 38, Issue 12, p.3664.

J. Van Zaen, L. Uldry, C. Duchene, Y. Prudat, R. A. Meuli, M.M. Murray, J.-M. Vesin. *Adaptive tracking of EEG oscillations*, J Neurosci Methods, 2010 Jan 30;186(1):97-106. Epub 2009 Nov 3.

## Conference Papers

V. Jacquemet, M. Lemay, L. Uldry, C. Duchêne, L. Kappenberger, A. van Oostrom, J.-M. Vesin. *The Role of Atrial Modeling in the Development of ECG Processing Tools*, World Congress 2009 - Medical Physics and Biomedical Engineering, Munich, September 7-12, 2009.

L. Uldry, N. Virag, J.-M. Vesin, L. Kappenberger. *Optimization of antitachycardia pacing protocols applied to atrial fibrillation: insights from a biophysical model*, Proceedings of the 31st Annual International Conference of IEEE EMBC 2009;3024-3027. September 2009.

L. Uldry, N. Virag, V. Jacquemet, J.-M. Vesin, L. Kappenberger. *Spontaneous termination of atrial fibrillation: study of the effect of atrial geometry in a biophysical model*, Proceedings of the 31<sup>st</sup> Annual International Conference of IEEE EMBC 2009;4504-4507. September 2009.

## Abstracts

L. Uldry, N. Virag, J.-M. Vesin, L. Kappenberger. *Influence of pacing site on the spatial extent of capture during atrial fibrillation rapid pacing*, Europace (2010) 12 (suppl 1): i59.

A. Forclaz, S. Narayan, A. Jadidi, I. Nault, L. Rivard, S. Myiazaki, N. Linton, O. Xhaet, A. Shah, X. Liu, L. Uldry, M. Wright, N. Derval, F. Sacher, P. Bordachard, P. Ritter, P. Jaïs, M. Hocini, M. Haïssaguerre. *Early spatial and temporal organization during atrial fibrillation ablation predicts arrhythmia termination*, Europace (2010) 12 (suppl 1):i165.

L. Uldry, N. Virag, J.-M. Vesin, L. Kappenberger. *Estimation of tissue wavelength predicts the feasibility of local capture by rapid pacing in atrial fibrillation*, Heart Rhythm (2010). Volume 7, Issue 5, Supplement (May 2010);S289.

L. Uldry, N. Virag, J.-M. Vesin, L. Kappenberger. *Effect of atrial fibrillation dynamics on the mechanisms of spontaneous termination*, Heart Rhythm (2010). Volume 7, Issue 5, Supplement (May 2010);S350.

A. Forclaz, S. Narayan, A. Jadidi, I. Nault, L. Rivard, S. Myiazaki, N. Linton, O. Xhaet, A. Shah, X. Liu, M. Wright, L. Uldry, N. Derval, F. Sacher, P. Jaïs, M. Hocini, M. Haïssaguerre. *Temporal and spatial regularization of persistent atrial fibrillation is associated with arrhythmia free outcome*, Heart Rhythm (2010). Volume 7, Issue 5, Supplement (May 2010);S404.

A. Forclaz, S. Narayan, A. Jadidi, I. Nault, L. Rivard, S. Myiazaki, N. Linton, O. Xhaet, A. Shah, X. Liu, L. Uldry, M. Wright, N. Derval, F. Sacher, P. Ritter, P. Jaïs, M. Hocini, M. Haïssaguerre. *Early temporal and spatial regularization during ablation of persistent atrial fibrillation predicts arrhythmia termination*, Heart Rhythm (2010). Volume 7, Issue 5, Supplement (May 2010);S33.

L. Uldry, N. Virag, J.-M. Vesin, L. Kappenberger. *The effect of pacing site and frequency on capture of atrial fibrillation observed in a biophysical model*, European Heart Journal 2009;30(Abstract Supplement):826.

L. Uldry, R. Meuli, I. Bourquin, A. Brioschi, J. Ghika, P. Maeder, E. Fornari. *Inter-hemispheric visual integration in Alzheimer's disease: changes in fMRI bold response in VP/V4 areas*, The International Society for Magnetic Resonance in Medicine, Toronto, May 2008.

L. Uldry, I. Bourquin, A. Brioschi, E. Fornari, J. Ghika, P. Maeder. *Alzheimer's disease and interhemispheric visual integration: changes in fMRI bold response in VP/V4 areas*, The 6<sup>th</sup> Forum of European Neuroscience, Geneva, July 2008.

L. Uldry, C. Duchene, Y. Prudat, R. Meuli, J.-M. Vesin, M.M. Murray. *Adaptive tracking of multiple EEG oscillations in single-trial data*, Frontiers in Human Neuroscience. Conference Abstract: 10<sup>th</sup> International Conference on Cognitive Neuroscience, Bodrum, 2008. doi: 10.3389/conf.neuro.09.2009.01.150.

J.-F. Knebel, L. Uldry, M.M. Murray. *Electrical neuroimaging resolves conflicting models of illusory contour processing in humans*, Frontiers in Human Neuroscience. Conference Abstract: 10<sup>th</sup> International Conference on Cognitive Neuroscience, Bodrum, 2008. doi: 10.3389/conf.neuro.09.2009.01.340.